STRATEGIES OPTIMISING THE THERAPEUTIC POTENTIAL OF INDUCIBLE NITRIC OXIDE SYNTHASE FOR THE USE IN CANCER GENE THERAPY

A thesis submitted to the University of Manchester for the degree of Doctor of Philosophy in the Faculty of Medicine, Dentistry, Nursing and Pharmacy

2004

RANA SOUFIAN AL-ASSAH

EXPERIMENTAL ONCOLOGY GROUP,
THE SCHOOL OF PHARMACY AND PHARMACEUTICAL SCIENCES,
UNIVERSITY OF MANCHESTER, MANCHESTER, UK

ProQuest LLC.
789 East Eisenhower Parkway
P.O. Box 1346
Ann Arbor, MI 48106 – 1346

List of Contents

List of Figures

List of Tables

List of Abreviations

A	
AAV	Adeno-associated Vectors
Ad	Adenovirus
B	
BH_4	Tetrahydrobiopterin
BSA	Bovine serum albumin
bp	Base pair
C	
CaM	Calmodulin
Carboxy-PTIO	2-(4-Carboxyphenyl)-4,4,5,5-tetramethylimidazoline-1-oxyl-3-oxide
CIP	Calf intestinal alkaline phosphatase
D	
dH_2O	Deionised water
ddH_2O	Double distilled water
DBD	DNA binding domain
DMSO	Dimethyl sulfoxide
DNA	Deoxyribonucleic acid
E	
EDTA	Ethylenediaminetetraacetate
F	
FAD	Flavin adenine dinucleotide
FCS	Foetal calf serum
FITC	Fluorescein isothiocyanate
FMN	Flavin mononucleotide
G	
GFP	Green fluorescent protein
GSH	Glutathione
GSNO	*S*-Nitroso-glutathione
GSSG	Glutathione disulfide
H	
HSV	Herpes simplex virus
HIF-1	Hypoxia-inducible factor 1
I	
IFNγ or INFγ	Interferon-γ
IL1β	Interleukin-1-β
IRES	Internal ribosome entry site
ITR	Inverted terminal repeats

J, K, L

L-NAME	Nitro-L-arginine methyl ester
L-NIO	N-Imino-ethyl-L-ornithine
L-NNA	N^{ω}-Nitro-L-arginine
L-NMMA or NMA	N^{G}-Monomethyl-L-arginine
LPS	Lipopolysaccharide
Kb	Kilobase

M

Moi	Multiplicity of infection
MTT	3-(4,5-Dimethylthiazole–2-yl)-2,5-diphenyltetrazolium bromide

N

NADPH	Nicotinamide adenine dinucleotide phosphate
NOC 5	1-Hydroxy-2-oxo-3-(3-aminopropyl)-3-isopropyl-1-triazene
NOC 18	1-Hydroxy-2-oxo-3,3 bis(2-aminoethyl)-1-triazene
NOR 4	3-[(+/-)-(E)-Ethyl-2'-[(E)-hydroxyimino]-5-nitro-3-hexenecarbamoyl]-pyridine
NO	Nitric Oxide
NOS	Nitric Oxide Synthase

O, P

pΔHSP	Minimal heat shock promoter
pCMV	Cytomegalovirus
PBS	Phosphate buffered-saline
Pon A	Ponasterone A
P_{450} reductase	NADH:cytochrome c (P_{450}) reductase

Q, R

RNA	Ribonucleic acid

S

SIN-1	3-Morpholinosydnonimine
SNAP	*S*-Nitroso-*N*-acetyl-penicillamine
SNP	Nitroprusside
TPZ	Tirapazamine (3-amino-1,2,4-benzotriazone1,4-dioxide, Tirazone™)
TNF-α	Tumour necrosis factor alpha

T, U, V

VEGF	Vascular endothelial growth factor
VP16	Herpes simplex virus promoter

W, X,

X-gal	5-Bromo-4-chloro-3-indolyl-β-D-galactoside

Y, Z

ABSTRACT

Nitric Oxide Synthases (NOS) are a family of enzymes that generate nitric oxide (NO) upon the conversion of L-arginine to citrulline. Two main types of NOS exist; constitutive and inducible. Inducible NOS (iNOS) is known to play a role in the immune system and has shown dual effects on tumour growth. At low levels, iNOS has exhibited pro-tumour effects while at higher levels the reverse has been observed.

This study aims to generate tools that tightly regulate iNOS expression and apply them to explore the therapeutic effects of iNOS for use in cancer therapy. Since stable clones that express high levels of iNOS are difficult to culture, as they generate high NO concentrations resulting in cell death, an inducible approach was sought. The ecdysone system was chosen because it demonstrated low basal levels, high fold induction, and the inducer had no known effects on iNOS. This system is comprised of a receptor and a response vector that have to be co-expressed in the cells in order to drive gene expression. Upon inducer addition, the receptor binds to the promoter of the response vector and thus gene expression occurs. Initially, the ecdysone system was evaluated *in vitro* and *in vivo* using the *Lac* Z reporter gene, then, ecdysone inducible iNOS stable clones were generated. The characteristics of the clone that showed the highest ecdysone inducible iNOS expression were fully examined *in vitro* and *in vivo*. This clone was later used to study the effect of iNOS expression on hypoxia and blood perfusion.

In order to be able to deliver iNOS in a gene therapy approach, recombinant adenoviruses encoding for the iNOS gene (and *Lac* Z as a control) were generated. Gene expression was tightly regulated in this system by varying the multiplicity of infection (moi) of the viruses.

Hypoxic cells are known to be chemo- and radio-resistant thus causing a major draw back in cancer therapy. Studies have revealed that iNOS is naturally up regulated in hypoxic cells. Since iNOS shares high sequence homology to P_{450} reductase, and since the latter metabolises bioreductve drugs like tirapazamine, iNOS was over expressed using the established tools to study its cytotoxic effects to tirapazamine in a gene directed enzyme prodrug therapy (GDEPT). Moreover, the hypoxia inducible factor, HIF-1, is known to be the key molecule that regulates the expression of genes under hypoxic stress. Current studies attempt to down regulate this molecule in order to reduce HIF-mediated gene expression. Hence, the effect of NO on HIF-mediated gene expression was studied using the NO donor GSNO as an exogenous NO source and using plasmids and the established adenoviruses as an endogenous non-chemical NO source.

In conclusion, this work emphasises the importance of iNOS expression in cancer gene therapy. Overexpression of this gene can be targeted to sensitise hypoxic cells to tirapazamine as well as be used to down regulate HIF-1. The transcriptional activity of this gene can be controlled using the ecdysone inducible system and clinically delivered using adenoviral vehicles.

DECLARATION

No portion of the work refered to in the thesis has been submitted in support of an application for another degree or qualification of this or any other university or institute of learning.

COPYRIGHT

Rana S. Al-Assah

بسم الله الرحمن الرحيم

قال رب اشرح لي صدري ﴿25﴾ و يسر لي امري ﴿26﴾
و احلل عقدة من لساني ﴿27﴾ يفقهوا قولي ﴿28﴾
و قل رب زدني علما ﴿114﴾

سورة طه

ACKNOWLEDGEMENTS

My deepest thanks go to my parents, Bassel, Mohammad, and Vida for their unlimited love, help, and encouragement.

I would also like to thank all my friends and colleagues in Experimental Oncology Group including Dr. Edwin Chinje and Brian Telfer for their help. A special thank you goes to Prof. Ian Stratford and Dr. Rachel Cowen for their continued support and invaluable advice.

Finally, I am grateful to my parents and the University Funding Scheme (ORS and URS awards) for funding my project.

THE AUTHOR

Rana Al-Assah, a Lebanese citizen, graduated from the American University of Beirut-Lebanon with a B.S degree in Biology in 2000. She then decided to persue a PhD degree at the University of Manchester-UK.

CHAPTER 1 INTRODUCTION

1.1 Nitric Oxide and Nitric Oxide Synthase

1.1.1 History and Discovery of Nitric Oxide

Nitric Oxide (NO) was first discovered by researchers trying to identify the agent responsible for regulating vascular tone. The agent discovered was called endothelium-derived relaxing factor (EDRF) and was assumed to be a protein like most signalling molecules. Later, studies showed that EDRF was in fact NO, which is a small gaseous molecule [1,2]. It then became known that NO is continuously produced in humans and animals, acting as a universal regulator of metabolism. These findings made *Science* announce NO as the "molecule of the year" in 1992 [3,4]. Moreover, in 1998 the Nobel Prize was awarded to R.F Furchgott, L.J Ignarro, and F. Murad for their fundamental discoveries of the physiological roles of NO [5]. Now, it is well known that NO plays a role in a variety of biological processes including neurotransmission, immune defence, and regulation of cell death (apoptosis) [2].

1.1.2 Biological Role of NO

NO is currently recognised as a ubiquitous biomessenger, existing in a wide variety of organisms. In mammals, NO is involved in a number of intercellular and intracellular functions including regulation of enzymes, altering vascular tone, inhibition of platelet aggregation and adhesion to vascular walls to cause blood vessel dilation. It has a role in lymphocyte proliferation, and mediates some of the cytotoxic action against pathogens and tumour cells. NO also plays a role in heart rhythm coordination and regulation of cellular respiratory activity [3,6,7].

Diseases Associated with NO

Many diseases are associated with either a hypo-functioning or hyperactive L-arginine/NO system. For example, hypertension and vasospastic diseases occur where

endothelial NO synthesis is lacking. On the other hand, septic shock, inflammation, and stroke are associated with massive induction of NO [8]. Diabetes also seems to be affected by this molecule. Constitutive NO may help in insulin release under physiologic conditions while induced NO may play a role in the destruction of the pancreatic β-cells during the development of type I diabetes [9]. Curiously, NO gas is being used by inhalation to relieve pulmonary hypertension while it should also be noted that continuous exposure of cells to high levels of NO could have cytotoxic effects leading to severe life-threatening organ damage [8].

1.1.3 Chemistry of NO

1.1.3.1 Chemical Properties of NO

NO plays a diverse role in the body because of its chemical properties. NO is a simple radical gas that has a small size and is soluble in both lipids and water. This makes it easily diffusible compared to other classical mediators that normally have complex structures and are stored in granules and released when needed. NO can also interact with other molecules by covalent bonding and redox reactions [8].

1.1.3.2 Reaction of NO with O_2 and $O_2^{\cdot-}$

NO reacts with oxygen (O_2) in a third order oxidation reaction whereby two molecules of NO react with one molecule of O_2 to give nitrogen oxides (NO_x). The half-life of NO highly depends on its concentration. In high concentrations, NO is more likely to react with oxygen yielding products called reactive nitrogen oxide intermediates (RNOI) or higher nitrogen oxides (NO_x). RNOI are highly reactive and short-lived. They exhibit much broader reaction spectrum towards bio-molecules than NO itself [10]. Therefore, NO can interact with a biological target directly (as NO itself) or indirectly (by producing RNOI species) depending on its concentration [10,11]. NO can also react with the superoxide anion radical

($O_2^{\cdot-}$) yielding the strong oxidant peroxinitrite [10]. Thus, the various roles mediated by NO may be explained by its complex chemistry (**Fig 1.1**).

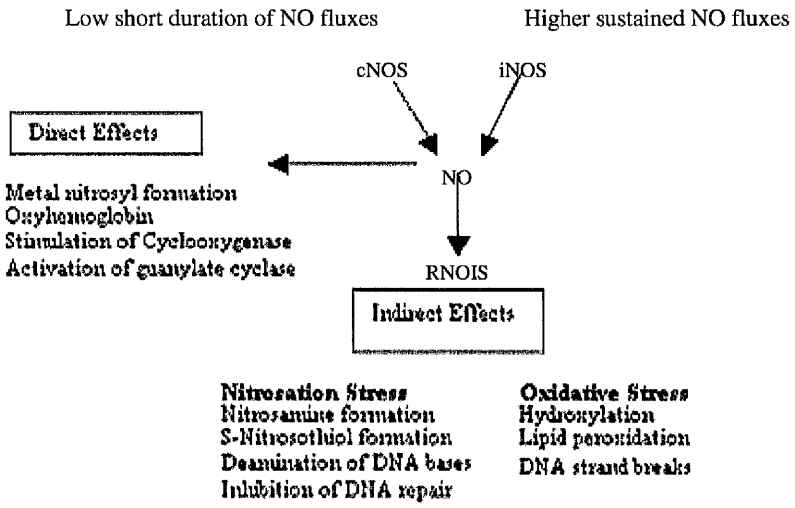

Fig 1.1 The source of NO and its chemical effects in biology [11].

1.1.4 Types of Nitric Oxide Synthases

Nitric oxide synthases (NOS) are a family of enzymes that convert L-arginine to citrulline and NO. Three main types of nitric oxide synthases (NOS) have been discovered: neuronal NOS (nNOS, NOS 1), inducible NOS (iNOS, NOS 2), and endothelial NOS (eNOS, NOS 3). A mitochondrial NOS has also been reported but its structure and regulation have not been defined [12]. It is important to note that members of the NOS family appear to be better distinguished by their mode of activation rather than the organ of their origin [6]. Constitutive NOS (cNOS) and iNOS are found in most types of tissue and their names only indicate the type of tissue they were first identified in [13].

nNOS and eNOS are constitutive NOS. They are inactive until intracellular Ca^{2+} levels increase sufficiently to allow calmodulin binding. When NOS containing cells are given the appropriate stimuli (for example: acetylcholine or glutamate) receptor activation leads to an increase in cytosolic calcium. This activates cNOS to produce a small amount of

NO for a short period of time. cNOS usually plays a regulatory role [8]. However, iNOS is Ca^{2+}/calmodulin (CaM) independent. When induced, it can bind tightly to calmodulin regardless of Ca^{2+} levels. iNOS releases large amounts of NO for a longer period of time and thus plays a host defence role [8]. The amount of NO released by iNOS per unit time is a thousand times higher than that released from cNOS [8] which could indicate that iNOS will generate RNOI [10]. As discussed below, the genomic structure of each of the three NOS isoforms is similar which suggests the divergence from a common ancestor [13].

1.1.4.1 Neuronal NOS (nNOS)

The human nNOS gene spans over 200 Kb on chromosome 12q24.2-q24.31. The major neuronal transcript is made up of 29 exons and encodes a 160 KDa protein. Its gene products are mainly expressed in neurons, skeletal and vascular smooth muscle, and bronchial and tracheal epithelia [12,14,15].

Mice with nNOS gene knockout mainly exhibit hypertrophy of the pyloric sphincter suggesting a role for nNOS in sympathetic smooth muscle relaxation at least in the gut. Moreover, increased aggressive behaviour in males and relative protection from ischemic neurological events compared to wild-type mice is also observed [12].

1.1.4.2 Inducible NOS (iNOS)

The human iNOS gene resides on chromosome 17 cen-q11.2 and contains 26 exons [12,15,16]. The full length of the iNOS gene is 37 Kb [13]. The first human iNOS cDNA was isolated in 1993 from lipopolysaccharide (LPS)-cytokine-stimulated primary human hepatocyte. The sequence revealed a 4,145 base pair (bp) cDNA containing a 3,459 bp open reading frame that encodes a polypeptide of 1,153 amino acids with a molecular mass of 131 KDa (**Fig 1.2**) [13,15].

The main phenotype observed in iNOS knockout mice is increased susceptibility to infection with intracellular pathogens. This suggests that iNOS is important for anti-bacterial

response [12,15]. iNOS knockout mice also exhibit impaired prostaglandin E2 production [12] and LPS induced hypertensions are markedly attenuated in iNOS lacking mice, which indicates that iNOS might be involved in septic shock in humans [15].

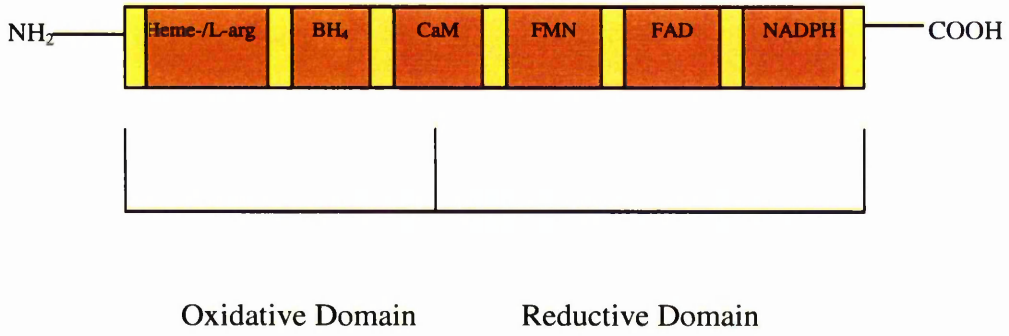

Fig 1.2 Organisational structure of the human iNOS protein: The polypeptide is 1153 amino acids with a calculated mass of 131 KDa and contains recognition sites for the cofactors FMN, FAD, NADPH, heme, BH_4, and CaM [13].

1.1.4.3 Endothelial NOS (eNOS)

The eNOS gene is expressed in the endothelium of a variety of tissues as well as in cardiac and myometrial myocytes, platelets, and airway epithelium. The human eNOS gene is located on chromosome 7q36 and contains 26 exons spanning approximately 21 Kb of genomic DNA [12,15].

Mice with eNOS gene knockout are hypersensitive and have a higher incidence of bicuspid aortic valves. They exhibit pulmonary hypertension (blood pressure aproximately 15 mmHg higher than controls [17]) with chronic, mild hypoxia, impaired wound repair, deficient growth factor-induced angiogenesis and markedly decreased bleeding times [12].

Features	cNOS	iNOS
Cellular Sources	Endothelial Cells	Macrophages
	Certain Brain Cells	Vascular Smooth Muscle Cells
Activators	Thrombin, ADP Acetylcholine Glutamate Calcium Ionophores Pressure Shear Stress	
Inducers	Physical Exercise	Lipopolysaccharide (LPS) Interferon-α LPS+ interlukin-1 LPS+ tumour necrosis factor α Oxidised low-density Lipoprotein
Amounts Released	Small, pulses	Large, continuous
Calcium Dependence	Yes	No
Molecular Targets	Heme Proteins Soluble guanylate cyclase Thiols	Fe-S proteins Thiols
Proposed Function	Regulation	Host Defense

Table 1.1 Comparison of constitutive NOS and inducible NOS [8].

1.1.5 Biochemistry of NOS

1.1.5.1 Structure of NOS

The catalytically active NOS is a homodimer. The molecular weight of the monomer ranges from 110 KDa to 160 KDa depending on the isoform. Each NOS monomer contains an oxidase domain at its amino-terminal end and a reductase domain at its carboxy-terminal end. The NOS reductase domain contains binding sites for the redox cofactors NADPH, FMN, while the oxidase domain tightly binds BH_4 and a cysteineyl thiolate-ligated heme group which is the reactive centre of the oxidation reaction [7,18]. CaM, which is located between the reductase and oxygenase domains, activates NOS function mainly by influencing the reductase domain **(Fig 1.3)**.

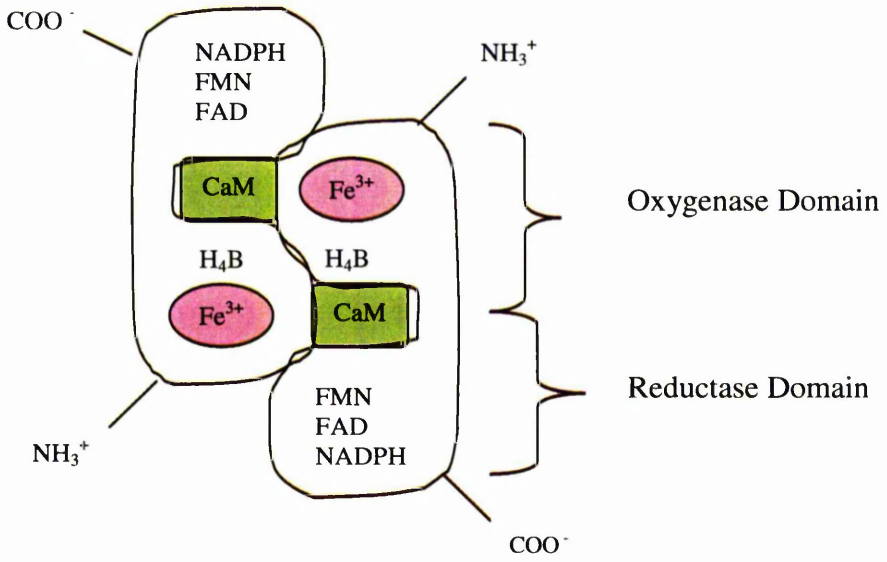

Fig 1.3 Schematic structure of NOS [7].

1.1.5.2 NOS Reaction

NOS catalyses the reaction of L-arginine to citrulline and NO. *N*-hydroxyarginine (NHA) is produced as an intermediate. The N-hydroxylation of L-arginine consumes one equivalent of each of NADPH and O_2 and it is typical of a P_{450} oxygenase reaction. During the reaction, NADPH is oxidised upon binding to NOS and $NADP^+$ is generated [7]. It is important to note that although NADH is similar in structure to NADPH, the former cannot be used in the NOS reaction [7]. In the second step, the heme group activates O_2 by recruiting only one reducing equivalent from NADPH and one from NHA **(Fig 1.4)** [7].

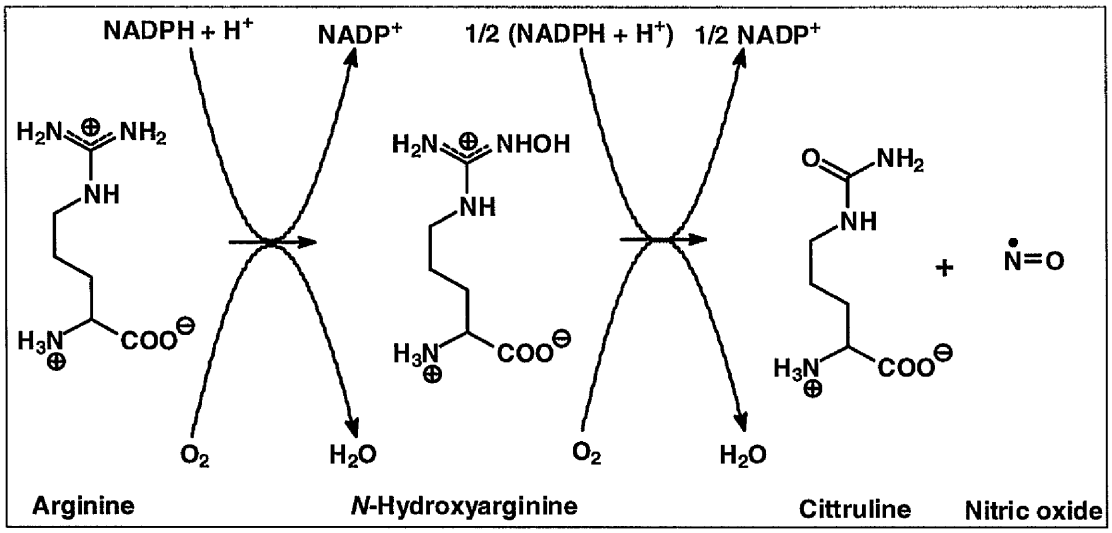

Fig 1.4 The reaction catalysed by Nitric Oxide Synthase [19].

1.1.6 Importance of iNOS over cNOS in Tumour Progression

The iNOS protein is available in very low (undetectable) basal levels in most cell types and its induction by cytokines generates higher NO concentrations for longer periods of time when compared to cNOS expression. Thus, studying the consequences of iNOS over expression would allow a more precise study of the effects of NO on tumour growth. Moreover, iNOS is Ca^{2+}/CaM independent, which means that the Ca^{2+} levels do not need to be controlled for in an experiment. iNOS is also produced by macrophages and plays an important role in the immune response [12,15].

1.1.7 iNOS Expression: Induction and Inhibition

The generation of iNOS is complex and occurs at multiple sites within the signal transduction pathway that lead to iNOS gene expression and includes transcriptional and post-transcriptional mechanisms of modification [13].

The list of iNOS inducers is increasing. The most important of which are cytokines (growth factors, tumour necrosis factor α: TNF-α, interferon-γ:IFNγ or INFγ, interleukin-1-

β: IL1β) and endotoxins (LPS). They induce iNOS at the transcriptional level [2,15]. Studies have also shown that hypoxia up regulates iNOS expression [20].

On the other hand, gluccocorticoids, transforming growth factor-β (TGFβ1), NO itself, Fe^{3+}, ethanol, and interleukin-4 (IL4) act at the transcriptional level to inhibit iNOS expression [15,21].

1.1.8 Inhibition of iNOS Activity

Some drugs like Dexamethasone (a synthetic analogue of hydro-cortisone [22]) appear to suppress iNOS activity post-transcriptionally [23]. Whereas, it is not known whether inhibition of iNOS activity by platelet- derived growth factors, insulin-like growth factor-1, and thrombin occurs during transcription and/ or post-transcription regulation [21,24].

Experimentally, iNOS activity can be inhibited using L-arginine analogues. Examples of such inhibitors include L-NMMA (also known as NMA) (N^G-monomethyl-L-arginine), L-NAME (nitro-L-arginine methyl ester), and L-NNA (N^{ω}-Nitro-L-arginine). This inhibition can be reversed by adding higher amounts of L-arginine [8].

1.2 Tumour Growth: Metastasis, Angiogenesis, and Apoptosis

The level of iNOS expression was observed to be high in urinary bladder cancer [25], colorectal carcinoma [26], breast cancer [27], and melanoma [28] amongst others. So, many studies were performed in order to establish a correlation between iNOS levels and cancer prognosis. In most cases, these experiments failed to find a clear relationship.

iNOS seems to play an important role in metastasis, angiogenesis, and apoptosis. However, the exact role is poorly understood. It seems that iNOS plays a dual role in tumour-growth depending on its level [12].

1.2.1 Metastasis

Metastasis is constituted of a series of events involving first the growth of a primary tumour followed by extensive angiogenesis. Cells with a metastatic phenotype invade the tissue stroma and penetrate the blood vessels to enter the circulation. The majority of these cells are rapidly destroyed but those that survive can be trapped by organ capillary beds and extravasate into the organ parenchyma. The metastatic process is completed upon cellular proliferation and vascularisation of the secondary deposit [29].

In some studies, induction of iNOS leading to high levels of NO has shown a direct correlation with metastasis. For example, upon addition of LPS, increase in growth of experimental lung metastasis and incidence of pleural metastasis was observed in an experimental murine model. The growth was compared to tumours induced with saline as controls and the growth effect was blocked upon the addition of the iNOS inhibitor NMA [30]. In another study, Zhang and Xu (2001) argue that NO should be considered as one of the factors involved in down-regulating the immune response -which is needed for metastasis to occur- as well as accelerating tumour metastasis. This argument was supported by the findings that the iNOS inhibitor L-NNA significantly inhibited lung metastasis of murine metastatic melanoma while L-arginine tended to enhance the metastasis. In addition, the cytotoxicity of the T-cells specific to these lung metastatic cells was significantly reduced when cultured with the metastatic cells themselves, an effect that was reversed in the presence of a selective iNOS inhibitor L-imi-noethyl-lysine [31].

On the other hand, NO appears to inhibit metastasis by causing vasodilation, inhibiting platelet aggregation, and inducing apoptosis [27,32]. In a study by Xie *et al.* (1996), a highly metastatic murine melanoma cell line showed low iNOS levels. When this cell line was transfected with the active iNOS gene, inactive iNOS gene, or control plasmid, only the cells transfected with active iNOS gene showed a high reduction in metastasis

compared to the controls [33]. Wang *et al.* (2001), found that disruption of the IFN-γ gene and a lack of physiologic IFN-γ production led to decreased iNOS expression and increased tumour growth and metastasis. In their study, highly metastatic murine pancreatic adenocarcinoma cells were implanted into IFN-$\gamma^{+/+}$ and IFN-$\gamma^{-/-}$ mice. Although in both cases the tumours grew, the ones implanted in the IFN-$\gamma^{-/-}$ mice developed more aggressively and metastasised more extensively [34].

One of the reasons for the discrepancy in the role of NO on metastasis is thought to be the presence of p53 mutations in some cells. Since p53 calls for apoptosis, these mutations can influence the fate of tumour cells and could indicate resistant to NO. Studies by Shi *et al.* (2000) demonstrated that disruption of host iNOS expression enhanced the growth and metastasis of NO-sensitive tumour cells but suppressed the metastasis of NO-resistant tumour cells, proposing that host-derived NO may differentially modulate tumour progression [35]. It was also observed that highly metastatic murine fibrosarcoma clones exhibited higher levels of iNOS than poorly metastatic cells even when both of these clones contained the same p53 mutation. Over expression of iNOS in the highly metastatic clone by infection with an iNOS retrovirus retarded tumour growth and completely suppressed metastasis. This could indicate the contribution of low iNOS expression to the progression of tumour cells even in the presence of p53 mutations, yet sustained iNOS over expression still suppressed tumour growth and metastasis [36].

1.2.2 Angiogenesis

Angiogenesis is the process of development of new blood vessels from pre-existing ones [37]. This process requires several important steps including matrix dissolution, endothelial cell proliferation, migration, and organisation into tubes, followed by lumen formation [38]. NO seems to play a role in all of these steps [39].

Some studies have shown that NO plays a pro-angiogenesis role whereas others have reported an opposite effect. The main reason for this discrepancy seems to be the varying levels of NO produced such that at high concentrations NO has an anti-tumour effect but at lower concentrations it promotes tumour growth and angiogenesis [40]. For example, iNOS knock-out mice showed delayed wound closure, which was corrected by iNOS transfection [41]. Moreover, when immunostained for iNOS protein expression in squamous cell carcinoma of the larynx, results showed a significant increase in iNOS expression in the transition from hyperplasia/mild dysplasia, to moderate/severe dysplasia, to invasive carcinoma [42]. Increased iNOS expression was also observed in invasive carcinomas of the head and neck region [43]. This suggests that iNOS inhibitors could act as promising anti-angiogenic therapeutic agents in these cases [42].

Jenkins *et al.* (1995) engineered human colon adenocarcinoma cells to generate NO continuously. When grown *in vitro*, these cells grew slower than the wild-type cells, an effect that was reversed upon the addition of the iNOS inhibitor N-imino-ethyl-L-ornithine (L-NIO). However, when the same cells were implanted in nude mice, the tumours grew faster than those derived from the wild-type and were more vascularised suggesting that NO may play a dual role in tumour growth [40].

Vascular endothelial growth factor (VEGF) is a key molecule in angiogenesis and when studying the role of NO on angiogenesis, many reports focus on the relationship between NO and VEGF. For example, upon exposure of choroidal endothelial cells to VEGF for 30 min, a dose dependent rise of NO production was observed in the medium. This effect was inhibited by the NOS inhibitor L-NAME [44]. Harris *et al.* (2002) regulated VEGF expression using the tetracycline inducible system in a breast carcinoma model and found that over expression of VEGF was associated with enhanced NOS activity. Both eNOS and iNOS were elevated suggesting that NOS is tightly regulated by VEGF at least in this tumour

model [45]. On the other hand, some studies focused on the role of NO on VEGF. For example, a study by Jozkowicz *et al.* (2001) revealed that NO derived from NO-donors or from NOS-transfected cells upregulates the synthesis of biologically active VEGF in vascular smooth muscle cells [39]. In the case of transfecting cells with eNOS or iNOS, the upregulated VEGF expression was reversed using L-NAME but not by its inactive enantiomer D-NAME and the addition of L-arginine restored VEGF production. The same authors also observed that cells stably transfected with NOS expressed more VEGF than those transiently transfected. This indicates a positive feedback loop between NO and VEGF [39]. On the other hand Tsurumi *et al.* (1997), used NO donors and found that NO seemed to down regulate VEGF by inhibiting its promoter [46].

To summarise, the effect of NO on angiogenesis remains unclear. iNOS induction can inhibit angiogenesis by inhibiting the proliferation of endothelial cells and vascular smooth muscle cells. NO may also be involved in the suppression of angiogenesis-related gene expression. NO suppresses both constitutive and hypoxia-induced platelet-derived growth factor expression at the level of transcription [27,47]. In contrast, sustained production of low levels of NO in solid tumours can promote tumour growth by enhancing vascular permeability, increasing blood flow, and increasing vascularisation (by stimulating endothelial cell growth and migration). Moreover, low levels of endogenous and exogenous NO can also serve as intracellular second messengers to induce interleukin-8 (IL-8) gene expression, an indirect angiogenesis factor [26].

1.2.3 Apoptosis

Apoptosis or programmed cell death occurs in response to several stimuli mainly to save the cells from replicating when mutations have occurred in the DNA. The pathway by which NO induces apoptosis is not clearly understood. NO might directly damage DNA [48] and inhibit protein and nucleic acid synthesis through modification of rate-limiting enzymes

[49]. Induction of apoptosis could also be due to inhibition of the tricarboxylic acid cycle and a subsequent drop in ATP production [50]. Moreover, NO induces abnormal intracellular Ca^{2+} mobilisation from mitochondria [51]. The decrease in intracellular pH and the redistribution of Ca^{2+} have been shown to trigger apoptosis [52]. Moreover, intracellular and extracellular acidification may lead to regeneration of NO from nitrite, thereby sustaining its cytotoxic activity [33,53]. It was also observed that NO-mediated down regulation of Bcl-2 may contribute to NO- mediated apoptosis [27].

Some studies have observed a relationship between iNOS expression and apoptosis. For example, iNOS was found to be expressed in human pancreatic cancer and its presence positively correlated with apoptosis. When measured by TUNEL staining, the apoptotic indices were significantly higher in positive iNOS expressers than negative expressers [54]. Cytokines-induced iNOS also showed a positive correlation with the degree of apoptotic cell death in ovarian cancer. In this case, the cells were treated with IFN-γ, IL-1β, and TNF-α and apoptosis was measured by gel electrophoresis and propidium iodide (PI) staining followed by flow cytometry analysis to monitor DNA fragmentation which is characteristic of apoptosis [55].

To the contrary, Xu *et al.* (2002) noticed that human colon cancer and human ovarian cancer tumours grown in nude mice formed significantly smaller tumours in the presence of NO-generating microencapsulated cells compared to control tumours. These microencapsulates are iNOS expressing cells entrapped in a semi-permeable alginate-poly-L-lysine membrane that is used as a delivery vehicle to tumour sites in mice. The tumours were injected subcutaneously along the microencapsulated cells. NO generation resulted in 54 % reduction in colon tumour volume 28 days after implantation and 100 % reduction in ovarian tumour volume 30 days after implantation at an estimated NOS activity of 223 $\pm$ 56 pmol/min/mg (measured 10 days postimplantation). It is noteworthy to mention that these

microencapsulated cells were expressing iNOS using the ecdysone system and were induced with Pon A at 10 mg/mouse for 14 days followed by 2 mg/mouse/week. Similar experiments were repeated *in vitro* whereby the NO generating cells were co-cultured with the other cell lines. In this case, iNOS expression was controlled using the tetracycline system (tet-On). More than 80 % cell death was observed using trypan blue staining in the induced co-culture while 15 % was observed in the uninduced and 30 % in the induced co-culture but in the presence of an iNOS inhibitor. Moreover, the induced colorectal coculture showed 45 % apoptosis when TUNEL stained. When implanted in vivo, 86 % reduction in the colorectal tumour volume was observed 30 days post implantation. In this case, the microencapsulated cells were induced by 0.5 mg/ml doxycycline in drinking water which was replaced 2 or 3 times a week [56].

A key regulator of apoptosis is the tumour suppressor gene p53. It is thought that 50 % of the tumours have a mutated or deleted p53 gene [5]. Recent studies have focused on the role of NO on p53 in an attempt to explain the dual role that NO plays in tumour growth. In normal cells, p53 levels are extremely low as a result of its rapid proteolytic degradation. However, DNA damage causes p53 stabilisation and accumulation. Then, p53 targets genes that affect cell cycle arrest and induce apoptosis [5]. To maintain somatic cell genomic integrity, the initial cellular response to NO-mediated DNA damage is p53 activation resulting in apoptosis [57-59]. In turn, p53 accumulation down regulates iNOS expression by binding to the iNOS promoter thus limiting the extent of NO-mediated damage. These cells are known as NO-sensitive [5]. Therefore, wild-type p53 protein expression in numerous tumours was associated with decreased iNOS expression [60,61]. However, when high levels of NO are present, and due to the continuous expression of p53, mutations in this gene may occur leading to its inactivation. Therefore, following p53 inactivation, the NO-p53 negative feedback loop fails and p53 mutated cells continue to produce high levels of NO unchecked.

These cells now become NO-resistant [5,61]. It is even thought that irrespective of the mechanisms contributing to NO resistance, NO resistance may lead to NO dependence [35]. Therefore, chronic induction of NO can be carcinogenic, partly because it causes p53 inactivation and thus NO-resistant cells may emerge during clonal evolution of tumours and these cells may eventually become NO-dependent [5,37]. For example, iNOS expression is positively associated with p53 mutation in tumours of the colon, lung, and oropharynx [37].

NO may interact with other molecules to promote tumour growth. It has been documented that NO activates cyclo-oxygenase-2 (COX-2), and the activation of (COX-2) confers NO resistance [5]. For example, when an NO-sensitive macrophage cell line was transfected with a COX-2 vector [62] or pre-treated with small amounts of NO to produce COX-2 [63], the cells became resistant to high doses of NO [5,37]. It has also been observed that over expression of COX-2 alters cell adhesion and protects cells against apoptosis by increasing the Bcl-2 protein production [64,65]. On the other hand, it was shown that NO could induce apoptosis by up-regulating the expression of Fas or Fas L proteins [56,66,67].

1.2.4 Conclusion

Whether iNOS has a pro- or anti- tumour effect could be due to many factors. The level of iNOS produced by tumours is of key importance. It has been demonstrated that overproduction of endogenous NO is auto-cytotoxic through the induction of apoptosis and suppression of tumour growth and metastasis, whereas low NO production may protect tumour cells from apoptosis and promote tumour growth [35,36]. Moreover, cells containing a mutated p53 tumour suppressor gene fail to decrease the levels of NO produced, a process that normally occurs via a p53-NO negative feedback loop. These cells are also unable to undergo apoptosis and might consequently become NO dependent and survive under high NO levels [60]. On the other hand, experimental conditions that exist *in vitro* might not exist *in vivo* and *visa versa*. For example, cytokine treatment *in vitro* could lead to high NO levels

as the experiment is performed in a contained flask and such a condition does not exist *in vivo*. So, it is possible that the levels induced, presumably by cytokines *in vivo*, may be very low and non-toxic and even facilitate survival and metastasis of tumour cells [36]. It is currently thought that the concentration of NO in human tumours (as opposed to murine macrophages that produce high iNOS levels) is at least one or two orders of magnitude lower than that required for anti-tumour effects to occur, with the levels formed being responsible for pro-tumour effects [68].

Other factors for such discrepancy include the use of different techniques to evaluate NOS expression [27,35], the use of different cell lines [35,36], different tumour types [27,35] and the varying cancer stage [11]. It is also noteworthy to mention that some clinical experiments have a small sample size which could misrepresent the true situation [26].

1.3 Resistance of Hypoxic Tumours to Therapy

1.3.1 Hypoxia

In addition to its dual role in tumour growth, iNOS is up-regulated under hypoxic conditions [20], has the ability to reduce some bioreductive drugs [69], and radiosensitise hypoxic cells [70].

1.3.1.1 Defining Hypoxia

Aggressive tumours often have reduced blood supply. This is due to their fast growth and thus their blood supply becomes insufficient. In addition, the newly formed blood vessels are disorganised which results in nutrient depletion, acidosis, and reduced oxygen tension and/ or hypoxia [71]. There are two types of hypoxia: chronic hypoxia which results from the tumour cells being further from the blood vessels than the normal diffusion distance of oxygen (about 100 μm [72]) and acute hypoxia that is caused by temporary stopping of blood flow through a particular blood vessel. It is noteworthy to mention that normal tissues typically have median oxygen concentrations in the range of 40-60 mmHg, whereas half of

all solid tumours have median values of less than 10 mmHg with fewer than 10 % in the normal range [72].

Hypoxic tumours are known to be resistant to radiotherapy and chemotherapy. Resistance to radiotherapy is explained by the fact that oxygen molecules react rapidly with the free-radical damage produced by ionising radiation in DNA, thereby "fixing", or making permanent, the DNA damage that leads to cell death. Hypoxic cells are furthest away from functioning blood vessels and cells at low oxygen levels divide much slower than those that are well oxygenated. This may result in chemoresistance especially since most anti-cancer drugs are only effective against rapidly proliferating cells and that these drugs need to reach the cells via blood vessels [72].

1.3.1.2 Hypoxia Inducible Factor

Hypoxia-inducible factor 1 (HIF-1) is a transcription factor that functions as a master regulator of oxygen homeostasis [73]. It is expressed in most cancers in response to hypoxia and it activates the transcription of genes whose protein products either increase O_2 delivery (example: erythropoetin, gene encoding VEGF) or provide metabolic adaptation under conditions of reduced O_2 availability [74]. HIF-1 is a heterodimeric protein consisting of HIF-1α and HIF-1β (also known as aryl-hydrocarbon nuclear translocator protein: ARNT) subunits. Both subunits contain amino-terminal-basis-helix-loop-helix-PAS (bHLH-PAS) that are required for dimerisation and DNA binding [74].

Immunocytochemical studies have showed that HIF-1α is over-expressed in most common human cancers in response to physiologic (hypoxia) and non-physiologic (genetic alteration) stimuli. For example, HIF-1α over-expression was detected in more than 90 % of colon, lung, and prostate cancers analysed, whereas no expression was detected in the corresponding normal tissue [74].

While the expression of HIF-1β is oxygen–independent, HIF-1α stability is tightly regulated by cellular oxygen tension. So, under hypoxic conditions, HIF-1α is stabilised and consequently binds to HIF-1β. The half-life of HIF-1α in post-hypoxic cells was found to be less than 5 minutes. In the presence of O_2, HIF-1α is subject to ubiquitination and proteosomal degradation which are blocked in hypoxic conditions [74].

1.3.1.3 Mechanism of HIF-1 Stabilisation

In the presence of oxygen, Pro402 and Pro564 in HIF-1α are hydroxylated by prolyl hydroxylases. This step is essential for the binding of the von Hippel-Lindau (VHL) tumour suppressor gene, which recruits an E3 ubiquitin-protein ligase that targets HIF-1α for proteasomal degradation. Under hypoxic conditions, oxygen becomes a rate-limiting factor for prolyl hydroxylation and consequently HIF-1α becomes stable. VHL also recruits histone deacetylases (HDAC) and factor inhibiting HIF-1 (FIH-1) that are required for transcriptional repression. In addition, oxygen-dependent hydroxylation of Asn803 in HIF-1α blocks its interaction with p300, a key co-activator that is needed for transcriptional activation [73,75] **(Fig 1.5)**.

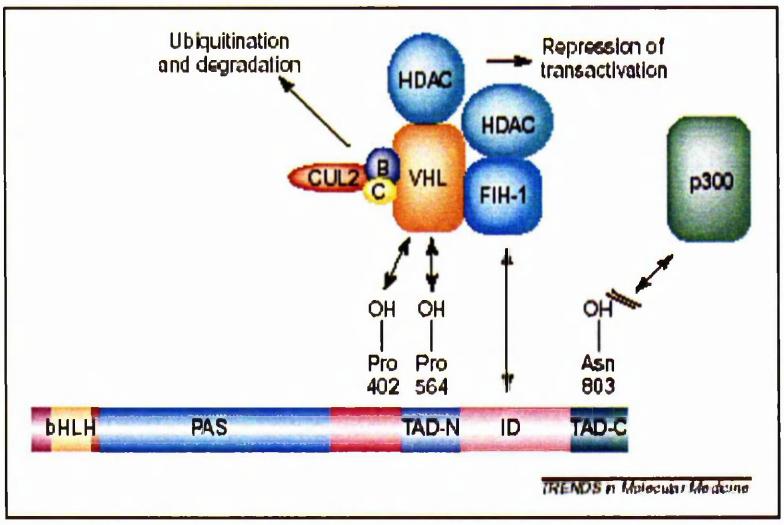

Fig 1.5 Regulation of HIF-1α protein expression and transcriptional activity by oxygen-dependent post-translational modifications (bHLH: basic helix-loop-helix, PAS: PAS domain, TAD-N: amino-terminal transactivation domain, ID: inhibitory domain, TAD-C carboxyl-terminal transactivation domain, Pro: proline, Asn: asparagine, p300: protein 300 FIH: factor inhibiting HIF-1, HDAC: histone deacetylases, VHL: von Hippel-Lindau, CUL2: cullin 2) [75].

1.3.1.4 Hypoxia Regulates iNOS Gene Expression

Hypoxia regulates the expression of several genes and this is mainly caused by the interaction of HIF-1 with its DNA recognition site known as the hypoxia responsive element (HRE) [71]. The expression of iNOS is thought to increase under hypoxic conditions as studies performed on the iNOS gene discovered an HRE site in its promoter [20]. It was found that hypoxic conditions in combination with INF-γ stimulate iNOS transcription and mRNA expression in murine macrophages [20]. This observation was further explained to be due to the physical interaction of two molecules HIF-1 and IRF (INF regulatory factor that is activated by INF-γ). These studies show that HIF-1 interacts with the HRE site present in the iNOS 5' regulatory region and that IRF-1 interacts with the HIF-1/HRE nucleoprotein complex thus inducing iNOS expression in macrophages [76]. On the other hand, although iNOS expression increases under hypoxic conditions and INF-γ, NO synthesis is markedly

reduced in activated macrophages in proportion to oxygen tension such that at 1 % oxygen tension, NO accumulation is reduced by 80-90 % [77].

However, other researchers found that HIF-1 alone can stimulate iNOS expression in pulmonary artery endothelial cells after exposure to hypoxic conditions. This increase in expression occurred as early as 24 h after hypoxia. Moreover, when a promoterless vector was used as a control, iNOS expression did not increase indicating once again the presence of an HIF-1 binding site in the iNOS promoter [78]. On the contrary, iNOS expression in rat aortic smooth muscle cells did not respond to hypoxia in the same manner as the endothelial cells. The discrepancy obtained with different cell lines indicates that other cell type-specific transcription factors may mediate the response to hypoxia [78].

1.3.1.5 HIF-1 Inhibition

As HIF-1 was observed to play a major role in regulating tumour growth, it has been targeted for anti-cancer therapeutic design [79]. For example, embryonic stem cells that are HIF-1α deficient (-/-) grew much slower than the wild-type cells (HIF-1α +/+) when implanted in nude mice [80]. Studies using tumour implants of the mouse hepatoma cell lines that were deficient in HIF-1β showed an 80 % reduction in ATP compared to the wild-type indicating that the low expression of the gene responsible for HIF-1β disrupts ATP synthesis probably by preventing the synthesis of adequate amounts of a crucial intermediate like glycine. The inability of these HIF-1β deficient tumours to up regulate the expression of glycolytic enzymes and glucose transporters could reduce the production of purine moieties needed for ATP production and thus contribute to the slower growth rate of these tumours compared to wild-type tumours [81].

Researchers are currently trying to inhibit HIF-1 using different approaches. Some methods include the use of anti-sense HIF-1 [82], HIF-1 dominant negative constructs [83],

RNAi technology [84], or small molecules that act by inhibiting the HIF-1 transcriptional activation pathway [85,86].

1.3.1.6 Regulation of HIF-1 by NO

In order to study the role of NO on HIF-1, different approaches were used. These include NO donors that produce NO chemically and exogenously, and cytokines and stable clones that express high levels of iNOS endogenously.

1.3.1.6.1 NO Stabilises HIF-1

In one study, Sandau *et al.* (2001) explain that lower NO concentrations induce a faster but transient HIF-1α accumulation compared to higher doses of the same NO donor. In their study, they have used the NO donor S-Nitrosoglutathione (GSNO) and observed that 100 μM elicited a rapid but transient accumulation of HIF-1α whereas 1 mM evoked a delayed HIF-1α accumulation when measured using western blot analysis even though the higher GSNO concentration resulted in higher NO production. These experiments were conducted under aerobic conditions. This study also explains that irrespective of the concentration of GSNO being used, the amount of HIF-1α protein being expressed appeared to be equal, although the time point of maximal expression varied significantly. Moreover, their experiments show that the NO triggered HIF-1α stabilisation is cGMP independent. Sandau *et al.* (2001) explain their observation to be due to the existence of two different transduction pathways [87,88]. On the other hand, under hypoxic conditions HIF-1α regulation was concentration and time dependent such that inhibition was only achieved at low concentrations of GSNO (100 μM). This was explained to be due to moderate stress that induces degradation by proteasomal system whereas enhanced stress may inhibit the 26S proteasome [87,88].

In another study, Metzen *et al.* (2003) used a hypoxia-inducible luciferase reporter gene and obtained a 2 fold luciferase induction when HEK 293 cells were induced with 1

mM GSNO in air. This induction was similar to that obtained with the cells induced with 1 % hypoxia or with cobalt chloride ($CoCl_2$) only suggesting that this HIF-1 was transcriptionally active. Further experiments showed that GSNO did not have any effect on the transcription and translation of HIF-1α. However, HIF-1α ubiquitination seemed to be dramatically down regulated. Moreover, the VHL-HIF-1α interaction that normally occurs under normoxic conditions seemed to be decreased in the presence of GSNO, hypoxia, or $CoCl_2$. This effect was explained to be either the result of a chemical modification of the oxygen-dependent degradation domain ODD and/or pVHL by GSNO or the result of attenuated prolyl hydroxylation of the ODD, which is required for pVHL binding. Further experimentation revealed that GSNO inhibited prolyl hydroxylase (PHD) domains PHD1, PHD2, and PHD3 as well as FIH-1 thus explaining the accumulation of HIF-1α [89].

In another study by Kimura *et al.* (2002), the effect of a variety of NO donors was studied. SNAP, GSNO, and NOC 18 activated a VEGF promoter in a dose-dependent manner under normoxic conditions and the effect was attenuated by an NO scavenger carboxyl-PTIO. These NO donors also induced HIF-1α accumulation and HIF-1 DNA binding activity suggesting that NO up-regulates the VEGF gene transcription by enhancing HIF-1 activity. On the other hand, NOR 4 enhanced the VEGF promoter activity under normoxic and hypoxic conditions, but this effect was not eliminated by carboxyl-PTIO which could be due to the lipophilic nature of NOR 4 allowing it to penetrate the cell membrane and the hydrophilic nature of carboxyl-PTIO making the latter unable to scavenge all the NO produced by NOR 4. Moreover, NOR 4 did not provoke HIF-1α accumulation. Another NO donor, SIN-1 had a positive effect on the VEGF promoter at high concentration under normoxic conditions and its effect was attenuated by carboxyl-PTIO. However, it showed no effect on hypoxic activation and did not enhance HIF-1 binding activity and HIF-1 accumulation. This could be due to the peroxynitrite by-product that may have a different

effect from NO on VEGF and HIF-1 activity. To the contrary, SNP showed an inhibitory effect on VEGF expression under hypoxic conditions only. However, this NO donor seems to be far from ideal as it produces ferrocyanide and ferricyanide and the latter has an inhibitory effect on the VEGF promoter activity [90]. This shows that different NO donors have different effects on HIF-1 regulation and also emphasises the need to precisely control for the concentration of the NO donor, the time needed to examine any effect, and the redox state of the experimental environment.

Other studies performed to understand the effect of NO donors (SNAP and NOC 5) on the VEGF promoter explain that the VEGF gene transcription is activated by NO as well as by hypoxia via the HIF-1 binding site and an adjacent sequence within the HRE of this gene in glioblastoma and hepatoma cells. However, it was also observed that optimal concentrations of these NO donors required for VEGF reporter gene expression under normoxic conditions cause an inhibitory effect on the gene expression under hypoxic conditions. This could be due to the production of higher NO concentration by the NO donors under hypoxic conditions than under normoxic conditions, and that exposure to excessive amounts of NO could be toxic [91].

Moreover, when iNOS was over expressed in tubular LLC-PK_1 cells producing 2 μM nitrite, HIF-1α stabilisation was observed [87]. Even when macrophages were activated using cytokines and then co-cultured with tubular LLC-PK_1 cells, HIF-1α accumulation was observed [87].

1.3.1.6.2 NO Inhibits HIF-1 Stabilisation

Some researchers studying the effect of NO on HIF-1 regulation observed a completely different result. For example, Yin *et al.* (2000) used the NO donor SNP to inhibit the luciferase activity driven by a VEGF promoter in a dose dependent manner. This inhibition was only observed under hypoxic conditions. However, SNP releases by-products

that can have their own effects on HIF-1 but so does GSNO that produces the oxidised glutathione GSSG upon NO release and a high concentration of the latter alone is a prominent source of oxidative stress [92].

Sogawa *et al.* (1998) observed an inhibition of activity again by hypoxia inducible luciferase reporter assay in Hep3B cells in the presence of any of the NO donors SNP, GSNO, or SIN-1. This inhibition was once again observed more dramatically under hypoxic conditions and barely observed under normoxic conditions. Sogawa *et al.* (1998) further explain this inhibition to be due to blocking the DNA binding activity of HIF-1. This is in accordance with the hypothesis that an oxygen sensing heme protein exists and is localised in the cell membrane. As NO binds to heme with a higher affinity than O_2, the binding of NO to the sensor would cause a conformational change that shuts down signal transduction even under hypoxic conditions [93].

Huang *et al.* (1999) observed the same inhibitory effect of SNP on HIF-1 and have again explained their observation to be to due to the ability of NO to bind to a heme protein in the oxygen sensor. Further experimentation showed that NO triggers destabilisation of HIF-1α via the ODD domain (but not through S-nitrosylation of the cysteine residue present in this domain) as well as via inhibiting the C-terminus activation domain [94].

Yin *et al.* (2000) showed that iNOS expression inhibits HIF-1 activity under hypoxic conditions in C6 glioma cells. They have transiently transfected the cells with the iNOS gene and a VEGF promoter-driven luciferase gene. The inhibition was partially reversed upon the addition of the antioxidant NAC possibly because NAC increases total intracellular glutathione concentrations with a lowered GSH/GSSG ratio to favour the formation of GSNO and prevent direct NO contact with HIF-1α or because NAC has shown to stabilise the HIF-1α protein under hypoxic conditions thereby facilitating the HIF-1 DNA-binding activity by an increased GSH/GSSG [92].

In a further study using stable clones that finely regulate iNOS expression using the tetracycline system, it was demonstrated that depending on its concentration NO has two opposite and independent effects. At low concentrations (<400 nM), NO inhibits HIF-1α accumulation under hypoxic conditions, an effect that is mitochondria-dependent possibly through inhibition of cytochrome c. However, at higher concentrations (>1 μM), NO stabilises HIF-1α in a mitochondria-independent manner [95,96].

1.3.2 Bioreductive Drugs

As previously described, hypoxic cells appear to be resistant to chemotherapy. This is because hypoxic cells are furthest away from functioning blood vessels and also because cells at low oxygen levels divide much slower than those that are well oxygenated, whereas most anti-cancer drugs are only effective against rapidly proliferating cells and that these drugs need to reach the cells through blood vessels [72]. However, hypoxia could be exploited in chemotherapy as it constitutes a major difference between tumour and normal tissue. Therefore, by designing a drug that is selectively toxic to hypoxic cells, toxicity to normal cells should be avoided.

Examples of these drugs include Mitomycin C, a quinone antibiotic that was introduced into clinical use in 1958 and has demonstrated activity against a number of tumours in combination with other chemotherapeutic drugs and radiation. This drug preferentially kills hypoxic cells compared to normoxic cells [72]. 1,4-Bis-[[2-(dimethylamino-N-oxide)ethyl]amino]5,8-dihydroxyanthrace ne-9, 10-dione (AQ4N), a di-*N*-oxide analogue of mitoxantherone, is another drug that selectively acts on hypoxic cells. Under reduced oxygen levels, AQ4N is converted to AQN that has high affinity to DNA and inhibits the enzyme topoisomerase II [72]. Another more promising drug, which is currently in Phase II and Phase III clinical trial, is tirapazamine (TPZ, SR 4233, WIN 59075, 3-amino-1,2,4-benzotriazone-1,4-dioxide, Tirazone ^{TM}) [97,98]. TPZ is a substrate for many reductase

enzymes that can add a single electron to the molecule, thereby producing a free radical intermediate. In the presence of oxygen, this free radical is rapidly oxidised back to the parent molecule with the formation of a superoxide radical; however, in the absence of oxygen, this does not occur and the highly reactive TPZ radical removes hydrogen from nearby macromolecules causing them structural damage [99]. If the nearby molecule is DNA, then the TPZ radical produces both single- and double-stranded DNA damage to chromosome aberrations and consequently cell death [69,72,100] **(Fig 1.6)**. Over expression of an enzyme under hypoxic conditions could facilitate the conversion of a non-toxic pro-drug into a toxic drug specially that this environment exhibits reduced oxygen tension [72].

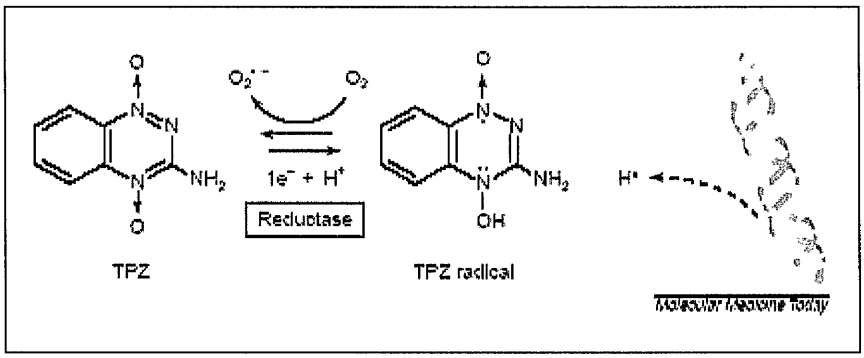

Fig 1.6 The metabolism of tirapazamine (TPZ) to its active free-radical moiety causing preferential toxicity to hypoxic cells by damaging the DNA double helix [72].

Previous studies have shown that P_{450} reductase is the major microsomal enzyme responsible for the reduction of TPZ to the radical intermediate [97,98,101,102]. As studies have revealed that the reductase monomer of iNOS shares a high degree of sequence homology with cytochrome P_{450} reductase [7,19,69], the ability of NOS to reduce tirapazamine amongst other compounds under hypoxic conditions was studied [69,97].

Garner *et al.* (1999) used the three NOS isoforms in their study and found that iNOS could reduce bioreductive drugs and had the highest affinity for tirapazamine. They also explain that all NOS isoforms may have a greater affinity for the drug than P_{450} reductase [69]. Chinje *et al.* (2003) have shown that an increase in cytosolic iNOS activity in a series of

transfected human breast carcinoma clones was associated with an increase in TPZ metabolism under hypoxic conditions and that there was no similar increase under aerobic conditions [97]. It has also been shown that in some cancers, NOS levels are elevated (unlike P_{450} reductase) and that NOS has an HRE site in its promoter and it might be highly expressed under hypoxic conditions. Moreover, there is a possibility that TPZ may inhibit NO formation *in vivo*, which could lead to reduction in tumour blood flow. This means that TPZ might potentiate its own toxicity by increasing the degree of hypoxia in tumours [69].

1.3.3 Radiation

Hypoxic cells have poor oxygen tension and thus are resistant to radiotherapy. This is because oxygen molecules are needed to react with free radicals produced by ionising radiation in order to cause perminant DNA damage and thus induce apoptosis [72]. Scientists are trying to overcome this drawback by finding hypoxic radiosensitisers. Recently, it has been found that NO effectively radiosensitises hypoxic mammalian cells with a substance enhancement ratio (SER) of 2.4. This indicates that NO is as effective as oxygen at enhancing the sensitivity of hypoxic cells to radiation [11].

For example, when authentic NO gas was used to treat hypoxic chinese hamster lung cells, results showed that NO was almost equally effective as oxygen [70,103,104]. Some NO donors were also used and gave similar results [103,105,106]. Moreover, when iNOS expression was induced by IFN-γ in hypoxic EMT-6 tumour cells, it was found that NO was the effector molecule responsible for radiosensitisation at a sensitivity that was almost similar to aerobic cells and counteracted using iNOS inhibitors [107]. In another study, murine tumours were transiently transfected to express iNOS encoded by either a constitutive promoter (CMV) or a radiation induced promoter (WAF1). In both cases, the results showed that iNOS delivered to cells *in vitro* and *in vivo* could generate sufficient NO to cause cytotoxicity and radiosensitisation to hypoxic cells [103,108].

The mechanism by which NO radiosensitises hypoxic cells is thought to be similar to that of oxygen. In the presence of ionising radiation, carbon-centered radicals are initially generated. In the absence of NO or O_2, these reactive radicals react with nearby protein hydrogen atoms which facilitates DNA repair. However, when it is present, NO might be reacting with the reactive C-radicals causing them to become incapable of reacting with the hydrogen-atoms. This increases radiation mediated cell-death [11]. Hirakawa *et al.* (2002) showed that a single 2-Gy dose in the presence of L-arginine induces iNOS expression and hence NO production in bovine aortic endothelial cells. When these cells were co-cultured with hepatoma cells, apoptosis was induced in the hepatoma cells. This effect was later inhibited by the addition of the iNOS inhibitor L-NAME. This indicates that iNOS expression could be induced by irradiation in the endothelial cells, an effect that could be beneficial to induce apoptosis in adjacent cells [109].

NO has an advantage over oxygen because it can penetrate farther into the tissue due to its higher diffusion coefficient even under lower concentrations than those of oxygen [11]. In addition, NO was found to cause vasodilation under certain iNOS levels. This could help in oxygenating hypoxic regions and therefore increase radiosensitisation. Yet, one disadvantage for NO radiosensitisation could be that NO reduces systemic blood pressure [11].

1.4 Importance of Studying the Role of iNOS in Cancer Gene Therapy

The role of iNOS in cancer therapy was evaluated in this study. iNOS was chosen over cNOS as it produces higher levels of NO when induced in the body and plays a major role in the immune system by targeting pathogens [12]. iNOS expression has also been correlated with many cancers including urinary bladder cancer [25] and breast cancer [27]. Although its role remains poorly understood, NO seems to have a dual effect on tumour growth. For example, low NO levels have shown pro-angiogenic and metastatic effects while

the opposite has been reported with higher concentrations. Moreover, NO appears to play an important role in apoptosis by controlling the p53 tumour suppressor gene. Lower levels of NO prduction induce p53 stabilisation, which commands the cells to undergo apoptosis as well as control the NO levels in a negative feedback loop. However, continuous NO production stabilises p53 for long periods of time and consequently increases the risk of mutations in this tumour suppressor gene. In the presence of a muated p53, the cells fail to undergo apoptosis and the level of NO remains uncontrolled for. These cells eventually become NO dependent and proliferate initiating tumour growth [59,60].

On the other hand, iNOS contains an HRE binding site in its promoter and is upregulated under hypoxic conditions [20]. NO seems to have a feedback effect on HIF but recent studies report conflicting results. Moreover, NOS shares high sequence homology to P_{450} reductase, which reduces the bioreductive drug TPZ [69]. iNOS was observed to have higher affinity to this drug than the cNOS or P_{450} reductase [69]. It was also reported that NO can radiosensitise hypoxic cells with an SER similar to O_2 [11]. Since iNOS is naturally upregulated under hypoxic conditions were TPZ can be reduced to produce a toxic species and since the cells surviving in this environment are resistant to chemo- and radio- therapy, studying the role of iNOS seems particularly interesting.

The work undertaken in this project aims to up regulate the level of iNOS in the cells in a gene therapy approach. This method was preferred over NO donors because the latter are chemical compounds that produce exogenous NO as well as other by-products. Since these by-products have their own biological effects, it would be difficult to confirm whether the obtained results are due to NO itself or the by-products. Moreover, these chemicals have extremely short lives (few hours) and are produced exogenously. In addition, the use of these compounds in the clinic has not as yet been reported possibly because of their chemical nature. On the other hand, NO donors produce NO directly without the production of NOS

and hence the role of iNOS as a bioreductive enzyme, for example, cannot be studied in this case. Therefore, these compounds appear to be far from ideal.

To the contrary, up regulating the levels of iNOS using a gene therapy approach allows for endogenous long-term expression of this gene. This method, however, has some disadvantages including triggering an immune response and the ability of some genes to integrate themselves in the host chromosomes. If the gene inserts itself adjacent to sequences that happen to code for tumour suppressor genes or oncogenes, loss of function of these crucial genes may occur. However, gene therapy has proven successful in some diseases like thalassaemia and cystic fibrosis. Gene expression can be driven using either a constitutive or an inducible promoter. This work utilises the latter approach to generate stable clones as clones that constitutivly over express iNOS are difficult to culture because the high levels of NO produced cause cell death. Different clones should also be generated in order to allow a range of iNOS activity, which might result in clonal variation. On the other hand, when an inducible system is used, gene expression is only switched on in the presence of an inducer in a dose dependent manner. This system should control for the toxicity of continous production of toxic genes like iNOS. Inducible systems may present a disadvantage when continuous expression is desired but become beneficial in case the disease is cured and gene expression is no longer required. In this study, the ecdysone system was chosen primarily because the inducer has not been reported to have any endogenous effects on NOS. Finally, adenoviruses, which have been previously used in the clinic, were chosen as a delivery vehicle of the iNOS gene in this study as they are able to transport the gene of interest into the nuclei but without integrating the DNA in the host genome.

1.5 Inducible Expression Systems

The need to study and precisely control the expression of many genes gave rise to the development of several inducible expression systems. To be beneficial, these systems must fulfil certain requirements including specificity whereby the system must be indifferent to endogenous factors and only activated by exogenous nontoxic drugs. The system should also insure non-interference with cellular pathway. High inducibility is needed: in the inactive state basal levels should be minimal, while in the active state, high levels of gene expression should be generated. The inducer must be bioavailable and should rapidly penetrate all tissues and cross the blood-brain barrier. A good system must insure reversibility such that when the inducer is cleared from all tissues, the system rapidly goes back to the inactive state. Finally, the system should be dose-dependent such that gene expression is proportional to the concentration of the inducer [110].

1.5.1 The Ecdysone System

The ecdysone system is a novel expression system discovered from the molting and metamorphosis of *Drosophila melanogaster* whereby a cascade of morphological changes is triggered by the steroid hormone 20-OH ecdysone. Induction using the ecdysone system requires the co-transfection of cells with two vectors: a receptor vector (pVgRXR) and a response vector (pIND SP1) [111].

1.5.1.1 Receptor Vector (pVgRXR)

The ecdysone vector pVgRXR encodes for a heterodimer consisting of the functional ecdysone receptor (EcR) and the product of the Ultraspirical gene (USP). USP was replaced by its mammalian homologue retinoid X receptor (RXR) and (EcR) was fused to the activation domain of VP16 (herpes simplex virus promoter) in order to increase induction levels (**Fig 1.7**). Even though EcR is not activated by mammalian hormones, some

modification in its DNA binding domain (DBD) was performed to avoid any potential interference with mammalian endogenous factors [110,112,113].

The final structure of the receptor is as shown in **Fig 1.7** below:

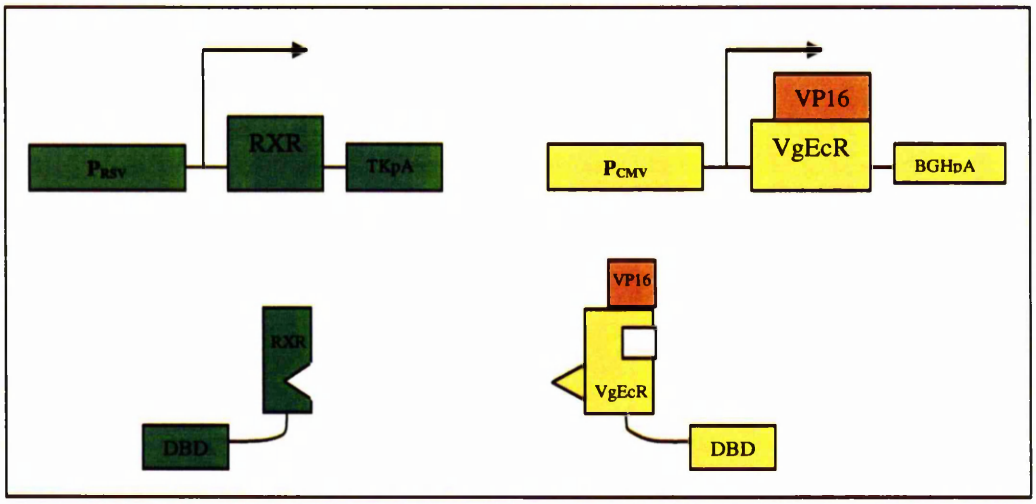

Fig 1.7 The ecdysone receptor pVgRXR is comprised of VgEcR and RXR. Each cassette has its own promoter (CMV or RSV) and poly A tail (BGH or TK) [111].

1.5.1.2 Response Vector (pIND SP1)

The actual ecdysone response element in the pINDSP1 vector is (E/GRE) and is situated directly upstream of the minimal heat shock promoter (PΔHSP). In order to reduce any possible interaction with any endogenous mammalian receptor, the natural ecdysone response element has been modified. It is now a hybrid consisting of one-half site from the natural ecdysone response element (5'AGTGCA 3') (EcRE) and one half-site from the glucocorticoid response element (5' AGAACA 3') (GRE); hence the name E/GRE [111,114].

To increase induction, five repeats of the (E/GRE) binding sites were engineered into the pIND SP1 vector. Also, 3 cis-acting elements (SP1) were inserted in order to increase absolute expression levels up to 5-fold **(Fig 1.8)**. The SP1 elements enhance expression at the level of transcription by interacting with SP1 transcription factors that are endogenous to mammalian cells. However, SP1 increases both induction as well as basal expression levels

[111]. Moreover, pIND SP1 has a multiple cloning site so that the gene of interest (in this case iNOS or *Lac* Z can be inserted).

Thus, the final structure of the response element is as presented in **Fig 1.8** below:

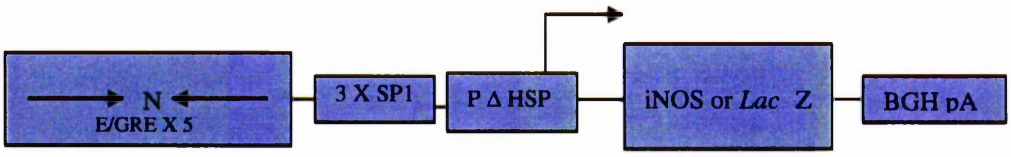

Fig 1.8 The pIND SP1 is made up of a modified ecdysone response element, SP1 sites that increase gene expression, a minimal heat shock promoter (PΔ HSP), as well as a multiple cloning site that allows the insertion of the gene of interest (N is a single base pair that separates the hybrid response elements).

1.5.1.3 Induction of Gene Expression

Finally, gene expression is induced once the steroid ecdysone (or its analogues: mainly muresterone A and Pon A) is introduced. The steroid binds to VgEcR so that it heterodimerises with RXR. The heterodimer receptor then binds to E/GRE in the response vector and this drives gene expression [113] **(Fig 1.9)**.

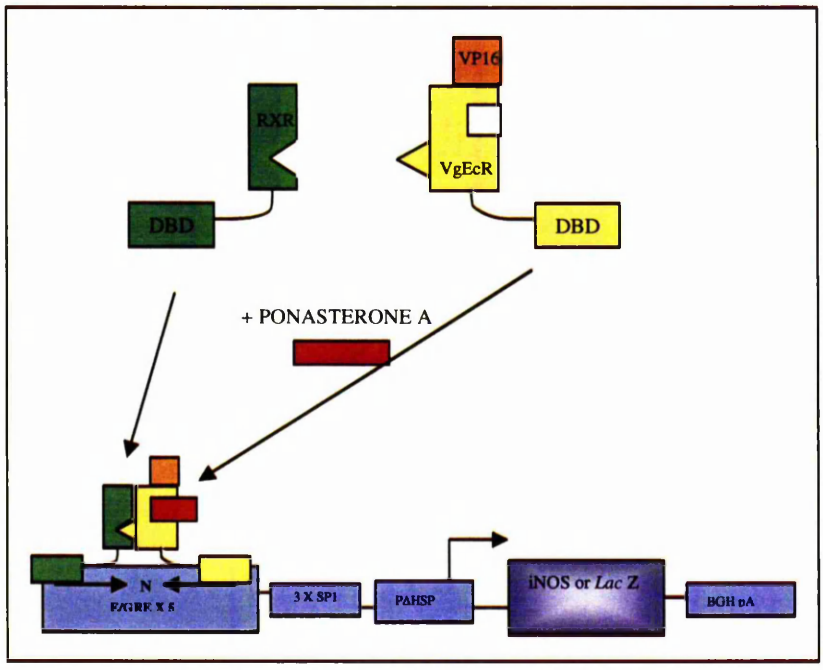

Fig 1.9 Upon addition of the inducer (Pon A), the 2 subunits of the ecdysone receptor bind together and then attach to the ecdsyone reporter. This drives gene expression [113].

1.5.2 Ligands Used in the Ecdysone System

The ligands used in the ecdysone system are mostly steroid in nature and therefore can penetrate all tissues and are quickly metabolised and cleared. Many ecdysone analogues were discovered but not all of them exhibited high induction ability. These include muresterone A, Pon A, ponasterone C, 20-hydroxyecdysone, inokosterone, makisterone amongst others. Studies showed that muresterone A and Pon A are the best inducers [112].

Muresterone A was isolated in 1970 from the seeds of a rare plant of Kaladana (*Ipomoea calonycto*) but because of the difficulty to find this plant and because muresterone A stocks were rapidly depleting, ponasterone A was found as an alternative [112].

Pon A -as well as other steroids- are found in common plants and are secreted as a self-protection mechanism against insect larvae that eat the leaves. These steroids mimic the action of endogenous insect hormone and bring about abnormal molting and premature demise. Surprisingly, these defensive steroids can represent over 1 % of total plant dry weight [112]. Saez *et al.* (2000) showed that Pon A and muresterone A are the best inducers with lowest basal activity. This property could be due to the absence of the hydroxy group at C-25 position [112] **(Fig 1.10)**. It is noteworthy to mention that Pon A has now commercially replaced muresterone A.

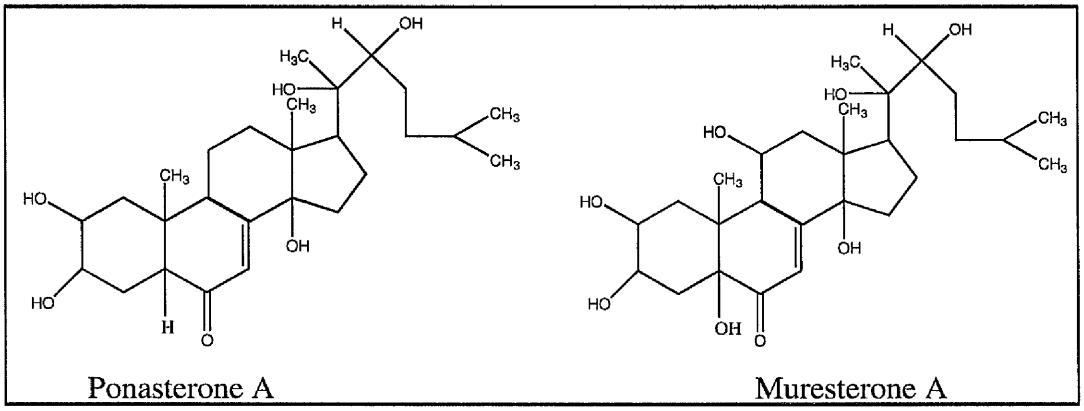

Fig 1.10 Structures of Pon A and muresterone A [112].

1.5.3 Ponasterone A

Pon A can be purified from the leaves of many plants including the *Podocarpacea* family- a widespread conifer species. *In vitro*, Pon A has been found to cause detectable induction within 4 h with a magnitude of induction reaching 250-400 fold within 14 h and continues to increase before stabilising at approximately 600 fold induction between 24 and 36 h [112]. It was also reported that even when exposed to high Pon A levels, once the inducer is removed, gene expression goes back to basal levels within 20 h **(Fig 1.11)** [112].

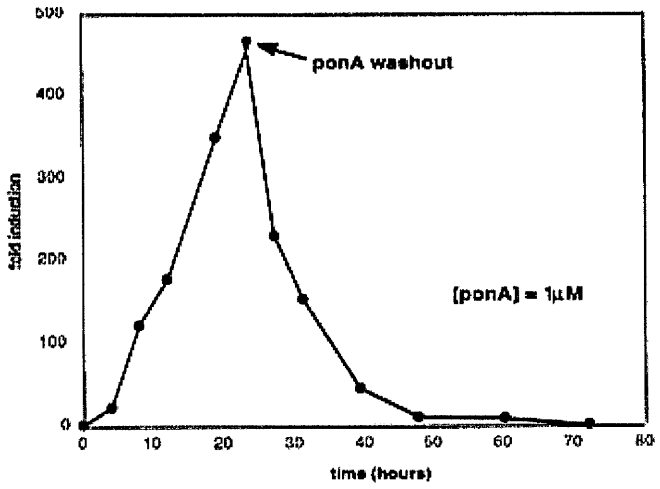

Fig 1.11 *In vitro* characterisation of Ponasterone A. Kinetics of induction and shutoff of the ecdysone system with 1 µM Ponasterone A as the inducer [112].

The *in vivo* studies showed easily detectable induction levels of luciferase gene expression 4-6 h after treatment, peaking at 9-12 h, and dropping significantly by 24 h and returning toward basal levels by 48 h. The level of induction reached 20-200 fold depending on the amount of Pon A used (3,5,10 mg/mouse) [112].

1.5.4 Advantages and Disadvantages of the Ecdysone System

Various studies have accounted for the tight regulation, dose responsiveness, and favourable uptake and clearance kinetics of the steroid inducer, which results in rapid gene switching [112]. Moreover, the non-mammalian origin of the system reduces the risk of

endogenous interference *in vivo*. Moreover, as mentioned earlier, the steroid nature of the inducer allows it to penetrate in all tissues including the blood-brain barrier [112].

However, Constantino *et al.* (2001) describe that muresterone A and Pon A have unexpected effects on cytokine signaling in hematopoietic mammalian cells. They showed that these 2 ecdysone analogues potentiate interleukin-3 (IL-3) dependent activation of the PI3-kinase/Akt pathway in the pro-B cell line (Ba/F3) which could ultimately affect the growth and survival of these cells [115]. If this reported observation is to be further validated by other scientists, it could indicate that these analogues might also indirectly induce iNOS by potentiating IL-3. However, other scientists continue to use the ecdysone system even when interleukins are vital for the mechanisms that they are studying [116-118]. In addition, some authors are cautious to use the ecdysone system in some organs of the body that are hormone- regulated (example: breast cells) because of the steroidal nature of the inducer [119].

1.5.5 Examples of the Use of the Ecdysone System

The ecdysone system has been used to study the role of a number of genes. When the Luciferase reporter gene was utilised, a dose response relationship was observed 24 h after Pon A induction (100 nM-10 μM) with inductions reaching 42-fold with 1 μM and 54-fold with 6 μM Pon A [120]. Other studies have used this system to obtain a therapeutic benefit like down regulating cyclin D_1(CD1) to understand its role in the cell cycle. A colon cancer cell line was stably transfected with the ecdysone inducible antisense CD1 and found that induction of cyclin D1 antisense mRNA by 1 μM Pon A resulted in a 55 % decrease in CD1 mRNA and 58 % decrease in CD1 protein levels 4 h post induction [120].

In another experiment and to study mammary gland tumourigenesis, a transgenic mouse model was developed whereby spatial and temporal specific mammary gland transgene expression was regulated by Pon A. This was performed by crossing mice bearing

the ecdysone response elements with mice bearing the ecdysone reporter elements. Gene expression was induced in the transgenic mice using Pon A pellets. In this case, gene expression was observed within 24 h and sustained using the implanted Pon A pellets. As a control, the expression of the *Lac* Z reporter gene was measured and found to be undetectable in the absence of Pon A and uniformly expressed in the mammary gland in the presence of 750 μg/mouse Pon A. There was almost no expression in other organs [121].

To study the role of BRCA1 in breast tumourigenesis, a human emberyonal kidney epithelial cell line was stably transfected by the ecdysone cassettes. This cell line was chosen particularly to evaluate the effect of BRCA1 in cells with modest endogenous levels of BRCA1 expression. Western blot results indicated 2-4 fold induction in protein levels 12 h after administration of 10 μM Pon A [122]. In addition, when the role of MAD2 expression in the mitotic checkpoint control was studied using the ecdysone system in ovarian cancer cell lines, 2-4 fold increase in MAD2 levels were observed after inducing with 5 μM Pon A for 20 h [123]. Moreover, using a *Drosophila melanogaster* cell line, a dose response relationship was observed in response to increasing Pon A dose (0.5 nM-5 μM) as well as increasing the time of exposure to Pon A (0-72 h) [124].

On the other hand, Xu *et al.* (2002) studied the role of iNOS on apoptosis *in vivo.* Human foetal kidney stable clones expressing iNOS in the ecdysone system were established and implanted in the mice. They acted as microencapsulated cells entrapped in a semi-permeable alginate-poly-L-lysine membrane, which is used as a delivery vehicle to tumour sites in mice. A dose of 10 mg/mouse Pon A was used to drive iNOS gene expression and resulted in an estimated NOS activity of 223 ± 56 pmol/min/mg (measured 10 days post implantation). Apoptosis in the cells injected alongside the microencapsulated Pon A-induced iNOS cells was monitored. This result was reproduced using the tetracycline system. When evaluated *in vitro*, a dose response relationship was also observed upon induction of

the ecdysone inducible iNOS gene. An iNOS activity of 6 ± 2 and 33 ± 4 pmol/min/mg was observed using 1 or 10 μM Pon A respectively. This induction was completely inhibited using the iNOS inhibitor L-NIO (20 μM) [56].

Moreover, the ecdysone system has proved useful in many different studies including those performed on apoptosis [125,126], cancer and cell cycle regulation [116,127], embryonic development [128], signal transduction [129,130], lipid metabolism [131], and neuronal function [112,132,133].

1.5.6 Other Inducible Systems

1.5.6.1 The Tetracycline Inducible System

The tetracycline inducible system is made up of the *tet* transactivator protein (tTA) which is a chimeric protein containing the VP16 activation domain fused to the *tet* repressor (*tet*R) of *Escherichia coli* [134]. In the absence of tetracycline (tet) or its derivative doxycyclin, tTA binds to the *tet* resistance operator (*tet*O) while in the presence of tetracycline, a conformational change in the repressor prevents tTA from binding to *tet*O. This is known as the Tet-Off system [135-137]. This system has been used *in vitro* and *in vivo*.

The major disadvantage of this system is the fact that tet must be present to repress gene expression, and tTA protein is toxic to mammalian cells [138]. To eliminate the need of tet, an auto regulatory system was designed by inserting multiple *tet*O sequences within tTA promoter [139]. This alteration causes constitutive expression of tTA in the absence of tet [135,136,140].

In order to eliminate the need of continuous availability of doxycycline to drive gene expression, a reverse transactivator (rtTA) was introduced. rtTA binds *tet*O in the presence of doxycycline. Thus, gene expression is induced by treatment with doxycycline and not in its absence. This system is known as Tet-On [134,138,141] (**Fig 1.12**). A disadvantage for

this is that long-term antibiotic treatment has major side effects *in vivo* and there is slow antibiotic clearance in the bone and liver of transgenic animals [135,137]. High basal levels have also been reported in some experiments [142,143].

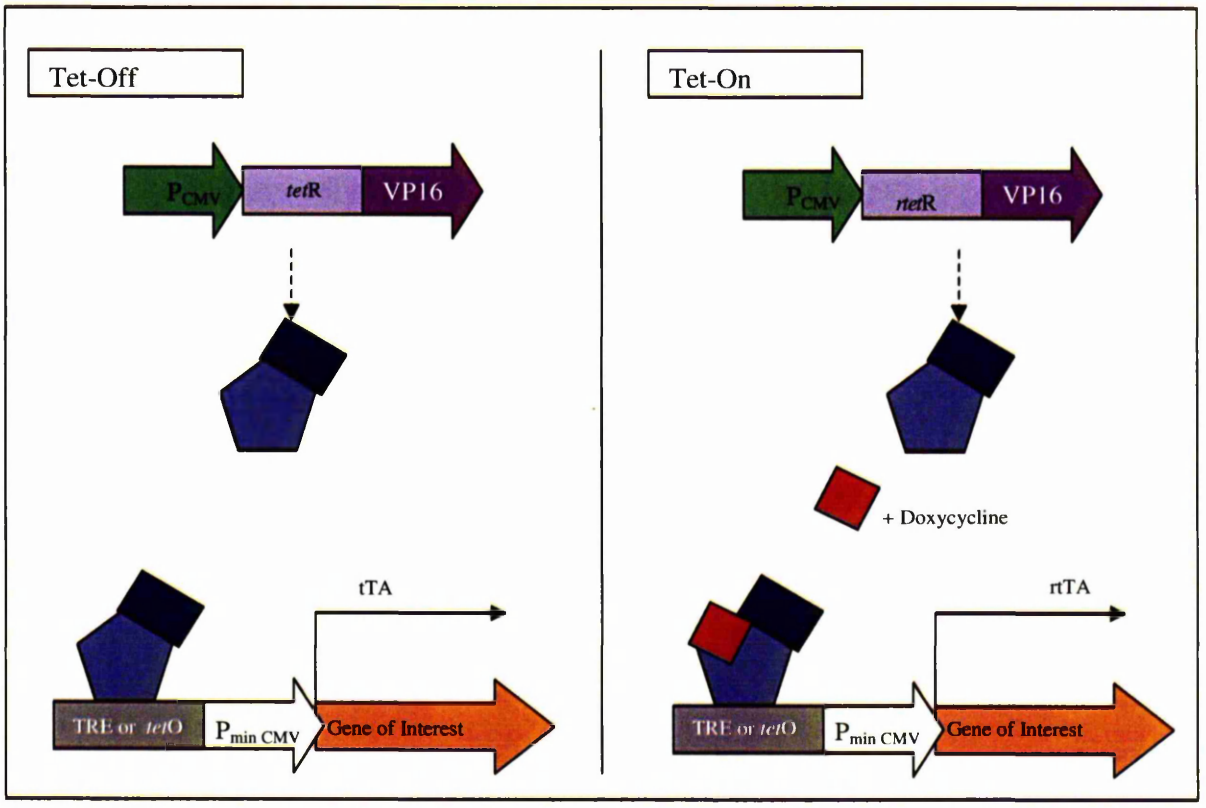

Fig 1.12 Gene expression using the tetracycline system. Addition of doxycycline is needed to drive gene expression in the tet-On but not in the tet-Off system (modified from [144]).

1.5.6.2 CID-based Regulatory System (Rapamycin-inducible System or Dimeriser System)

This system uses chimeric inducers of dimerisation (CIDS) to regulate gene expression. The system is based on the ability of rapamycin to induce dimerisation of two cellular proteins, FKB12 and FRAP. A DNA binding domain (ZFHD1) that binds to a novel DNA response element and is not recognised by any endogenous transcription factors was fused to FKBP12 [135,136,140].

The activation domain of p65 was added to FRAP to be able to activate target gene expression. Therefore, in response to rapamycin, FKBP12 and FRAP dimerise, and activate transcription of a down stream target gene **(Fig 1.13)**.

A disadvantage of this system is that rapamycin is involved in many signaling pathways and thus can induce other possible side effects in eukaryotic cells [135,136,140].

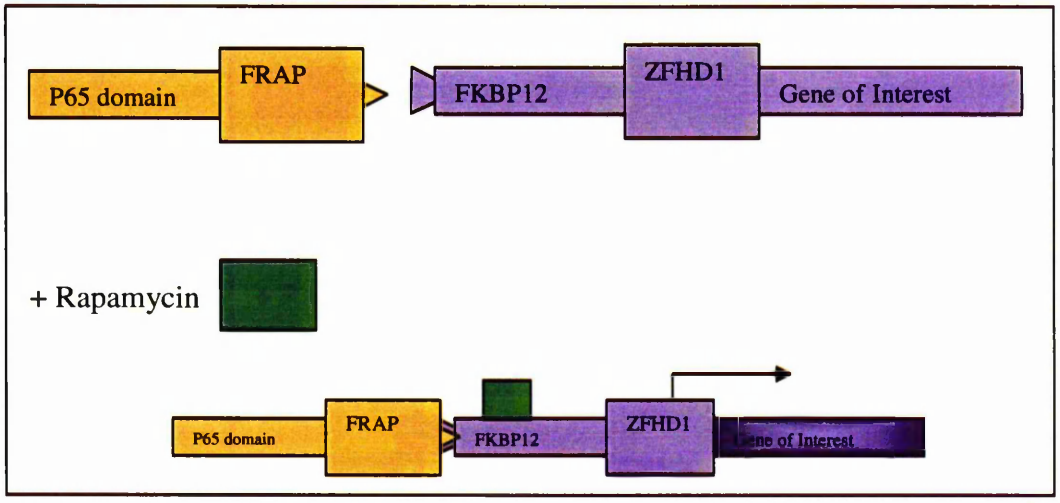

Fig 1.13 Induction of gene expression using the CID based regulatory system. In the presence of rapamycin, FRAP amd FKBP12 dimerise in order to drive gene expression.

1.5.6.3 Estrogen-based Inducible Systems

This system is based on a chimeric molecule containing the estrogen receptor, the yeast GAL 4 DNA binding domain and the VP16 activation domain. In response to estrogen, the chimeric molecule dimerises, binds to GAL 4- responsive promoters and leads to activation of target gene expression **(Fig 1.14)** [135,136].

A 100-fold induction has been achieved with this system *in vitro*. However, endogenous estrogen may activate basal transgene expression resulting in leaky expression [135,136]. Moreover, it is not ideal to control iNOS expression using this system as estrgen is known to regulate endogenous iNOS [145].

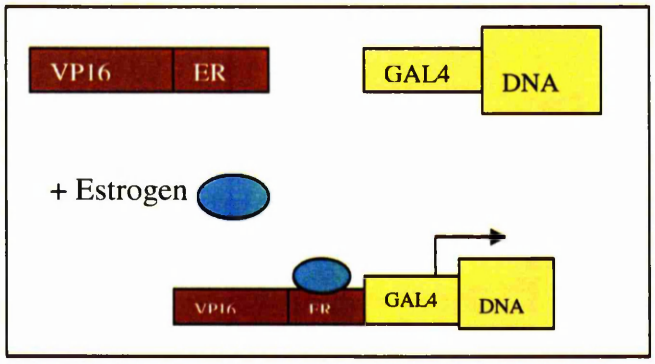

Fig 1.14 Upon estrogen administration, ER and GAL4 bind in order to drive gene expression.

1.5.6.4 Progesterone-based Inducible Systems

This system uses a chimeric regulator GLVP which is a hybrid protein consisting of the GAL 4 DNA binding domain, VP16, and a truncated form of the human progesterone receptor that retains the ability to bind the ligand. When a progesterone antagonist, RU486 is added, GLVP forms a functional dimer that binds to promoters containing GAL 4 up stream activator sequences and activates gene transcription [135,136] (**Fig 1.15**).

A possible disadvantage of this system could be the generation of immune response because of the yeast origin of GAL 4 DNA binding domain [135,136]. Again, it is not ideal to use this system to regulate iNOS expression as progesterone can interact with NO [146].

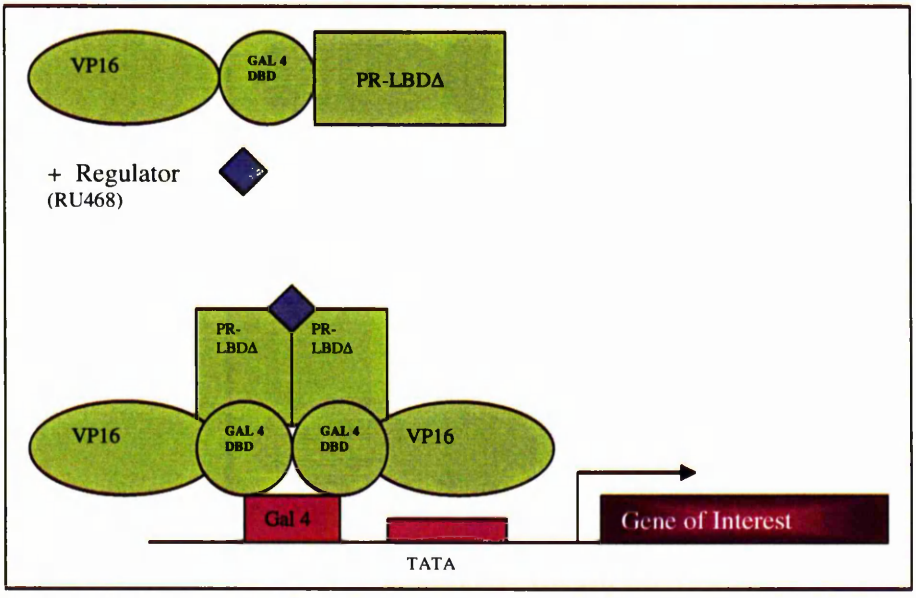

Fig 1.15 Induction of gene expression using the progesterone-based inducible system [135].

1.5.6.5 IPTG-based Regulatory Systems

This system is based on the bacterial lactose repressor protein (*lac*R). *lac*R binds to a specific DNA element, the *lac* operator (*lac*O) in the presence of isopropyl-β-D-thiogalactoside (IPTG). To be used for regulation of eukaryotic genes, the *lac* operon was inserted up stream of a TATA box. *lac*R was also modified by excision of its repressor function and fusion of the active domain of the herpes simplex virus protein VP16 to the IPTG- and DNA- binding site for *lac*R. Thus creating a *lac*I activator protein (LAP) that can drive the expression of *lac*O- bearing genes. Administration of IPTG causes the chimeric regulator to bind to *lac*O and activate the TATA box coupled reporter gene **(Fig 1.16)**.

Very high induction levels (up to 1200 fold induction within 24 h) can be achieved; however, IPTG is toxic to mammalian cells thus limiting the scope of application of this system [135,136].

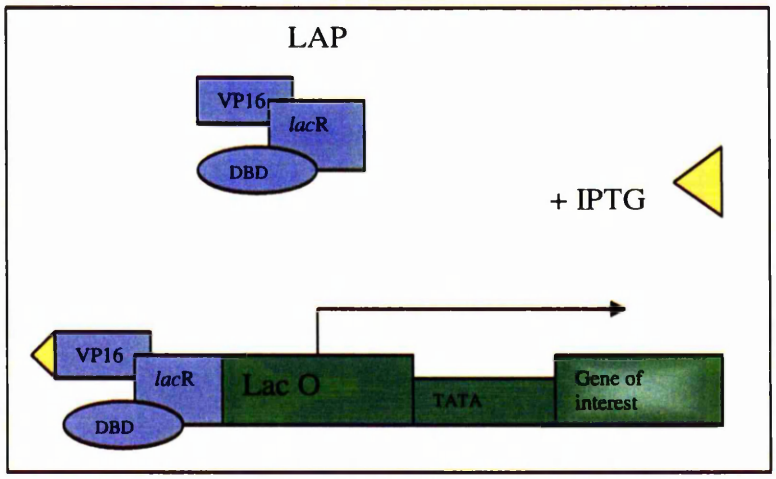

Fig 1.16 Induction of gene expression using the IPTG based regulatory system.

1.5.6.6 Cumate System

The Cumate inducible system (Q-mate™) is based on the *cym* operon that in *Pseudomonas putida* F1 regulates the expression of genes intervening the transformation of p-cymene into p-cumate. A *cmt* operon is located downstream from the *cym* operon and controls the further degradation of the cumate molecule. The *cymR* gene located up stream of

the *cym* operon encodes a repressor molecule CymR, which monitors the expression of the *cym* and *cmt* operons. CymR is induced by p-cumate [147,148] **(Fig 1.17)**.

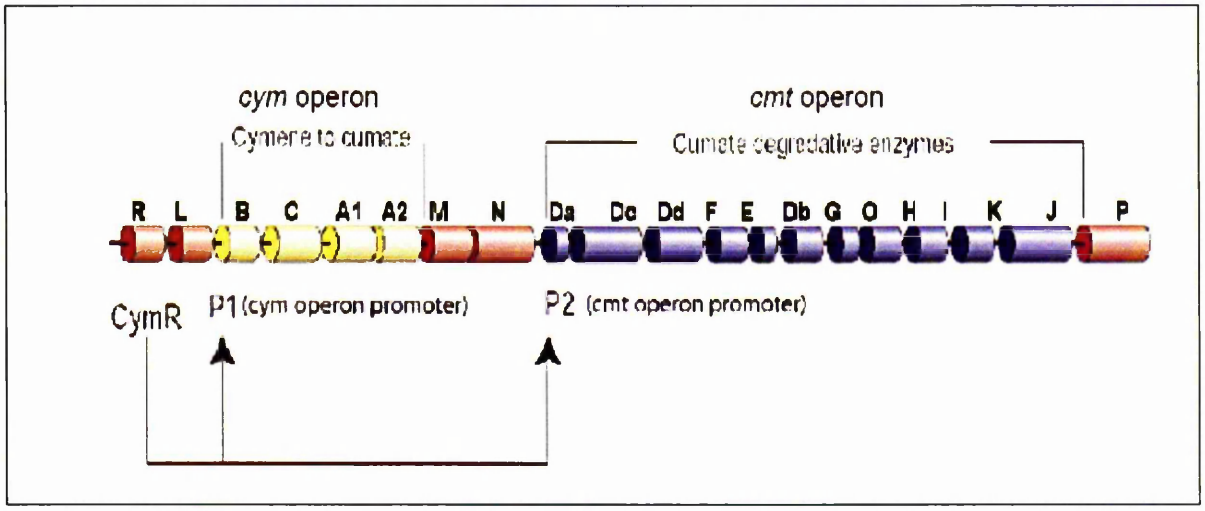

Fig 1.17 Regulation of the degradation of cymene by the repressor CymR mediated by the cym and cymt operons [147].

Normally, the cumate repressor CymR is bound to the operator site and represses gene expression. Only in the presence of cumate will CymR bind to this inducer (cumate) and undergo a conformational change making it unable to bind to the operator site. Hence, gene expression is driven in the presence of cumate [147] **(Fig 1.18)**.

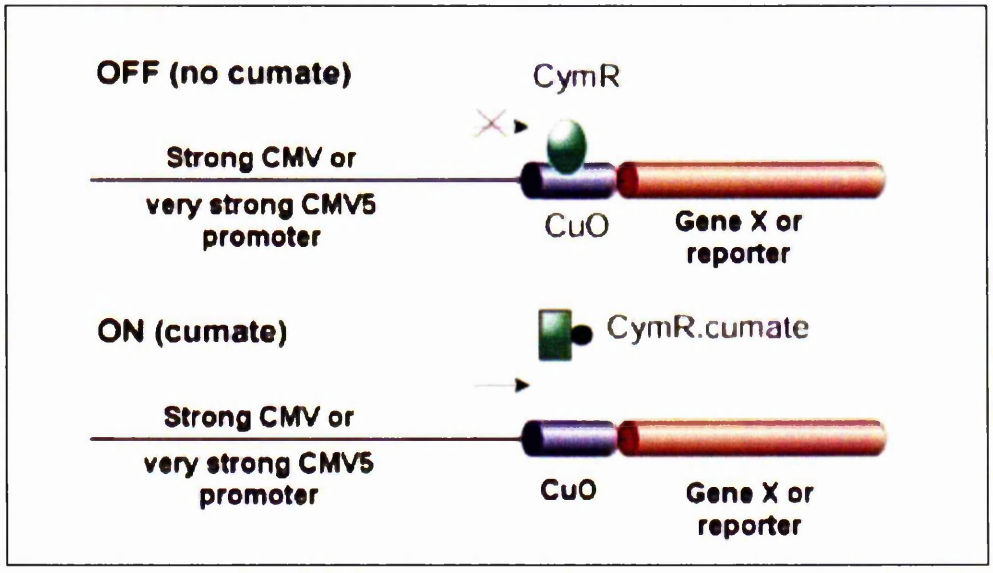

Fig 1.18 Components of the Cumate System. In the presence of the inducer, CymR binds to cumate instead of the operator site and gene expression is driven [147].

This system promises tight gene regulation and dose dependent expression in response to cumate [147]. However, little research has been conducted using this system to date.

1.5.7 Comparative Studies Using Several Inducible Systems

A study using glioma cells compared three inducible systems: tetracycline (tet-off), dimeriser, and the ecdysone system. Cells were transiently transfected with the *Lac* Z reporter gene and it was found that the ecdysone system had the highest induction activity followed by tet-off and dimeriser systems [149]. On the other hand, Xiao *et al.* (2003) observed only a moderate 15 fold induction of the *Lac* Z reporter gene when measured 24 h after addition of 24 μM Pon A. However, it is noteworthy to mention that in this case, the CMV promoter was replaced with a tissue specific promoter, which may have implications on the reduction of both basal and induction levels [150]. Moreover, when the cassettes of the tetracycline, ecdysone, antiprogestin, and dimeriser-based systems were expressed using adenoviruses in order to compare these systems using several parameters, the dimeriser system proved to be the best. However, the nearly undetectable basal level was the advantage of the ecdysone system allowing its use to study the gene function and therapy of toxic proteins where leakiness should be avoided. On the other hand, insensitivity to its inducer and relatively low induced expression seemed to be the drawbacks of this system in this study [151].

1.6 Gene Therapy Vectors

1.6.1 Viral Vectors

1.6.1.1 Adenoviruses

Adenoviruses are non-enveloped double-stranded DNA viruses (**Fig 1.19**), which are usually associated with mild human infections including those of the respiratory tract [152]. They deliver target genes to a wide variety of cell types, including dividing and non-dividing

cells, with high efficiency and minimum toxicity [140,152]. Adenoviruses do not provoke insertional mutagenesis because they do not integrate their DNA into the cellular chromosome. However, the disadvantage of adenoviruses is the inflammatory immune response that they cause in response to the production of their continuous viral proteins even in the absence of the disease causing genes [153].

The adenovirus genome is 36 Kb in length. It has inverted terminal repeat (ITR) sequences at both ends, and the gene transcripts can be divided into 2 phases of gene expression: early genes (E) and late genes (L) expressed before or after the onset of viral DNA replication respectively [152].

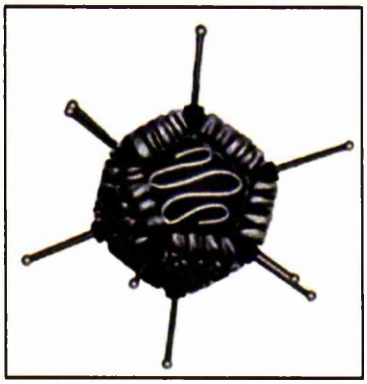

Fig 1.19 Adenoviruses have non-enveloped double stranded DNA.

1.6.1.2 Replication-deficient Ad-based Vectors (rAds)

First generation recombinant adenoviruses (rAds) are mainly based on the human adenovirus serotypes 2 and 5. The E1 gene region has been deleted so that the virus becomes replication defective and to allow insertion of the gene of interest. In some cases, the E3 gene region is also deleted to allow insertion of a larger gene of interest. The size of inserted DNA into rAds can be a total of 7-8 Kb only [140]. Because these adenoviruses have lost the E1 gene and thus can no longer replicate, they must be propagated in a cell line that stably expresses the E1 region [152].

The disadvantages of these rAds are the immune response and limited capacity for foreign DNA. Because of an immune response being generated *in vivo*, rAds have been shown to be relatively short in the periphery being optimal at 3-4 days and disappearing around 1-2 weeks [152].

Less immunogenic second generation rAds have been developed whereby they are deficient in E2, E3, or E4 gene regions. These rAds can be propagated on *trans*-complementary cell lines [152]. However, the small size of insert remains a disadvantage [140].

"Gutless" vectors are another type of rAds whereby all viral genes have been deleted. Their genome contains only the inverted terminal repeats (ITR) and packaging signal of the wild-type virus. Thus, they can theoretically accommodate a 35 Kb DNA insert [152]. In order to be propagated, the gutless vector needs a helper virus to provide, in *trans*, all the genes needed for virion assembly [152]. Gutless adenoviruses give more prolonged gene expression than first generation adenoviruses [152]. However, it is difficult to produce high titres of gutless adenovirus and preparations are often contaminated with the helper virus.

Examples on the use of rAds in gene therapy include the promising clinical trials currently being performed on the administration of adenoviruses encoding for the herpes simplex virus-1-thymidine kinase (HSV-1-TK) expression followed by administration of ganciclover for the treatment of brain tumours [154-157]. Moreover, currently at phase I clinical trials is the TNFerade viral vector. TNFerade is a replication deficient adenovirus that encodes for TNF-α under the control of a radiation inducible -Egr-1 promoter. After treatment with an external beam of radiation, TNF-α is expressed. This expression system aims at using the beneficial effects of TNF-α only. Preliminary data indicate that 43-70 % of patients showed positive response to this treatment but it is unknown how much of a positive

response would have been achieved with radiation alone. Side effects include fever, pain at the injection site, and chills [158,159].

1.6.1.3 Adeno-associated Vectors (AAV)

In humans, AAV are not associated with any disease. The structure of AAV is simple, made up of a short linear, single-stranded DNA composed of 2 open reading frames (ORFs), rep (regulation) and cap (structure), and 2 small (145 bp) inverted terminal repeats (ITR). The ITRs are responsible for the encapsidation and stable integration of the viral genome into a special locus on human chromosome 19. AAV infect both dividing and non-dividing cells. However, AAV also need the presence of a helper virus (example: adenovirus or Herpes simplex virus) in order to replicate and the insert gene is limited to 4-5 Kb in size [152,153].

1.6.1.4 Herpes Simplex Virus Vectors (HSV)

HSV-1 is an enveloped, double-stranded DNA virus with a 152 Kb genome encoding more than 80 genes [160]. HSV-1 has a wide host range and can express genes for a significant period of time. Its large genome allows the cloning of more than one therapeutic gene in the same virus [153]. There are two types of HSV vectors: recombinant HSV vectors and amplicon vectors. Recombinant HSV vectors are generated by the insertion of transcription units directly into the HSV genome through homologous recombination events. Amplicon vectors are based on plasmids bearing the transcription unit of choice, an origin of replication, and a packaging signal. The plasmid is transfected into a cell line, which is also infected with a helper virus. The latter provides replication and packaging function in *trans*, enabling the amplicon to be packaged into infectious HSV-1 virions [160].

1.6.1.5 Vaccina Virus

The vaccina virus is a smallpox virus used for immunisation. It is a large virus that can infect a variety of hosts. This virus, however, can only be used to treat patients who were

not vaccinated against smallpox or have a compromised immune system. Little research has focused on using this virus [153].

1.6.1.6 Retroviruses

The first developed recombinant viral vector for gene delivery was the retrovirus [161]. Retroviruses are enveloped single stranded-RNA viruses [152]. Many retroviral vectors have been engineered from the mouse leukaemia virus and the adult T-leukaemia virus. In order to be beneficial, the genetic material needed for viral production should be removed. These include the genes necessary for viral replication, encapsulation, infection, and reverse transcription. Instead, a packaging cell line provides those genes in order to produce replication deficient viruses. The disadvantage of retroviruses is their ability of infecting only dividing cells but lentiviruses -which are retroviruses- are currently being engineered from the human immunodeficiency virus such that they do not require dividing cells for infection [152,153,162]. Moreover, their ability to randomly integrate their DNA into the host chromosome might disturb the cell cycle regulation [153] or cause oncogene activation or tumour-suppressor gene inactivation [152]. However, retroviruses have high transfection efficiency [153].

1.6.2 Non-viral Vectors

The non-viral vectors use physical methods for gene transfer. Although they do not cause an immune response like viral vectors, but they are more difficult in the targeting of specific cells and tissues [153]. Non-viral vectors include: naked DNA whereby gene length is not a limitation, lipid or liposome (fatty acids) coating of the DNA, electroporation technique which is based on DNA transfer using high electric voltage, ballistic DNA injection whereby plasmid DNA is coated by tungsten or gold and transferred using a gene gun; however, this method causes a large amount of cell damage. All of these methods aim at

protecting the DNA from degradation by the endosome, the cell, and the nuclear membranes before reaching the nucleus [153].

1.6.3 Examples on the Use of Adenoviruses Encoding for the iNOS Gene

The iNOS gene has been inserted in adenoviruses and has been successfully used in a variety of *in vivo* experiments. For example, Kibbe *et al.* (1998, 1999, 2001) used AdiNOS in porcine vein grafts to inhibit intimal hyperplasia [160,163,164] and Li *et al.* (2003) as well as Zanetti *et al.* (2003) used AdiNOS to study heart diseases [165,166]. While Tzeng *et al.* (1997, 1998) used AdiNOS to inhibit hepatocyte and endothelial apoptosis [167,168], Wang *et al.* (2004) used AdiNOS to study the role of iNOS on radiation in human colorectal cell lines and have found a 63 % tumour regression when AdiNOS and radiation (2 Gy x 3 fractions) were used compared with 6 % when radiation alone was used. Apoptosis was also significantly higher in the combined therapy (22 ± 4 %) as compared to each of radiation and a control vector (9 ± 1 %), AdiNOS only (9 ± 3 %), or no treatment (2 ± 1 %) [169]. In addition, Weller *et al.* (2003) used AdiNOS to study the role of NO in UVB-induced keratinocyte apoptosis and found that iNOS reduced apoptosis in this case [170]. Gunnett *et al.* (2002) used the same vehicle to show that gene transfer of iNOS impairs vascular relaxation in the cerebral arteries of rabbits and humans [171].

1.6.4 Examples on the Use of Adenoviruses Encoding for the Ecdysone Cassettes

The ecdysone system has been previously used in a gene therapy approach by cloning its receptor and reporter cassettes into adenoviruses [133,172-174]. The cells were then infected with these adenoviruses at varying multiplicity of infection (moi) and gene expression was induced after Pon A administration (**Fig 1.20**).

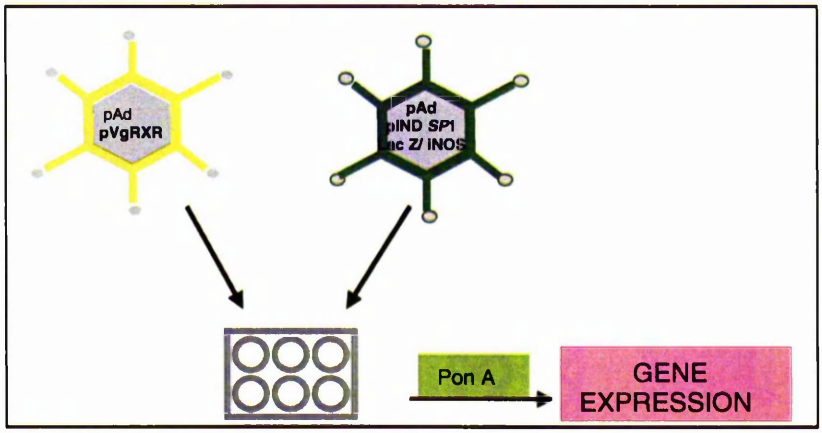

Fig 1.20 The ecdysone reporter and receptor cassettes are cloned in the viral backbone to generate 2 viruses. These viruses are then used to infect a variety of cell lines, and only upon administration of Pon A, gene expression should be driven.

For example, Johns *et al.* (1999) used the ecdysone system to transfer "electrical silencing" genes into neurons in order to suppress neuronal excitability which is a causative agent for epilepsy and intractable pain. The expression cassettes of each of pVgRXR and pIND-1 (with the gene of interest) were cloned into the adenovirus vector pAdLox and were then used to infect primary neuron cells. Expression was induced by muresterone A 24 h post viral infection. Their results demonstrated the ability to modify neuronal excitability genetically in an inducible and reversible manner and that the ecdysone has low basal and high inducible activities [133] (**Fig 1.21**). It is noteworthy to mention that the ratio of receptor: reporter viral particles should be monitored as excess receptor virus could increase basal levels as well as slightly decrease fold induction [133].

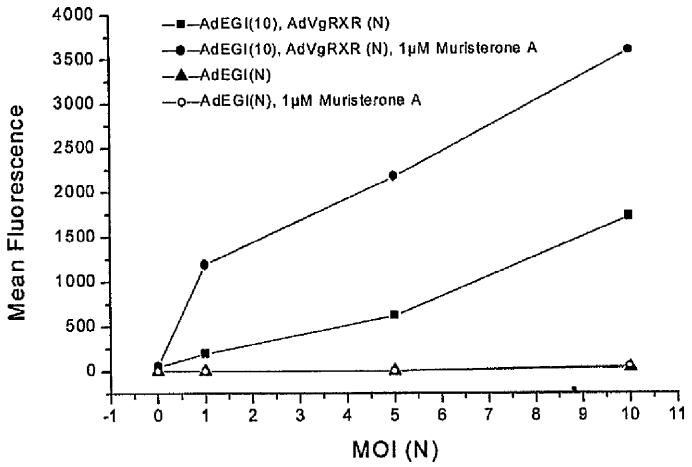

Fig 1.21 Infection of neurons with variable mois of both an adenovirus that contains an ecdysone-inducible promoter controlling expression of a cassette containing GFP, an IRES, and a multiple cloning site (AdEGI) and an adenovirus that expresses the modified ecdysone receptor and the retinoid X receptor (AdVgRXR) resulted in muristerone A-dependent and -inducible expression of GFP. In the absence of AdVgRXR, background expression was minimal, and such cells were entirely refractory to muristerone A [133].

In another study, the ecdysone system was used in an adenoviral context to study the role of PI 3-kinase, a cytoplasmic signalling molecule. Again several mois of the viruses were used and Pon A was added 24 h post-infection and gene expression was measured after a further 24 h. Low basal levels and 2-3 fold induction was observed with 3 μM Pon A [172]. Other examples using a combined ecdysone system and adenovirus approach include studies to suppress oxygen sensitive K^+ current in chemoreceptor cells [173], and studies aiming at expressing genes in mammalian sensory hairs [174].

1.6.5 Conclusion

The importance of tightly regulating the level of iNOS in order to achieve therapeutic benefit as well as the ability of the ecdysone system to precisely regulate gene expression with low basal level and high fold induction encouraged us to control the expression of iNOS using this inducible system. Moreover, the previous use of adenoviruses to express iNOS or the ecdysone cassettes prompted us to use this therapeutic vehicle as a tool to further control and deliver this therapeutic gene.

1.7 Aims and Objectives

The role of iNOS in tumourigenesis and cancer therapy cannot be underestimated. The conflicting opinions towards whether iNOS plays a pro- or anti-tumourigenic effect emphasised the importance of tightly controlling its expression in order to obtain therapeutic benefit. Moreover, since the natural iNOS promoter has an HRE-binding site, this indicates that iNOS is over expressed under hypoxic conditions and so could be tailored for use in a gene-directed–enzyme-prodrug-therapy (GDEPT). The ability of NO to radiosensitise hypoxic cells similarly to aerobic cells and its availability in areas of reduced oxygen tension as well as its ability to mediate vascularisation leading to increased oxygenation adds to its therapeutic benefits. Finally, HIF-1 plays a key role under hypoxic conditions and the potential ability of NO to inhibit HIF-1 might hold an interesting therapeutic future.

This study aims to precisely control iNOS gene expression using an inducible mammalian expression system as well as deliver this gene using adenoviruses in order to optimise the use of iNOS in cancer gene therapy. Therefore, these specific objectives were set:

- Evaluation of the ecdysone inducible system *in vitro* and *in vivo* using the *Lac* Z reporter gene
- Generation of stable clones that express ecdysone inducible iNOS and the evaluation of these clones *in vitro* and *in vivo*
- Generation of type 5 adenoviruses that encode for the expression of iNOS
- Study the role of iNOS on tumour vascularisation using the established iNOS clone
- Measure the effect of iNOS mediated hypoxic cytotoxicity to the bioreductive drug, TPZ
- Decipher the effect of NO on HIF-mediated gene expression using NO donors and the generated adenoviruses

CHAPTER 2 MATERIALS AND METHODS

2.1 Water and Chemicals

2.1.1 Water

Deionised water (dH_2O) was prepared by reverse osmosis using Millipore distillation system and was used for general purposes. In the nucleic acid experiments, double distilled water (ddH_2O) was used (Sigma, UK), which was prepared by reverse osmosis followed by autoclaving at 121 ^{0}C for 15 min.

2.1.2 Chemicals

All the chemicals were purchased from Sigma, UK unless otherwise stated.

2.2 Plasmid Cloning Techniques

All experiments involving recombinant DNA technology were performed in Category II containment laboratories.

2.2.1 Preparation of LB (Luria-Bertani) Media and LB-agar plates

LB media was prepared using LB broth (Sigma, UK) (2 g/100 ml distilled water). LB-agar solution (Agar: Gibco BRL, Paisley, UK) was prepared by adding agar (1.5 g/100 ml LB media). LB Low Salt medium was made up by mixing 10 g/l Tryptone (Becton Dickinson, San Jose, California, USA) 5 g/l NaCl (BDH, Merck Ltd, Poole, Dorset, UK), and 5 g/l Yeast Extract (Gibco BRL, Paisley, UK). The pH was adjusted to 7.5. This media was recommended by the manufacturer to keep Zeocin active in order to grow the pVgRXR plasmids.

The solutions were autoclaved and stored at room temperature. The desired antibiotic selection was added in the recommended concentration (**Table 2.1**) to the LB media that was then stored at 4 ^{0}C once opened. In order to prepare the LB-agar plates, the LB-agar solution was microwaved until completely dissolved and left to cool to 50 ^{0}C and then any antibiotic

selection was added. The solution was poured into sterile plastic petri dishes and allowed to settle before storing at 4 ^{0}C. The plates were pre-warmed at 37 ^{0}C before use.

Plasmid	*Medium*	*Antibiotic*	*Antibiotic Concentration*
pVgRXR	LB Low Salt	Zeocin	25 µg/ml
pShuttle vectors	LB Medium	Kanamycin	50 µg/ml
All Others	LB Medium	Ampicillin	100 µg/ml

Table 2.1 Transformation and culture requirements for different vectors

2.2.2 Preparation of *E. coli* stocks

Stocks of competent *E. coli* DH5α were prepared by streaking previously purchased DH5α (Gibco BRL, Paisley, UK) onto LB-agar plates without selection followed by incubating at 37 ^{0}C overnight. One colony was then picked and left to grow with agitation in 5 ml LB medium overnight at 37 ^{0}C. Then, 1:100 (v/v) of this culture was added to 400 ml LB medium placed in conical flasks and left to grow with agitation (225 rpm) for 3 h to reach the exponential growth phase. This was determined by measuring the optical density (OD_{600}) using a spectrophotometer (DU650, Beckman). Once the OD_{600} value reached 0.6-0.8, the culture was left to cool on ice for 15 min and then spun down at 6 g for 5 min at 4 ^{0}C. The pellet was resuspended in 34 ml cold sterile calcium chloride ($CaCl_2$ at 50 mM) and 6 ml of glycerol (BDH Limited Poole, England). The preparation was divided into 1 ml aliquots and placed in freezing tubes (Nalgene), snap frozen in liquid nitrogen, and then stored at –80 ^{0}C.

2.3 DNA Manipulation and Cloning

2.3.1 iNOS cDNA Source

EcoR I-linked iNOS cDNA (GenBank accession no. X73029) cloned as a *Not* I fragment into pBluescript SKII (+), was kindly provided by Prof. Ian Charles (The Rayne Institute, University of London, UK). The iNOS cDNA was then isolated by partial *EcoR* I

digestion followed by restriction with *Xho* I /*Not* I and then cloned into a mammalian expression vector, F373 (kindly provided by Dr. Stephen Hobbs, CRUK Centre for Cancer Therapeutics, ICR, London, UK) cut with the same enzymes. The resultant plasmid (pEF-iNOS-puro) encoded a bicistronic message driven by the human elongation factor 1α promoter. This allowed the translation of both iNOS and *pac* (the gene responsible for puromycin resistance) from a single transcript by virtue of an internal ribosomal entry site upstream of the *pac* gene [97].

2.3.2 DNA Digests

Plasmid DNA were cut using type II restriction endonucleases (New England Biolabs, Hertfordshire, UK). In an eppendorf, 1-5 μg of DNA was digested with 1 μl of the enzyme (10-20 Units) in a total volume of 20 μl containing 1x enzyme buffer and 1x BSA (bovine serum albumin) (the enzyme buffer and BSA are provided with each enzyme and diluted to 1x using ddH_2O). The total volume was adjusted by adding ddH_2O. The reaction was incubated overnight at 37 ^{0}C (or the optimum temperature for other enzymes). The digested DNA fragments were separated on a 1 % agarose gel and the fragments of appropriate sizes were excised and gel extracted using the QlAquick Gel Extraction Kit (Qiagen LTD, Crawley, UK). The DNA was eluted in 30 μl ddH_2O.

2.3.3 Blunting

In some cases, the vector and the insert were digested with enzymes that generate incompatible cohesive ends and therefore they had to be blunt in order for a ligation to occur. So, to the digested DNA preparation, 1x thermopol buffer (supplied as 10x), 1.5 μl (3 Units) Vent enzyme (New England Biolabs, Hertfordshire, UK) and 2.5 μl nucleotide mixture (dNTPs 1:1:1:1 dTTP:dCTP:dATP:dGTP, each dNTP was supplied at 100 mM making the final concentration at 25 mM for each dNTP) were added. The volume was adjusted to 40 μl

by adding ddH_2O. The Vent enzyme was used to blunt the generated DNA ends as it digests the hanging nucleotides in a 3'-5' direction. The nucleotides were used to fill in the gaps generated by enzymes that create a 5' overhang. The reaction was incubated at 75 ^{0}C for 30 min and then column extracted using the QlAquick Gel Extraction Kit. The DNA was eluted in 50 µl ddH_2O.

2.3.4 Dephosphorylation

In order to prevent the religation of a vector digested with an enzyme that generates compatible ends, a dephosphorylation step was performed on the digested vector only. Alkaline dephosphorylation removes the 5' phosphate group from the linearised plasmid. A volume of 1 µl CIP (calf intestinal alkaline phosphatase- 10 Units) and 1x enzyme buffer (supplied as 10x), (New England Biolabs, Hertfordshire, UK) were added to 5 µg DNA. The reaction was incubated at 37 ^{0}C for 1 h and then column extracted using the QlAquick Gel Extraction Kit. The DNA was eluted in 30 µl ddH_2O.

2.3.5 DNA Ligation

The linearised DNA fragments were run on a 1 % agarose gel against a 1 Kb DNA ladder to compare the DNA concentrations. For each ligation, 100 ng of the vector was added to different ratios of the insert (1:1, 1:3, 1:6 vector: insert). A sample of the vector only was also included to control for any religated vector. In each ligation mixture, 1x DNA ligase buffer (supplied as 10x) and 1 µl (20 Units) T4 DNA ligase enzyme (New England Biolabs, Hertfordshire, UK) were added. The volume was adjusted to 20 µl by ddH_2O. The ligation mixture was set up on ice and the reaction was initiated by the addition of the T4 DNA ligase and then allowed to proceed at 16 ^{0}C for 18-20 h. The ligations were then transformed into DH5α or BJ5183 Electroporation Competent Cells (Stratagene, The Netherlands). BJ5183 Electroporation Competent Cells are a bacterial strain and were used for DNA transformation using electroporation. They were utilised to generate adenoviruses as they have the

components needed to allow the homologous recombination between a vector that contains the gene of interest and a second vector that contains the adenoviral genome, provided that sites of homology are shared between these two vectors.

2.4 Transformation of Plasmid DNA into Competent *E. coli*

2.4.1 Using Heat-shock Techniques

2.4.1.1 Into DH5α

Transformations were performed into competent DH5α *E. coli.* A vial of DH5α was thawed slowly over ice. Then, 100 ng of the plasmid was added to 100 µl of DH5α and left 10 min on ice. Samples were heat shocked at 42 ^{0}C for 45 s and then 900 µl S.O.C. Ultra Pure Medium (2 % Tryptone, 0.5 % yeast extract, 10 mM NaCl, 2.5 mM KCl, 10 mM $MgCl_2$, 10 mM $MgSO_4$, and 20 mM glucose) (Gibco BRL, Paisley, UK) was added. After shaking in a 37 ^{0}C incubator for 1 h, 200 µl of the transformation mixture was plated onto LB agar plates containing the appropriate antibiotic selection marker **(Table 2.1)** and left overnight in a 37 ^{0}C incubator.

2.4.1.2 Into SCS 110

Transformation into non-methylating SCS 110 (Stratagene, The Netherlands) was performed when a certain digest was methylation sensitive. This is due to the presence of a methylase enzyme encoded by the Dam, Dcm, or Mec gene in some *E. coli.* This enzyme causes the addition of a methyl group to certain nucleotides in certain sequences thus causing resistance to digestion by the restriction enzymes that target these sites [175]. To allow these digests to occur, the non-methylating SCS 110 *E. coli* were used.

A volume of 1.7 µl β-mercaptoethanol (Stratagene, The Netherlands) was added to a 110 µl suspension of SCS 110 that was thawed slowly over ice. The samples were left on ice for 10 min. Then, 10 ng of DNA was added to each sample and left on ice for 30 min. The samples were heat shocked at 42 ^{0}C for 45 s and incubated on ice for 2 min. Then, 900 µl

S.O.C. Ultra Pure Medium was added. After shaking in a 37 ^{0}C incubator for 1 h, 200 µl of the transformation mixture was plated on LB-agar plates and incubated at 37 ^{0}C overnight.

2.4.2 Using Electroporation

The BJ 5183 Electroporation Competent Cells were used for DNA transformation using electroporation to generate adenoviruses. These cells have the components needed to allow the homologous recombination between a vector that contains the gene of interest and a second vector that contains the adenoviral genome, provided that regions of homology are shared between these two vectors.

The vector that contains the gene of interest was linearised and dephosphorylated in preparation for a homologous recombination with the second vector that contains the viral genome.

The linearised vector (1 µg) and the second vector (100 ng) were co-transformed into BJ 5183 Electroporation Competent Cells (40 µl) by electroporation. Each sample was mixed, placed in a cuvette, and tapped to remove air bubbles. The electroporation machine (EquiBio-Easyject, Middlesex, UK) was run until it reached 2500 V to allow for transformation of DNA into the electroporation competent cells. Then, 1 ml of S.O.C medium was added and the sample was shaken at 37 ^{0}C for 1 h. The transformants were plated on agar plates containing antibiotic selection.

2.5 DNA Separation and Sequencing

2.5.1 Agarose Gel Electrophoresis

2.5.1.1 Preparation of the Gel

Agarose gel electrophoresis was preformed in order to separate, quantify, and characterise the digested DNA. A 1 % agarose (Gibco BRL, Paisley, UK and Helena BioSciences Ltd, UK) gel was prepared in 1x TAE buffer. Ethidium bromide at a final concentration of 0.5 µg/ml was added and the DNA was loaded using the DNA loading

buffer (1x). A suitable DNA marker (10 µl) was run along side as a source of guidance for DNA size and quantity. The gel was run in 1x TAE buffer at 90-100 V until the DNA bands were clearly separated. The gel was viewed using a UV transilluminator at 302 nm (T2201 Sigma Chemical Company) and a photograph was taken using a Polaroid Gel camera and Polaroid 667 film.

2.5.1.2 Preparation of Gel Electrophoresis Reagents

- TAE is made up of 2 M Tris-acetate and 0.05 M EDTA pH 8.3 (ethylenediaminetetraacetate Gibco BRL, Paisley, UK)
- DNA loading buffer: 40 % (w/v) sucrose, few crystals of bromophenol blue were added (until a deep purple colour was visualised). It was sterile filtered.
- DNA Ladders (λ-*Hind* III digest, 100 bp, and 1 Kb) were prepared by adding a ratio of 1:2:7 of 500 ng purchased ladder (New Englands Biolabs, Hertfordshire, UK), DNA loading buffer, and ddH_2O respectively. The mixture was stored at 4 ^{0}C.

2.5.2 Gel Extraction

Gel extraction was performed using the QlAquick Gel Extraction Kit (Qiagen LTD, Crawley, UK). After excising the DNA with a clean sharp scalpel and weighing it in an eppendorf, 3 volumes of buffer QG were added to 1 volume of the gel. This buffer helps in dissolving the agarose residues. The mixture was incubated at 50 ^{0}C for 10 min (until the gel dissolved completely). Then, 1 volume of isopropanol was added to the sample and mixed. To bind the DNA, the sample was applied to the QlAquick column and centrifuged at 16,060 g for 1 min. The flow-through was discarded and 0.5 ml of buffer QG was added and the sample was respun at 16,060 g for 1 min. To wash, 0.75 ml of buffer PE was added and the mixture was respun at the same speed. The flow-through was discarded and the sample was respun another time. Then, the QlAquick column was placed into a clean eppedorf and the DNA was eluted by adding 50 µl of buffer EB or ddH_2O, leaving the sample to stand for 1

min, and centrifuging for 2 min at 16,060 g. This procedure allows the precipitation of the linearised DNA removing all buffers and enzymes or agarose gel residues. The above-mentioned buffers are all supplied in the QlAquick Gel Extraction Kit.

2.5.3 DNA Sequencing

2.5.3.1 Primer Annealing and DNA Extension

Sequencing was performed using the ABI Prism® Big Dye Terminator™ Cycle Sequencing method (ABI Prism, UK) method. To 250-500 ng of DNA, 8 µl Terminator Ready Reaction Mix (which contains the polymerase enzyme and dNTPs and is provided in the kit) (ABI Prism, UK) and 10 pmol pShuttle forward or reverse primer (Stratagene, UK) were added. The volume was adjusted to 20 µl by the addition of ddH_2O. As a control, 2.5 µl of pGEM DNA at 0.2 µg/µl was used, 4 µl of M13 primer at 0.8 pmol/µl and 8 µl of Terminator Ready Reaction Mix were added. The volume was adjusted to 20 µl by the addition of ddH_2O. Then, 40 µl of mineral oil were added to each sample.

The tubes were spun for few seconds and were placed in a thermal cycler (Genius-Techne, Jepson Bolton and Co. Ltd - Watford, UK). The machine was pre-warmed at 96 ^{0}C for 1 min after which the samples were placed in the machine at this temperature for another 1 min. Then, the following cycles were repeated 30 times. Rapid thermal ramp to 96 ^{0}C, and left 30 s at 96 ^{0}C, rapid thermal ramp to 50 ^{0}C, and left 15 s at 50 ^{0}C, followed by rapid thermal ramp to 60 ^{0}C, and left 4 min at 60 ^{0}C. Then, rapid thermal ramp to 4 ^{0}C and held until ready to purify. This process ensures template denaturation at 96 ^{0}C, primer annealing at 50 ^{0}C, and DNA extension and polymerisation at 60 ^{0}C. Then, the 20 µl reaction was removed from underneath the oil layer and placed into clean eppendorfs.

2.5.3.2 Polymerase Chain Reaction (PCR) Product Purification

To precipitate the PCR product using ethanol/ sodium acetate precipitation, 2 µl of 3 M sodium acetate at pH 4.6 and 50 µl of 100 % ethanol was added to each 20 µl reaction.

The tubes were incubated on ice for 10 min and then spun for 30 min at 16,060 g. The supernatant was aspirated and discarded. Then, 250 µl of 70 % ethanol was added to wash the DNA and the tubes were spun at 16,060 g for 15 min. The supernatant was aspirated again. The samples were dried and stored at –20 ^{0}C until sequenced (Sequencing Service, University of Manchester).

2.6 Preparation of Plasmid DNA from *E. coli*

2.6.1 Mini Preparation

Colonies were picked using plastic loops and grown in 5 ml LB plus antibiotic and were left shaking at 225 rpm and 37 ^{0}C overnight. Then, 2 ml were centrifuged at 16,060 g for 10 min.

The plasmid DNA was extracted using a QIAGEN mini preparation kit (Qiagen LTD, Crawley, UK). Mini preparations (also called mini-prepped colonies) were performed in order to obtain pure plasmid DNA that could be digested with restriction enzymes or sequenced to check the ligation of an insert DNA into a vector.

The pellet was resuspended in 250 µl buffer P1 and mixed with 250 µl of buffer P2. The mixture was incubated at room temperature for 5 min to which 350 µl buffer P3 was added. The mixture was centrifuged at 16,060 g for 10 min at 4 ^{0}C. Then, the DNA lysate was transferred to a QIAGEN spin column and spun for 1 min at 16,060 g. The column was washed with 750 µl buffer PE and spun for another minute at 16,060 g. The eluant was removed and the column was respun for 1 min at 16,060 g. Then, 50 µl of buffer TE or sterile distilled water was added to the DNA. The mixture was left to stand for 1 min and then spun for 2 min at 16,060 g to elute the DNA. All of the above mentioned buffers constitute part of the QIAGEN mini preparation kit and are needed to purify the DNA preparations.

2.6.2 Maxi Preparation

After being tested for the desired ligation, the positive colonies were grown in 5 ml LB plus antibiotic to maintain the selection. Colonies were left shaking overnight and 1:100 (v/v) of the culture was transferred to conical flasks with 200 ml medium and antibiotic. The bacteria were left shaking overnight at 37 ^{0}C and 225 rpm.

The culture was centrifuged at 21.9 g for 15 min at 4 ^{0}C and the DNA was extracted using a QIAGEN Endofree plasmid maxi preparation kit (Qiagen LTD, Crawley, UK). The aim of this procedure is to obtain a pure plasmid preparation that is free of chromosomal DNA, RNA, protein, and any cellular debris. The bacterial pellet was resuspended in 8.5 ml buffer P1 (50 mM Tris-HCl pH 8, 10 mM EDTA, 100 μg/ml RNase A). A volume of 8.5 ml of buffer P2 was added in order to lyse the cells (Buffer P2: 200 mM NaOH, 1% SDS). SDS causes the solubilisation of the phospholipids and proteins in the cell membrane and thus the release of cell contents while NaOH denatures the chromosomal and plasmid DNA. Then, 8.5 ml of buffer P3 (acidic potassium acetate) was added to neutralise the mixture and precipitate the SDS with the cellular debris and chromosomal DNA only leaving the renatured plasmid DNA. The plasmid was separated by centrifugation at 15,522 g for 15 min. The supernatant was poured into QIAfilter cartridge to make sure all the excess SDS has been removed. A volume of 2.5 ml buffer EB (endotoxin removal buffer) was added to the filtrate and incubated on ice for 30 min. Buffer EB prevents the endotoxin molecules or lipopolysaccharides from binding to the DNA purification resin in the QIAGEN tip. Endotoxins are undesirable as they have strong, negative influence on the transfection efficiency in primary and sensitive cultured cells. To purify the plasmid DNA, a QIAGEN tip 500 was used. The tip was pre-equilibrated with 10 ml buffer QBT (1 M NaCl, 50 mM MOPS, pH 7.0, 15 % isopropanol). The solution in the tip was washed with 2x 30 ml of buffer QC (1 M NaCl, 50 mM MOPS pH 7, 15 % isopropanol) to completely remove any

remaining contaminants. The plasmid DNA was then eluted with 15 ml buffer QN (1.6 M NaCl, 50 mM MOPS pH 7.0, 15 % isopropanol) into a clean endo-free eppendorf. The DNA was precipitated by addition of 10.5 ml isopropanol and immediate centrifugation at 15,522 g and 4 ^{0}C. The pellet was washed with 5 ml endotoxin-free 70 % ethanol and centrifuged for 10 min at 4 ^{0}C. The supernatant was aspirated in sterile conditions and the pellet was left to dry for 5 min. The pellet was then resuspended in 200 µl endotoxin-free TE buffer in an endotoxin-free eppendorf. All of the above mentioned buffers constitute part of the QIAGEN maxi preparation kit.

2.6.3 Quantification of Plasmid DNA using a UV Spectrophotometer

DNA concentration and purity was determined by diluting 10 µl of the plasmid DNA with 990 µl sterile distilled water and read on a spectrophotometer (DU650, Beckman) at OD_{260} and OD_{280}. The concentration was calculated using the following formula:

[OD_{260} x dilution factor (100) x 50 (DNA constant)/1000=µg/µl DNA]

(50 is the extinction coefficient since 50 µg/ml DNA gives an OD_{260} of 1)

A protein-free preparation should give an OD_{260}/OD_{280} of 1.8.

2.7 Tissue Culture

All tissue culture experiments were performed in Category I containment laboratories.

2.7.1 Cell lines

MDA-MB-231 (human breast adenocarcinoma), HT-1080 (human fibrosarcoma), CHO-K1 (chinese hamster ovary), HCT-116 (human colorectal carcinoma), HEK 293 (human embryonic kidney, transformed with adenovirus type 5 DNA), T47D (human breast carcinoma) were obtained from American Type Culture Collection (ATCC, VA, USA) and were grown in RPMI 1640 medium (Gibco BRL, Paisley, UK) with a final L-glutamine (Gibco BRL, Paisley, UK) concentration of 2 mM and 10 % v/v Foetal Calf Serum (FCS)

(LabTech International) at 37 ^{0}C in a humidified air/5 % CO_2 atmosphere. Unless otherwise mentioned, a media volume of 20 ml/T-75, 5 ml/T-25 flasks and 2 ml/well, 1 ml/well, 0.2 ml/well in 6, 24, and 96-well plates was used respectively.

2.7.2 Trypsinisation

The cells were detached by trypsinisation. The media was removed and the cells were washed with PBS (phosphate buffered-saline) and then enough trypsin-EDTA (0.05 % Trypsin and 0.53 mM EDTA-4Na) (Gibco BRL, Paisley, UK) was added to cover the cells. Both PBS and trypsin were pre-warmed at 37 ^{0}C. After incubating at 37 ^{0}C for 5 min, the cells were observed for detachment. Media (including L-glutamine and FCS) was added in order to inhibit the effect of trypsin and to allow for further culturing of the cells.

2.7.3 Freezing and Defrosting of the Cells

In order to freeze down, the cells were trypsinised and spun at 412.5 g for 5 min and then resuspended in a suitable volume of freezing media (made up of 50 % media, 40 % foetal calf serum, and 10 % DMSO). The media was filter sterilised and stored in aliquots at –20 ^{0}C). The cells were divided into 1 ml aliquots initially stored at –80 ^{0}C and then placed in liquid nitrogen for long-term storage.

To defrost, the cells were removed from liquid nitrogen and immediately thawed at 37 ^{0}C. Fresh media was added to the defrosted cells and then spun at 412.5 g for 5 min in order to remove any DMSO residues present in the frozen media. The pellet was then resuspended in fresh media and placed in a T-75 flask. The media was changed the following day.

2.8 Transfection

2.8.1 Transient Transfection

Cells were seeded in 6-well plates (Falcon, UK) at $1x10^5$ cells/well and incubated at 37 ^{0}C overnight. On the second day, the cells were transfected using Lipofectin or

Lipofectamine reagents (Gibco BRL, Paisley, UK) as described below. On the second or third day, the transfection medium was removed, the cells were washed with PBS, and fresh RPMI medium containing 10 % v/v foetal calf serum was added.

2.8.1.1 Using Lipofectin

Lipofectin is a 1:1 (w/w) liposome formulation of the cationic lipid N-[1-(2,3-dioleyloxy)proplyl]-n,n,n-trimethylammonium chloride (DOTMA), and dioleoyl phosphotidylethanolamine (DOPE) in membrane filtered water [176]. A mixture of 1 µg/well of each vector was added to 100 µl/well Opti-MEM® I reduced serum medium (Opti-MEM® I is a modification of Eagle's Minimum Essential Medium and contains GlutaMAX™ I (L-Alanyl-L-Glutamine), 2.4 g/l sodium bicarbonate, HEPES, sodium pyruvate, hypoxanthine, thymidine, trace elements, growth factors, and 1.1 mg/l phenol red and has 50 % reduced serum with no cell adaptation needed [111]) (Gibco BRL, Paisley, UK). In another tube, 20 µl/well Lipofectin, and 100 µl/well Opti-MEM® I were used. The tubes were left seperate for 30 min and then mixed together and incubated at room temperature for 15 min. The cells were washed with 2 ml/well Opti-MEM® I media followed by incubation with the transfection media for 4 –24 h.

2.8.1.2 Using Lipofectamine

Lipofectamine reagent is a 3:1 (w/w) liposome formulation of the polycationic lipid 2,3-dioleyloxy-N-[2(sperminecarboxamido)ethyl]-N,N-dimethyl-1-propanaminium trifluoroacetate (DOSPA) and the neutral lipid dioleoyl phosphatidylethanolamine (DOPE) in membrane filtered water [177]. A mixture of 1 µg/well of each DNA was added to 100 µl/well Opti-MEM® I. In another tube, 10 µl/well Lipofectamine, and 100 µl/well Opti-MEM® I were mixed. When Lipofectamine was used, the two tubes were immediately mixed together and then incubated for 45 min at room temperature. The cells were washed with 2 ml/well Opti-MEM® I media followed by incubation with the transfection media for 4 –24 h.

2.8.2 Stable Transfection

Cells were seeded at 1-2 x10^5 cells/well. The following day, they were transfected with Lipofectamine or Lipofectin as mentioned in the previous section. A concentration of 0.5-2 μg/well of each vector as well as Opti-MEM® I media was used. The media was replaced 24 h post transfection with 10 % v/v foetal calf serum-containing media. After another 48 h, the media was replaced with antibiotic selection media. The cells were incubated until colonies formed. The colonies were picked using plastic loops and cultured in the same antibiotic selection media awaiting screening for positive gene expression.

2.9 Induction of Gene Expression

Ponasterone A (Pon A) (Invitrogen, Groningen, The Netherlands, Stratagene, The Netherlands, and A.G Scientific, UK) was reconstituted in 100 % ethanol. To prepare a 1 mM stock, 250 μg of Pon A powder were mixed with 500 μl ethanol and stored at –20 ^{0}C. Varying concentrations of Pon A were freshly made up in media and added to the transfected cells to induce gene expression. Pon A was left for 24 h (unless otherwise stated) and then the relevant assays were performed.

2.10 *Lac* Z Expression

2.10.1 X-gal Staining

The principle of this assay is based on the ability of transfected cells (coding for the β-Galactosidase enzyme) to react with X-gal (5-bromo-4-chloro-3-indolyl-β-D-galactoside) and give a blue insoluble compound.

The cells were washed with PBS, fixed with 10 % formalin (Sigma, UK) for 10 min and then washed with PBS again. The cells were stained for β-Galactosidase expression using the X-gal (Helena Bioscience Ltd, UK) solution (for 20 ml preparation: 40 μl of 1 M magnesium chloride (BDH Limited Poole, England), 100 μl of 1 M potassium ferricyanide,

100 µl 1 M potassium ferrocyanide, 1 ml X-gal with a concentration of 20 µg/ml. The volume was adjusted to 20 ml by adding PBS).

After adding this mixture, the cells were incubated between 2-24 h at 37 ^{0}C, 5 % CO_2. The properties of the blue cells were evaluated under the microscope.

In some experiments, 1 ml DMSO/well was added in order to dissolve the blue colouring of the cells and the absorbance was read at 650 nm to allow quantification [178].

2.10.2 β-Galactosidase Enzyme Activity Assay

The principle of this assay is based on the ability of transfected cells (expressing the *Lac* Z reporter gene) to undergo the following reaction:

$$\text{Ortho-nitrophenyl-β-galactoside (ONPG)} \xrightarrow{\beta\text{-galactosidase}} \text{Ortho-nitrophenyl (ONP)}$$

ONPG is colourless while ONP is yellow. The colour absorbance was measured using a spectrophotometer (DU650, Beckman, USA). It is noteworthy to mention that since human cells do not have the β-Galactosidase enzyme, no background should be observed.

Transfected cells were lysed with 200 µl lysis buffer [12.5 ml 100 mM Tris-HCl (pH 7.8), 7.5 ml glycerol, 500 µl 1 M $MgCl_2$, 500 µl Triton X-100, 100 µl 0.5 M EDTA (pH 8). The volume was adjusted to 50 ml by adding sterile distilled water]. Then, the supernatant was transferred to a clean tube and 45 µl of 10 mM $MgCl_2$/0.45 M β-mercaptoethanol [0.02 g $MgCl_2$, 320 µl β-mercaptoethanol, 9.68 ml distilled water], 100 µl substrate solution (o-nitrophenol-β-D-galactopyranoside 4 mg/ml in PBS), and 345 µl PBS were added. The mixture was left on ice for 5 min and then incubated at 37 ^{0}C for 1 h until a yellow colour developed. The tubes were placed on ice and the reaction was stopped by the addition of 510 µl 1 M sodium carbonate (Na_2CO_3). The absorbance was read at 420 nm (DU650, Beckman). The enzyme activity in the sample was determined according to the formula:

$$\text{Enzyme Activity (Units)} = \frac{380 \times A_{420} \times \text{dilution factor}}{T \text{ (min)}}$$

(380 is a constant needed in this equation)

2.11 The Luciferase Assay

Firefly luciferase is a protein that does not require post-transcriptional processing for enzymatic activity [179] [180] and thus functions as a genetic reporter immediately upon translation. Photon emission is achieved through oxidation of beetle luciferin in a reaction that requires ATP, Mg^{2+}, and O_2. This reaction produces Oxyluciferin and light that is detected using a luminometer [181].

Renilla luciferase is another protein that originates from *Renilla reniformis* [182]. Like Firefly luciferase, *Renilla* luciferase does not requires post-translational modifications for its activity and thus functions as a genetic reporter immediately after translation. The luminescent reaction catalysed by *Renilla* luciferase utilises O_2 and coelenterate-luciferin (coelenterazine). In the DLR™ assay Chemistry (Promega, UK), the kinetics of the *Renilla* luciferase reaction provide a stabilised luminescent signal that decays slowly over the course of the measurement [181]. The *Renilla* luciferase was used as a control reporter to check for variability in the experiments that could be caused by toxic compunds.

Luciferase expressing cells were placed in anoxic or aerobic conditions for 18 h after which the cells were reoxygenated for 3 h. The media was then removed, the cells were washed with PBS, and lysed using 50 µl/well of the Lysis Buffer (diluted to 1x in ddH_2O) provided by the Luciferase Kit (Promega, UK) The plates were mixed on a plate shaker for 15 min and 20 µl/well were read using a Luciferase plate reader (Titertex- Multiskan MCC/340, UK). The substrates provided by the Luciferase Kit were used to initiate the enzymatic reactions.

2.12 Protein Quantification

The protein assay was performed in order to quantify the amount of protein in a sample. A 1:50 dilution of copper sulphate (4 % w/v) (Sigma, UK) in bicinchoninic acid (Sigma, UK) was prepared [183]. A volume of 200 µl of this reagent was added to 10 µl of each unknown sample or standard in a 96 well micro-titre plate. The following Bovine Serum Albumin (BSA) (New England Biolabs, Hertfordshire, UK) concentrations were prepared (4000, 3000, 2000, 1000, 500, 100, 10, 0 µg/ml) as a set of protein standards. The plate was incubated at 37 ^{0}C for 60 min until a deep purple colour developed at the higher standard concentrations and the absorbance was read at 540 nm using a micro-titre plate reader (Titertek Multiskan MCC/340, UK).

A standard curve was obtained by plotting the absorbance versus protein concentration for the BSA standards. The curve was used to determine the protein concentration for each unknown protein sample.

2.13 Staining for iNOS Protein Expression

2.13.1 Immunocytochemistry

Upon staining with a primary antibody that binds to iNOS followed by a FITC (Fluorescein isothiocyanate) conjugated secondary antibody that binds to the primary anti-body, the cells that code for the iNOS gene should fluoresce when examined under a fluorescent microscope.

The cells were fixed with 10 % formaldehyde for 20 min and then permeabilised by the addition of 0.1 % (v/v) Triton X-100 (Sigma, UK) in PBS for 10-15 min. Then, 10 % horse serum (Gibco BRL, Paisley, UK) in PBS (blocking solution) was added to the cells and left at room temperature for 30 min. This was followed by the addition of a primary rabbit anti-iNOS antibody (raised against human iNOS) (ZYMED, San Francisco, USA) that was diluted at 1:500 in 0.1 % blocking solution and incubated at room temperature for 1 h. After

washing with PBS, the cells were incubated in the dark for 30-60 min at room temperature with the secondary goat anti-rabbit FITC conjugated antibody (Sigma, UK) that was diluted at 1:100 in 0.1 % blocking solution. Then, DAPI (4,6-diamidino-2-phenylindole) stain (1:500 dilution in distilled water) was added to stain the nuclei and each cover slip was mounted with Mowiol (12 % Mowiol, 34.5 % glycerol, 0.12M Tris-HCl pH 8.5) onto a microscope slide.

Cells were observed under the fluorescence microscope (Eclipse E800, Japan), nuclei stained blue by DAPI stain and NOS protein stained green due to FITC present in the secondary antibody. FITC is excited at 488 nm and the emission is collected at 530 nm [147].

2.13.2 Flow Cytometry

Another method used to monitor the percentage of cells that express the iNOS gene was by flow cytometry. Cells that were expressing iNOS were first stained by a primary anti-body that binds to the iNOS protein followed by a FITC conjugated secondary antibody that binds to the primary anti-body. The samples were then analysed using the FACS machine (Becton Dickinson, San Jose, California, USA) with the FL-1 channel that detects light at 530 nm.

The cells were fixed with 4 % paraformaldehyde (Sigma, UK) for 15 min at 4 ^{0}C and permeabilised using a permeabilisation buffer [1% Heat Inactivated FCS, 0.1% sodium azide solution, 0.1% Triton X-100, and the total volume was adjusted to 50 ml with PBS at pH 7]. The cells were washed gently with PBS and pelleted. The primary rabbit anti-iNOS antibody was diluted (1:500) in 1 % BSA and the samples were incubated with the primary antibody at room temperature for 1 h. They were then washed with PBS containing 1 % BSA. Then, the secondary goat anti-rabbit FITC conjugated antibody was diluted (1:100) in PBS containing 1 % BSA and the cells were incubated with the secondary antibody in the dark for 30 min at

room temperature. The samples were washed with PBS and analysed using the FACS machine.

2.13.3 Measuring Apoptosis by PI staining

In order to study the extent of apoptosis, the cells were stained with propidium iodide (PI), which binds to DNA. The percentage of fluorescence due to PI staining was measured using the FACS machine. PI is excited at 536 nm and the emission is collected at 617 nm in the FL-3 channel that detects light at 650 nm.

The cells were fixed with 4 % paraformaldehyde for 15 min at 4 ^{0}C and permeabilised using a permeabilisation buffer [1 % Heat Inactivated FCS, 0.1 % sodium azide, 0.1 % Triton X-100, and the total volume was adjusted to 50 ml with PBS at pH 7]. The cells were washed gently with PBS and pelleted. The cells were stained for iNOS in order to compare the percentage of apoptosis relative to the iNOS expression in the sample. Hence, the same antibodies and the same protocol were followed as mentioned in the flow cytometry experiment with the addition of PI (10 μg/ml) in PBS in the final step.

2.14 Quantification of the Activity of the iNOS enzyme

In order to measure the activity of the iNOS enzyme in the cells, three distinct methods were used.

2.14.1 The L-citrulline Assay

This assay is based on the ability of NOS to convert L-arginine to citrulline. ^{14}C-radio-labelled arginine (Specific Activity =50.5 MBq/mg) (Amershampharmacia biotech, UK) was added to cell extracts and the amount of radio-labelled citrulline was measured. Any endogenous unlabelled arginine was removed by resin (Dowex-50WX8-400) (Sigma, UK).

2.14.1.1 Preparation of Cell Extracts

Exponentially growing cells were washed in cold PBS and harvested with trypsin-EDTA solution. The cells were then pelleted in cold PBS by centrifuging at 264 g for 10 min. The resulting cell pellet was re-suspended in 0.5 ml ice-cold buffer containing HEPES (10 mM, pH 7.4), sucrose (320 mM), EDTA (100 μM), dithiothreitol (0.05 mM), leupeptin (10 μg/ml), soybean trypsin inhibitor (10 μg/ml), and aprotinin (2 μg/ml) and sonicated using an MSE Soniprep 150 for 3x5 s at a nominal frequency of 23 KHz and an oscillation amplitude of between 5 and10 μm. The samples were placed on ice between each sonication. These suspensions were allowed to stand on ice for a further 10 min, and then centrifuged at 9,500 g for 15 min at 4 ^{0}C.

2.14.1.2 The Assay

The resultant pellet was discarded and the post-mitochondrial supernatant (cytosol and microsomes) was treated with a strong cation exchange resin to remove the endogenous arginine. The supernatant was incubated with the resin for 5 min and centrifuged at 9,500 g for 5 min in order to pellet the resin. This process was repeated twice, after which the cytosol was considered to be free of endogenous arginine.

NOS activity was measured by monitoring the conversion of L-[U^{14}-C]-arginine to L-[U^{14}-C]-citrulline. The reaction mixture (final volume 150 μl) consisted of HEPES buffer (20 mM, pH 7.4), L-valine (150 mM), L-citrulline (100 μM), 10 μM L-arginine and 50 μCi/ml L-[U^{14}-C]-arginine, tetrahydrobiopterin (10 μM), calmodulin (400 U/ml), dithiothreitol (2.5 mM), calcium chloride (250 μM), BSA (75 mg/ml) and 1 mM NADPH. The reaction was initiated by the addition of 50 μl of cell extract (100-300 μg protein) and incubated at 37 ^{0}C for 10 min. The reaction was terminated by the addition of 1.5 ml of 50 % (v/v) Dowex-50WX8-400 resin in water (to bind any remaining arginine in the incubation mixture). A volume of 5 ml of water was then added to the resin-incubate mix and then left to settle for

20 min before taking an aliquot of the supernatant for analysis by scintillation counting machine (Wallac 1409 Liquid Scintillation Counter). The enzyme activity associated with iNOS (calcium-independent activity) was measured as a difference in activity in the absence and presence of 1 mM ethylene-bis-(oxyethylenenitrilo) tetra-acetic acid (EGTA, a calcium chelating agent) and NOS inhibitor (100 μM L-NNA) [184] [185].

2.14.1.3 Calculation of Specific NOS activity

To calculate the activity of NOS, the background dpm (B) (B is the background count with resin added and no enzyme) was subtracted from the dpm for the 100 μl assay buffer (A) (A is the total count without the resin and no enzyme). So, A-B=C for 100 μl assay buffer. Next D was calculated as follows: [C/1500]x[3.325/2]=D (dpm/pmol). In this case, 1500 pmol is the number of pmol of arginine in 100 μl assay buffer and 2 ml is the volume counted of a total 3.325 ml in the assay protocol. So, with the specific activity D known, the pmol of radio-labelled arginine converted to radio-labelled citrulline for each sample was calculated by dividing this value by D. As the incubation time was 20 min for 50 μl of enzyme, D was divided by 20 and multiplied by 20 to express the activity in pmol min^{-1} ml^{-1}. Then, the value was divided by the protein content to express the unit of NOS activity as pmol of ^{14}C-citrulline formed/min/mg protein.

2.14.2 The Griess Assay

After it is produced by NOS, NO is converted into nitrite and nitrate. This assay measures the total nitrite in the media and thus indirectly quantifies iNOS expression in the samples.

Stably transfected cells were seeded in RPMI 1640 medium. On the second day, the media was replaced with Pon A in DMEM (Serum Free) medium (Gibco BRL, Paisley, UK) with 1 % volume by volume 2 M L-glutamine. The medium was changed because RPMI 1640 as well as foetal calf serum have shown high background of nitrite and nitrate. On the

third day, the griess assay was performed according to the manufacturer's protocol (R&D Systems, Abingdon, Oxon, UK). This assay is based on the conversion of NO into nitrate and nitrite. Nitrate reductase was used to reduce the nitrate back to nitrite and thus the total amount of nitrite was measured. This detection was determined as a coloured azo-compound product of the Griess reaction that absorbs visible light at 540 nm.

The medium of the cells was aspirated and mixed with 2-fold reaction buffer (detergent) and filtered or centrifuged for 10 min at 16,060 g to ensure that no cells were present. In a 96 well plate, 100 µl of medium was loaded per well. To each sample, 25 µl nitrate reductase (diluted in the reaction buffer) and 25 µl NADH (diluted 1:2 in dH_2O) was added. Nitrite standards (50 µl/well) were also prepared and 200 µl of the reaction buffer, 50 µl of nitrate reductase and 25 µl NADH were added to each well. The plate was then incubated at 37 ^{0}C for 30 min.

A volume of 50 µl of Griess reagent I and 50 µl of Griess reagent II were added to each well and left at room temperature for 10 min. The plate was then read at 540 nm using a micro-titre plate reader (Titertek Multiskan MCC/340, UK) and the amount of nitrite was deduced from the standard curve. All the reagents were supplied in the Nitric Oxide (NO_2^- /NO_3^-) Kit (R&D Systems, Abingdon, Oxon, UK).

2.14.3 The iNOS Reductase Assay

The NOS enzyme has an oxidative and a reductase domain. This assay measures the activity of the reductase domain and thus provides an indirect measure of the activity of the iNOS enzyme.

2.14.3.1 Preparation of Cell Extracts

The cells were split into T-75 flasks and left until confluent. Then, they were induced with 20 µM Pon A (5 ml of media/flask) and left for 24 h. The cells were later trypsinised and cell lysates were prepared [as mentioned for the L-citrulline assay but by replacing the

buffer mentioned above with Nuclear buffer A that is made up of 100 mM HEPES, 150 mM $MgCl_2$, 1 M KCl (potassium chloride), and 1 M KOH (potassium hydroxide)].

2.14.3.2 The Assay

The following reagents were also prepared: 100 mM phosphate buffer containing 3 μM Ca^{2+} (prepared from $CaCl_2$), 10 mM KCN (potassium cyanide) freshly prepared in distilled water, 400 μM cytochrome c (prepared freshly in phosphate buffer), 7.5 μM tetrahydrobiopterin (THB_4), 250 U/ml calmodulin, and 10 mM NADPH (freshly prepared in phosphate buffer). Then the assay was performed as follows. Into each cuvette, 0.5 ml of cytochrome c (final concentration 200 μM), 0.1 ml 10 mM KCN (final concentration 1 mM), 5 μl 1.5 mM THB_4 (final concentration 7.5 μM), and 5 μl of 50,000 U/ml calmodulin (final concentration 250 U/ml) were added. A suitable concentration of protein (0.1-0.3 mg/ml) was added to the mixture. Then, the total volume was adjusted to 1 ml using the phosphate buffer (containing 3 μM Ca^{2+}). The contents were mixed well and the cuvettes were transferred to the 37 ^{0}C thermostatted cell compartment of the spectrophotometer (DU650, Beckman). The baseline was recorded and the reaction was initiated by adding 20 μl of 10 mM NADPH (final concentration 200 μM) to the sample cuvette only. The increase in absorbance with time at 550 nm for 2 min was recorded.

2.14.3.3 Calculation of iNOS Activity

The results were calculated by first reading the initial rate of cytochrome c reduction in units of Δ A550 nm/min from the spectrophotometric chart recording. The extinction coefficient of reduced cytochrome c at 550 nm has been determined to be 21.0 cm^2/mmol [186]. Hence, NADPH-cytochrome c reductase activity (nmol/min/ml lysate) was calculated by the formula:

$$\frac{\Delta \text{ A550 nm/min}}{1} \times \frac{1000}{21.0} \times \frac{\text{Total cuvette volume (ml)}}{\text{volume of suspension (ml)}}$$

The enzyme activity was expressed as nmol/min/mg protein at 37 ^{0}C by dividing by the protein content of the suspension.

2.15 Cell Survival Assays

2.15.1 The MTT Assay

The MTT Assay is a colourimetric assay that measures the level of cell proliferation of drug treated cells as a percentage of untreated control cells. After having administered the drug and exposed to anoxic and then to aerobic conditions, MTT [(3-(4,-5 Dimethylthiazole –2-yl)—2,5-diphenyltetrazolium bromide] (stock concentration prepared at 5 mg/ml in PBS) was added at a final concentration of 0.5 mg/ml. This assay is based on the cleavage of the yellow tetrazolium salt (MTT) to produce a dark formazan derivative (Thiazolyly blue) [187,188] as MTT is actively transported into the cell and reduced to the formazan by-product via mitochondrial dehydrogenases [188,189]. After MTT addition, the plate was incubated at 37 ^{0}C for 4 h. The media was fully aspirated without disturbing the purple-formed crystals that were afterwards dissolved in 500 µl/well DMSO when a 24-well plate was used and 200 µl/well when a 96-well plate was used. The plate was shaken on the plate shaker (Heidolph TITRAMAX 1000-Germany) for 10 min. When the 24-well plate was used, 200 µl/well was transferred into a 96-well plate. The absorbance at 540 nm was read using the plate reader (Titertek Multiskan MCC/340, UK). A curve representing the percentage survival (determined from the absorbance readings at 540 nm for the sample and untreated control) versus the drug concentration was plotted and the IC_{50} (the value of the drug concentration that corresponds to 50 % cell survival) was calculated.

2.15.2 Clonogenic Assay

This assay was used to study the colony forming effeciency after drug treatment and incubation under aerobic and anoxic conditions. The cells were seeded in 60 mm-plastic dishes (5 ml/dish) and treated with the drug and incubated under the required oxygen

conditions. After 8 days, the cells were PBS washed and fixed with 70 % ethanol. They were PBS washed again and stained with 0.5 % methylene blue (prepared in 70 % ethanol) for 2-3 min. The plates were washed with tap water 2 min after staining and were left to air dry. The colonies (each colony is defined to be about 50 cells)-now stained blue- were counted in each plate [190]. The plating efficiency was calculated by dividing the number of counted colonies/plate by the seeding number. This value was multiplied by 100.

2.16 Virus Generation

All experiments involving adenoviruses were performed in Category I containment laboratories.

In order to generate recombinant adenoviruses, two main methods exist. The first involves direct ligation of the gene of interest into the adenoviral genome. However, this method is extremely difficult because the adenovirus genome is large (36 Kb) and contains few useful restriction sites [147]. The second method, which is more commonly used involves cloning the gene of interest into a shuttle vector and transferring the gene into the adenovirus genome by means of homologous recombination in an adenovirus packaging cell line [191]. This homologous recombination step was further adjusted and now occurs in certain *E. coli* that employ the efficient homologous recombination machinery [192] (example: the BJ 5183 Electroporation Competent cells). Thus, a recombinant adenovirus is produced by a double-recombination event between co-transformed adenoviral backbone plasmid vector (pAdEasy-1) and a pshuttle vector carrying the gene of interest [147] (**Fig 2.1**).

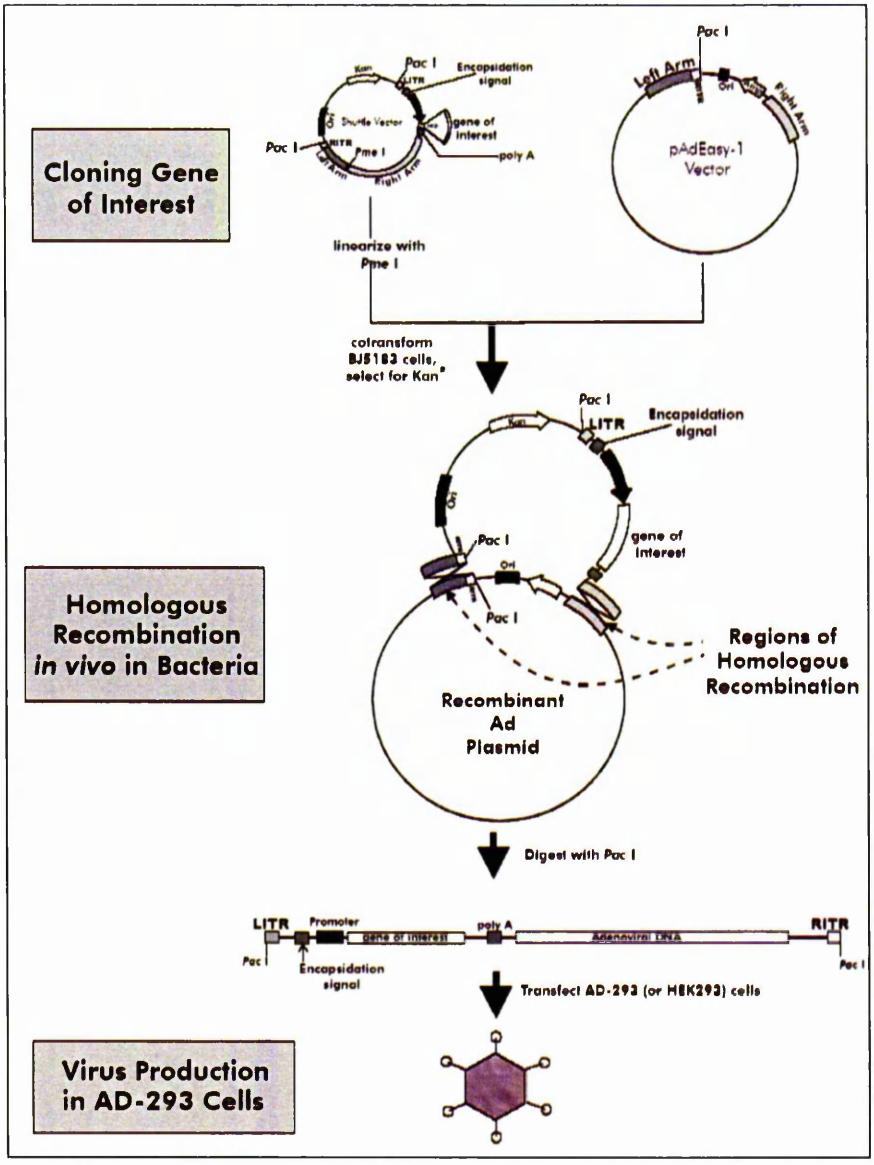

Fig 2.1 Production of Recombinant adenovirus using the pAdeasy system.

2.16.1 Preparation of the Primary Inoculum

In order to prepare a primary inoculum of the virus, HEK 293 cells were transfected with the pAdeasy vector containing the cassette of interest. The HEK 293 cell line was chosen because it provides the E sites needed for viral replication. For each viral preparation, 10 µg of the pAdeasy vector containing the cassette of interest was digested with 1 µl (10 Units) *Pac* I enzyme in a reaction containing 1x BSA and 1x restriction enzyme buffer (supplied as 10x). The digest was left overnight at 37 ^{0}C. Then, the digested plasmid was

column extracted **(Section 2.5.2)** to a final volume of 30 µl in ddH_2O and used to transfect the HEK 293 cells that were seeded in a T-75 flask until 40 % confluent. The transfection was performed using Lipofectamine at 30 µl/flask. The cells were incubated at 37 ^{0}C until 100 % cytopathic effect was observed indicating that all of the cells were infected with the virus formed. It is noteworthy to mention that the pAdeasy-iNOS virus was grown in presence of 100 µM L-NNA inhibitor to avoid any possible NO-induced cell-toxicity. Then, the media from each flask was collected and spun at 412.5 g for 5 min. The pellet was resuspended in 1 ml PBS. After 3 cycles of thaw-freezing in a 37 ^{0}C water bath and liquid nitrogen, the samples were spun at 16,060 g for 10 min. The supernatants were then frozen down at –80 ^{0}C.

2.16.2 Virus Replication

To scale up the virus stocks, 10-15 T-175 flasks of HEK 293 were grown until 80 % confluent and were then infected with 30-50 µl viral primary inoculum. The cells were incubated at 37 ^{0}C until 100 % cytopathic effect was observed. Then, the media was poured into 50 ml tubes and was either stored immediately at –80 ^{0}C or was spun at 412.5 g for 30 min and the pellets were stored at –80 ^{0}C for later viral purification.

2.16.3 Virus Purification

The 50 ml media (or pellet) from the flasks was freeze-thawed 3 times using liquid nitrogen and a 37 ^{0}C water bath to release all the adenovirus particles from the HEK 293 cells. The media was spun at 412.5 g for 30 min. The virus purification kit (BD Biosciences Kit, CA, USA) was used. The following procedure was performed based on the manufacturer's protocol. A 0.45 µm Millipore filter available in the kit was pre-wet with PBS. The supernatant was filtered and an equal volume of 1x Dilution Buffer was passed through the filter so that the colour of the eluant turned pink due to a pH change. Another small filter was then pre-wet with PBS and attached to the given plastic wire. The pink

filtrate was aspirated slowly through this wire so that the virus was allowed to stick on the small filter. A 50 ml of 1x Wash Buffer was also passed through the filter to make sure no residue was left (**Fig 2.2**). The virus was then eluted using 1ml of 1x Elution Buffer into a small bijou. The eluant was either aliquoted in small volumes and stored at –80 ^{0}C or concentrated by spinning at 16,060 g for 30 min at 4 ^{0}C. The supernatant was then immediately removed and the pellet was resuspended using 1x Formulation Buffer, aliquoted and stored at –80 ^{0}C.

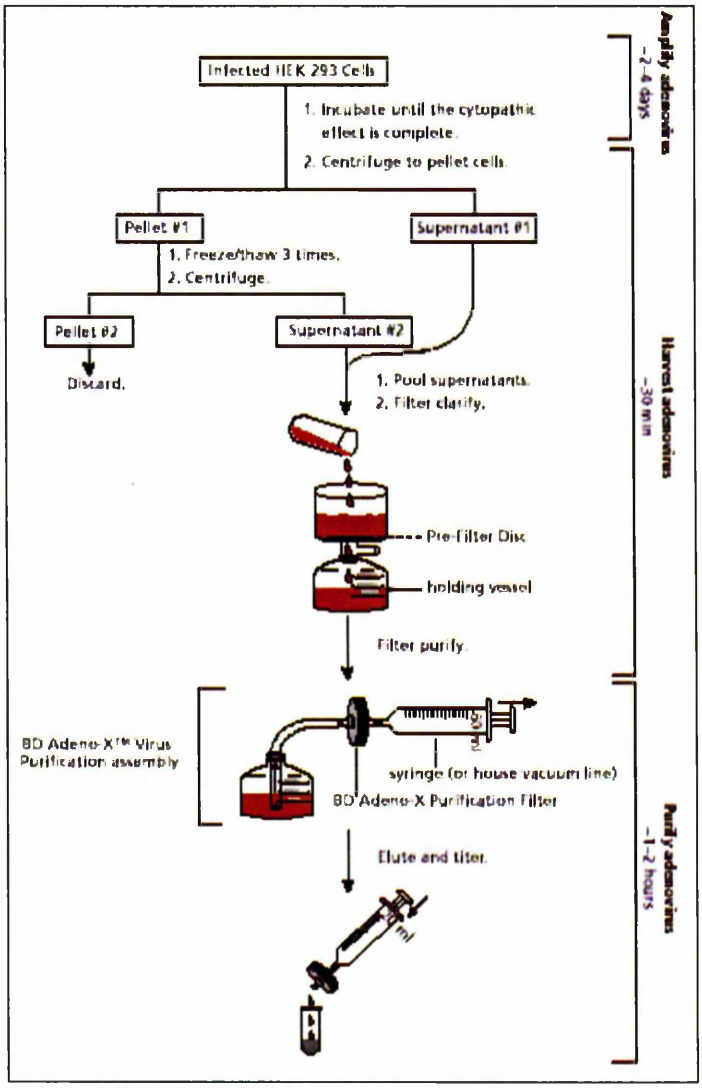

Fig 2.2 Overview of the BD Adeno-X™ Virus Purification Kit protocol [193].

2.16.4 Virus Titration

The titration was performed in order to calculate the number of plaque forming units (pfu/ml) in a viral stock. HEK 293 cells were seeded at $5x10^3$ cells/well in a 96-well plate leaving the upper and the lower rows empty (**Fig 2.4**). The plate was incubated at 37 ^{0}C. The following day, a triplicate-well serial dilution of the virus ranging from 10^{-2} to $7.63x10^{-12}$ was performed in a 24-well plate leaving the last 2 wells empty as a control (**Fig 2.3**). Then, from each well in the 24-well plate, 300 µl were taken and added to the 3 wells in the 96-well plate (100 µl/well in triplicates). After 2 days, the media was replaced with 200 µl fresh media. After 8-10 days, the last well that was infected was recorded and used to calculate the pfu/ml of the virus vial (**Fig 2.4**).

990 1	900 2	900 3	900 4	900 5	500 6
500 7	500 8	500 9	500 10	500 11	500 12
500 13	500 14	500 15	500 16	500 17	500 18
500 19	500 20	500 21	500 22	500 23	500 24

Fig 2.3 A 24-well plate format used for the viral dilutions. A volume of 10 µl of the virus was added to 990 µl of media to the first well. Then, 100 µl (wells 1 to 4) or 500 µl (wells 5-22) - as per the table- was taken from each well to the following to perform the needed serial dilutions. The last 2 wells were left empty as a control.

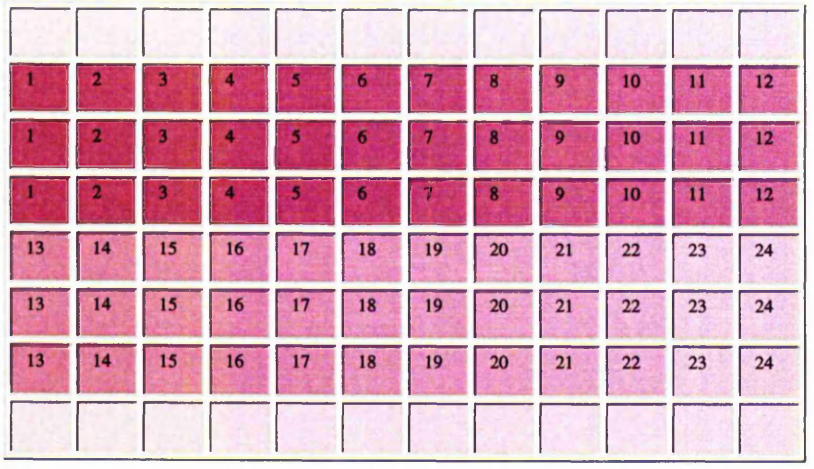

Fig 2.4 HEK 293 cells were seeded at $5x10^3$ cells/well. Then, 100 µl of the diluted virus (24 well-plate) was added to the wells of this plate in triplicates.

Well	**1**	**2**	**3**	**4**	**5**	**6**
Dilution	10^{-2}	10^{-3}	10^{-4}	10^{-5}	10^{-6}	$5x10^{-7}$
Pfu/ml	$1.0x10^3$	$1.0x10^4$	$1.0x10^5$	$1.0x10^6$	$1.0x10^7$	$2.0x10^7$
Well	**7**	**8**	**9**	**10**	**11**	**12**
Dilution	$2.5x10^{-7}$	$1.25x10^{-7}$	$6.25x10^{-8}$	$3.12x10^{-8}$	$1.56x10^{-8}$	$7.81x10^{-9}$
Pfu/ml	$4.0x10^7$	$8.0x10^7$	$1.6x10^8$	$3.2x10^8$	$6.4x10^8$	$1.28x10^9$
Well	**13**	**14**	**15**	**16**	**17**	**18**
Dilution	$3.91x10^{-9}$	$1.95x10^{-9}$	$9.77x10^{-10}$	$4.88x10^{-10}$	$2.44x10^{-11}$	$1.22x10^{-10}$
Pfu/ml	$2.56x10^9$	$5.12x10^9$	$1.02x10^{10}$	$2.05x10^{10}$	$4.10x10^{10}$	$8.19x10^{10}$
Well	**19**	**20**	**21**	**22**	**23**	**24**
Dilution	$6.10x10^{-11}$	$3.05x10^{-11}$	$1.53x10^{-11}$	$7.63x10^{-12}$	Uninfected	Uninfected
Pfu/ml	$1.64x10^{11}$	$3.28x10^{11}$	$6.55x10^{11}$	$1.32x10^{12}$	Controls	Controls

Fig 2.5 This figure represents the calculations based on the above dilutions. Example: if the last infected well was number 12 in the 96-well plate, then the virus would have a pfu/ml of $1.28x10^9$.

2.17 *In vivo* Experiments

For all the *in vivo* studies, the experiments were performed in 8-week-old female nude (nu /nu cba) mice. All procedures were carried out by approved protocols (Home Office Project License 40-1770) in accordance with the Scientific Procedures Act 1986 and in line with the United Kingdom Coordinating Committee on Cancer Research guidelines on the Welfare of Animals in Experimental Neoplasia [194].

Tumour implantation, drug injections, animal care, animal sacrifice, and tumour excision were performed by Brian Telfer and David Garvey.

2.17.1 Tumour Implantation and Pon A Treatment

Cells were injected subcutaneously (s.c) at 2-5x10^6 cells/implant in 0.1 ml from a suspension of 2-5x10^7 cells/ml in PBS into the nude mice. Once a tumour volume of 200-400 mm^3 was achieved, Pon A concentrations of 1 or 2 mg/mouse dissolved in 30 µl DMSO and 270 µl of pre-warmed olive oil were injected intraperitoneally (i.p). The mice were sacrificed by neck dislocation 12-48 h post Pon A injection and the tumours were excised, fixed (10 % formalin for 24 h followed by 70 % ethanol) and stained or frozen (in liquid nitrogen) and β-galactosidase **(Section 2.10.2)** and iNOS enzyme **(Section 2.14.1)** activity assays were performed.

2.17.2 Injection of Hypoxia and Blood Perfusion Markers

In order to monitor certain aspects of tumour growth, some markers were injected into the tumour bearing mice. To stain for hypoxic regions, 0.2 ml of Pimonidazole (Natural Pharmacia International, RTP, NC, USA) (66 mg/kg) was administered i.p 2 h before sacrificing. Hoechst 33342, a blood perfusion marker, was injected intravenously (i.v) at 0.1 ml (3 mg/0.5 ml-dissolved in 0.9 % saline) 1 min before sacrificing. The tumours were collected and stored half fixed and half frozen waiting for sectioning and immunostaining.

2.18 Sectioning and Staining of Tumours

2.18.1 Tumour Sectioning

The tumours were formalin-fixed and then wax embedded (Histology, Stopford Bldg, Manchester University). They were then sectioned at 5 µm/section (unless stated otherwise) using a microtombe. The sections were placed on either APES (3-aminopropyl-triethoxysilane) coated slides or on Polylysine slides (BDH SuperFrost, UK).

Cryostat sections were performed on frozen tumours at 5 µm/section using a cryostat-microtome (Bright, Starlet 2212, Instrument Company LTD, UK).

2.18.2 APES Coating

APES coating provides a better attachment of the sample to the slide compared to non-coated slides. Non-coated slides (BDH SuperFrost, UK) were placed in 95 % alcohol for at least 2 min. The slides were then rinsed 3 times with tap water followed by one rinse in distilled water and one rinse in acid alcohol (1 % HCl, Sigma, UK in 70 % IMS-industrial methylated solvents made up of a 99 % ethanol mixture Chemix, UK). The slides were left to dry and were then placed in 3 % APES (freshly prepared in acetone) for 2 min and rinsed by emersion in acetone for 2 min. They were later washed in distilled water and dried at 37 ^{0}C overnight.

2.18.3 Immunostaining of the Tumours

The sectioned tumours were immunostained using the suitable antibodies that bind to the injected markers. The slides were placed for 10 min in xylene (Fisher Scientific, UK) to remove the wax. They were then rinsed with an ethanol gradient (6 min in each of 100 %, 90 %, and 70 % ethanol). This was followed by rinsing in a solution made up of distilled water and 0.1 % Tween 20 for 3 min. The slides were then washed with PBS and 0.1 % Tween 20 for another 3 min. A PAP pen was used to draw a circle around the sectioned tumour. Hydrogen peroxide (H_2O_2) drops -used as a blocking agent- (0.03 % H_2O_2 containing sodium azide) (provided in the DAKO EnVision Kit, DAKO Corporation, CA, USA) were added to the sections and left for 5 min. The slides were then washed for 3 min in PBS and 0.1 % Tween 20. Then, they were incubated in 0.05 % pronase diluted down in PBS for 20 min and washed for 3 min in PBS and 0.1 % Tween 20. The sections were incubated with horse serum (Sigma, UK) at a dilution of 10 % in PBS and 0.1 % Tween 20 PBS for 1 h. This step as well as the pronase addition is important to block non-specific binding. The sections were again washed with PBS and 0.1 % Tween 20. The primary antibody diluted in 1 % horse serum in PBS and 0.1 % Tween 20 was added to the sections and left for 45 min. A negative

control with no primary antibody was included. Either a 1/50 dilution of Pimonidazole (hydroxyprobe) or a 1:500 dilution of rabbit-anti-iNOS antibody was used. After incubation with the primary antibody, the sections were washed with PBS and 0.1 % Tween 20 for 3 min after which the secondary antibody was added and left for 30 min. In the case of Pimonidazole staining, the drops of secondary antibody from DAKO EnVision Kit were used while in the case of iNOS staining; goat anti-rabbit IgG horse- radish peroxidase (Sigma, UK) was used at a dilution of 1:100. Again a negative control slide with no secondary antibody was included. The slides were then washed with PBS and 0.1 % Tween 20 for 5 min. This step was repeated 3 times. Then, DAB (DAB + Chromogen: 3,3'-diaminobezidine chromogen solution) from the DAKO EnVision kit was added to the sections until a brown stain developed. Later, the slides were washed with PBS and 0.1 % Tween 20. The slides were then quickly dipped in haematoxylin solution (2 g/l haemtoxylin, 17.6 g/l aluminium sulphate, 0.2 g/l sodium iodide -Sigma, UK) to counter stain followed by washing in running tap water until the water became clear. Then, they were dipped 6 times in tap water, after which they were washed with PBS and 0.1 % Tween 20. The slides were placed in xylene for 5-10 min and then dipped 6 times through the reverse of the ethanol series (70 %, 90 %, 100 %). The slides were finally mounted using DPX mountant (BDH SuperFrost, UK).

2.19 Microscopy and Software

Fluorescent microscopy was used to view fluorescent staining. All other samples were viewed using light microscopy. Images were captured using a digital camera attached to a fluorescent microscope and later adjusted on Adobe Photoshop. DNA sequencing was analysed using Chromas software.

The Endnote software was used to organise the references and the statistics were performed on Excel (t-test).

CHAPTER 3

Results 1 EVALUATION OF THE ECDYSONE INDUCIBLE SYSTEM

3.1 Introduction

To study the role of iNOS in tumour growth, precise control of gene expression is vital. The ecdysone mammalian inducible system was chosen to regulate gene expression because it has demonstrated low basal level, high fold induction, and inducer-dose dependent gene expression [112,120,121]. The ecdysone inducible system is comprised of 2 vectors: pVgRXR and pIND SP1. The gene of interest was cloned in the multiple cloning site of pIND SP1. Only upon addition of the inducer (Pon A) should gene expression be driven [110].

Prior to regulating iNOS gene expression using the ecdysone system, this inducible system was evaluated using the *Lac* Z reporter gene. Preliminary experiments were conducted using transient transfections and then stable clones encoding for *Lac* Z in the ecdysone cassette were generated to evaluate the ecdysone system *in vitro* and *in vivo*. The following parameters were studied: basal levels, fold induction, inducer-dose dependence, effect of time on induced gene expression, as well as reversibility of gene expression after Pon A removal.

3.2 Evaluation of the Ecdysone System Using Transient Expression of the *Lac* Z Reporter Gene

In order to evaluate the ecdysone system, the *Lac* Z reporter gene was used. The ecdysone inducible plasmids pVgRXR and pIND SP1 were purchased from Invitrogen (Invitrogen, Groningen, The Netherlands). The pIND SP1 vector into which a *Lac* Z gene has already been inserted was also purchased (Invitrogen, Groningen, The Netherlands). Initially, the ecdysone system was evaluated *in vitro* by transiently transfecting a range of cell lines with both vectors of the ecdysone system (pVgRXR and pIND SP1 *Lac* Z) and *Lac* Z gene expression was monitored.

MDA-MB-231 (human breast cancer), HT-1080 (human fibrosarcoma), and CHO-K1 (chinese hamster ovary) were transiently transfected with pVgRXR and pIND SP1 *Lac* Z **(Section 2.8.1)**. The cells were seeded at $1x10^5$ cells/well in a 6-well plate. The following day, 1 µg/well of each vector was mixed with 10 µl/well Lipofectamine in the MDA-MB-231 and HT-1080 cell lines. The same DNA concentration was mixed with 20 µl/well Lipofectin in the CHO-K1 cell line in an attempt to improve the transfection efficiency. After 24 h, the cells were exposed to varying concentrations of Pon A. Following a further 24 h, the cells were formalin-fixed and X-gal stained. Cells successfully expressing the *Lac* Z gene which encodes for β-galactosidase, produce a blue coloured product upon addition of X-gal. The number of blue cells in each well was counted.

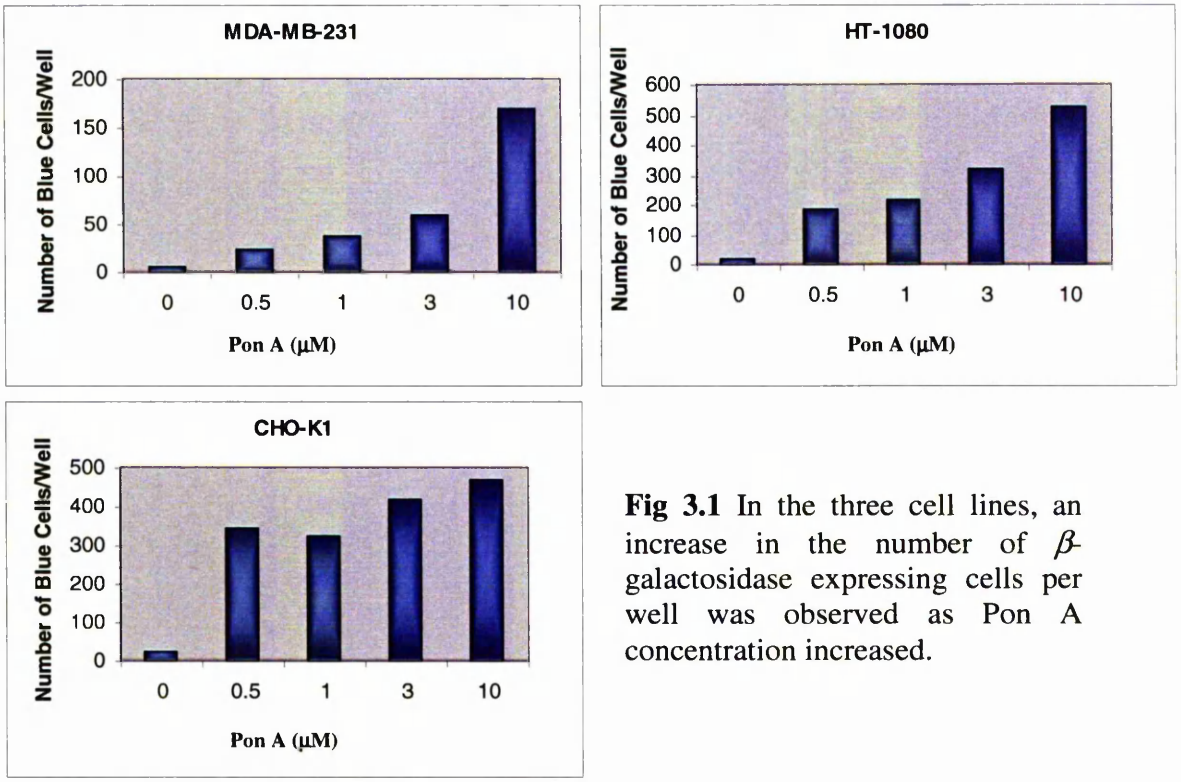

Fig 3.1 In the three cell lines, an increase in the number of β-galactosidase expressing cells per well was observed as Pon A concentration increased.

Fig 3.1 shows that with increased Pon A concentration, an increase in *Lac* Z gene expression was observed. The Pon A doses were chosen based on the manufacturer's suggestion of a maximal 10 μM dose and an induction period of 24 h. Gene expression was detected even at 0.5 μM Pon A and reached 20-26 fold induction at 10 μM (fold induction was calculated by dividing the number of blue cells observed at 10 μM Pon A by the number of blue cells observed in the absence of Pon A). Although the number of blue cells varied between cell lines, the fold induction remained similar (24.3 fold in MDA-MB-231, 25.8 fold in HT-1080, and 20.3 fold in CHO-K1 at 10 μM Pon A). This could be due to the different transfection efficiency, which is dependent on each cell line. It is noteworthy to mention that the MDA-MB-231 and HT-1080 cell lines showed better Pon A-dose dependent gene expression than the CHO-K1 cell line in this case. Moreover, in the absence of Pon A, very minimal expression was observed especially in the MDA-MB-231 cell line (7 blue cells/well)

indicating that the ecdysone system shows tight regulation of reporter gene expression in the human tumour cell line and in the rodent cell line at least *in vitro*.

3.3 Generation of Stable Clones Expressing the Ecdysone Cassettes

To eliminate the need to control for transfection efficiency and to evaluate the system *in vivo*, stable clones expressing both ecdysone vectors pVgRXR and pIND SP1 *Lac* Z were generated.

3.3.1 Antibiotic-dose Tolerance of Wild-type Cells

In order to generate stable clones containing the vector of interest, antibiotic administration was used to select for the positively transfected clones.

The pVgRXR vector has a Zeocin resistance marker for mammalian selection while the pIND SP1 vector has a neomycin resistance marker (G418.Sulphate antibiotic-PAA Lab, GmbH, Weiner Strasse, Austria). To select for transfected clones, the extent to which wild-type cells tolerate each antibiotic was measured. Wild-type cells were seeded at $1x10^3$ cells/well in a 24-well plate and grown in selection medium with a range of antibiotic concentration (0, 100, 250, 500, 750, 100 μg/ml for Zeocin and 0, 100, 250, 500, 750, 1000, 2500, 500 μg/ml for G418.Sulphate). The cells were observed daily. The concentration and the time that caused the death of all the cells (as visualised under the microscope) were recorded. **(Table 3.1)**

	Zeocin (μg/ml) (pVgRXR)	G418.Sulphate (μg/ml) (pIND SP1)	Both Antibiotics (μg/ml)
MDA-MB-231	100 (10 days)	1000 (8 days)	G418.Sulphate 1000 (μg/ml) Zeocin 100(μg/ml) (10 days)
HT-1080	100 (10 days)	500 (8 days)	G418.Sulphate 250 (μg/ml) Zeocin 50 (μg/ml) (10 days)

Table 3.1 Cell lines grown with varying antibiotic concentration. The concentration and time corresponding to complete death were recorded.

3.3.2 Stable Transfection to Generate Ecdysone Inducible *Lac* Z Clones

The aim of this experiment was to stably transfect the HT-1080 and MDA-MB-231 cell lines with both pVgRXR and pIND SP1 *Lac* Z. Initially, the cells were transfected with pVgRXR.

HT-1080 cells were seeded in 6-well plates at $1x10^5$ cells/well and incubated at 37 ^{0}C overnight. The following day, transfections were performed using Lipofectin reagent (**Section 2.8.2**). In the first 50 ml Falcon tube, 2 µg/well pVgRXR vector was diluted with 100 µl/well Opti-MEM® I medium. Opti-MEM® I is a modification of Eagle's Minimum Essential Medium purchased with reduced serum and was used to optimise the transfection effeciency [111]. A volume of 20 µl/well Lipofectin and 100 µl/well Opti-MEM® I were mixed in another tube. Each tube was left separate for 30 min after which they were both mixed and incubated at room temperature for 10-15 min. The transfection medium was added to the cells and left overnight. On the third day, the medium was replaced with RPMI medium containing 10 % v/v foetal calf serum. After 48 h, the medium was replaced with antibiotic selection medium (Zeocin-**Table 3.1**) and the cells were trypsinised and placed in culture plates and left 10-14 days to allow for colony formation. Colonies were then picked using plastic loops and placed into 24-well plates and subsequently transferred to 6-well plates, T-25, and T-75 flasks for culturing under continued selection pressure until screened.

3.3.3 Screening for Clones Expressing the pVgRXR Plasmid

From the cells that were transfected with pVgRXR, 14 MDA-MB-231 clones and 9 HT-1080 clones were able to grow in the presence of selection medium. Some of these clones were then transiently transfected with pIND SP1 *Lac* Z to screen for expression of the ecdysone receptor. Wild-type MDA-MB-231 and HT-1080 were transiently transfected with both pVgRXR and pIND SP1 *Lac* Z and acted as a positive control. The cells were seeded at

$1x10^5$ cells/well and induced with Pon A concentrations of 0,1, or 5 µM. After 24 h, the samples were formalin-fixed, X-gal stained, and the blue cells were counted (**Fig 3.2**).

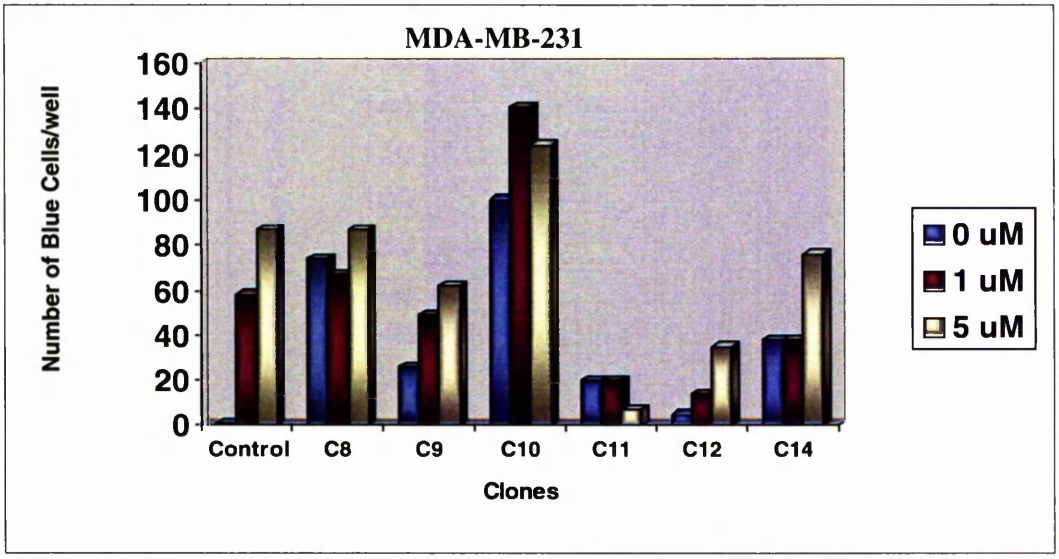

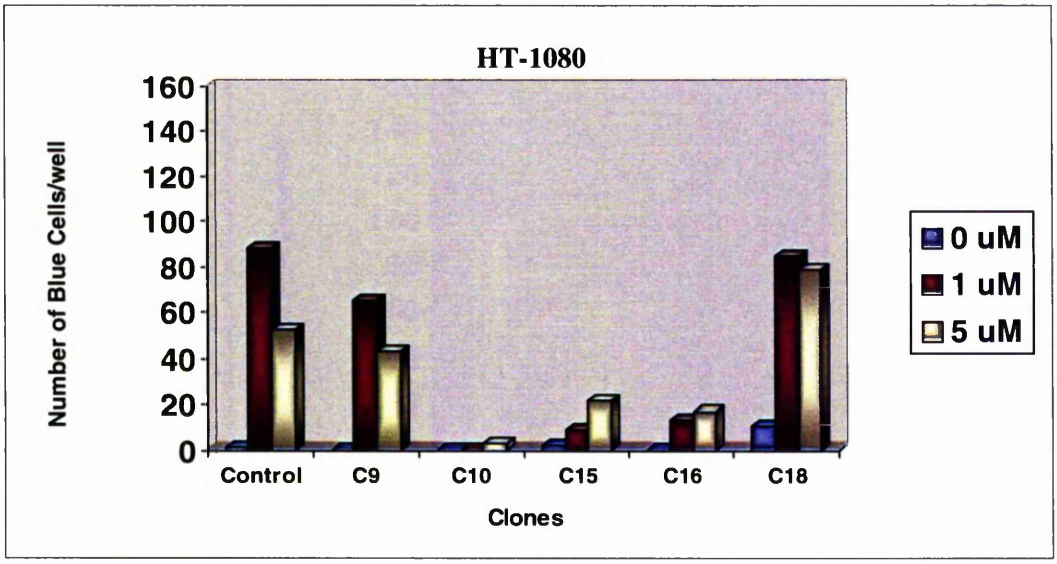

Fig 3.2 To select for positive clones, the cells were transiently transfected with pIND SP1 *Lac* Z, induced with Pon A (0,1,5 µM), fixed, and X-gal stained. Then, the number of blue cells was counted.

Based on tight gene expression in response to Pon A, promising clones from each cell line were chosen (MDA-MB-231: C9, C12 and HT-1080: C16). High-uninduced gene

expression was observed in some MDA-MB-231 clones. This could be due to the ecdysone promoter being inserted downstream of a stronger promoter in the host genome hence allowing for gene expression in the absence of Pon A. These clones were discarded. Gene expression in the control samples were almost similar to those observed in **Fig 3.1** with differences being attributed to variation in the transfection efficiency.

3.3.4 Stable Transfection of the pVgRXR Clones with pIND SP1 *Lac* Z to Generate Double Stable Ecdysone Inducible Clones

MDA-MB-231 clones 9 and 12 and HT-1080 clone 16 that stably express pVgRXR were used for stable transfection with pIND SP1 *Lac* Z. The transfection was performed using 1 µg/well pIND SP 1 *Lac* Z DNA and 20 µl/well Lipofectin. The cells were allowed to recover from the transfection process for 3 days after which selection media containing G418.Sulphate and Zeocin was added (**Table 3.1**). After 10-13 days, 24 colonies were picked from each cell line, cultured, and screened for ecdysone-inducible *Lac* Z expression. In order to test for gene expression, the cells were seeded at $1x10^5$ cells/well in a 6-well plate and induced with 5 µM Pon A. The cells were formalin-fixed and X-gal stained. None of the MDA-MB-231 clones showed inducible gene expression but the HT-1080 clone that showed the highest ecdysone inducible *Lac* Z gene expression represented by the number of blue cells/well was picked (**Fig 3.3**) and used to further evaluate the ecdysone system.

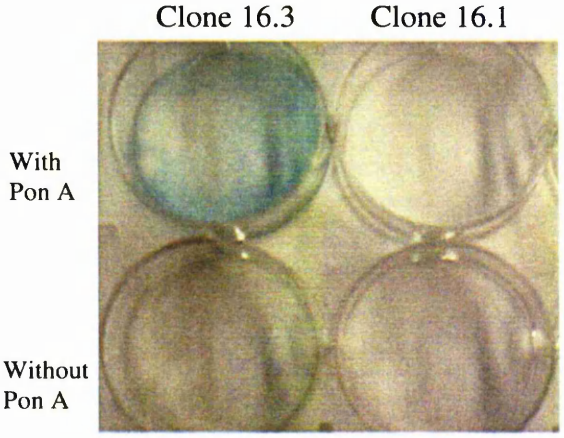

Fig 3.3 Blue cells were observed in the presence of 5 µM Pon A in clone 16.3 (positive clone) while no blue cells were observed in clone 16.1 (negative clone).

Stability of the HT-1080 Lac Z Clone

To confirm that clone HT-1080 16.3 (that expresses pVgRXR and pIND SP1 *Lac* Z) is a stable clone, it was grown either in the presence or absence of antibiotic selection for 2 weeks and then tested with the β-galactosidase colour assay after adding 5 µM Pon A for 24 h. The cells gave the same intensity of blue colour/well in both cases indicating that this clone was stable.

3.4 *In vitro* Evaluation of the Ecdysone System Using the HT-1080 *Lac* Z Stable Clone

3.4.1 X-gal Staining of the HT-1080 Inducible *Lac* Z Clone

In order to evaluate the ecdysone system, cells from the HT-1080 *Lac* Z clone 16.3 were seeded at $1x10^5$ cells/well in a 6-well plate and exposed to varying concentrations of Pon A for 24 h. Then, the cells were formalin-fixed and stained with X-gal. Blue cells were counted. An increase in number of blue cells as the concentration of Pon A increased was observed which indicated a tight dose response relationship as well as low basal expression **(Fig 3.4)**.

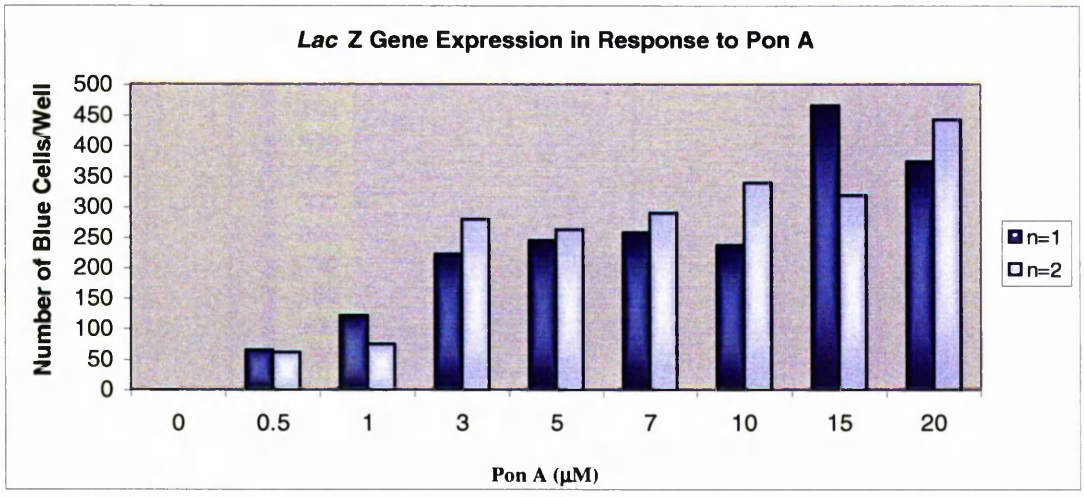

Fig 3.4 The ecdysone system was evaluated using the HT-1080 pVgRXR and pIND SP1 *Lac* Z double stable clone. After inducing with Pon A and staining with X-gal, blue cells were counted. At 0 µM Pon A, 1 blue cell was observed in n=1 and no blue cells were observed in n=2 (duplicate wells were used in this experiment and hence the results for n=1 and n=2 are shown).

Although the number of *Lac* Z expressing cells was lower, a higher fold induction was obtained in this experiment (578 fold at 10 μM Pon A) compared to the same experiment conducted in the HT-1080 cell line but using transient transfection (26 fold at 10 μM Pon A) **(Fig 3.1)**. This was due to the lower basal levels obtained in this case. Higher Pon A doses were also used in this experiment to try to increase the level of gene expression further.

3.4.2 Measuring the β-Galactosidase Activity of the HT-1080 *Lac* Z Clone

Another method to evaluate the ecdysone system is to measure the β-galactosidase activity of the HT-1080 ecdysone inducible *Lac* Z clone. This activity reflected the expression of the *Lac* Z reporter gene that encodes for β-galactosidase. Cells were seeded at $1x10^5$ cells/well in a 6-well plate and induced with varying concentrations of Pon A for 24 h. Then, the cells were lysed and the β-galactosidase enzyme assay was performed. An increase in activity as the concentration of Pon A increased was shown **(Fig 3.5)**. This experiment was performed separately from the X-gal staining experiment.

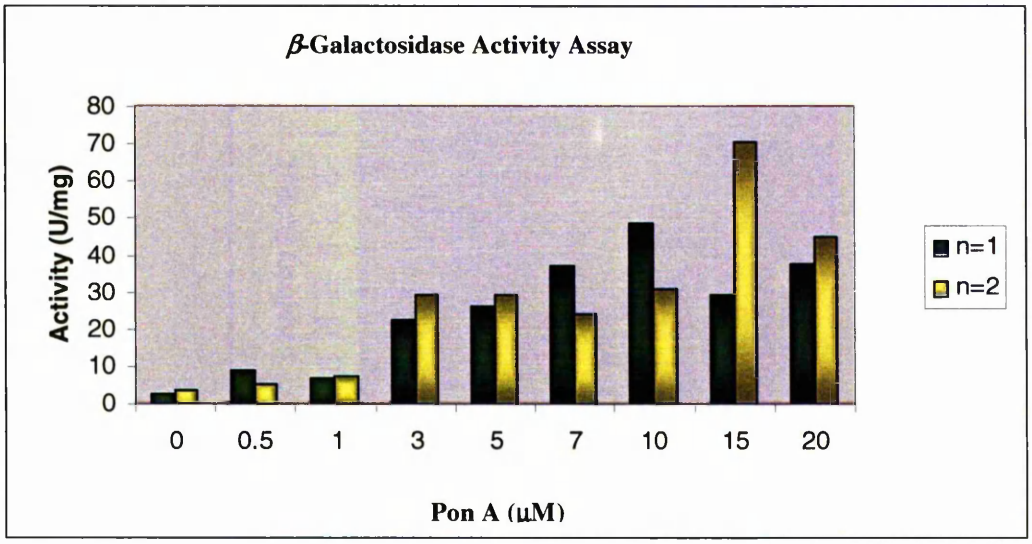

Fig 3.5 The β-galactosidase activity of the HT-1080 pVgRXR- pIND SP1 *Lac* Z double stable clone was measured. Cells showed an increase in activity as the Pon A concentration increased (this experiment was performed in duplicate wells and hence the results for n=1 and n=2 are shown).

This assay measured the activity of each cell expressing the β-galactosidase gene and therefore gave the extent to which the induced cells/well expressed the inserted gene rather than the positive/negative result obtained upon X-gal staining whereby cells that express *Lac* Z were stained blue upon X-gal addition regardless of the degree of gene expression. This assay also eliminated the human error in counting blue-stained cells. In this case, a 13.7 fold induction was obtained at 10 μM Pon A. This lower fold induction could be attributed to the different assays used and to the higher basal levels compared to the X-gal experiment.

3.4.3 Effect of Pon A Availabilty Over Time

To study the effect of Pon A availability over time, the HT-1080 clone 16.3 *Lac* Z was used. The cells were seeded at $5x10^4$ cells/well in a 6-well plate and induced with Pon A the following day. The cells were left without changing the media for 18, 24, 48, or 72 h and were then lysed and assayed using the β-galactosidase activity assay **(Fig 3.6)**.

n=1

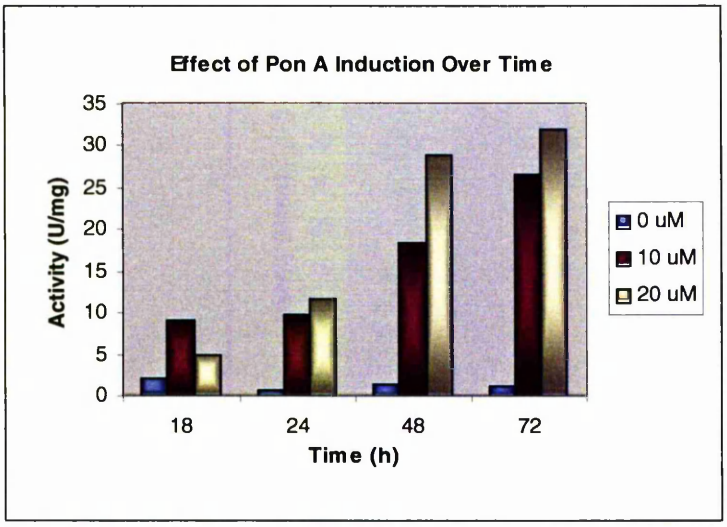

n=2

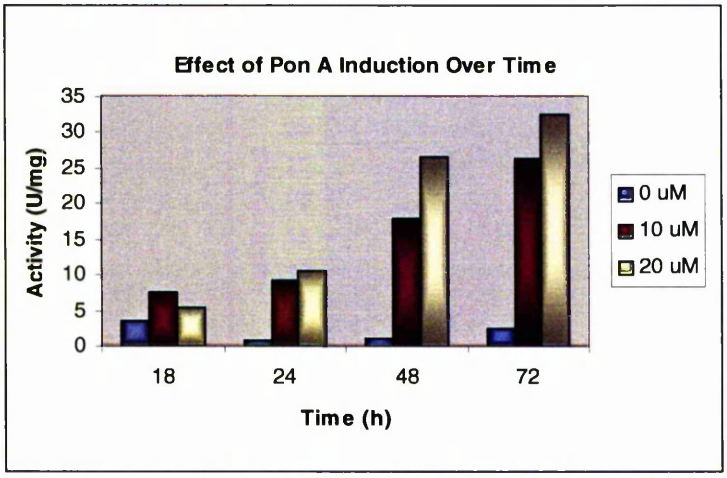

Fig 3.6 β-galactosidase activity in response to increasing time of Pon A exposure. The cells were induced with Pon A for 18-72 h (this experiment was performed in duplicate wells and hence results for n=1 and n=2 are shown).

This experiment shows that the β-galactosidase protein expression still increases even 72 h post Pon A exposure, which indicates that Pon A is not a limiting factor for *Lac* Z gene expression. Moreover, in order to obtain a clear dose-response effect, gene expression should be monitored at least 24 h after inducer administration.

3.4.4 Effect of Pon A Removal Over Time

The ecdysone inducible *Lac* Z clone 16.3 was also used to study the rate at which gene expression returns back to basal levels after Pon A removal. After seeding the cells at $5x10^4$ cells/well in a 6-well plate and inducing with Pon A for 24 h, the cells were washed with PBS and fresh Pon A-free RPMI media was added. The cells were lysed either immediately or after 24, or 48 h and were then assayed using the β-galactosidase activity assay **(Fig 3.7)**.

n=1

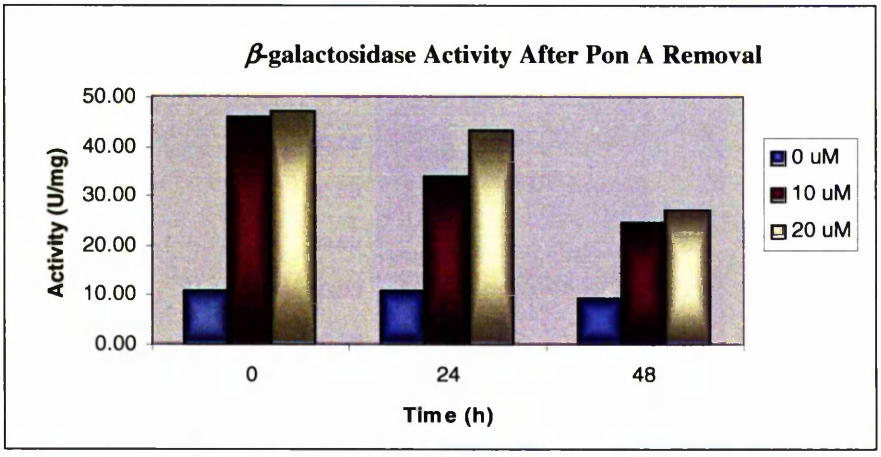

n=2

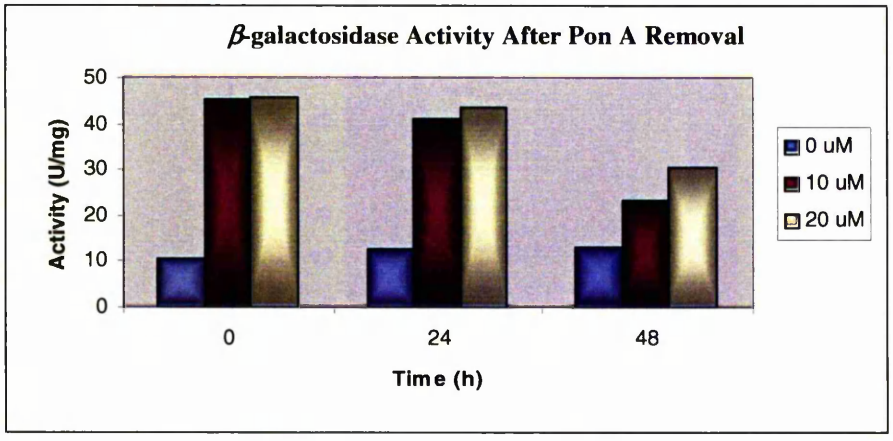

Fig 3.7 This graph shows that after Pon A was removed (time 0 h), gene expression decreased. The cells were exposed to Pon A for 24 h after which the media was replaced by Pon A –free RPMI media. The cells were lysed 0, 24, or 48 h after Pon A removal and the β-galactosidase activity assay was performed (duplicate wells were performed in this experiment and hence results for n=1 and n=2 are shown).

The results indicated that 24 h after Pon A removal, β-galactosidase protein levels began to decrease but did not return to basal levels even after 48 h. Based on the experiments performed by Saez *et al.* (2000), it was expected that Pon A induced expression should return to basal levels 20 h after Pon A removal. The difference in the results could be due to the fact the Saez *et al.* (2000) used 1 μM Pon A whereas we have used 10 and 20 μM and hence Pon A was depleted earlier when the lower dose was used [112]. Moreover, Saez *et al.* (2000) used the Luciferase reporter gene to measure induction while in these experiments the *Lac* Z reporter gene was used. It could be that the degradation of the β-galactosidase protein is slower than that of the Luciferase enzyme.

3.5 *In vivo* Evaluation of the Ecdysone System Using the HT-1080 Inducible *Lac* Z Clone

In order to evaluate the ecdysone system *in vivo* using the *Lac Z* reporter gene, the ecdysone inducible clone HT-1080 *Lac Z* 16.3 was used. Cells were injected s.c at $2x10^6$ cells/ 0.1 ml/mouse into nude mice. Once a tumour volume of 200-250 mm^3 was achieved, Pon A was administered. Because of its steroidal nature, Pon A was dissolved in olive oil that was pre-warmed and mixed with DMSO to increase solubility [112]. A minimal volume of DMSO was used as this compound is toxic at high concentrations, and hence, Pon A concentrations of 1 and 2 mg/mouse dissolved in 30 μl DMSO and 270 μl of pre-warmed olive oil were injected i.p. The mice were sacrificed 17 h post Pon A injection and the tumours were excised, fixed and X-gal stained or frozen and the β-galactosidase activity assay performed. Only very few experiments in the literature that use the ecdysone system *in vivo* describe the kinetics of Pon A in *in vivo* models. Initially, this experiment was performed to find the minimum Pon A dose needed for high gene expression as well as to try to find the time needed for gene induction after Pon A injection. Saez *et al.* (2000) have showed that Luciferase gene expression peaked 9-12 h post Pon A administration (3-5

mg/mouse), dropped dramatically at 24 h and that Pon A was almost fully cleared from the body 48 h after its injection with gene expression returning to basal levels [112]. For this reason, a time point of 17 h was chosen to sacrifice the mice after Pon A administration and *Lac* Z gene expression was expected to be observed.

3.5.1 Growth Profile of the Ecdysone Inducible *Lac* Z clone

The volume of each tumour was measured every few days and the growth profile was plotted (**Fig 3.8**). The mice were injected with Pon A once the tumours reached a volume of 200-250 mm^3.

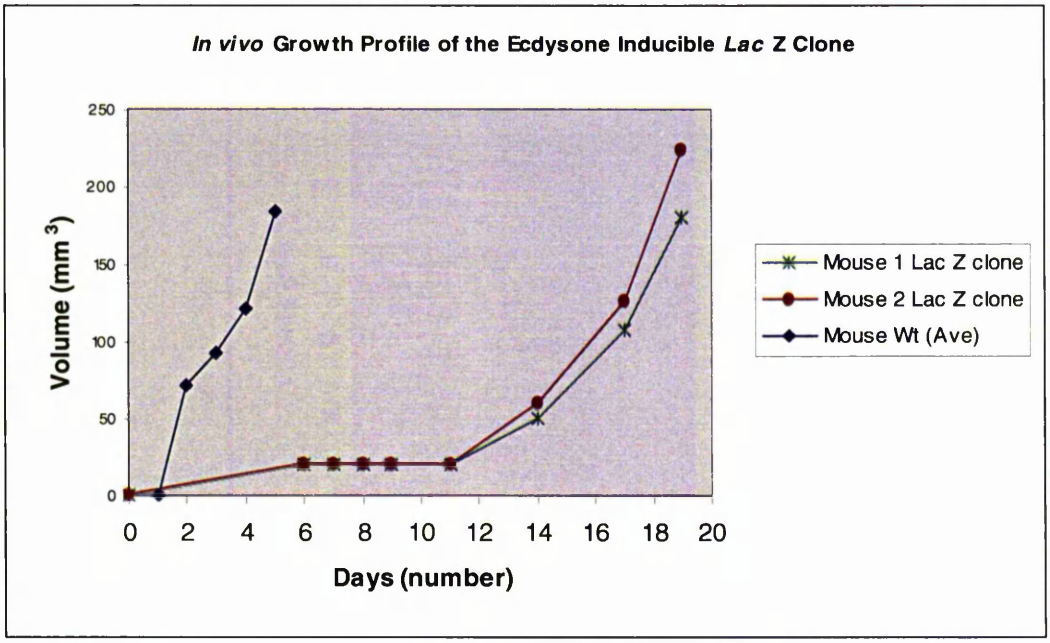

Fig 3.8 Tumour growth profile of the ecdysone inducible *Lac* Z clone (Wt: wild-type HT-1080 tumours).

The doubling time of the HT-1080 ecdysone inducible *Lac* Z clone was 3 days. This was compared to previous experiments performed in our laboratory using the wild-type HT-1080 cells whereby a doubling time of 2.5 days was obtained (unpublished data).

3.5.2 Measuring the Ecdysone Inducible *Lac* Z Expression *in vivo*

The fixed tumours were stained with X-gal for 48 h. The induced tumours turned blue indicating the switching on of gene expression. This is exemplified by the tumour that was

induced with 1 mg/mouse Pon A **(Fig 3.9)** although the tumour stained from the 2 mg/mouse Pon A showed a slightly darker colour upon X-gal staining. The same tumour was also sectioned and stained with β-galactosidase antibodies that are HRP (horse raddish peroxidase)-conjugated. Upon addition of the chromogen substrate (DAB + Chromogen), HRP reacts with this substrate to give a brown-coloured staining **(Fig 3.10)**. The minimum Pon A dose (1 mg/mouse) that showed high gene expression was selected for future use.

The tumour take rate or the percentage of implanted mice that developed tumours was 25 % in this experiment (2/8). An uninduced control was not included in this case due to the limited number of developed tumours. Instead, a dose of 2 mg Pon A was used to treat the second mouse. This experiment was not repeated due to ethical reasons especially that the outcome of high gene expression was clearly seen using 1 mg/ mouse Pon A.

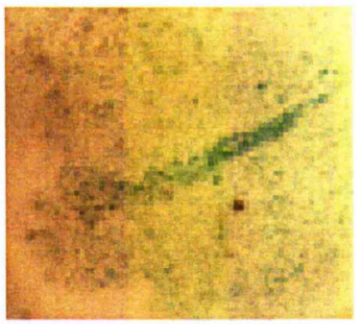

General View- Xgal Staining (5 µm)

Fig 3.9 Upon injecting the mouse with 1 mg Pon A and excision of the tumour 17 h later, the tumour turned dark blue after X-gal staining (the darker region in the middle is due to a fold in the tumour section).

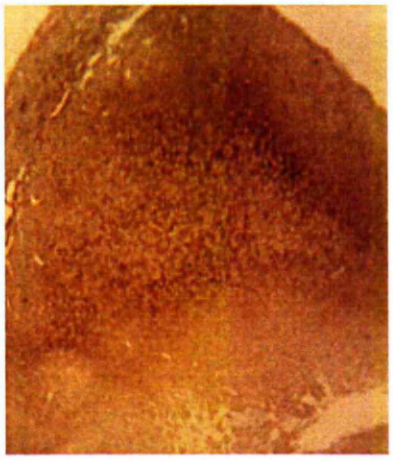

β-galactosidase antibody 10x

β-galactosidase antibody 4x

Fig 3.10 Staining of the tumour (induced with 1 mg/mouse Pon A) by β-galactosidase antibodies. Stained regions produced a brown colour (5 μm section).

Upon X-gal staining of the fixed tumour half **(Fig 3.9)**, homogenous dark blue colour was initially observed. The darker region in the middle of this figure is due to a fold in the tumour section. However, when the tumour was further stained with β-galactosidase antibodies **(Fig 3.10)**, some regions showed darker staining than the others. This suggested that Pon A reached the centre of the tumour as only half of the tumour was fixed and X-gal stained and the dark blue colour was observed at all the edges of this half. However, Pon A might be unable to reach regions that have reduced blood vessels as observed when stained with the β-galactosidase antibodies.

3.5.3 β-galactosidase Enzyme Activity Assay of the Tumour

The tumour was homogenised and sonicated to release the enzymes. After centrifuging at 16,060 g for 10 min, the β-galactosidase enzyme activity assay was performed in order to measure the amount of β-galactosidase enzyme present in the tumour. Increasing absorbance as volume of lysate increased indicated switching on of gene expression in response to Pon A **(Fig 3.11)**. To control for the blood content, the absorbance of the same lysate volume was tested without the addition of the ONPG substrate. However, the activity of this tumour was only 0.002 U/mg. This value is an underestimation of the true

activity due to the high amount of blood present in this tumour whereby the experiment appears to reach saturation (dark yellow colour) before the reaction is complete.

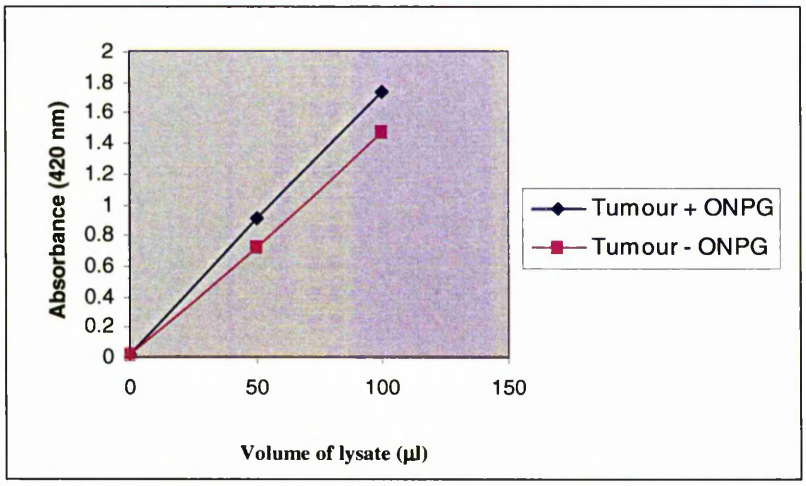

Fig 3.11 This graph shows increasing absorbance with increasing volume of tumour lysate in the presence and absence of substrate (ONPG), which was needed to drive the *β*-galactosidase assay.

3.6 Conclusion

In this chapter, the ecdysone mammalian inducible system was evaluated using the *Lac* Z reporter gene. Transient transfection experiments showed an induction of 20-25 folds at 10 µM Pon A in the MDA-MB-231, HT-1080, and CHO-K1 cell lines.

A double stable clone expressing the *Lac* Z reporter gene in the ecdysone cassette was generated using the HT-1080 cell line. *In vitro* evaluation of the system showed low basal levels, high gene expression in response to Pon A (39.7 U/mg *β*-galactosidase activity at 10 µM), and the existence of an inducer-dose dependent relationship. The fold inductions obtained were moderate (13.7 folds at 10 µM Pon A using the *β*-galactosidase activity assay). A range of fold inductions have been reported in the literature depending on the Pon A dose, time of exposure to Pon A before testing for gene expression, and the type of therapeutic gene used. For example, 42-fold at 1 µM and 54-fold at 6 µM Pon A were

observed 24 h after Pon A administration using the Luciferase reporter gene [120], while only 2-4 folds were observed by Welcsh *et al.* (2002) 12 h after 10 μM Pon A administration in the study of the role of BRCA1 [122]. Again, 2-4 fold induction was observed when MAD2 was studied 20 h after 5 μM Pon A addition [123]. Moreover, we observed that gene expression continues to increase even 72 h post Pon A addition provided that the media was unchanged. However, gene expression did not promptly return to basal levels when the inducer was removed in contrast to what was observed by Saez *et al.* (2000), yet in their experiment 1 μM Pon A was used [112] while these experiments utilise 10 and 20 μM. On the other hand, when cells from the inducible *Lac* Z clone were implanted into mice, high gene expression was observed 17 h after Pon A administration even at 1 mg/mouse.

In conclusion, the ecdysone system seems to be a suitable tool to regulate gene expression both *in vitro* and *in vivo*.

CHAPTER 4

Results 2 *IN VITRO* AND *IN VIVO* REGULATION OF iNOS GENE EXPRESSION USING THE ECDYSONE SYSTEM

4.1 Introduction

Stable clones that constitutively over express iNOS at high levels are difficult to culture because they generate high levels of cytotoxic NO. They are often cultured in the presence of iNOS inhibitors and only for short periods of time as their stability is difficult to maintain due to their high iNOS activity. Moreover, several clones need to be generated in order to obtain varying iNOS expression levels, which might result in clonal variation (Previous work done in our laboratory by Dr. Edwin Chinje). For this reason, an inducible approach to regulate gene expression was sought.

The ecdysone system was initially evaluated *in vitro* and *in vivo* using the *Lac* Z reporter gene. Low basal levels and tight gene regulation in response to the inducer suggested that this system was suitable for regulation of iNOS expression. After ligating the iNOS gene into the ecdysone response vector, gene expression was initially monitored using transient transfection experiments. Then, stable clones that express iNOS in the ecdysone cassette were generated. The expression of the iNOS gene was measured by determining nitrite levels, iNOS activity, as well as by immunostaining for the iNOS protein. Finally, this clone was implanted *in vivo* in order to study its stability and monitor the kinetics of iNOS induction in mice. Then, the tumour that showed highest iNOS expression was cultured *ex vivo* and a higher iNOS gene expression was obtained. This clone was established as xenografts in nude mice again and used to study the effect of iNOS over expression on hypoxia and blood perfusion.

4.2 Ligation of the iNOS cDNA into the Ecdysone Inducible Vector pIND SP1

Having obtained a dose-dependent *Lac* Z gene expression in response to Pon A, similar experiments were performed using iNOS. Initially, the iNOS gene was ligated into the pIND SP1 vector. A source of iNOS cDNA was available from the plasmid vector pEF iNOS IRES-puro [97] and used for the ligation. The iNOS gene is 4164 bp long.

To regulate the expression of iNOS, the iNOS gene had to be inserted into the multiple cloning site of the pIND SP1 vector. Both, the iNOS gene (in pEF IRES-puro) and the pIND SP1 vector were cut by *Nhe* I and *Not* I enzymes (New England Biolabs, Hertfordshire, UK) and run on a 1 % agarose gel. The iNOS gene and the now linear pIND SP1 vector were excised from the gel and extracted. Then, the iNOS cDNA was ligated into the pIND SP1 vector using T4 DNA ligase. Since the same two enzymes cut both insert and vector, the cloning was directional **(Fig 4.1)**.

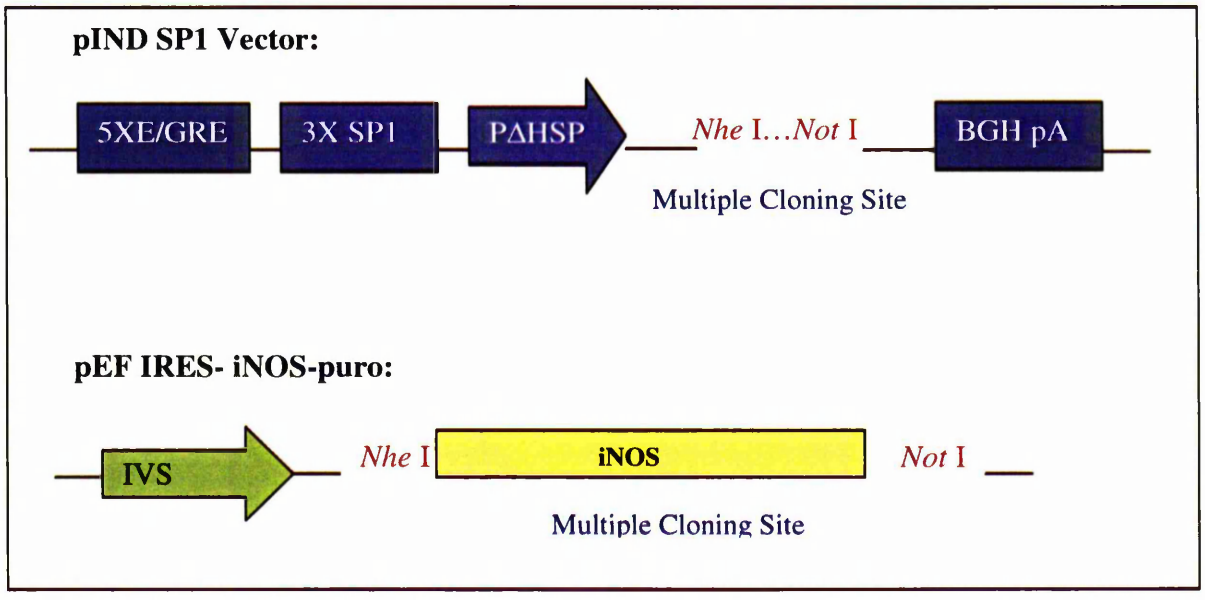

Fig 4.1 Cloning of the iNOS gene into the pIND SP1 vector.

The ligated vector was transformed into *E. coli* (DH5α) as mentioned in **Section 2.4.1**. Mini-preparations and maxi-preparations were performed using the Qiagen Kit

(Section 2.6). To verify that the ligated vector was correct, the new plasmid was cut with *Nhe* I and *Not* I to release the iNOS gene. **(Fig 4.2)**

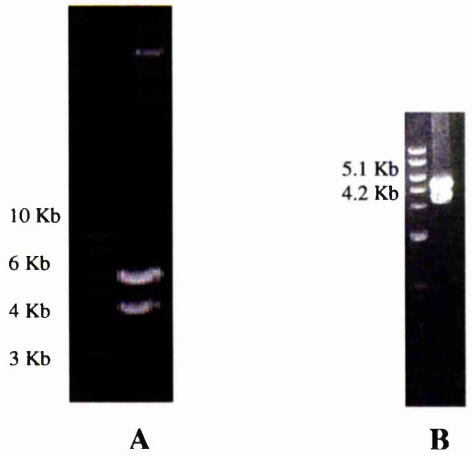

Fig 4.2 A Ligation: Digesting the iNOS gene (4.2 Kb) from pEF IRES puro (5.7 Kb). The iNOS gene is the lower fragment. **B:** Digesting the ligated pIND SP1 iNOS into pIND SP1 (5.1 Kb) and iNOS gene (4.2 Kb) to test for the positive clone. Again the iNOS gene is the lower fragment.

4.3 Ecdysone Inducible iNOS Expression Using Transient Transfection

4.3.1 Flow Cytometry Analysis of Ecdysone Inducible iNOS Expression

To estimate the level of iNOS gene expression achievable using the ecdysone system, HT-1080 and CHO-K1 cell lines were seeded at $1x10^5$ cells/well in a 6-well plate and transiently transfected with pVgRXR and pIND SP1 iNOS (1 µg DNA/well of each vector and 6 µl/well Lipofectin) **(Section 2.8.1)**. After 24 h, varying Pon A concentrations were added. After another 24 h, the cells were formalin-fixed then incubated with a primary rabbit anti-iNOS antibody and secondary goat anti-rabbit FITC conjugated antibody. The samples were assayed using flow cytometry. The cells that express iNOS fluoresced due to the presence of FITC in the secondary antibody. This fluorescence was detected on the flow cytometry machine as FITC is excited at 488 nm and the emission is collected at 530 nm [147]. Fluorescence in each sample was measured by gating (or comparing) against the fluorescence of the control. A gate (usually labelled M) was chosen to measure the

background fluorescence in the control sample. The same gate was used to measure the fluorescence in the other samples. Fluorescence is detected by the percentage of cells that shift to the right hand side in the case of FITC staining. Then, the % fluorescence values (also known as % gated) of each sample and the control were compared. It is noteworthy to mention that in this experiment when the graph of the cells that underwent transfection but were uninduced with Pon A was compared with the control that did not undergo transfection, a shift in the peak (usually reflecting fluorescence due to gene expression) was observed. This could be due to the toxicity associated with the transfection process whereby some cells die because they cannot tolerate the penetration of DNA as well as the lipid carrier (Lipofectin in this case) or due to high iNOS basal expression **(Fig 4.3)**.

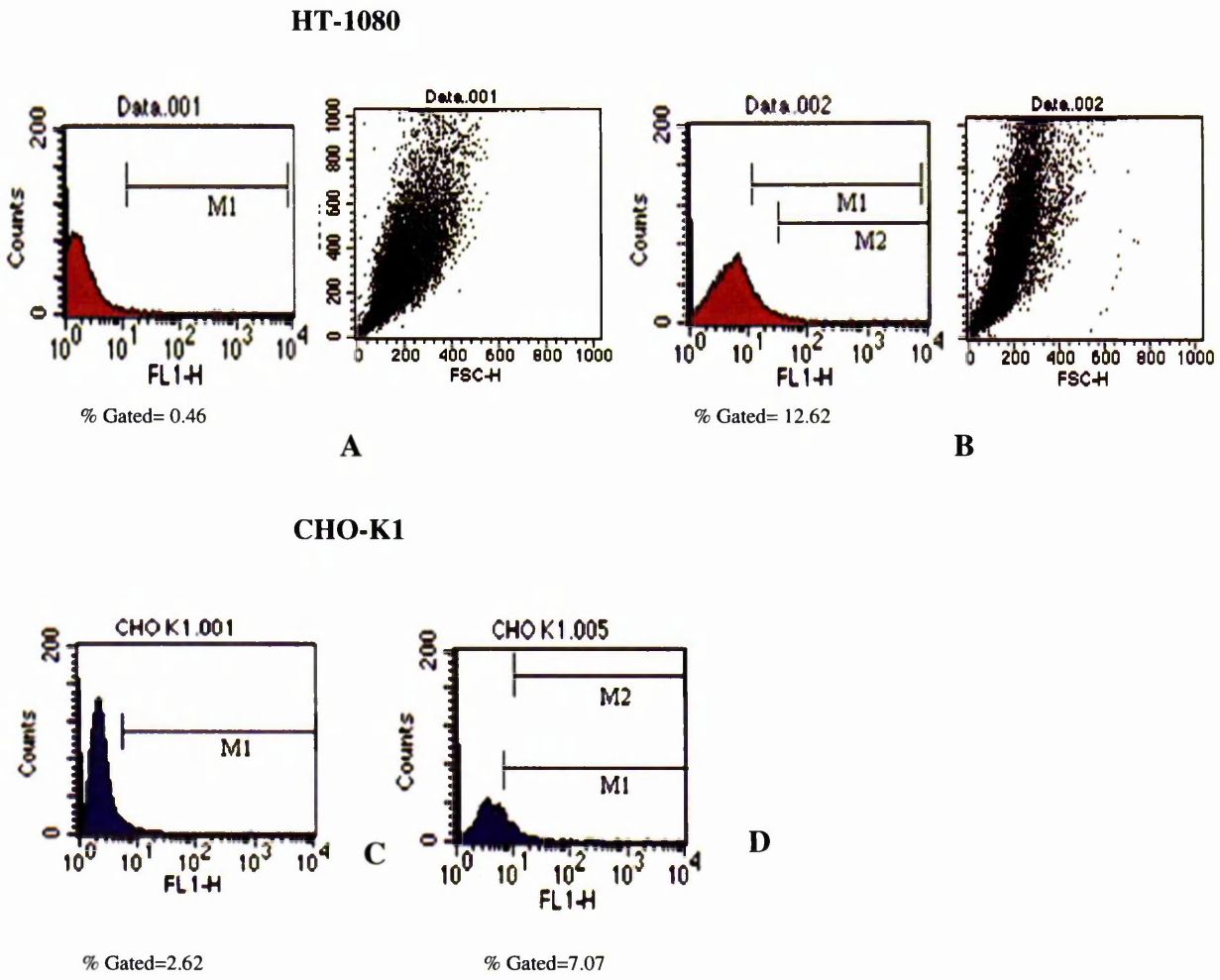

Fig 4.3 In this experiment, gating against wild-type HT-1080 cells (A) did not act as a true control because a shift in peak (FL1-H) was observed after transfection and in the absence of Pon A. Change in cell morphology (FSC-H) was also observed. Thus, the true control was the cells that were transfected but were uninduced with Pon A (B). M1 is the gate set at the background fluorescence of the control sample resulting in 0.46 %. The same gate was used to compare the fluorescence of the transfected cells. Fluorescence has increased from 0.46 % in the wild-type HT-1080 cells (A) to 12.62 % (B) in transfected but uninduced HT-1080 cells. Again a shift in peak (from 2.62-7.07 %) was observed with the untransfected CHO-K1 cells (C) and the transfected uninduced cells (D).

In order to find the % fluorescence due to iNOS gene expression, a new gate (M2) was set in the DNA transfected and uninduced cells. This gate was used as a reference to compare the % fluorescence of the other induced samples **(Figs 4.4, 4.5, and 4.6)**.

HT-1080

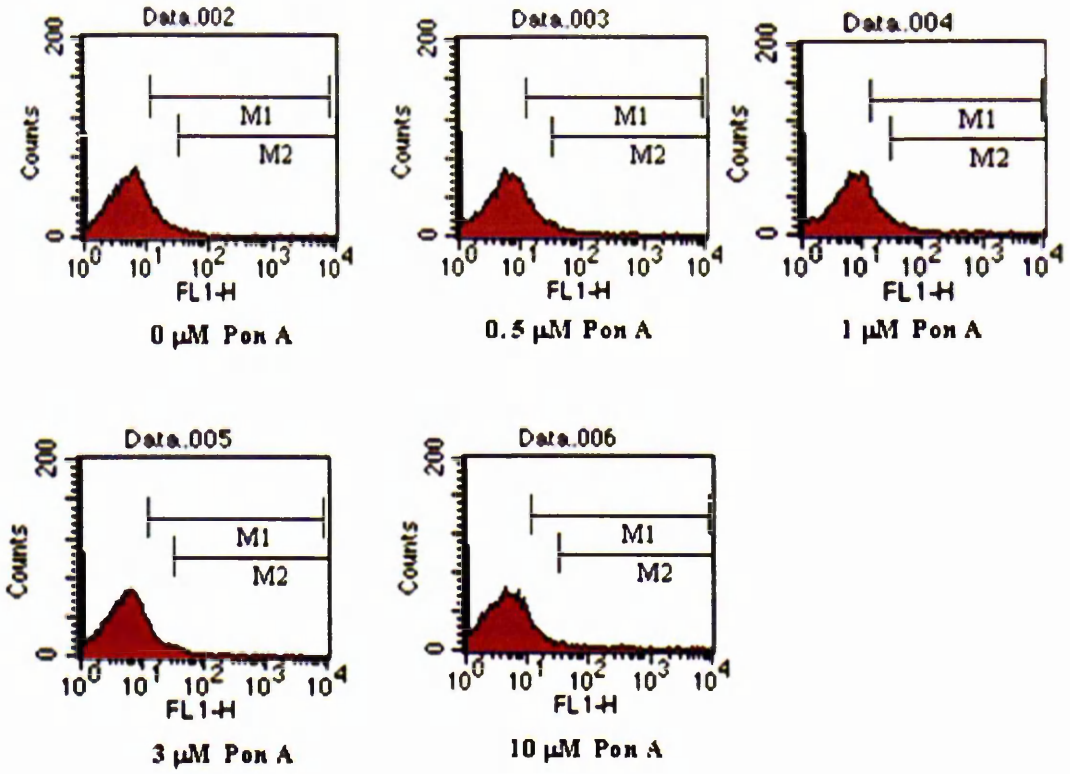

Fig 4.4 To measure the % fluorescence due to iNOS gene expression in the HT-1080 cell line, a new gate (M2) was set in the transfected uninduced (0 µM Pon A) cells as the old gate (M1) did not act as a true gate due to the shift in peak after transfection.

CHO-K1

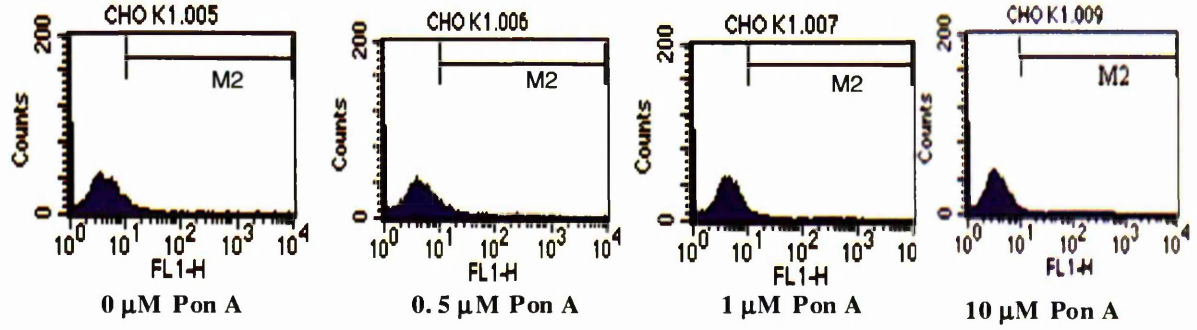

Fig 4.5 To measure the % fluorescence due to iNOS gene expression in the CHO-K1 cell line, a new gate (M2) was set in the transfected uninduced (0 µM Pon A) cells; as the old gate (M1) did not act as a true gate due to the shift in peak after transfection

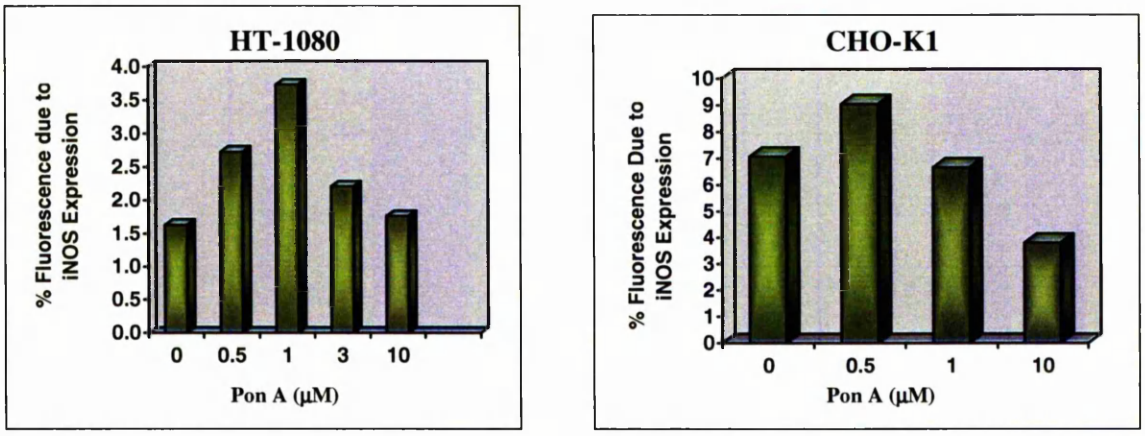

Fig 4.6 The bar chart above shows the % of HT-1080 or CHO-K1 cells immunostaining positive for the iNOS protein as assessed by flow cytometry. The % of positive cells was determined by gating against uninduced transfected cells (M2 in **Figs 4.4 and 4.5**).

In this experiment, gene expression was not in an inducer-dose dependent manner in both cell lines. However, this could be attributed to the inability of the cells to tolerate the transfection process. This experiment was later repeated (using stable clones) and dose-dependent gene expression was observed **(Section 4.5.2)**.

4.3.2 Immunocytochemical Analysis to Determine iNOS Expression

Immunocytochemical experiments were performed in order to detect iNOS expression. The principle behind this experiment was based on the fact that cells expressing iNOS would fluoresce (green) after staining them with the primary rabbit anti-iNOS antibody followed by the secondary goat anti-rabbit FITC conjugated antibody. In this case, the cells were grown on cover slips and staining was detected by fluorescent microscopy. NOS positive cells would fluoresce green whereas nuclei would stain blue due to DAPI stain.

The CHO-K1 cell line was seeded at $1x10^5$ cells/well in a 6-well plate and transiently transfected with pIND SP1 iNOS and pVgRXR (1 μg DNA/well of each vector and 20 μl/well Lipofectin-**Section 2.8.1**). Pon A was added 24 h later for a period of 48 h. This timing was chosen in an attempt to increase gene expression. After staining, the samples were analysed using a fluorescent microscope (**Fig 4.7**). The same experiment was performed

using the HT-1080 and MDA-MB-231 cell lines but iNOS expressing cells were not detected due to the low transfection efficiency.

CHO-K1

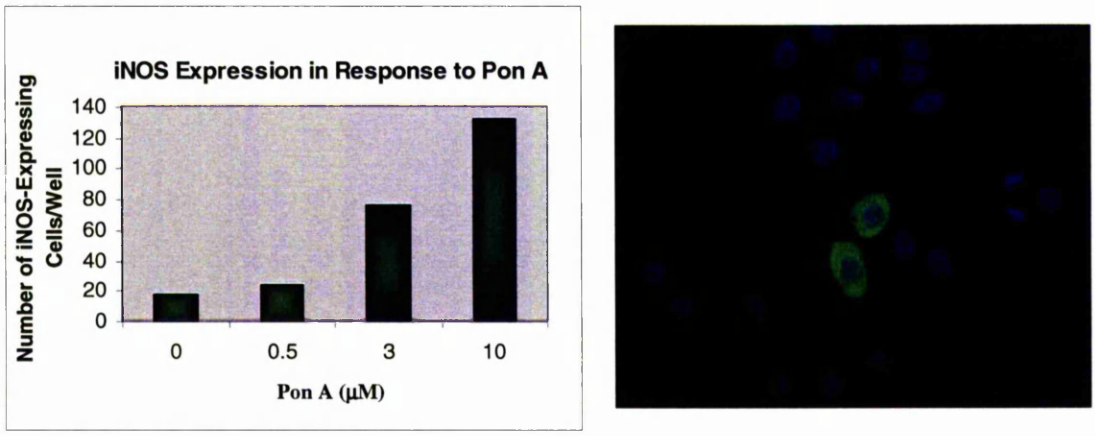

A **B**

Fig 4.7 A Green CHO-K1 cells were counted per cover slip (10 fields of view per cover slip) for varying Pon A concentrations. **B** Nuclei stain blue with the DAPI stain while cells expressing the iNOS protein stain green due to FITC.

Again, the results showed dose-dependent induction with minute basal expression and 7.4 fold induction at 10 μM Pon A. The above picture also shows that iNOS (green) is a cytosolic protein. The results were consistent with those of the X-gal stained cells that transiently express the *Lac* Z reporter gene in the ecdysone cassette **(Section 3.2)**.

4.4 Generation of Stable Ecdysone Inducible iNOS Clones

Having confirmed the functionality of the pVgRXR and pIND SP1 iNOS plasmids and in order to obtain reproducible gene expression, a stable clone expressing the iNOS gene in the ecdysone cassette was generated. This allowed the study of the dual role of iNOS in tumourigenesis *in vitro* and *in vivo*.

4.4.1 Stable Transfection of the pVgRXR Clones with pIND SP1 iNOS

Previously established clones that stably express pVgRXR (namely MDA-MB-231 clones 9 and 12 and HT-1080 clone 16) were stably transfected with pIND SP1 iNOS (1

μg/well) and using 20 μl/well Lipofectin (**Section 2.8.2**). The iNOS inhibitor L-NNA (100 μM) was used to avoid any iNOS-mediated cell-toxicity which might be caused in case the ecdysone cassette integrates next to a promoter in the host genome that might result in unregulated switching on of gene expression. L-NNA competes with L-arginine to bind to the active site of NOS.

Potential clones were grown and induced with 5 μM Pon A to test for stable transfection with both pIND SP1 iNOS and pVgRXR. The griess assay was used to screen for positive clones.

4.4.2 Screening for Positive Clones Using the Griess Assay

The cells were seeded at $2.5x10^4$ cells/well in a 96-well plate and dosed with 5 μM Pon A. After 24 h, the griess assay was performed. After it is produced by NOS, NO is converted into nitrite and nitrate. The griess assay measures the total nitrite in the media and thus indirectly quantifies NOS expression in the samples. Absorbance of the induced samples was measured at 540 nm and compared to that of the uninduced cells. Clone 16.10 showed a positive result (**Figs 4.8 and 4.9**).

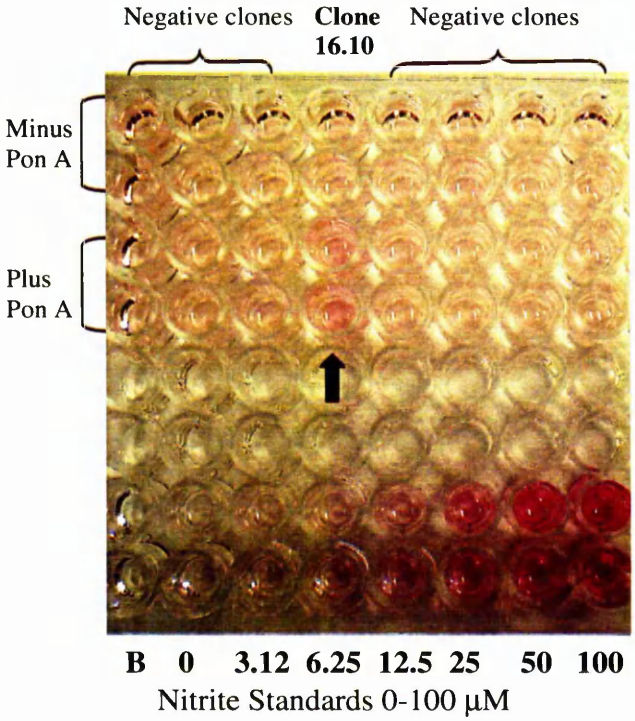

Fig 4.8 In the presence of 5 μM Pon A, clone 16.10 produced more nitrite than in the absence of Pon A. This is due to the expression of the iNOS gene. All other clones were negative (B is the blank containing only the reaction buffer used in the assay).

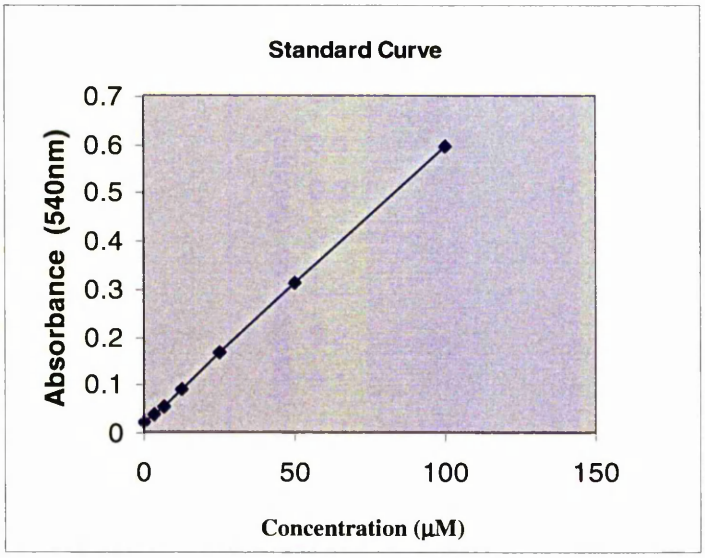

Fig 4.9 A standard curve that was used to calculate the concentration of nitrite from the unknown sample.

Clone 16.10 showed an average absorbance of 0.046 in the absence of Pon A and an average absorbance of 0.1 in the presence of 5 μM Pon A. This corresponds to a nitrite concentration of 4.36 μM and 13.85 μM respectively. Thus, a 3-fold induction was observed and this indicates that clone 16.10 is positive. Only one clone was positive in the HT-1080 cell line and none in the MDA-MB-231. This could be due to the need to stably transfect the cells with 2 plasmids. The possibility of cell death due to NO production was unlikely due to the addition of L-NNA. Stocks of the HT-1080 clone 16.10 were frozen in liquid nitrogen for later use.

4.5 *In vitro* Evaluation of the Stable HT-1080 iNOS Clone

4.5.1 Quantification of NOS Activity Using the L-citrulline Assay

In order to evaluate the stable HT-1080 iNOS clone, the L-citrulline assay was performed. This assay provides functional analysis of the clone and measures NOS activity after inducing the cells with varying concentrations of Pon A.

The cells were split into T-75 falcon flasks and were induced with varying Pon A concentrations and left for 24 h. Then, the L-citrulline assay was performed.

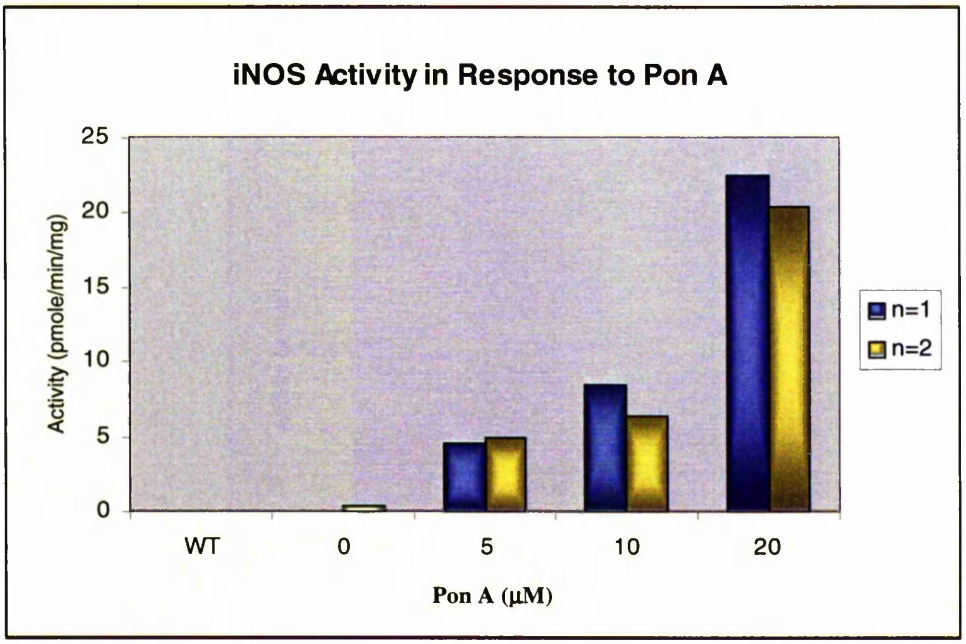

Fig 4.10 NOS activity measurements in the presence of increasing Pon A concentration. WT is HT-1080 wild-type and has an activity of 0 pmol/min/mg at 20 μM Pon A. All other samples are the stable clone HT-1080 16.10 iNOS induced with Pon A (this experiment was performed in duplicate wells and hence both results n=1 and n=2 are showed). No activity was observed with the uninduced clone in n=1.

The L-citrulline assay showed an increase in NOS activity with increasing Pon A concentration **(Fig 4.10)**. NOS activity reached a maximum of 21.5 pmol/min/mg with 20 μM Pon A. At 10 μM, 7.4 pmol/min/mg was achieved. This activity was lower than that obtained by Xu *et al.* (2002) who generated stable human foetal kidney cells that express iNOS using the ecdysone system. At 10 μM Xu *et al.* (2002) obtained 33 ± 4 pmol/min/mg [56]. A reason for this difference in results could be due to the different cell lines used. It is expected from previous work in our laboratory that these levels of iNOS expression may cause pro-tumour effects [47].

4.5.2 Immunocytochemical Staining of the iNOS Protein

In order to observe whether all the cells are stimulated to over express iNOS at 20 μM Pon A, the ecdysone inducible iNOS clone was further evaluated using an immunocytochemical approach whereby iNOS protein was stained. The cells were seeded at

$1x10^5$ cells/well on cover slips in a 6-well plate and induced with varying concentrations of Pon A the following day. After 24 h, the cells were fixed and stained using iNOS antibodies. The samples were then visualised using a fluorescent microscope **(Fig 4.11)**

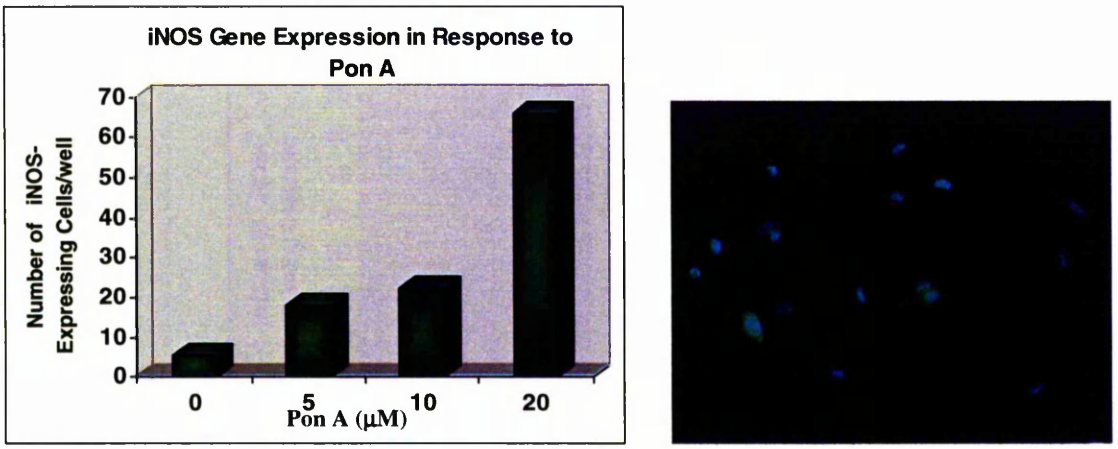

Fig 4.11 A As Pon A concentration increased, the number of iNOS expressing cells increased **B** An image showing fluorescence due to iNOS expression with 20 μM Pon A. iNOS expressing cells were stained green and the nuclei were stained blue (20x magnification).

These results showed gene expression in response to Pon A administration. It was also observed that even at 20 μM Pon A, many cells did not express iNOS. This could be due to the impurity of the clone whereby some cells possibly retained the selection markers but lost the iNOS cDNA due to its large size as compared to the backbone vector pIND SP1. On the other hand, an increase in the dose of Pon A could drive higher gene expression. However, it was noticed that at high Pon A concentration levels, cell death was observed which might reflect some Pon A mediated toxicity, an effect that was similarly observed in the inducible *Lac* Z clone.

4.5.3 Measuring Pon A Toxicity Using the MTT Assay

To monitor the toxic effects of Pon A, an MTT assay was performed. The HT-1080 wild-type cells were seeded at $2.5x10^3$ cells/well in a 96-well plate. After 2 h, the cells were induced with varying concentrations of Pon A (0,5,10,15,20,30,40,50,75,100 μM). After

another 24 h, the media was replaced with fresh Pon A-free RPMI media. After 2 days, the MTT assay was performed (**Fig 4.12**).

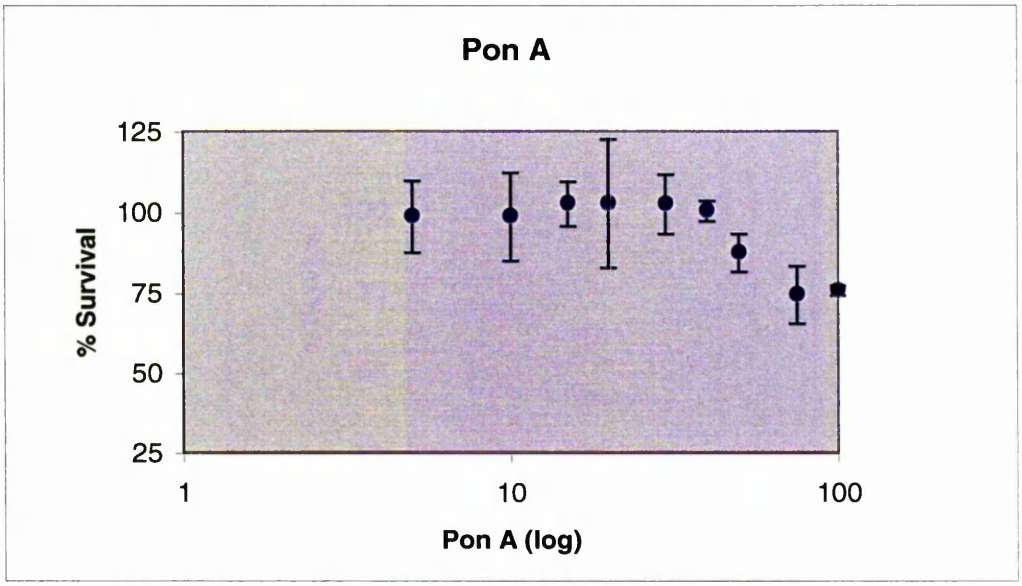

Fig 4.12 Measuring Pon A toxicity using the MTT Assay (average values of triplicate wells).

The results show 12 % cell death at 50 μM Pon A. However, because in this experiment the Pon A containing media was removed after 24 h and the cells were allowed to proliferate for 2 more days in the absence of Pon A, concentrations of less than 30 μM were used in further experiments to avoid any toxic effects of this inducer.

4.5.4 Flow Cytometric Analysis of iNOS Expression

This clone was also evaluated using flow cytometry to detect iNOS gene expression. The cells were seeded at $1x10^5$ cells/well in a 6-well plate and induced with varying concentrations of Pon A. After 24 h, the cells were formalin-fixed, immunostained with iNOS antibodies and the results were interpreted using flow cytometry (**Fig 4.13**). Fluorescence of the induced cells was compared to that of the uninduced cells.

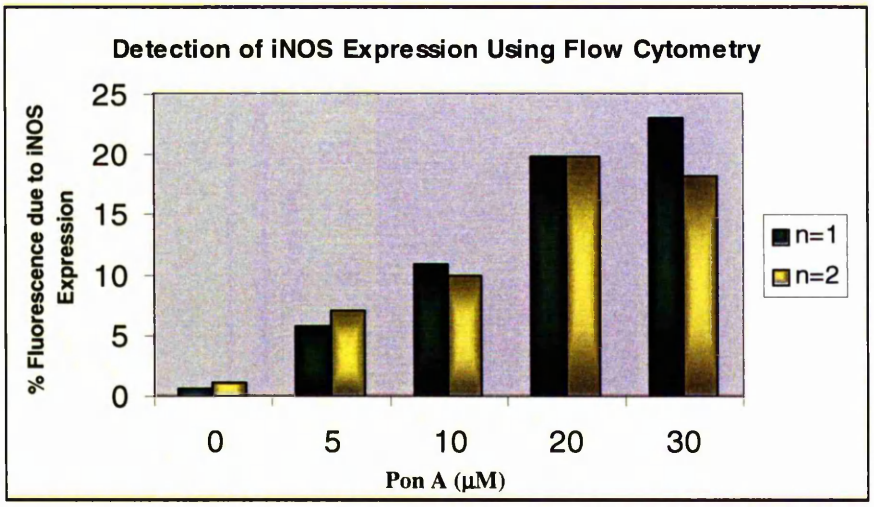

Fig 4.13 Detection of inducible iNOS expression using flow cytometry. As Pon A concentration increased, fluorescence increased reaching up to 20 % with 20 μM Pon A (this experiment was performed in duplicate wells and both results are shown: n=1 and n=2).

As observed in the immunocytochemical staining experiment **(Section 4.5.2)**, gene expression increases with increasing Pon A concentrations. In this experiment, iNOS gene expression was estimated to be 20 % when induced with 20 μM Pon A. In order to try to increase this expression, higher Pon A doses were used. However, cell death was microscopically viewed at 30 μM Pon A. This can also be observed in **Fig 4.14** by the shift in peak in the wild-type cells that were treated with 20 μM Pon A (2.21 % fluorescence) as opposed to those untreated with Pon A (0.67 % fluorescence). This fluorescence could be caused by Pon A.

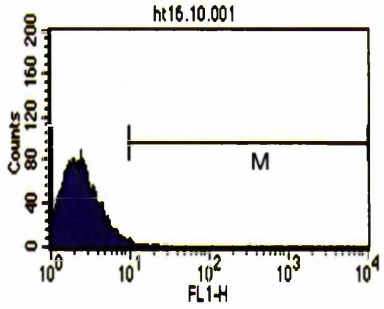

Wt- 0 μM Pon A
(0.67 %)

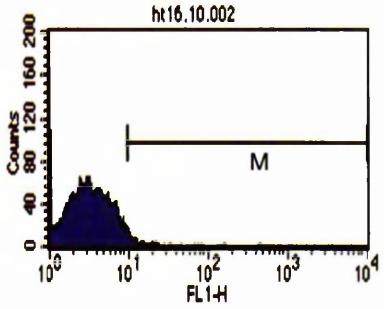

Wt- 20 μM Pon A
(2.21 %)

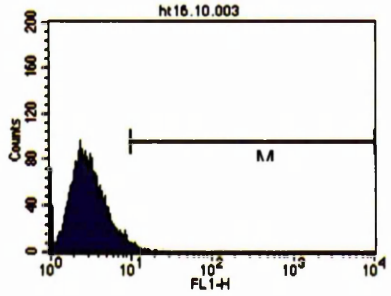

Clone- 0 μM Pon A
(0.70 %)

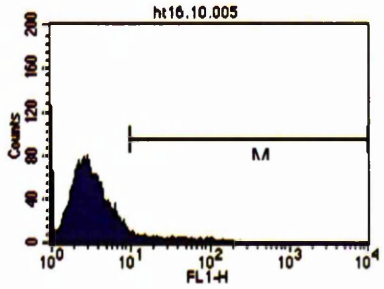

Clone- 5 μM Pon A
(5.81 %)

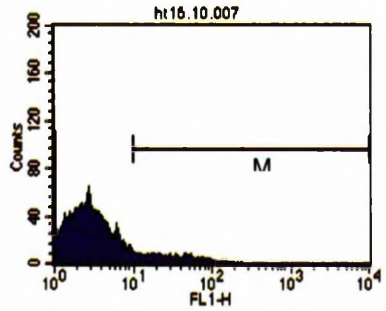

Clone- 10 μM Pon A
(10.95 %)

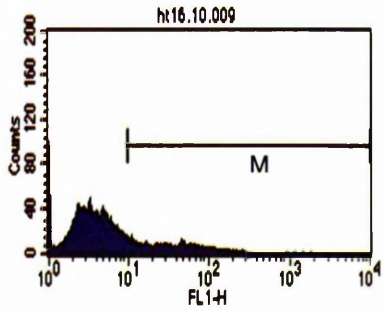

Clone 20 μM Pon A
(19.88 %)

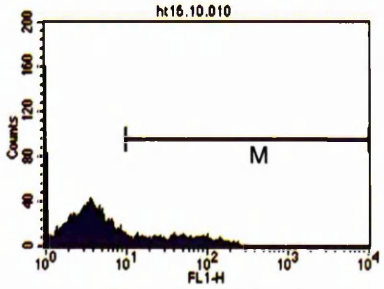

Clone -30 μM Pon A
(23.07 %)

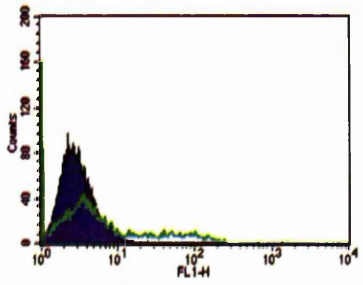

Overlay of the Clone at 0 (blue) and 30 μM Pon A (green)

Fig 4.14 Representative graphs showing the increase in fluorescence due to iNOS gene expression in response to increasing Pon A concentrations. M is the gate set at 0.67 % in the uninduced wild type (Wt) and at 0.70 % in the uninduced clone to account for the background fluorescence. The same gate was used to compare fluorescence of the induced cells. The last graph shows an overlay of fluorescence of the 30 μM-induced (green line) and uninduced (purple) clone.

4.5.5 Growth Curves of the Wild type, Ecdysone Inducible *Lac* Z and iNOS HT-1080 Clones

The growth curves of the HT-1080 wild-type cells, the ecdysone inducible *Lac* Z, and ecdysone inducible iNOS clones were determined in the presence and absence of Pon A. This allowed the comparison of the growth properties of the wild-type and the clones as well as monitor any effects caused by Pon A administration or NO generation.

The cells were seeded in 6-well plates at $1x10^4$ cells/well and induced with Pon A (0 or 20 μM) after 4 h. Every day, the content of each well was trypsinised in 1 ml trypsin and counted in order to plot a growth curve **(Fig 4.15)**.

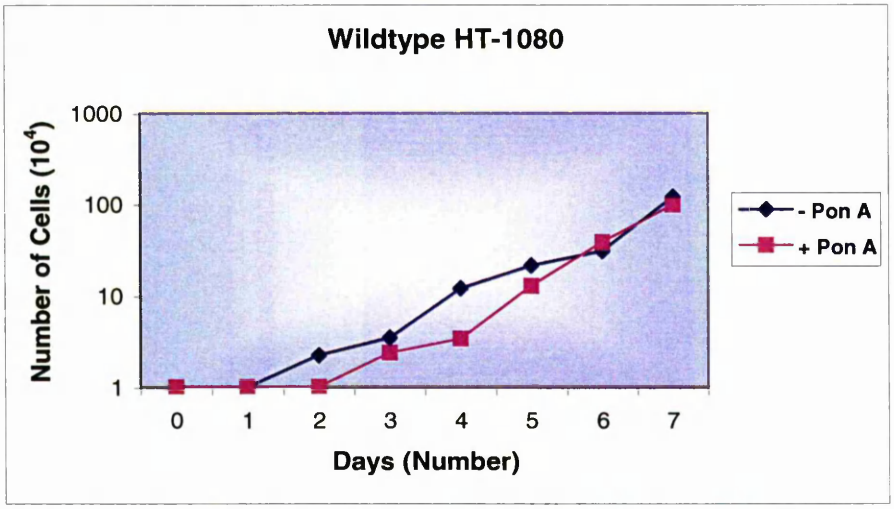
Wildtype HT-1080
Number of Cells (10^4)
1000
100
10
1
0 1 2 3 4 5 6 7
Days (Number)
- Pon A
+ Pon A

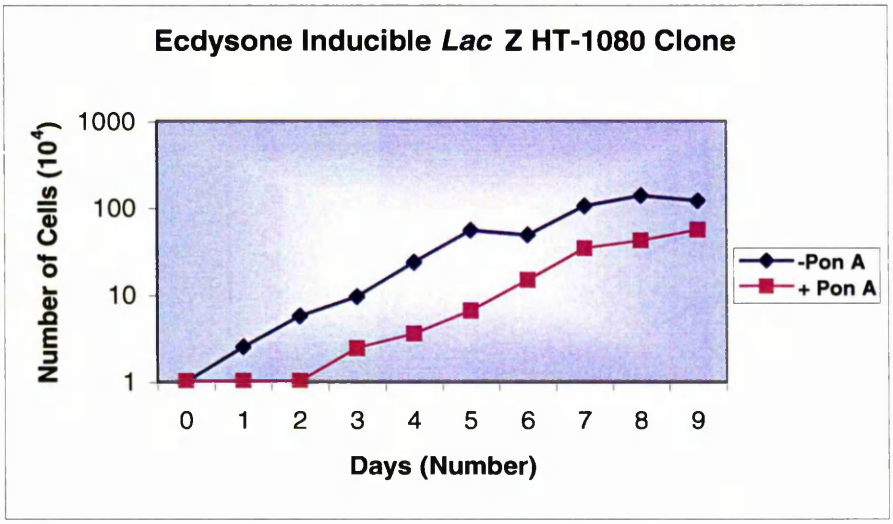
Ecdysone Inducible *Lac* Z HT-1080 Clone
Number of Cells (10^4)
1000
100
10
1
0 1 2 3 4 5 6 7 8 9
Days (Number)
-Pon A
+ Pon A

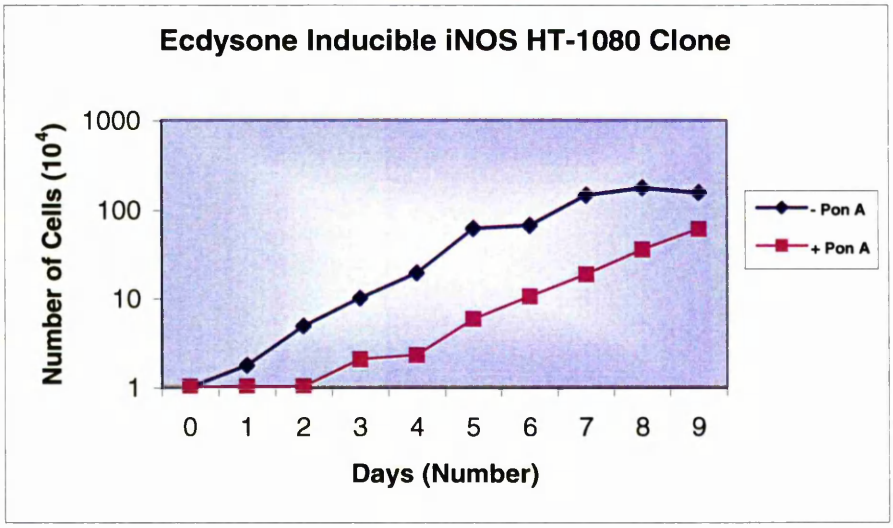
Ecdysone Inducible iNOS HT-1080 Clone
Number of Cells (10^4)
1000
100
10
1
0 1 2 3 4 5 6 7 8 9
Days (Number)
- Pon A
+ Pon A

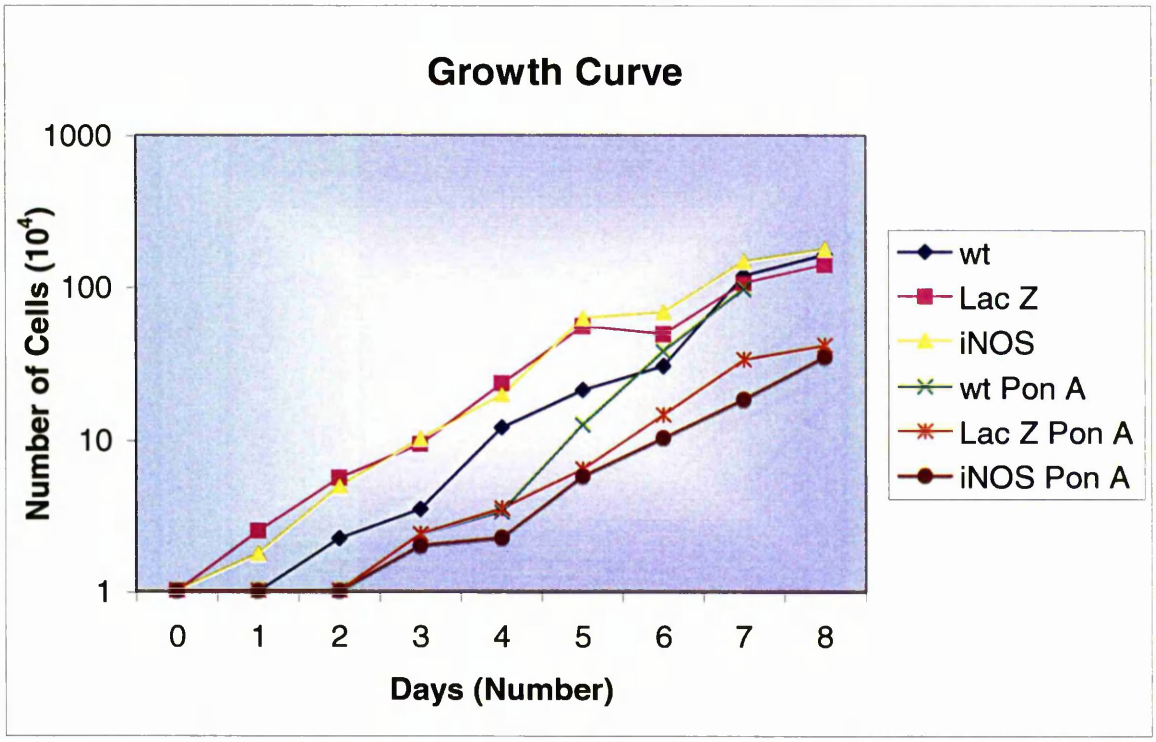

Fig 4.15 The above graphs show the growth curves of the wild-type HT-1080 and the ecdysone inducible *Lac* Z and iNOS HT-1080 clones in the presence and absence of Pon A ($1x10^4$ cells/well were seeded). The last curve is an overlay of all graphs (this experiment was performed in duplicate wells and the average values are shown).

In the absence of Pon A, the doubling time of the wild-type HT-1080 cell line was 2 days. The doubling time for the *Lac* Z clone was 1 day and that of the iNOS clone was 2 days. In the presence of Pon A, the doubling time was not affected and was 1 day for the wild-type cells and 2 days for each of the clones. However, Pon A caused a growth delay of 1 day in the wild type and 3 days in each clone before the cells reach the logarithmic phase of growth. This experiment also indicated that NO did not cause toxicity in the iNOS clone since the growth delay in the iNOS and *Lac* Z clone was the same.

4.5.6 Effect of Multiple Pon A Dosing on Gene Expression

To study the effect of multiple Pon A dosing on iNOS expression, cells from the HT-1080 inducible iNOS clone were seeded at $1x10^5$ cells/well in a 6-well plate and induced with 20 μM Pon A. The cells were treated with either 1 dose of Pon A for 1 day, 2 doses for

2 days, 3 doses for 3 days, 1 dose for 3 days or 2 doses for 3 days. The media was replaced each day. In addition, in one sample, 2 doses of Pon A were administered but the same Pon A containing medium was left till the third day. The samples were formalin-fixed on the second, third, or fourth day depending on the conditions mentioned above. Then, the cells were immunostained with iNOS antibodies and assayed using flow cytometry.

Sample Label	Sample Description	% Fluorescence Due to iNOS Expression
A	No Pon A 3days	0.83
B	1dose 1day (media was changed on day 2)	22.14
C	2doses 2days (media was changed on day 2)	29.93
D	3doses 3days (media was changed on day 2 & 3)	24.60
E	1dose 3days (media was changed on day 2)	6.87
F	2doses 3days (media was changed on day 2 & 3)	12.24
G	2doses 3days (media was unchanged on day 3)	30.52

Table 4.1 Values in this table represent gene expression in response to multiple Pon A dosing (average values of duplicate wells).

The results showed that dosing twice on 2 consecutive days increases gene expression the most indicating that Pon A does not reach saturation when given at 1 dose. Dosing for more days did not increase gene expression indicating that Pon A could have reached the saturation limit by which it can induce iNOS gene expression using this clone. Moreover, when the media was changed after 1 Pon A dose (E), gene expression was reduced by 3.2 fold 48 h after Pon A removal but was still 8.3 fold higher than the basal level (**Table 4.1**).

4.5.7 Examining the Stability of the HT-1080 Inducible iNOS Clone Over Time

To study the stability of this clone (16.10), fresh vials of stored cells were defrosted from liquid nitrogen and used. The cells were grown in the presence or absence of antibiotic selection since defrosting and for a total period of 4 weeks. The cells were then split into T-

75 falcon flasks and were treated with varying Pon A concentrations. After 24 h, the cells were assayed for iNOS activity using the L-citrulline assay (**Fig 4.16**).

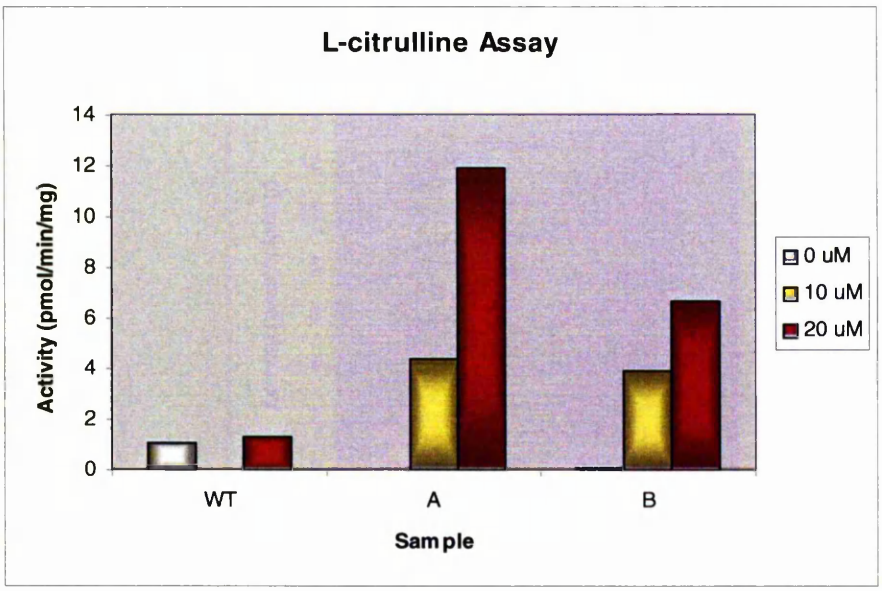

Fig 4.16 The cells were induced with Pon A for 24 h and then assayed using the L-citrulline assay (WT is the wild-type HT-1080, A is the clone cultured with selection, and B is the clone cultured without selection. Each sample was induced with 0, 10, and 20 μM Pon A. Note that the activities of the WT at 10 μM and clone A at 0 μM was 0 pmol/min/mg).

A Pon A-dose response relationship was observed in all the samples; however, the cells that were cultured out of selection (**Fig 4.16** B) showed a decrease in fold induction indicating that the clone could lose activity if cultured for long periods of time.

In order to confirm this finding, new vials of the same clone (16.10) were defrosted from the stocks stored in liquid nitrogen and assayed for their activity using the L-citrulline assay. After defrosting, the cells were grown until confluent in T-75 flasks. Then, each sample was divided (1:10) into a T-75 flask, induced the following day with 20 μM Pon A, and assayed 24 h after induction. Again, the vial that was cultured least before freezing (approximately 2 weeks-designated as 16.10/2) showed higher NOS activity (33.8 pmol/mg/min) as compared with the vial cultured longer before freezing (approximately 8 weeks-designated 16.10/8) (24.8 pmol/mg/min). It was also observed in this experiment that

the clone that was cultured for the longest period of time (approximately 12 weeks after defrosting -designated 16.10/2/12) lost almost all the activity (0.53 pmol/mg/min).

In order to monitor iNOS gene expression, the same vials were cultured and induced with 20 μM Pon A. They were immunostained with iNOS antibodies, and the % fluorescence due to iNOS expression was interpreted using flow cytometry. Once again, the least cultured clone (16.10/2) showed highest expression as compared with the other clones (16.10/8 and 16.10/2/12) **(Fig 4.17)**.

% Fluorescence Due to iNOS Gene Expression:

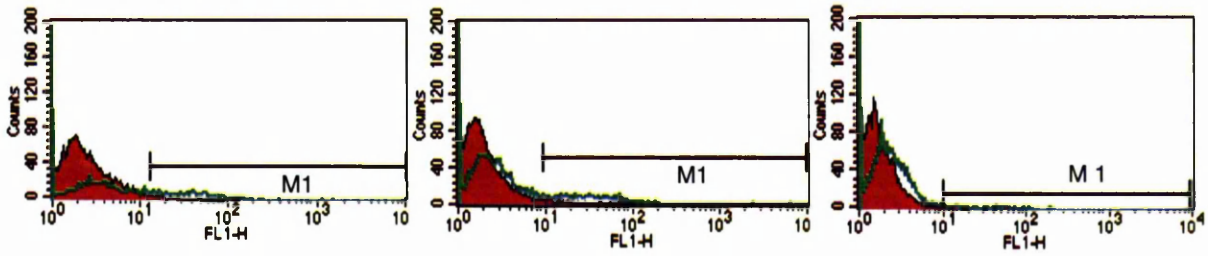

16.10/2 **16.10/8** **16.10/2/12**

Sample	16.10/2	16.10/8	16.10/2/12
- Pon A	0.70	0.45	0.16
+ Pon A	13.67	11.1	2.07

Fig 4.17 Three batches of the clone were tested for iNOS gene expression using flow cytometry. These graphs represent an overlay of the percentage fluorescence due to iNOS gene expression in the presence (green line) or absence (red graph) of Pon A. M1 is the gate get set at the background fluorescence in each uninduced sample.

At the same time and in order to refine the ecdysone inducible iNOS clone and increase the percentage of iNOS expressing cells, the 16.10 clone that was in culture for approximately 10 weeks (16.10/2/10) was seeded at 100 cells/well in a 6-well plate and cultured to reach a T-75 flask. This dilution aims to kill any wild-type cells present in the clone due to the presence of antibiotic selection. It was expected that at this low cell density, the selection pressure was higher. However, only 2 sub-cultures survived and when they were induced with 20 μM Pon A for 24 h and tested using the L-citrulline assay, a very low

activity of 0.5 and 0.16 pmol/mg/min was observed indicating that the wild-type cells had a better chance of survival even in the presence of antibiotic selection. This could be due to initially integrating the ecdysone plasmids that carry the resistance selection markers into the cells but the later loss of the iNOS gene possibly due to selection pressure. For this reason, in all the subsequent studies the 16.10/2 iNOS clone was used (unless mentioned otherwise) and was only allowed to remain in culture for a maximum period of 4 weeks after which it was replaced with fresh vials of the same stock.

4.5.8 Effect of the iNOS Inhibitor L-NNA on the Clone

Since some basal iNOS expression was observed in the absence of Pon A, the cells were cultured in the presence of the iNOS inhibitor L-NNA (100 μM). This inhibitor blocks the formation of NO and therefore should stop any basal NO-mediated toxicity that might be causing the clones to lose the iNOS cDNA even though the levels of NO seemed modest when uninduced.

In this experiment, the effect of culturing the cells in the presence or absence of the iNOS inhibitor L-NNA was studied. Fresh vials of the HT-1080 iNOS 16.10/8/1 clone were cultured either in the presence or absence of L-NNA for 4 weeks. After that, the cells were seeded at $1x10^5$ cells/well in a 6-well plate, induced with 20 μM Pon A for 24 h and immunostained with iNOS antibodies. Gene expression was assayed using flow cytometry **(Table 4.2)**. The results indicate that cells cultured in the presence of L-NNA showed slightly higher levels of iNOS expression.

% Fluorescence Due to iNOS Expression:

Sample	0 μM Pon A	20 μM Pon A
Without L-NNA	2.09	9.18
With L-NNA	2.05	14.23

Table 4.2 The effect of the iNOS inhibitor L-NNA on gene expression.

Although this result was unexpected, culturing the cells in the presence of an inhibitor has shown better iNOS expression.

4.6 Stable Transfection of the Ecdysone-iNOS Cassettes in Other Cell lines

In order to produce higher iNOS activity for apoptotic studies, another attempt to generate stable clones using the MDA-MB-231 and HCT-116 cell lines was performed.

4.6.1 Stable Transfection

HCT-116 and MDA-MB-231 cell lines were transfected with both pVgRXR and pIND SP1 iNOS together in order to obtain stable clones **(Section 2.8.2)**.

Some modifications to the protocol used to generate stable HT-1080 clones were performed in an attempt to obtain clones that express higher levels of iNOS. The cells were seeded in a 6-well plate at $2x10^5$ cells/well and incubated at 37 ^{0}C overnight. On the second day, the transfections were performed using Lipofectamine reagent instead of Lipofectin. In the first tube, 0.5 µg/well of pVgRXR and 0.5 µg pIND SP1 iNOS/well were mixed with 100 µl/well Opti-MEM® I medium. In another tube, 10 µl/well Lipofectamine were added to 100 µl/well Opti-MEM® I medium. Both tubes were mixed immediately and then left for 45 min. After washing the cells with 2 ml/well Opti-MEM® I medium, the transfection medium was added to the cells and left overnight. Then, the medium was replaced with fresh RPMI medium that contains 10 % v/v foetal calf serum. After 48 h, the medium was replaced with selection medium (**Table 3.1 and Table 4.3** in addition to 100 µM L-NNA inhibitor) and the cells were placed in culture plates and left 12-14 days. Colonies were then picked and cultured while maintained under antibiotic selection.

A number of 48 colonies of HCT-116 and 11 colonies of MDA-MB-231 were picked from each experiment. It is noteworthy to mention that different antibiotic concentrations **(Table 4.3)** were used with the HCT-116 cell line in an attempt to get high gene expression.

Plate	*Zeocin (μg/ml)*	*G418. Sulphate (μg/ml)*
A	100	250
B	100	500
C	100	1000
D	200	500

Table 4.3 Concentration of antibiotics used in order to generate stable pVgRXR and pIND SP1 iNOS clones in the HCT-116 cell line. In each plate, Zeocin and G418.Sulphate were added.

The clones were induced with 20 μM Pon A and screened to find those that express high levels of iNOS.

4.6.2 Screening of the HCT-116 and MDA-MB-231 Transformants for Positive Ecdysone Inducible iNOS Clones

In order to screen for stable ecdysone inducible iNOS expression, 24 HCT-116 and 11 MDA-MB-321 clones were tested using the L-citrulline assay, NOS reductase assay, and by immunostaining. Once enough cells were obtained for screening, the cells were induced with 20 μM Pon A for 24 h. The samples were then assayed for iNOS activity (**Table 4.4**). The NOS reductase assay was performed as it utilises a smaller number of cells ($1x10^5$ cell/well) than the L-citrulline assay and therefore the clones could be screened at an earlier time point. Although some clones showed a high iNOS activity when measured using the L-citrulline assay, this activity was not observed using the reductase assay nor was a high iNOS expression level observed by immunostaining. Only the clones that gave the highest activities are shown in **Table 4.4**.

Sample	L-Citrulline (pmol/min/mg)	NOS-Reductase (nmol/min/mg)
MDA-MB-231-Wt	12.2	7.1
MDA-MB-231-3	13.6	9.6
HCT-116-Wt	1.49	8.2
HCT-116-1	34.0	9.1
HCT-116-22	18.82	11.6

Table 4.4 Potential MDA-MB-231 and HCT-116 clones were screened once using the L-citrulline and once using the NOS-reductase assays. In this experiment, the MDA-MB-231 wt gave higher activity than the expected (0.87 pmol/min/mg-data previously generated in our laboratory by Dr. Edwin Chinje) (wt:wild type).

After screening with the L-citrulline and the NOS-reductase assays, the clones that gave the highest iNOS activity were immunostained with the iNOS antibodies and assayed using flow cytometry (**Table 4.5**). However, all of these clones confirmed lower gene expression than the already established HT-1080 ecdysone inducible iNOS clone that was used as a control in this experiment.

% Fluorescence due to iNOS Gene Expression:

Sample	- Pon A	+ Pon A
HT-1080 iNOS clone	0.94	25.65
MDA-MB-231-3	3.95	7.4
HCT-116-1	4.15	5.55
HCT-116-22	6.84	13.16

Table 4.5 Gene expression in the absence and presence of Pon A as detected by immunostaining and flow cytometry.

After being screened with 3 differernt assays, the HCT-116 and the MDA-MB-231 clones were found to express lower iNOS levels than the HT-1080 ecdysone inducible iNOS clone and were consequently discarded. The experiments were continued using the HT-1080

ecdysone inducible iNOS clone (16.10/2). The inability to produce highly expressing iNOS clones might be due to the fact that 2 plasmids are needed for gene expression.

4.7 *In Vivo* and *Ex Vivo* Evaluation of the HT-1080 Ecdysone Inducible iNOS Clone

4.7.1 Implanting the Ecdysone Inducible iNOS Clone *in vivo*

Although the ecdysone inducible iNOS clone has shown an activity of 21.5 pmol/min/mg and the percentage of iNOS fluorescing cells was 20 % when induced with 20 μM Pon A, this clone (16.10/2) was evaluated *in vivo* in order to measure its tumour take rate, its stability *in vivo*, as well as study the kinetics of iNOS induction in mice. In order to maintain high activity, cells from the 16.10/2 iNOS clone were defrosted from liquid nitrogen and cultured for less than 1 week before implanting into mice. The ability of i.p-injected-Pon A to reach the tumour site at a minimal dose to drive iNOS gene expression was monitored. Cells were injected s.c at $2x10^6$ cells/0.1 ml/mouse into the nude mice. Once a tumour volume of 300-400 mm^3 was achieved, Pon A concentrations of 1 and 2 mg/mouse dissolved in 30 μl DMSO and 270 μl of pre-warmed olive oil were injected i.p. (Control mice were injected with pre-warmed olive oil and DMSO only). The mice were sacrificed 18-26 h after Pon A injection. These doses and time points were chosen based on the previous experiments conducted using the inducible *Lac* Z clone whereby high *Lac* Z gene expression was observed at 1 mg/mouse 17 h post Pon A injection. **(Section 3.5)**

The tumours were excised and stored frozen. Then, the L-citrulline assay was performed.

4.7.2 Tumour Take Rate

The take rate in this experiment was only 16.7 % (4 mice out of 24). Possible reasons include clonal characteristics and a possibility of some leakiness in the system whereby iNOS was expressed as the tumour was developing and thus high NO levels might have

caused tumour death at an early stage although this was not expected from the *in vitro* characterisation of the clone.

4.7.3 Quantifying the iNOS Activity of the Tumour Lysates Using the L-Citrulline Assay

The mice were sacrificed 18-26 h post Pon A injection. The tumour xenografts were homogenised and the L-citrulline assay was performed on the lysates. It was observed that only the mouse that was treated with 1 mg Pon A had a measurable amount of NOS activity detected in the tumour lysate (**Table 4.6**).

Sample	Pon A dose (mg/mouse)	Activity (pmol/min/mg)
Mouse-26 h after Pon A injection	0	0
Mouse-26 h after Pon A injection	1	6.57
Mouse-26 h after Pon A injection	2	0
Mouse-18 h after Pon A injection	2	0

Table 4.6 iNOS activity in response to i.p Pon A administration to mice bearing the ecdysone inducible HT-1080 iNOS clone. After inducing the mice with Pon A, the tumours were excised and homogenised. The lysates were assayed using the L-citrulline assay.

The fact that most of the obtained tumours showed undetectable NOS activity levels could reflect the difficulty to maintain stability of clones expressing 2 plasmids and a toxic gene *in vivo*. However, one tumour resulted in an iNOS activity of 6.57 pmol/min/mg indicating that in this case the clone was able to survive the stability pressure. This activity was compared to two previously established constitutive MDA-MB-231 iNOS clones that express 8.94 pmol/min/mg and 33.1 pmol/min/mg *in vivo*. These clones have an *in vitro* activity of 11.62 and 66.20 pmol/min/mg respectively. The wild-type MDA-MB-231 cell line

has shown no activity *in vivo* (Dr. Edwin Chinje). The activity of any clone appears to be lower *in vivo* than *in vitro* as iNOS levels can accumulate in *in vitro* culture conditions [36].

4.7.4 Measuring the Activity of iNOS in the *Ex Vivo* Cultured Cells

Cells from the tumour that showed 6.57 pmol/mg/min iNOS activity were cultured *ex vivo* for 4 weeks. The cells were later dosed with 20 μM Pon A for 24 h. Then, cell-lysates were prepared and analysed using the L-citrulline assay (**Table 4.7**).

Sample	WT	*Ex-vivo*	*Pre- in vivo*
0 μM Pon A	0	1.83	0.2
20 μM Pon A	6.68	21.9	21.5

Table 4.7 NOS activity (pmol/min/mg) of the *ex vivo* cultured tumour compared to that of the clone before being implanted in the mice (labelled pre-*in vivo*)

The unexpected high level of iNOS activity observed in the induced cells even after being implanted *in vivo* and cultured *ex vivo* indicated that this particular clone (designated 16.10/T) was stable.

4.7.5 Flow Cytometry Analysis of the *Ex Vivo* Culture

iNOS gene expression in the *ex vivo* culture was also evaluated using flow cytometry. After being in culture for 4 weeks, the iNOS 16.10/T cells were seeded at $1x10^5$ cells/well in a 6-well plate. The following day, the cells were induced with 20 μM Pon A for 24 h, after which the cells were immunostained with iNOS antibodies and assayed using flow cytometry. A higher fold of induction was observed in the *ex vivo* culture as compared to the original 16.10/2 iNOS clone (**Table 4.8 and Fig 4.18**).

% Fluorescence Due to iNOS Gene Expression:

Sample	-Pon A	+Pon A
Ex-Vivo	1.61	27.08
Pre-in vivo	0.90	19.88

Table 4.8 *Ex vivo* cultured cells were induced with 20 µM Pon A and immunostained with iNOS antibodies. Fluorescence due to iNOS gene expression was analysed using flow cytometry and compared to the pre-*in vivo* values (average values of 2 separate experiments).

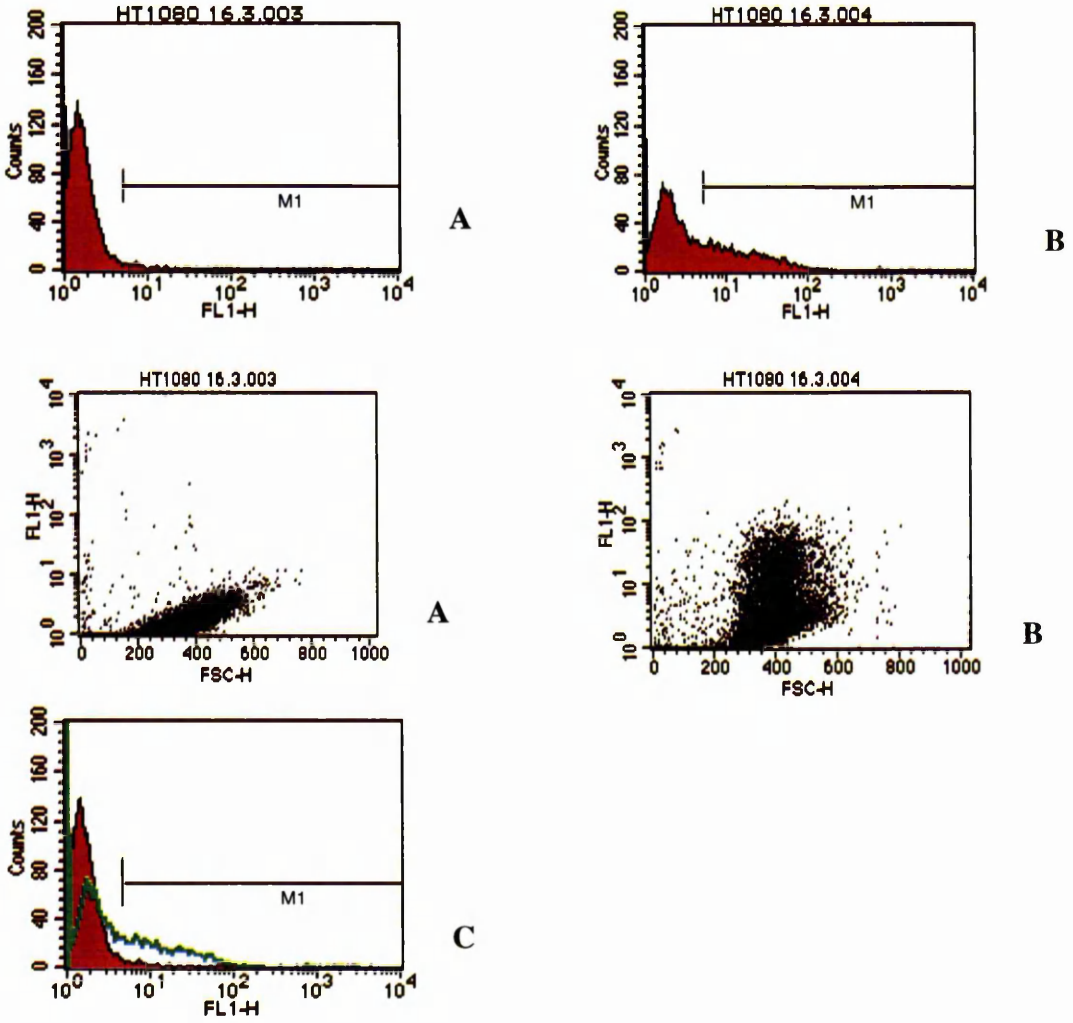

Fig 4.18 Cells from the tumour that was induced with 1 mg Pon A for 26 h were cultured *ex vivo*. These graphs represent the percentage of fluorescence due to iNOS gene expression detected with the flow cytometry. **A** Uninduced cells **B** Induced cells (20 µM Pon A). **C** An overlay graph of the induced (green) and uninduced (red) cells. M1 is the gate set at the background fluorescence of 1.21 % in the uninduced sample and used to compare fluorescence of the induced sample (representative graphs of 2 separate experiments).

This indicated that the clone was still expressing high levels of iNOS upon Pon A induction. It is noteworthy to mention that fluorescence of the clone increased when the clone was cultured *ex vivo* compared to the experiment performed before the clone was implanted *in vivo*. This flow cytometry experiment of the 16.10/T iNOS clone was repeated 3 weeks later and the same % of gene expression was observed (data combined in **Table 4.8**). This indicated that the clone seemed to have been slightly purified when implanted *in vivo*. Stocks of this 16.10/T iNOS clone were frozen and stored in liquid nitrogen. Future experiments were conducted using this ecdysone inducible HT-1080 iNOS 16.10/T clone.

4.8 Studying the Role of iNOS on Tumour Vascularisation Using the HT-1080 Purified Ecdysone Inducible iNOS Clone

This experiment aimed to evaluate the ecdysone system *in vivo* using the ecdysone inducible HT-1080 iNOS clone. In addition, the early effects of iNOS expression on tumour physiology, perfusion, and hypoxic fraction were studied.

4.8.1 Cell Implanting and Administration of Staining Markers

Cells from the HT-1080 ecdysone inducible iNOS clone (16.10/T) were grown as tumour xenografts. The cells were implanted s.c at $5x10^6$ cells/0.1 ml/mouse. Once a tumour volume of 200-250 mm^3 was achieved, a Pon A concentration of either 0 or 1 mg/mouse was administered i.p. Pon A was dissolved in 270 µl of pre-warmed olive oil and 30 µl DMSO (Control mice were injected with pre-warmed olive oil and DMSO only). The mice were sacrificed and the tumours were excised 12, 24, or 48 h post Pon A administration (**Table 4.9**). The concentration and the duration of Pon A were chosen based on the experiments performed by Saez *et al.* (2000) [112] and the previous evaluation of the ecdysone system using the HT-1080 ecdysone inducible *Lac* Z clone **(Section 3.5)** whereby a high level of reporter gene expression was obtained with 1 mg/mouse Pon A, 17 h post Pon A administration. The purchase price of Pon A was a limiting factor.

Hypoxic and blood perfusion markers were administered to all of the mice in order to study the effect of iNOS on tumour physiology. A volume of 0.2 ml of Pimonidazole (a marker for hypoxia) (Natural Pharmacia International, RTP, NC, USA) at 66 mg/kg was injected i.p 2 h before sacrificing and 0.1 ml of Hoechst 33342 (a blood perfusion marker) at 3 mg/0.5 ml was injected intravenously (i.v) 1 min before sacrificing. After sacrificing the mice, the tumours were collected and stored half fixed and half frozen for later sectioning and immunostaining.

Pon A(mg/mouse)	0	0	0	1	1	1
Time to Excision (h)	12	24	48	12	24	48
Number of Tumours	1	1	2	2	2	2
Mouse Label	G	D	E,H	C,F	B,J	A,I

Table 4.9 Pon A dosage and excision time after Pon A administration for each mouse.

4.8.2 Tumour Growth Profile

In this experiment, the tumour take rate increased to 50 % (10/20). This might be explained due to trypsinising the cells and suspending them with serum free medium instead of serum containing medium. This higher tumour take rate could also be due to the purified clone (16.10/T) now being used. It was observed that 3 tumours required a longer period of time to start growing, but once they reached a volume of 50 mm^3 they entered the log phase of growth. The tumour growth profiles of all the 10 tumours are plotted in **Fig 4.19**.

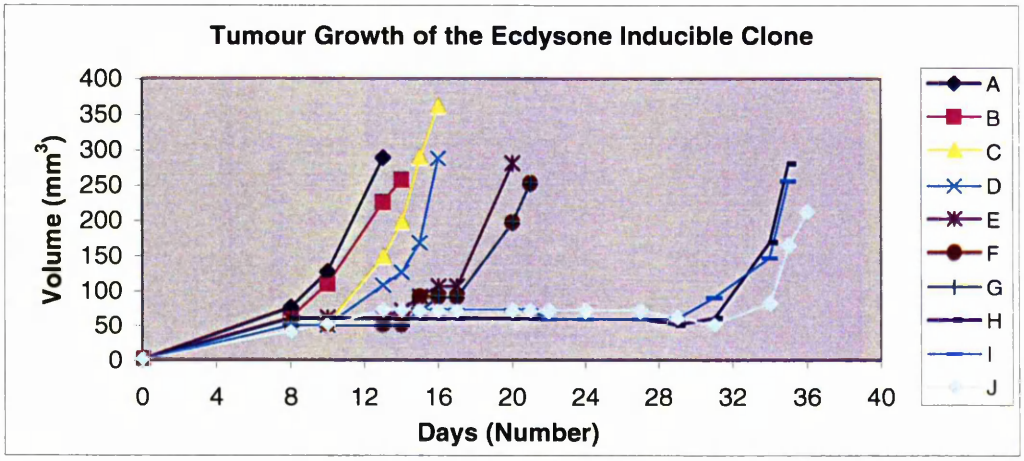

Fig 4.19 A graph showing the growth of ecdysone inducible iNOS HT-1080 tumours *in vivo*.

As soon as the tumours were established and reached a volume of 50 mm^3, the doubling time of the tumours was measured. The doubling time of this clone *in vivo* was an average of 2.2 days, which is similar to that of the wild-type (2.5 days) **(Section 3.5.1)**.

4.8.3 Staining of the Tumours to Determine Hypoxic Regions

In order to study whether increased iNOS levels regulate the hypoxic fraction, mice implanted with the ecdysone inducible iNOS clone were first administered with Pon A to induce iNOS expression and then injected 2 h before sacrificing with Pimonidazole, which binds to hypoxic cells. Pimonidazole is well distributed to all tissues in the body including the brain but only binds to cells that have oxygen concentrations less than 14 μM. This is equivalent to a pO_2 of 10 mm Hg at 37 ^{0}C [195,196].

After sectioning, the tumours were stained with the Hydroxyprobe^{TM}-1 Mab1 (Natural Pharmacia International, RTP, NC, USA), which is a primary antibody that binds to the protein adducts caused by the reduced Pimonidazole [197]. A secondary antibody provided by DAKO EnVision Kit was added. The secondary HRP-antibody binds to the primary antibody and stained regions produce a dark brown colour upon addition of the chromogen substrate (DAB + Chromogen). Control sections were stained with the secondary antibody only to control for non-specific binding.

Two sections/tumour were stained to detect hypoxic regions. For each tumour, the section that showed the highest intensity of staining was scored from 1-5 (1 being the least). **(Table 4.10)**. Samples B, F, and G showed an increased intensity of Pimonidazole staining compared to the background, while sample E for example did not show any staining **(Fig 4.20)**. However, no correlation was observed between hypoxic staining and the pattern of Pon A injection in mice. This may be because Pon A could not reach the hypoxic regions due to the reduction in blood vessel functioning within these sites.

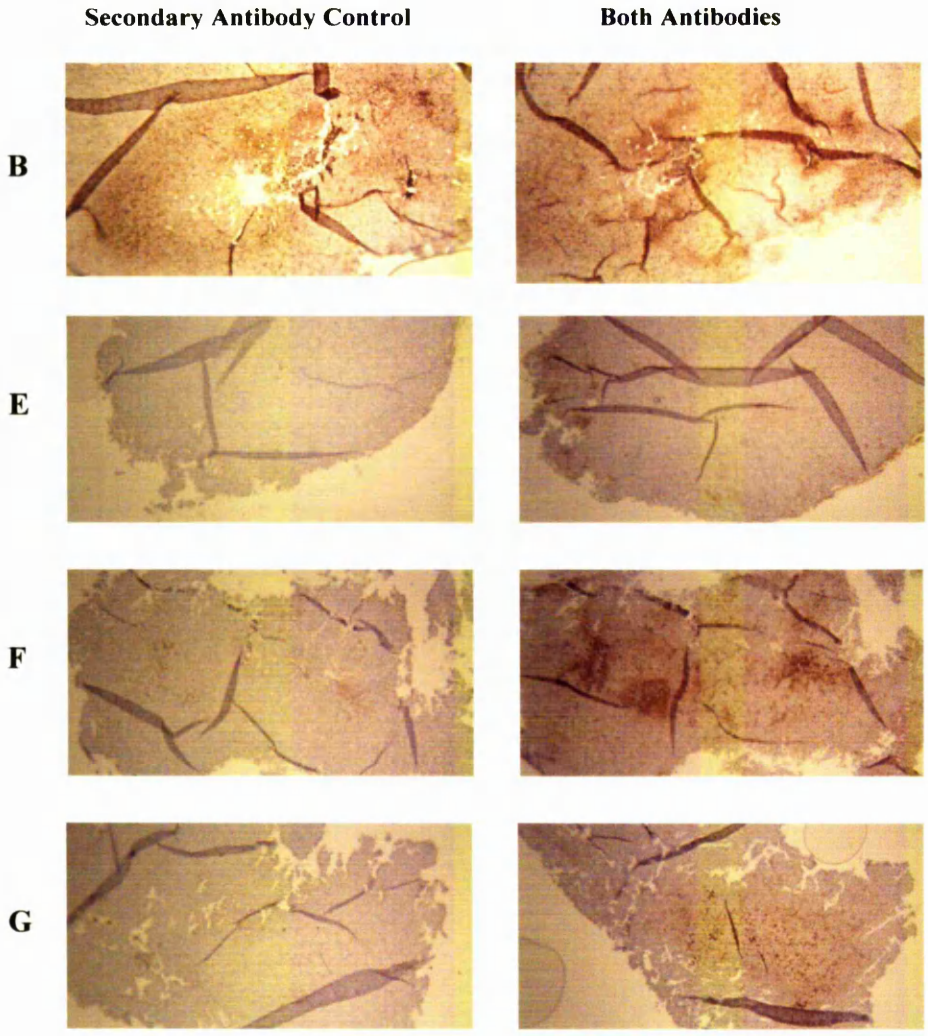

Fig 4.20 Staining for hypoxic regions using Pimonidazole. Tumour sections shown in this figure were stained with both primary and secondary antibodies or simply the secondary antibody that acted as a background control for non-specific binding (10x magnification).

Sample	A	B	C	D	E	F	G	H	I	J
Score (1-5)	3	5	2	1	1	5	3	1	2	1
Pon A (mg/ mouse)	1	1	1	0	0	1	0	0	1	1
Time to Excission	48	24	12	24	48	12	12	48	48	24

Score	12 h	24 h	48 h
0 mg Pon A	3	1	1,1
1 mg Pon A	2,5	1,5	2,3

Table 4.10 Score for Pimonidazole intensity for each sample.

Previous experiments in our laboratory showed that the HT-1080 cell line has a hypoxic fraction, which is estimated to be 6.2 % in the wild-type tumours [198]. The ecdysone inducible HT-1080 clone has shown considerable amount of heterogeneity in hypoxic fraction, which was independent of Pon A dosing. Some studies suggest that low NO levels could promote hypoxia [199] and in that case an increase in the hypoxic fraction should have been observed in our experiment. However, other studies suggest that NO may have a pro-tumourigenic role [26] and therefore cause a decrease in hypoxia. For this matter and since the wild-type tumours have a small percentage area of hypoxic regions, locating tumours with even a lower percentage could be difficult and might explain our results.

4.8.4 Hoechst Staining as a Marker for Blood Perfusion

To study the effect of iNOS expression on vascular formation, a blood perfusion marker (Hoechst 33342) was used [200]. Mice implanted with the ecdysone inducible iNOS HT-1080 clone were injected with Pon A to induce iNOS expression and then injected with Hoechst 33342 i.v. 1 min before sacrificing.

After excision, frozen tumours were cryostat sectioned and visualised under a fluorescent microscope. Photographs of the regions with the highest brightness (coloured blue and correspond to blood perfusion) were captured from each section and were viewed on the computer. Then, a single and random threshold for brightness was set as a reference to compare the brightness of the samples (**Fig 4.21**). The percentage area of brightness/field of view above the defined threshold was calculated by the computer and was used to estimate blood perfusion (**Table 4.11**).

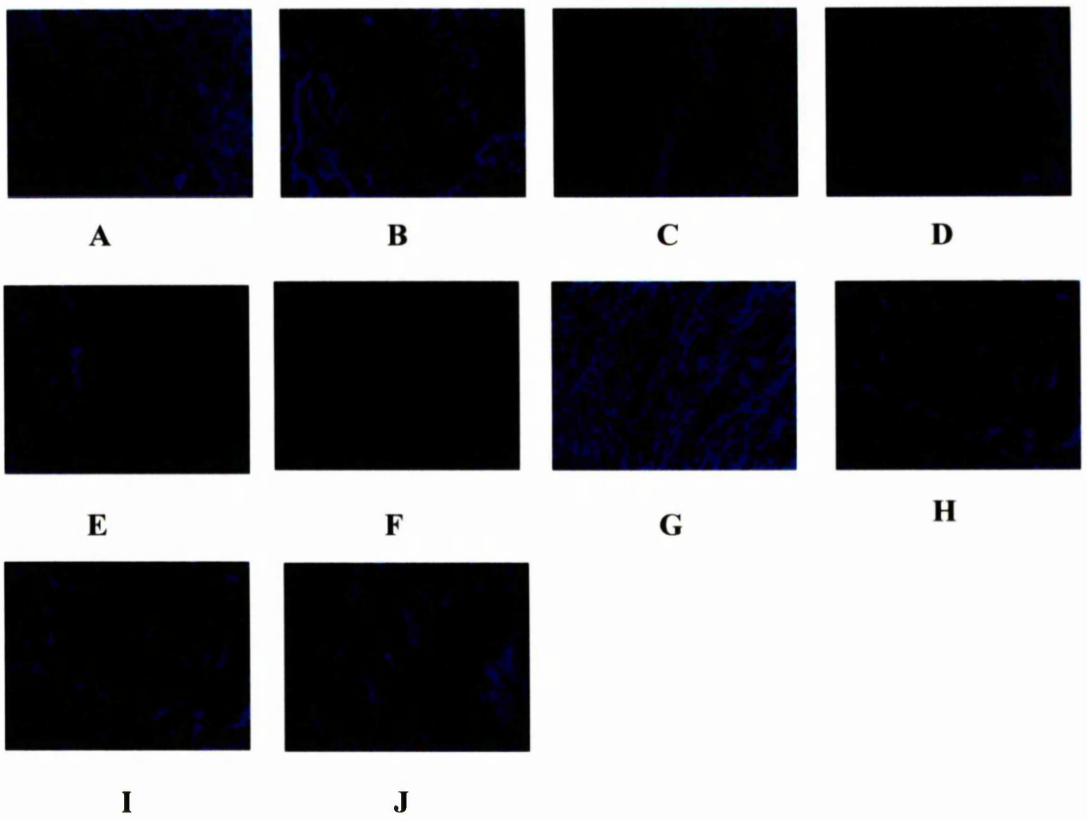

Fig 4.21 Hoechst staining photos of tumour sections. The bright blue represents blood perfusion (40x magnification).

Sample	A	B	C	D	E	F	G	H	I	J
% Area Above Threshold	7.23	7.25	8.88	5.00	5.57	4.22	12.87	6.44	5.15	10.98

Average % Area Above Threshold	12 h	24 h	48 h
0 mg Pon A	12.87	5.00	5.57, 6.44
1 mg Pon A	8.88, 4.22	7.25, 10.98	7.23, 5.15

Table 4.11 These tables show the % area that is above the set threshold. The values represent blood perfusion.

This experiment suggested a peak in % area-above-threshold at 24 h in the mice dosed with 1 mg Pon A. This hinted to a possibile increase in blood vessel perfusion in response to iNOS up-regulation at this time point. The only exception to this was the mouse excised after 12 h and untreated with Pon A (mouse G). However, because this was only one sample and since the other untreated mice (n=3) showed a minimal degree of hoescht staining, mouse G was excluded in this case.

In this experiment, different sections were used to stain for hypoxic regions and blood perfusion. Therefore, a clear correlation was not observed between the Pimonidazole and Hoechst staining. However, the results hinted that only in the presence of Pon A, and when iNOS expression was expected to be at its maximum levels (24 h), the highest degree of blood perfusion was observed (9.12 %). This correlated with lowering the degree of hypoxic fraction (3 on the scoring system).

4.8.5 Detection of iNOS Expression

Tumour sections were stained with iNOS antibodies using varying antibody concentrations in order to improve the staining protocol, yet no iNOS expression was detected in any of the samples (performed at least 3 separate times in duplicate sections).

4.9 Conclusion

In this chapter, the ecdysone system was used to tightly regulate iNOS gene expression. Initially, the iNOS gene was ligated into the ecdysone response vector. Then, preliminary iNOS-immunostaining experiments showed inducer-dose dependent gene expression. To avoid the low transfection efficiency obtained in transient experiments and in order to be able to use this system *in vivo*, ecdysone inducible iNOS stable clones were generated. However, after careful screening, only one HT-1080 clone showed reasonable gene expression. An iNOS activity of 21.5 pmol/min/mg was obtained at 20 μM Pon A. Moreover, a 20 % shift in fluorescence due to iNOS over expression at the same Pon A dose

was observed when assayed by flow cytometry. Since high doses of Pon A (20 μM) showed delayed cell growth as observed by the growth curve, using higher Pon A concentrations was inappropriate. This toxicity was further proven to be due to Pon A and not due to NO because the growth delay was also observed in the wild-type cells and the ecdysone inducible *Lac* Z HT-1080 clone.

The ecdysone inducible iNOS clone initially showed a decrease in activity over time. However, when this clone was implanted *in vivo*, an activity of 6.57 pmol/min/mg was achieved in the tumour that was induced with 1 mg/mouse Pon A for 26 h. This activity was significant especially as NOS activity *in vivo* is known to be lower than that *in vitro* [47]. After culturing the tumour *ex vivo*, an activity of 21.9 pmol/min/mg was obtained when induced with 20 μM Pon A. This activity was similar to that of the clone before being implanted *in vivo* (21.5 pmol/min/mg). Moreover, when immunostained, a 27.08 % shift in fluorescence due to iNOS expression was observed at 20 μM (compared to a pre-*in vivo* 19.88 % shift in fluorescence). Even when repeated 3 weeks later, the same fluorescence was obtained indicating that this particular clone was stable. This clone was used in all the forthcoming experiments to study vascular formation and to study the role of iNOS on cell sensitivity to TPZ.

When implanted *in vivo* again to study the relationship of iNOS with hypoxia and blood perfusion, a trend was observed between iNOS expression and blood perfusion. The highest blood perfusion staining occured 24 h after administration of 1 mg/mouse Pon A and declined at 48 h possibly due to Pon A being cleared by the body.

CHAPTER 5

Results 3 GENERATION AND EVALUATION OF iNOS-ENCODING ADENOVIRUSES

5.1 Introduction

In order to be able to use iNOS in a gene therapy approach, type 5 adenoviruses were used as a delivery vehicle. The original aim was to generate adenoviruses that express iNOS (and *Lac* Z) in the ecdysone system, an approach that was previously documented in the literature [133,172-174] without disruption of ecdysone inducible gene regulation. This showed that the genes present in the viral backbone did not interfere with the inducible promoter.

The required cassettes were digested and ligated into the pShuttle vector. Homologous recombination between this vector and pAdeasy vector inserted the gene of interest into the viral genome. These potential viruses were then allowed to replicate in a cell line that provides the E1 gene products in a *trans* configuration (which was needed for viral replication) to produce the recombinant adenoviruses. The viruses were then examined for functionality.

However, after careful evaluation of gene expression, it became clear that the generated adenoviruses had a constitutive (CMV) promoter instead of the ecdysone inducible one. Yet, these adenoviruses were also used to precisely regulate gene expression through varying the multiplicity of infection (moi) in the cells rather than by Pon A induction.

Gene expression generated by the established adenoviruses was measured and compared to the ecdysone inducible iNOS clone and another iNOS clone that constitutively expresses iNOS (previously generated in our laboratory by Dr. Edwin Chinje). The viruses and the iNOS clones were then used to study the impact of iNOS over expression on apoptosis since some studies have shown different effects of iNOS over expression on cell

death. For example, iNOS was found to be over expressed in human pancreatic cancer and its presence positively correlated with apoptosis [54]. Cytokine induced iNOS also showed a positive correlation with the degree of apoptosis in ovarian cancer [55]. On the other hand, apoptosis was observed by Xu *et al.* (2002) in colorectal cells that were cocultured with iNOS expressing cells [56].

5.2 Generation of Recombinant Adenoviruses

In order to generate recombinant adenoviruses, the gene of interest was ligated in the multiple cloning site of the pShuttle vector. The pShuttle vector was needed because it contains regions of homology with another vector-pAdeasy. This second vector expresses the viral genome. The homologous recombination between the 2 vectors allowed the gene of interest to be integrated into the viral cassette.

5.2.1 Ligation of the pVgRXR cassette into pShuttle

The ecdysone receptor cassette was cut from the pVgRXR vector by *Dra* III enzyme and ligated into the pShuttle vector that was cut by *Bgl* II enzyme. Both pVgRXR and pShuttle were blunted and pShuttle was dephosphorylated. Then, the pVgRXR fragment was ligated into pShuttle using T4 DNA ligase **(Section 2.3)** **(Fig 5.1)**. It is noteworthy to mention that the pVgRXR cassette is 7402 bp and this is the size limit of the insert that can be inserted into these adenoviruses [140].

After transforming into DH5α **(Section 2.4.1)** and plating on kanamycin-containing plates (which is the selection marker for the pShuttle vector), 17 colonies were picked, mini-prepped **(Section 2.6.1)**, and digested by *Hind* III to check for the correct ligation **(Fig 5.2)**. Results showed that colony 17 was ligated in the forward direction while colonies 12 and 13 were ligated in the reverse direction. All the other colonies did not contain the correct insert. The direction of ligation is not important in this case, as the entire ecdysone receptor cassette has been ligated into the pShuttle vector. Moreover, cloning a full cassette in the opposite direction in adenoviruses has the advantage of reduced viral interference on gene expression [201].

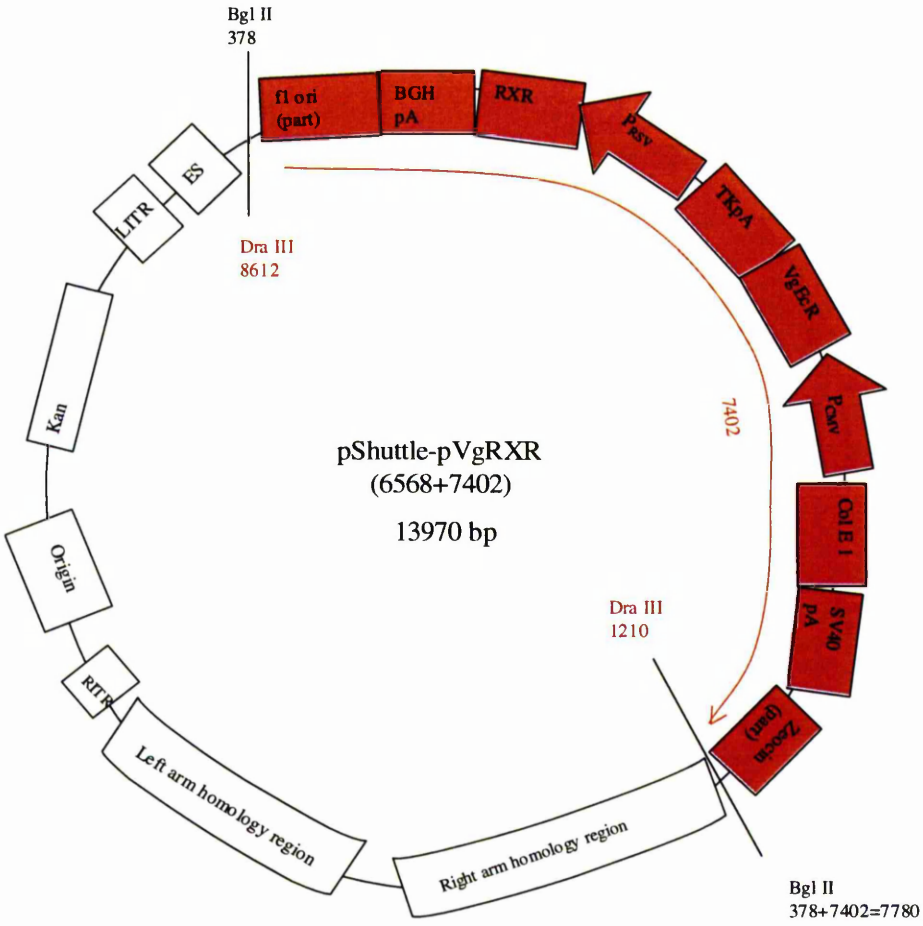

Fig 5.1 Map of the pVgRXR cassette ligated into pShuttle.

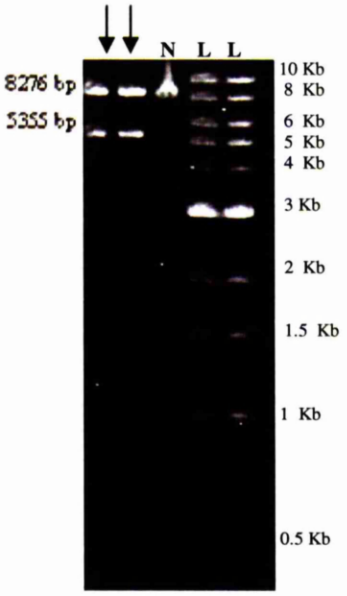

Fig 5.2 A DNA digest confirming the ligation of pVgRXR cassette into the pShuttle vector in the reverse orientation. The expected bands sizes were 339 bp, 5355 bp, and 8276 bp. The smallest band was detected at an earlier time point (N:negative colony, L: 1 Kb ladder).

5.2.2 Ligation of the pIND SP1 cassette into pShuttle

In order to express genes using the ecdysone system, a second virus encoding for the ecdysone reporter had to be generated. The pIND SP1 vector was cut by *Nhe* I and *Sal* I to release a 547 bp fragment constituting the ecdysone promoter. The pShuttle vector was linearised using *Not* I. Both vector and insert were blunted and pShuttle was dephosphorylated. Then, the pIND SP1 fragment was ligated into pShuttle using T4 DNA ligase **(Section 2.3)** **(Fig 5.3)**. In this case, pShuttle-pIND SP1 promoter vector was developed as it was not possible to digest the full pIND SP1 cassette (which included the multiple cloning site and the poly A) due to the presence of *Pme* I recognition sites in this cassette. The presence of these sites will interfere later on in the process of homologous recombination and would result in the loss of part of the insert.

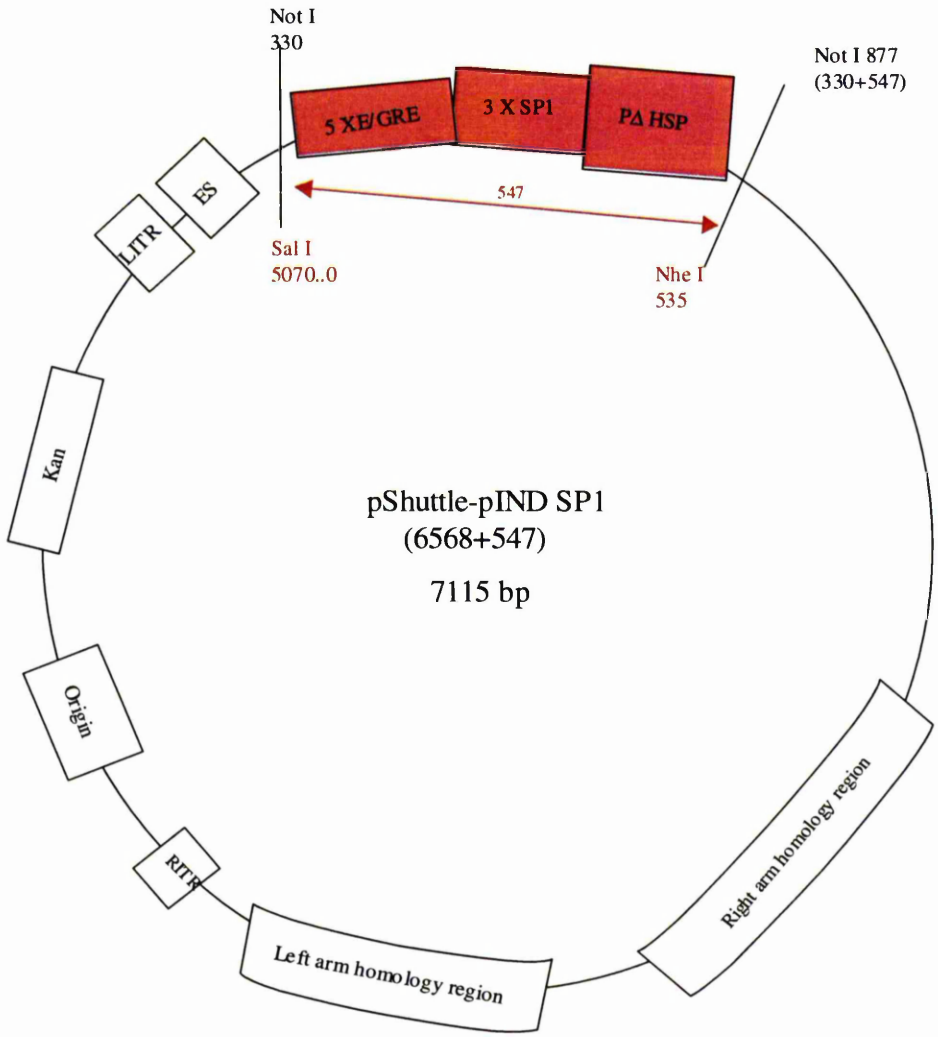

Fig 5.3 Map of the constructed pShuttle-pIND SP1

After transforming into DH5α **(Section 2.4.1)** and plating on kanamycin-containing plates, 17 colonies were picked and mini-prepped **(Section 2.6.1)**. Since the inserted cassette was only 547 bp, finding enzymes that would confirm the orientation of the insert was difficult. So, the mini-prepreparations were linearised using *Sal* I enzyme and colonies with the correct total size were sequenced. The forward primer of pShuttle vector was used (5'

GAAGTGAAATCTGAATAAT TTTGT 3'). Colony number 8 had the correct ligation in the correct orientation **(Fig 5.4)**. All other colonies were negative.

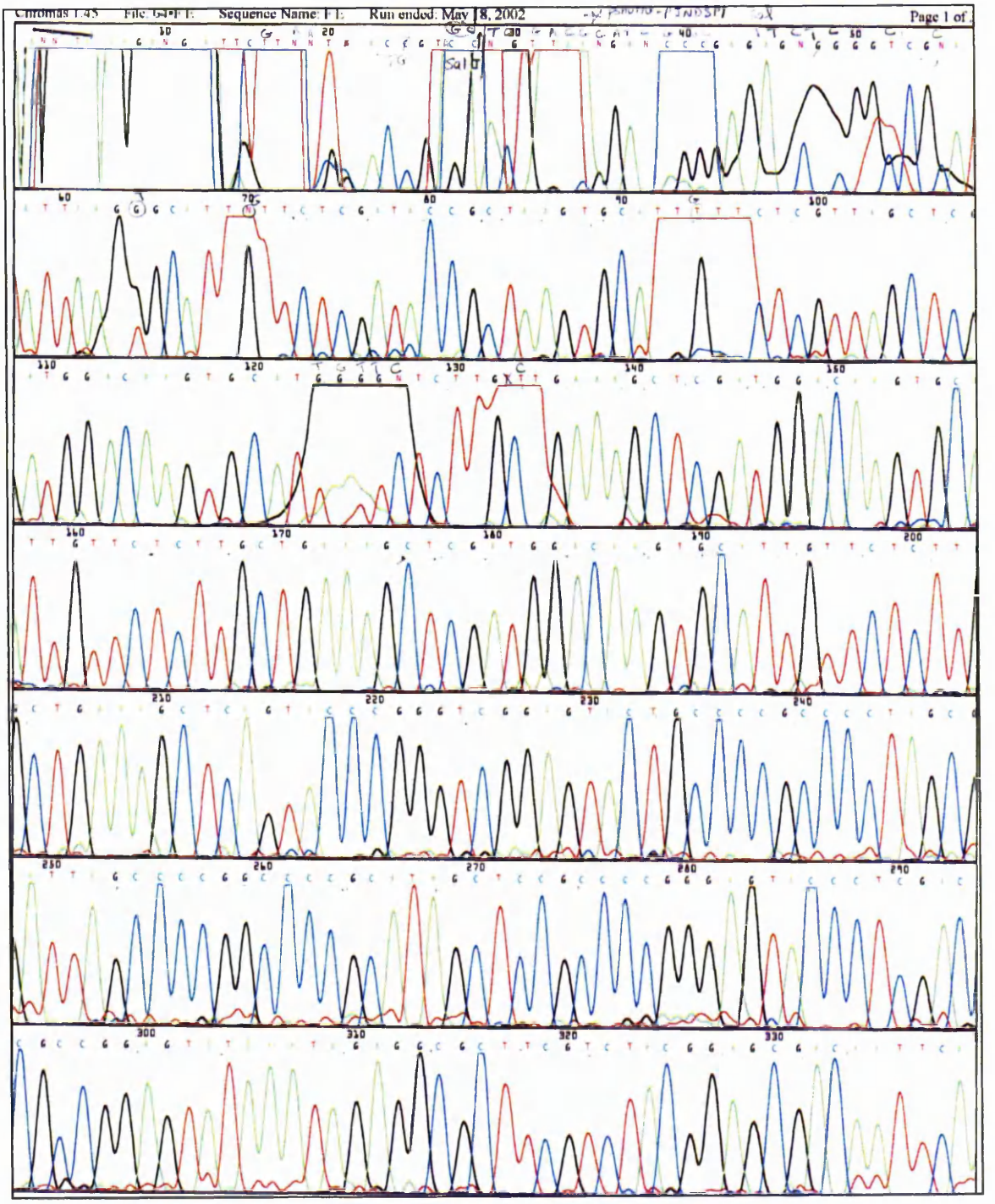

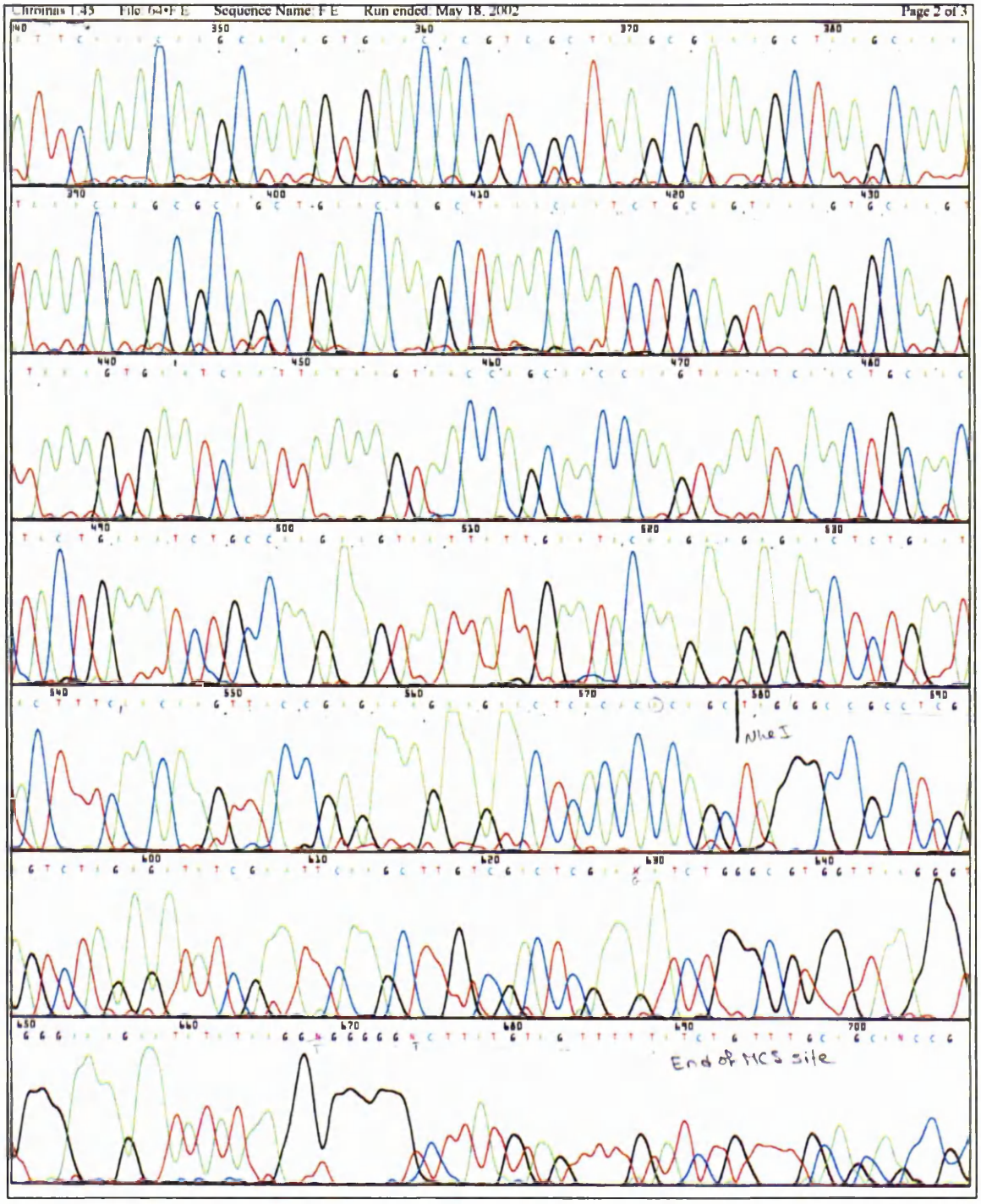

Fig 5.4 Sequence of pShuttle-pIND SP1 (colony 8) using the forward pShuttle primer. This showed the sequence of the insert read from *Sal* I to *Nhe* I in the correct forward orientation. The sequence continued reading the region after the insert until it reached the end of the multiple cloning site (MCS) of the pShuttle backbone. The sequence shows peaks for each nucleotide as follows: green A (adenine), black G (guanine), blue C (cytoseine), and red T (thymine). Broad bands result due to non-specific binding and could therefore be corrected for by comparing to the literature sequence.

5.2.3 Ligation of *Lac* Z-poly A into the pShuttle-pIND SP1 Vector

To generate adenoviruses that encode for the inducible *Lac* Z gene, the previously established pShuttle-pIND SP1 vector was linearised by *Hind* III and a *Lac* Z-poly A fragment (from pShuttle CMV *Lac* Z-purchased from Stratagene, The Netherlands) was digested by *Sal* I and *Sph* I. Both vector and insert were blunted and the pShuttle-pIND SP1 vector was dephosphorylated. Then, the *Lac* Z-poly A fragment was ligated into pShuttle-pIND SP1 using T4 DNA ligase **(Section 2.3)** **(Fig 5.5)**.

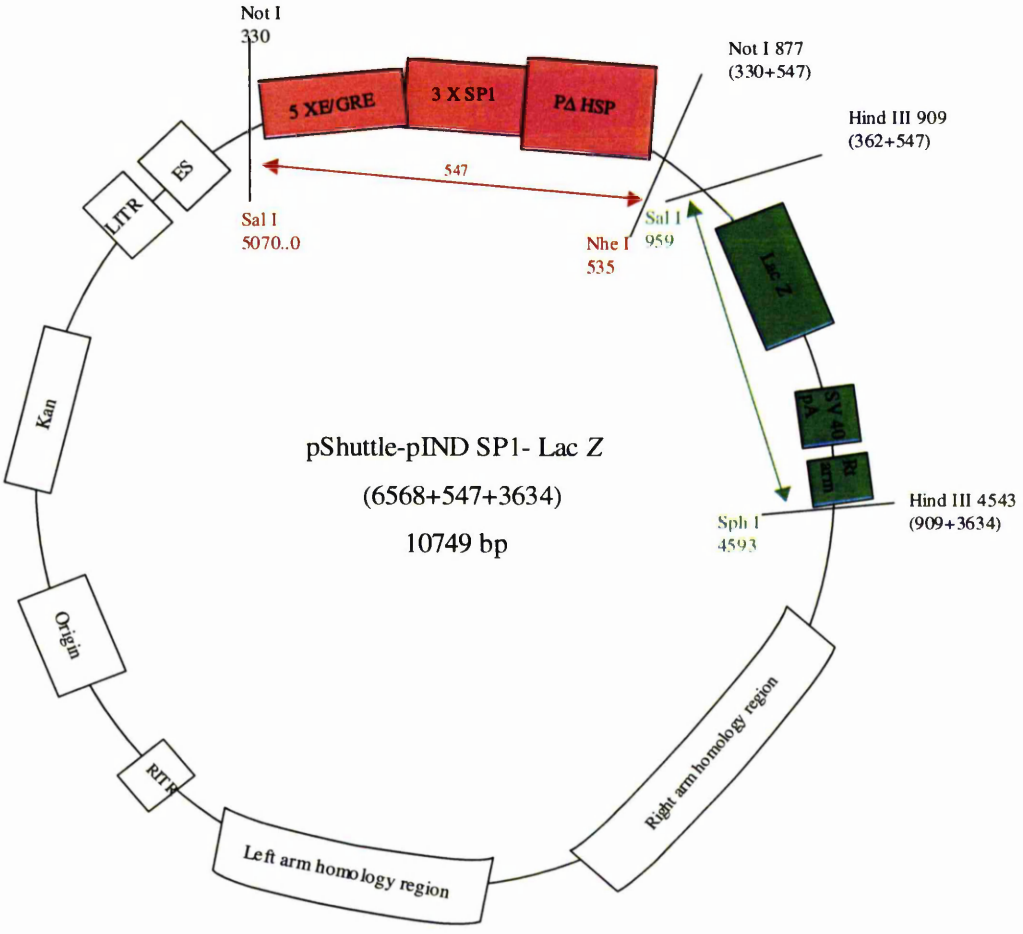

Fig 5.5 Map of the constructed pShuttle-pIND SP1 *Lac* Z vector

After transforming into DH5α **(Section 2.4.1)** and plating on kanamycin -containing plates, 33 colonies were picked, mini-prepped **(Section 2.6.1)**, and digested by *Kpn* I and *Hind* III to check for the correct ligation. Three colonies showed sizes similar but not exact to

the expected band sizes. For this reason, another digest was performed using *Not* I and *Hind* III but this digest confirmed the size and not the orientation of the insert. The colonies that showed the required sizes were sequenced using the pShuttle reverse primer (5' GTGGGGGTCTTATGTAGTTTTG 3') to confirm directionality. This sequence confirmed the existence of the Poly A as well as part of the *Lac* Z gene. The promoter region was previously sequenced when cloning the pShuttle pIND SP1 promoter vector (**Section 5.1.2**). The sequencing showed that colony number 14 had both a *Lac* Z fragment and Poly A (**Fig 5.7**). **Fig 5.6** shows the test digest of colony number 14.

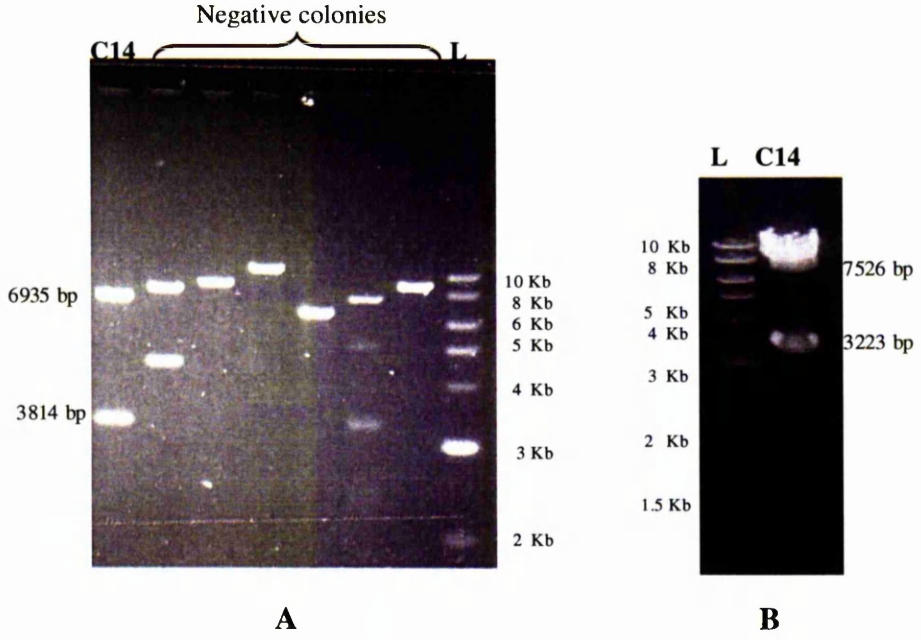

Fig 5.6 Test digests performed after colonies were picked to check for the pShuttle pIND SP1 *Lac* Z ligation. **A** *Kpn* I and *Hind* III digests; the expected sizes were 3814 bp and 6935 bp. Colony number 14 (C14) was picked as it showed similar but not the exact band sizes. To confirm the ligation, C14 was digested using *Not* I and *Hind* III (**B**). This digest confirmed that the ligation was correct (expected sizes: 3223 bp and 7526 bp) but did not confirm orientation hence the need to sequence using the reverse pShuttle primer (L: 1Kb ladder).

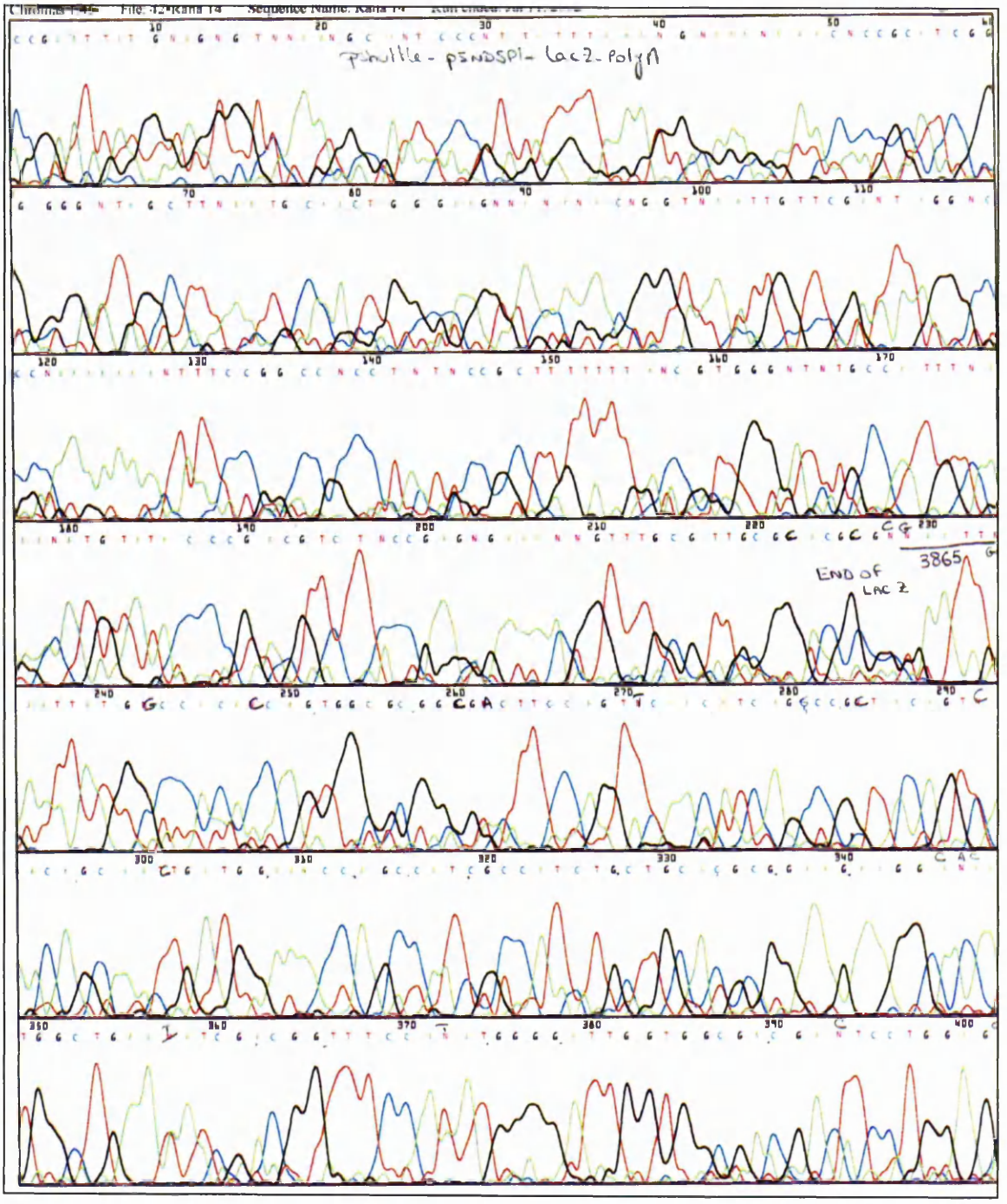
Pshuttle - pENDSPI - lac2 - polyA
END OF LAC Z
3865

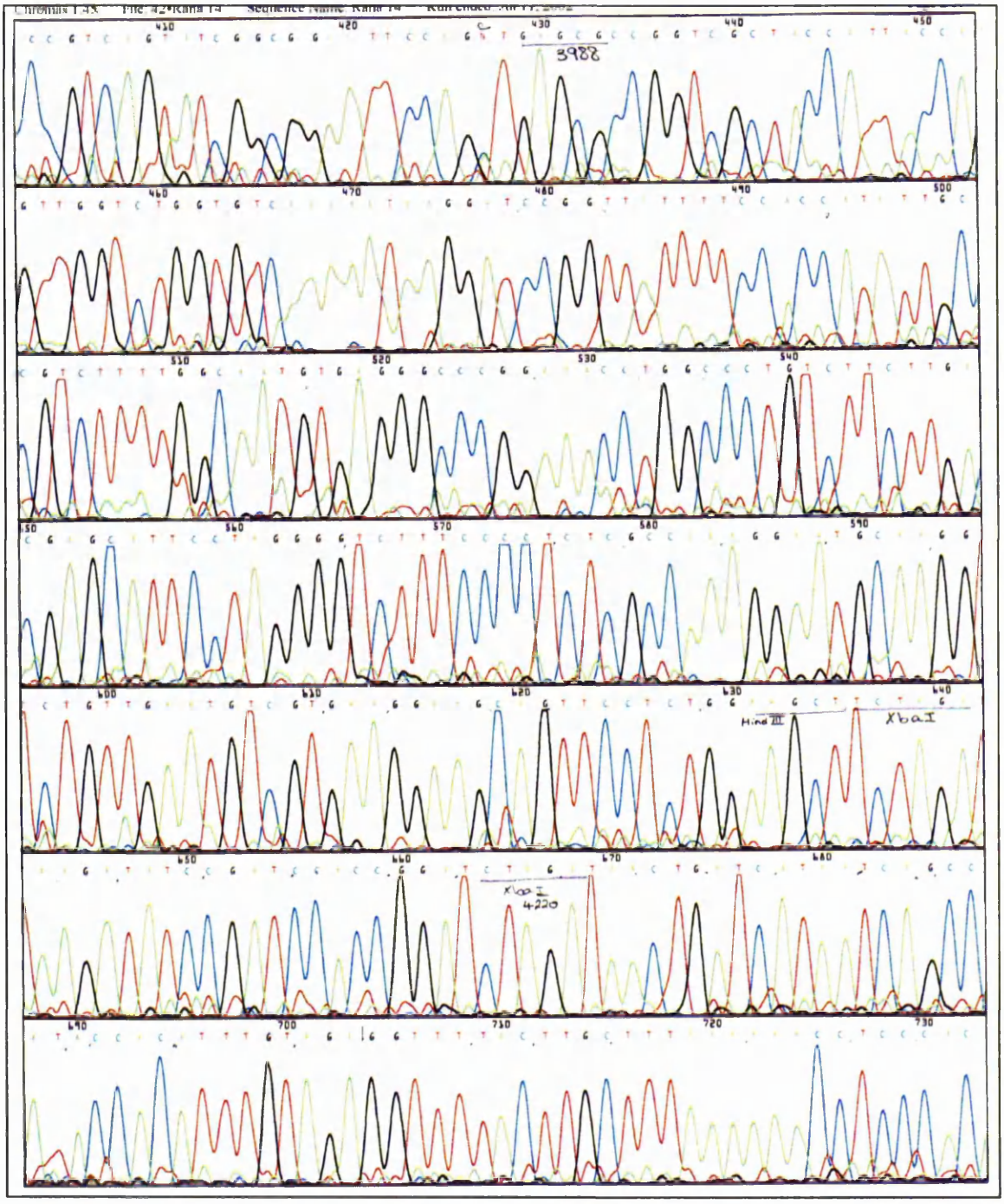
3988
Hind III
XbaI
Xba I
4220

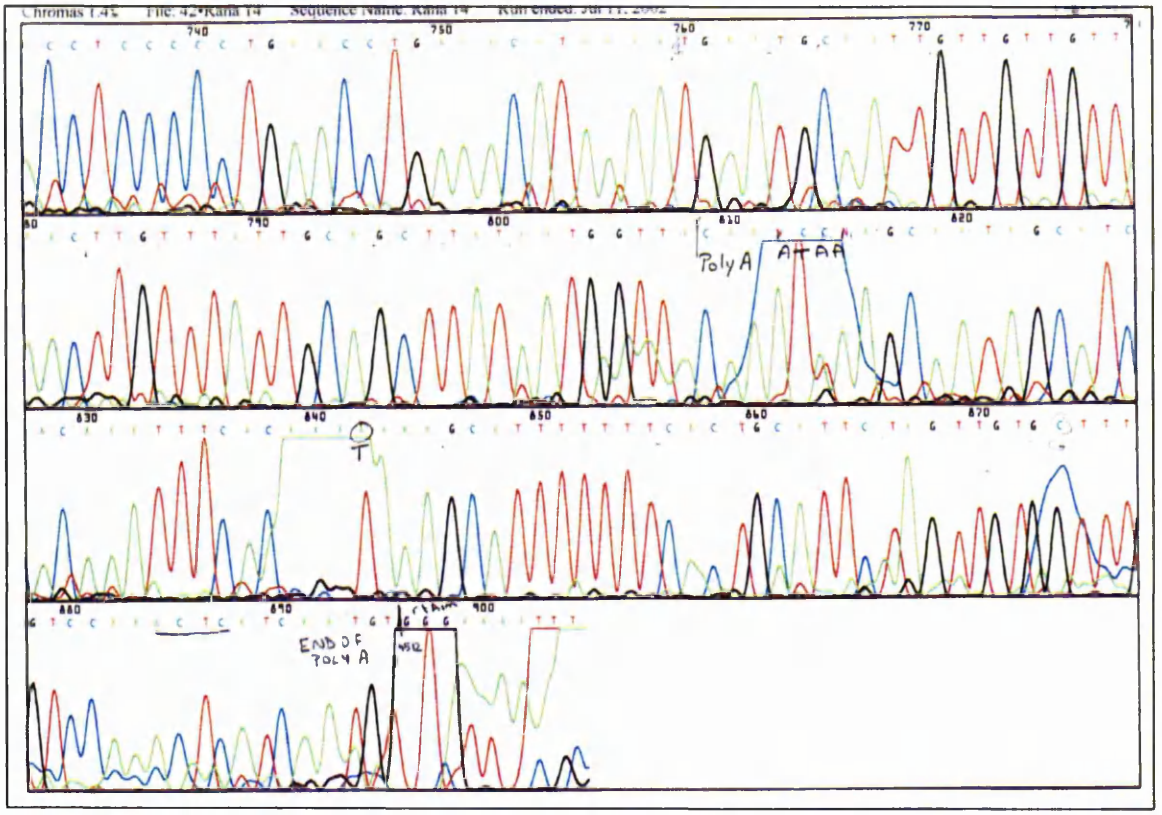

Fig 5.7 Sequence of pShuttle-pIND SP1 *Lac* Z using the reverse pShuttle primer. The regions from the end of Poly A to part of the *Lac* Z cDNA were sequenced.

To further confirm the constructs, a functionality test was performed. T47D cells were seeded at $2x10^5$ cells/well in a 6-well plate and transiently transfected with the pVgRXR original plasmid (1 µg/well) and the pShuttle-pIND SP1-*Lac* Z colony number 14 (10 µl of the mini prep/well) using Lipofectamine (20 µl/well). The following day, the cells were induced with 20 µM Pon A for 24 h. Then, the cells were formalin-fixed and X-gal stained. Blue cells were observed indicating that this colony was functional. Colony number 14 was maxi-prepped **(Section 2.6.2)** and later used.

5.2.4 Ligation of iNOS cDNA into the pShuttle-pIND SP1 vector

Having obtained a pShuttle-pIND SP1 *Lac* Z vector, the *Lac* Z cDNA was replaced by the iNOS gene. The *Lac* Z fragment was excised by *Hind* III and *Not* I enzymes. The iNOS cDNA was derived from the previously ligated pINDSP1 iNOS vector, which was

digested with *Nhe* I and *Not* I to release the iNOS fragment. Then, both vector and insert were blunted and the vector was dephosphorylated using the CIP enzyme. The ligation was performed at 16 ^{0}C overnight using T4- DNA ligase **(Section 2.3)** **(Fig 5.8)**.

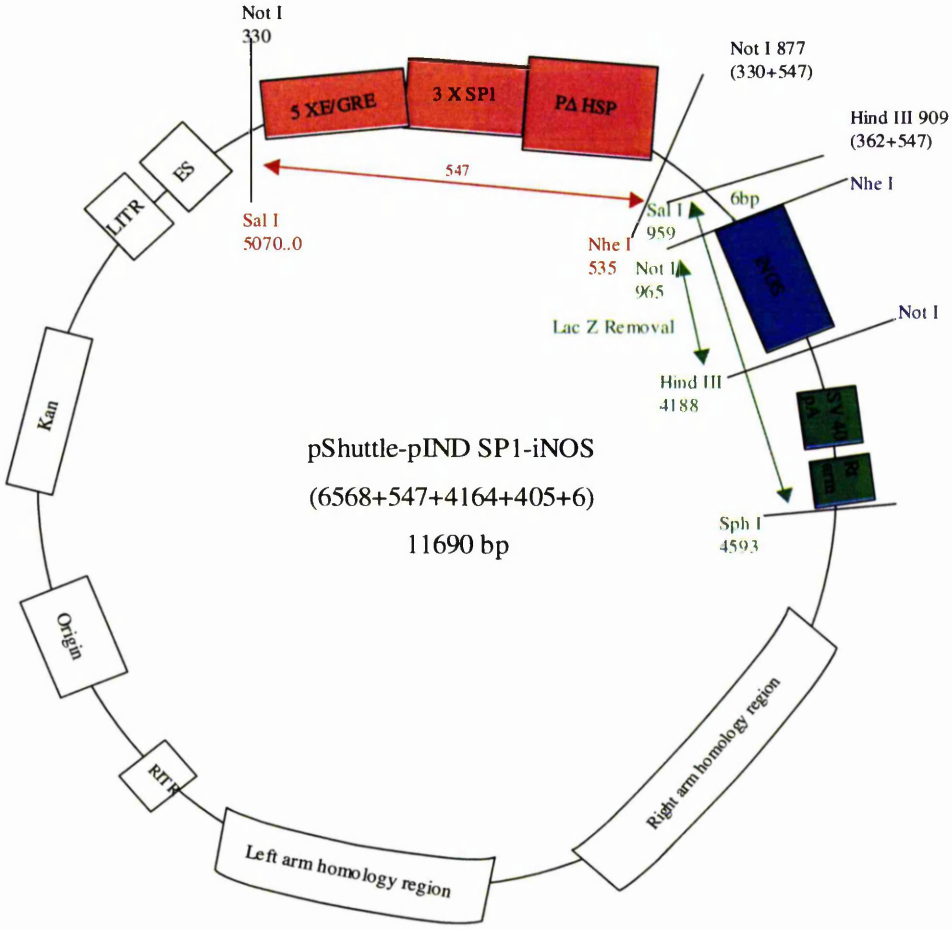

Fig 5.8 Map of the constructed pShuttle-pIND SP1 iNOS (regions coloured in green constitute backbone pieces from the pShuttle-pIND SP1 *Lac* Z vector).

After transforming into DH5α **(Section 2.4.1)**, and plating on kanamycin-containing plates, 26 colonies were picked, mini-prepped **(Section 2.6.1)**, and digested with *EcoR* I to test for the correct ligation. The colonies with the correct band sizes (5758 and 5932 bp) were sequenced using the pShuttle reverse primer (5' GTGGGGGTCTTATGTAGTTTTG 3') vector for further confirmation **(Fig 5.9)**. The right colony (number 3) was then grown and maxi-prepped **(Section 2.6.2)**.

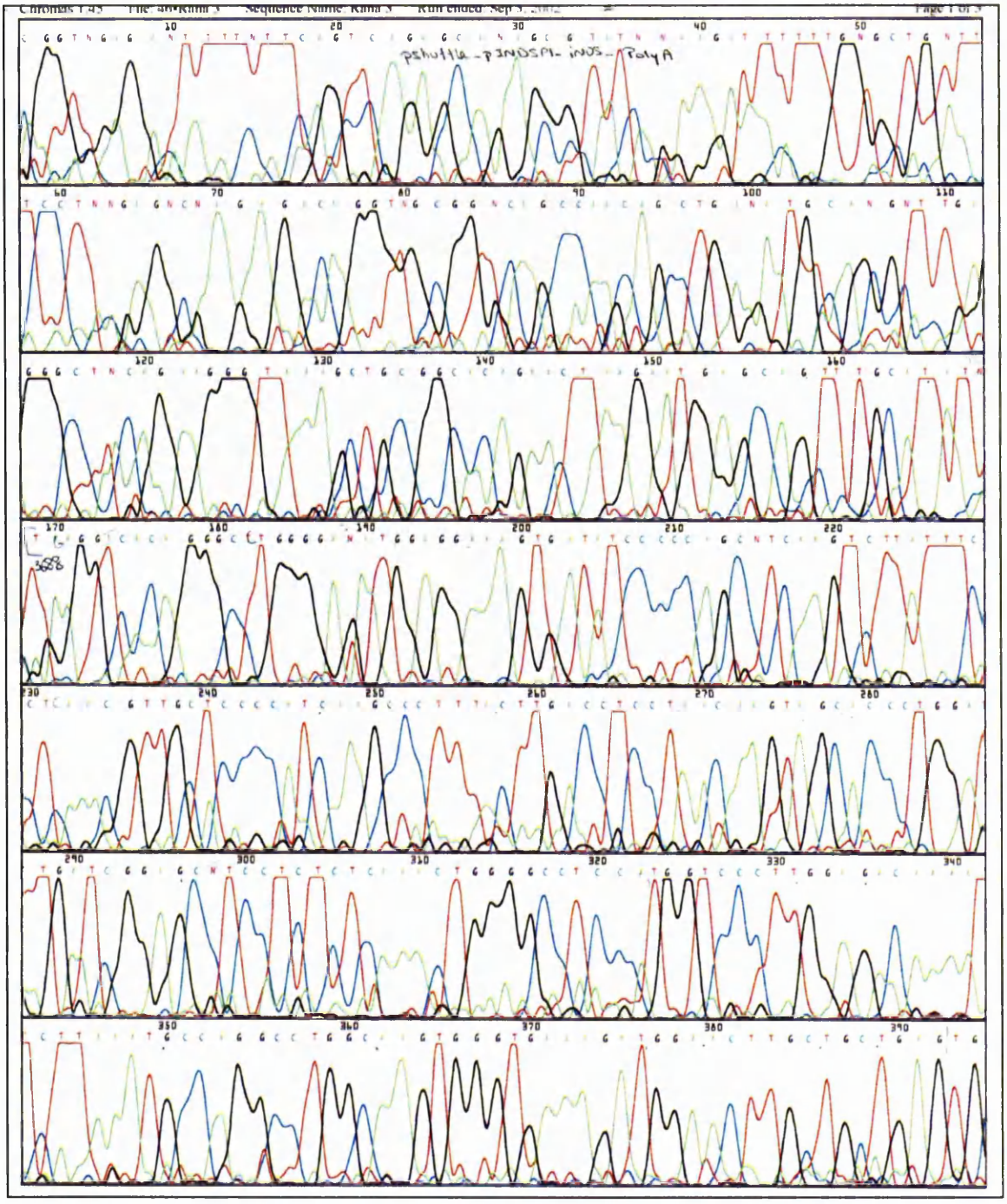
pshuttle-pINOS-iNOS-PolyA

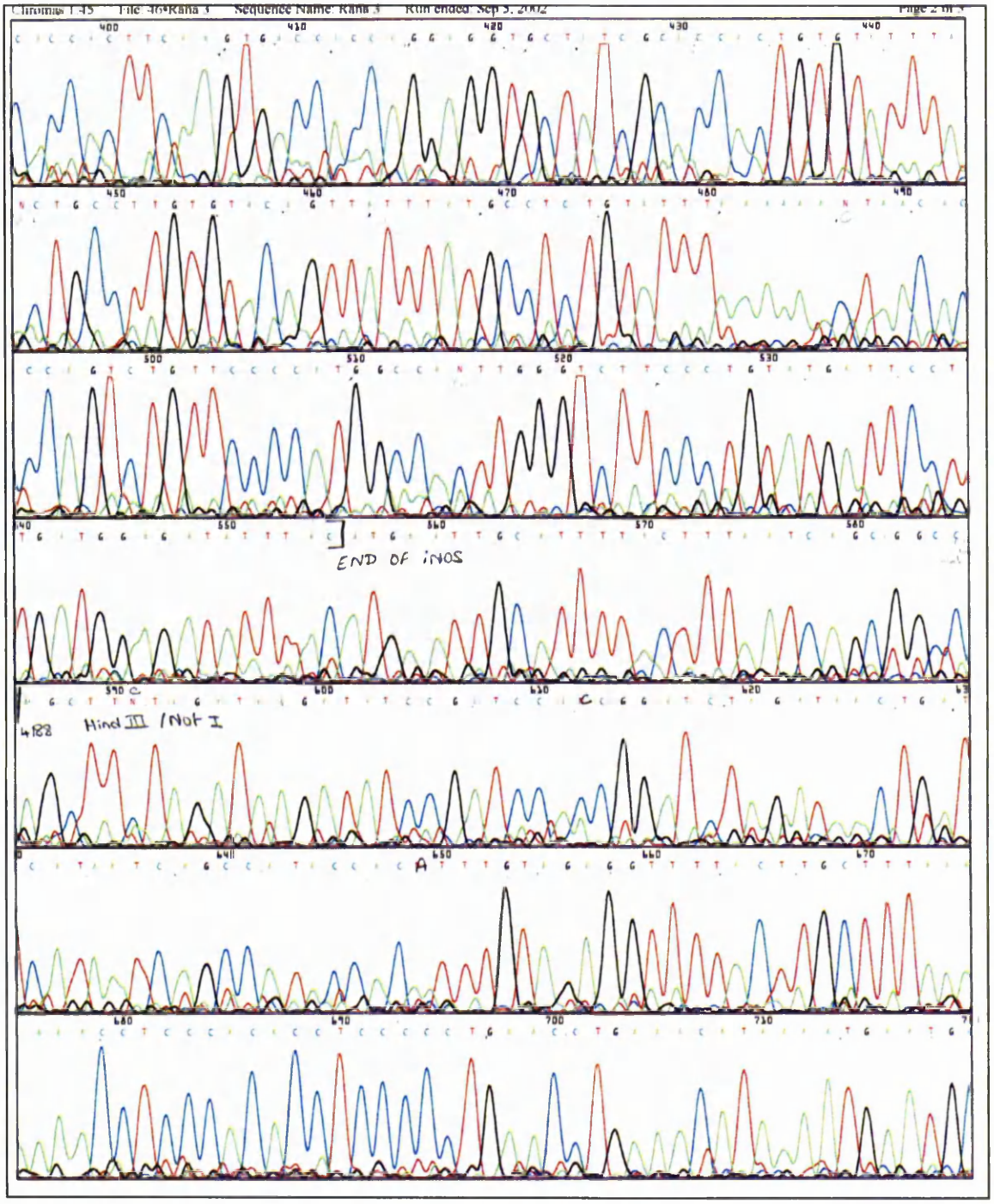
END OF iNOS
4188
Hind III / Not I

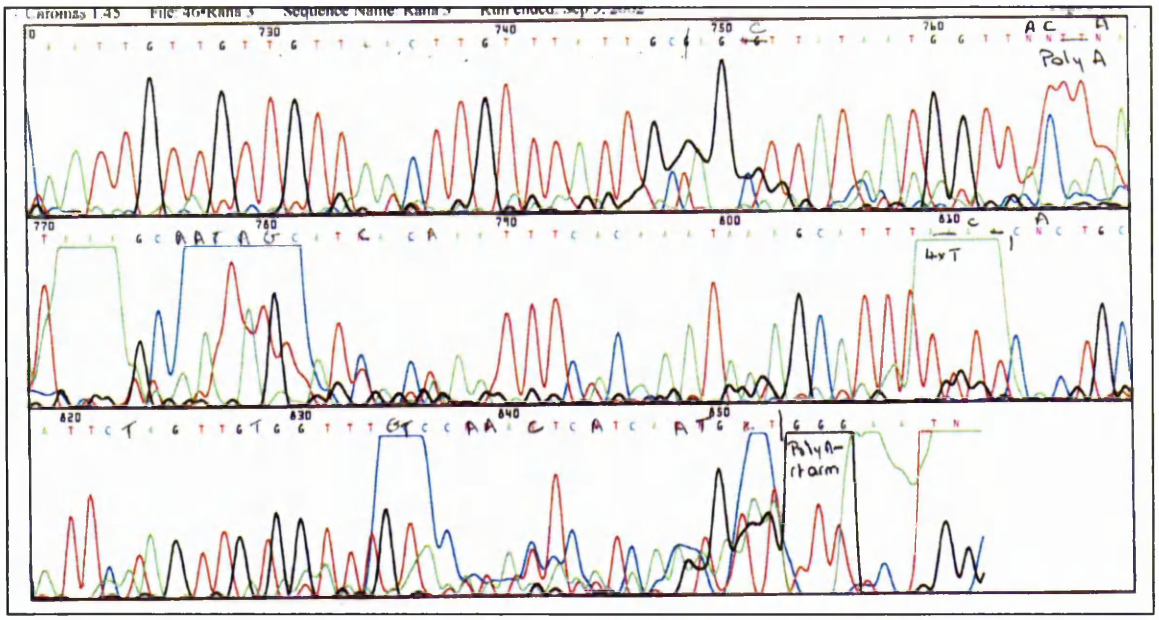

Fig 5.9 Sequence of pShuttle-pIND SP1 iNOS by the reverse pShuttle primer. In this sequence the Poly A and part of the iNOS gene were observed.

5.3 Co-transformation of the pShuttle Vectors with pAdeasy

Each of the following vectors: pshuttle-pVgRXR, pshuttle-pIND SP1 *Lac* Z, and pshuttle- pIND SP1 iNOS was cotransformed with pAdeasy in order to allow homologous recombination between pAdeasy and each of the other vectors to occur. Each vector was linearised with *Pme* I and dephosphorylated by the CIP enzyme to ease the homologous recombination process **(Section 2.16)**.

The linearised cassette (1 µg), and pAdeasy (100 ng) were co-transformed into BJ 5183 Electroporation Competent Cells (40 µl) by electroporation **(Section 2.4.2)**. Each sample was mixed, placed in a cuvette, and tapped to remove air bubbles. The electroporation machine (EquiBio-Easyject, Middlesex, UK) was run until it reached 2500 V to allow for transformation of DNA into the electroporation competent cells. Then, 1 ml of S.O.C medium was added and the sample was shaken at 37 ^{0}C for 1 h. The transformants were plated on kanamycin-containing plates.

The colonies were mini-prepped **(Section 2.6.1)** and digested with *Pac* I enzyme to check for the recombination. Two bands should be observed, the first at around 23 Kb and

the second at 3 to 4 Kb (depending on the site of homologous recombination). These sizes correspond to the viral and insert genes upon digestion with *Pac* I enzyme **(Fig 5.10)** The colonies with the correct band sizes were transformed using heat-shock into competent DH5α *E. coli* **(Section 2.4.1)** and plated on kanamycin-containing plates. Colonies were picked, mini-prepped and digested with *Pac* I to confirm the band sizes again. After that, maxi-preparations **(Section 2.6.2)** were established.

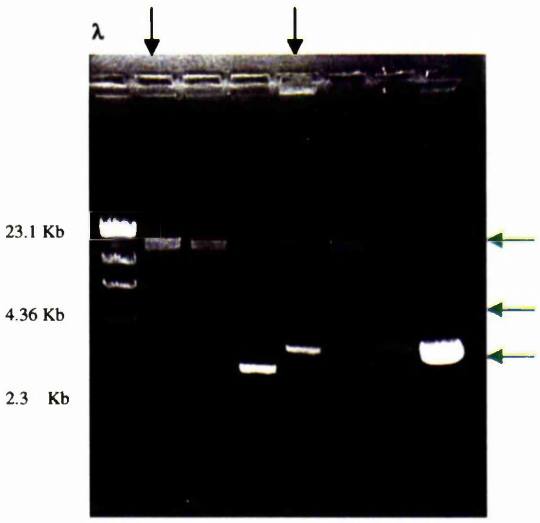

pAd pVgRXR

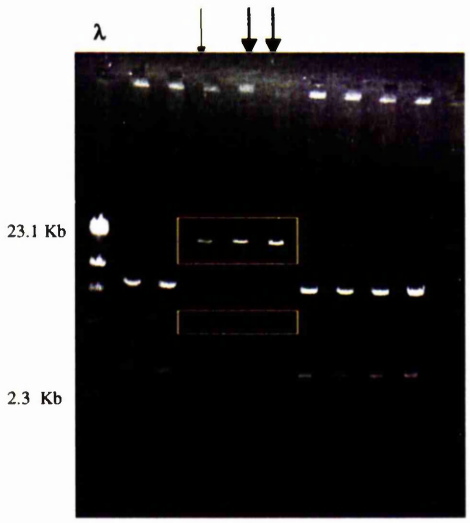

pAd pIND SP1 *Lac* Z

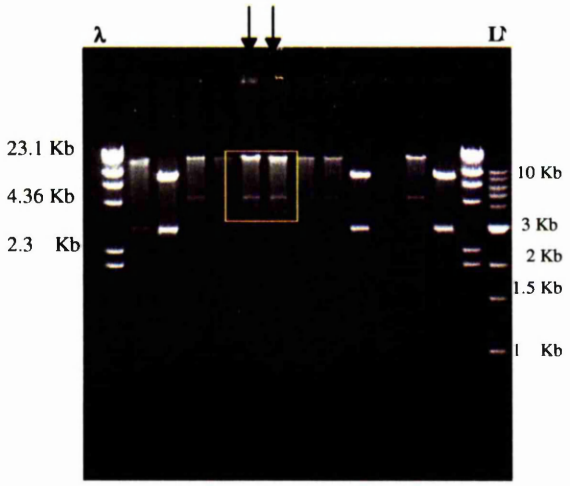

pAd pIND SP1 iNOS

Fig 5.10 The pAdvectors digested with *Pac* I enzyme. Two bands were observed the first at 23 Kb and the second at either 3 or 4 Kb (depending on the site of homologous recombination). The colonies indicated with arrows have been picked. (λ:λ-*Hind* III digested ladder L: 1 Kb Ladder, unlabelled columns are other digested colonies that were later discarded).

5.4 Virus Replication and Purification

Having obtained viral genomes that contain each of the cassettes and in order to allow the viral DNA to be expressed and packaged, the pAd vectors were linearised using *Pac* I enzyme and used to transfect HEK 293 cells. This cell line was chosen as it provides the E1 gene products in a *trans* configuration and thus allows the generation of the replication deficient adenoviruses. When a 100 % cytopathic effect was observed, the cells were harvested and subjected to thaw-freezing to release the viral particles in order to obtain a primary inoculum. Then, this inoculum was used to generate larger volumes of viruses that were purified using a virus purification kit (BD Biosciences, CA, USA) **(Section 2.16)**. Then the viruses were titred **(Section 2.16.4)** and stored at –80 ^{0}C for later use.

5.5 Testing the Functionality of the Generated Viruses

The purpose of this experiment was to test that the newly generated viruses were functional. So, before being quantified, the viruses were used to infect HCT-116 wild-type cells. These cells were split into 2 T-25 flasks and incubated for 24 h. Then, in the first flask, 10 µl of each of pAdpVgRXR and pAdpIND SP1 *Lac* Z were added. In the second flask, 10 µl of each of pAdpVgRXR and pAdpIND SP1 iNOS were added. The next day, the flasks were treated with 20 µM Pon A. After 24 h, the cells were either formalin-fixed and stained with X-gal to test for *Lac* Z expression or immunostained with iNOS antibodies and iNOS expression was detected using flow cytometry. In both cases, gene expression was compared to uninfected wild-type cells. More than 90 % of the cells turned blue indicating *Lac* Z gene expression (data not shown). High gene expression was also detected with the cells infected with the iNOS viruses **(Fig 5.11)**.

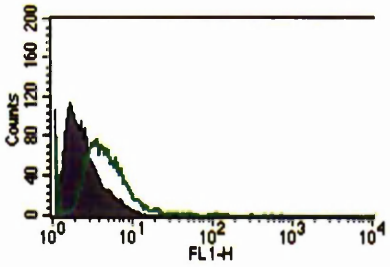

Fig 5.11 A shift in peak was observed due to iNOS expression when treated with 20 μM Pon A (green line) as compared to the uninfected wild type cells (grey).

5.6 Regulation of Gene Expression Using the Established Adenoviruses

5.6.1 Determining the Optimum Conditions for Highest Ecdysone Inducible *Lac* Z Expression with Minimal Leakiness

In order to find the best conditions to achieve regulatable gene expression, the number of viral particles/cell or multiplicity of infection (moi) and the ideal ratio of pAdpVgRXR to pAdpIND SP1 were studied. HT-1080 wild-type cells were seeded in a 24-well plate at $1x10^4$ cells/well. After 4 h, the cells were infected with varying moi of both pAdpVgRXR and pAdpIND SP1 *Lac* Z to give a total moi of 30. The following day, the infected cells were dosed with Pon A and left for 24 h after which the β-galactosidase activity assay was performed **(Table 5.1 and Fig 5.12)**.

Unexpectedly, this experiment indicated that *Lac* Z gene expression increased as the moi of pAdpVgRXR decreased. High basal expression was also observed. Morever, even in the absence of pAdpVgRXR, Pon A caused an increase in *Lac* Z gene expression.

Pon A (μM)	*3:27*	*1.5:28.5*	*Lac Z only (30)*
0	4.3	5.6	4.9
10	6.0	6.4	8.8
20	5.5	6.9	9.7

Table 5.1 β-galactosidase activity (U/mg) measurement in response to cellular infection with adenoviruses encoding for ecdysone inducible *Lac* Z expression. The following moi ratio of pAdpVgRXR to pAd pIND SP1 *Lac* Z were used: 3:27, 1.5:28.5, and a control sample with moi 30 of pAd pIND SP1 *Lac* Z only.

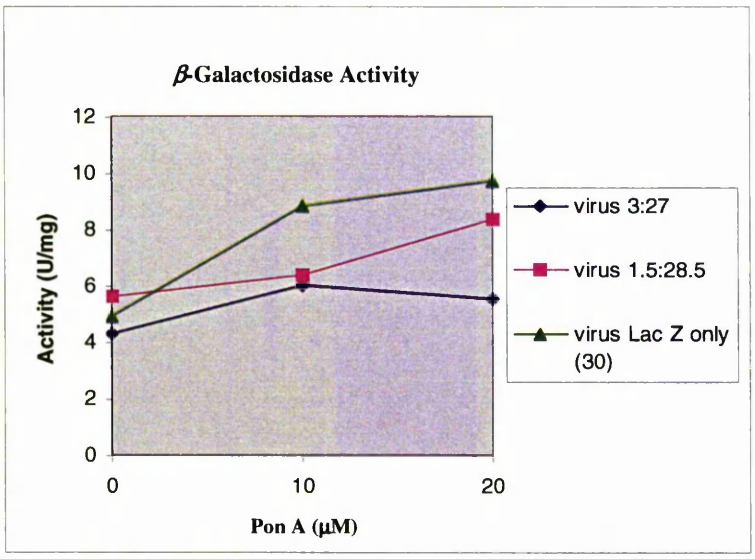

Fig 5.12 A graph showing β-galactosidase activity of wild-type HT-1080 cells infected with the adenoviruses encoding for *Lac* Z in the ecdysone cassette.(ratios of pAdpVgRXR: pAd pIND SP1 *Lac* Z)

5.6.2 Using an External pVgRXR Source to Retrieve Inducible Gene Expression

From these results, it was suspected that the pAdpVgRXR was non-functional. Although previously tested, yet another source of pVgRXR was sought in order to confirm the functionality status of this virus. Hence, the HT-1080 inducible iNOS clone 16.10/T was used solely as a source of pVgRXR and was therefore infected with pAdpIND SP1 *Lac* Z. The HT-1080 wild-type cells were used as a control.

Cells were seeded at $1x10^4$ cells/well in a 24-well plate and infected 4 h later with pAdpIND SP1 *Lac* Z only or both pAdpVgRXR and pAdpIND SP1 *Lac* Z. The moi of pAdpIND SP1 *Lac* Z in this experiment was fixed at 30. The following day, the infected cells were induced with Pon A and left for 24 h after which the β-galactosidase activity assay was performed (**Table 5.2**).

Pon A (μM)	Wt 3:30	Wt 1.5:30	Wt Lac Z only (30)	iNOS clone Lac Z only(30)	iNOS clone 3:30
0 A	3.72	3.54	5.05	11.74	11.17
0 B	4.16	2.99	5.05	8.42	10.59
0 Ave	3.94	3.27	5.05	10.08	10.88
5 B	4.81	8.04	9.77	7.54	7.28
5 A	9.40	7.42	8.67	7.66	4.32
5 Ave	7.11	7.73	9.22	7.6	5.80
10 A	6.90	6.37	8.33	10.33	8.92
10 B	5.90	8.25	11.02	7.36	7.63
10 Ave	6.40	7.31	9.68	8.85	8.25

Table 5.2 β-galactosidase activity measurement (U/mg) using different sources of pVgRXR. The moi of pAdpIND SP1 *Lac* Z was fixed at 30 (this experiment was performed in duplicate wells –A and B, the average was also calculated) (Wt:wild-type).

If the pAdpVgRXR virus was non functional, highest gene expression would have been expected in the iNOS clone that was infected with pAdpIND SP1 *Lac* Z. However, this was not the case and high *Lac* Z expression was observed in almost all samples with the highest occurring in the absence of pVgRXR regardless of its source. Moreover, gene expression did not seem to be responding to Pon A in some cases.

5.6.3 DNA Test Digests to Re-confirm the Ligation of the pVgRXR Cassette

For further assurance of the functionality status of pAdpVgRXR, a test digest to reconfirm the cloning of the pVgRXR cassette into pShuttle and to make sure that this cassette was not lost when pShuttle-pVgRXR was cotransformed with pAdeasy was performed. pAdpVgRXR (2 μg) was digested with *Hind* III enzyme and run on a 1 % agarose gel. The following controls were also included in this experiment: the pVgRXR plasmid, 2 colonies of pShuttle- pVgRXR (forward and reverse orientation of ligation), and pShuttle empty vector. All digests showed the expected band sizes confirming that the ligation was correct **(Fig 5.13)**.

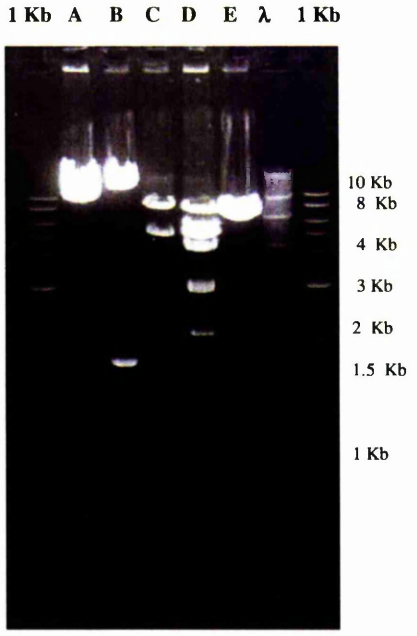

Fig 5.13 A DNA test digest to confirm the expected sizes of: **A** pVgRXR original plasmid (339 bp and 8464 bp) **B** pShuttle pVgRXR Forward cassette (339 bp, 1740 bp, 11891 bp) **C** pShuttle pVgRXR Reverse orientation (339 bp, 5355 bp, 8276 bp) **D** pAdpVgRXR (several bands including those of the pshuttle-pVgRXR plasmid) **E** pShuttle (6568 bp) λ Ladder-Hind III digest: 23.1 Kb, 9.4Kb, 6.6 Kb, 4.4 Kb, 2.3 Kb, 2.0 Kb (small size bands were clearly observed on the same gel at an earlier time point) (1 Kb=1000 bp).

5.6.4 Transient Transfections Using pVgRXR and pIND SP1 *Lac* Z Plasmids

Having realised that *Lac* Z was being expressed in the absence of pAdpVgRXR or pVgRXR when the viral pAdpIND SP1 *Lac* Z was used, it was important to reconfirm that this phenomenon does not occur when the plasmid pIND SP1 *Lac* Z is used. Therefore, a transient transfection experiment using the pVgRXR and pIND SP1 *Lac* Z plasmids was conducted.

HT-1080 wild-type cells were seeded at $2x10^5$ cells/well in a 6-well plate and transfected with the ecdysone plasmids (1 µg/well of each plasmid) using Lipofectamine (10 µl/well). The following day, the cells were induced with Pon A for 24 h and the *β*-galactosidase activity was measured (**Fig 5.14**).

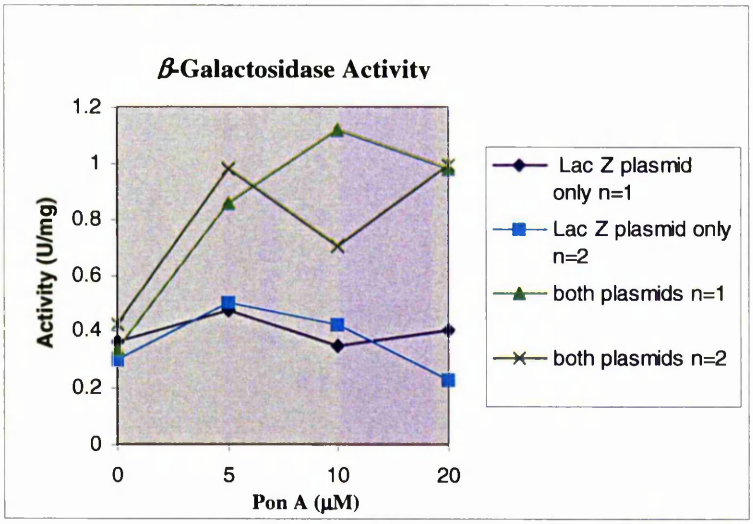

Fig 5.14 β-galactosidase activity measurements (U/mg) in HT-1080 cells transiently transfected with pVgRXR and pIND SP1 *Lac* Z (this experiment was performed in duplicate wells; so, n=1 and n=2 are shown).

The results indicated that although activity values were modest (due to low transfection efficiency), gene expression in the absence of pVgRXR remained basal compared to that in the presence of pVgRXR.

5.6.5 Comparison of iNOS and *Lac* Z Expression Using the Adenoviruses

The pAdpIND SP1 iNOS virus was tested in order to compare the results with those of pAdpIND SP1 *Lac* Z. HT-1080 wild-type cells were seeded at 2.5×10^4 cells/well in a 24-well plate. The following day, the cells were infected with either pAdpIND SP1 iNOS alone (moi 30) or both pAdpIND SP1 iNOS (moi 30) and pAdpVgRXR (moi 3). After inducing with varying concentrations of Pon A for 24 h, the cells were immunostained with iNOS antibodies and assayed using flow cytometry **(Fig 5.15)**.

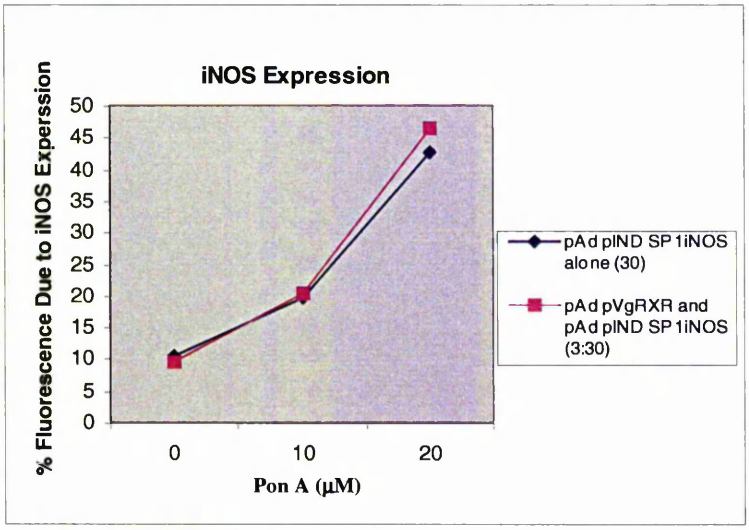

Fig 5.15 iNOS gene expression as determined by flow cytometry. Wild-type HT-1080 cells were infected with pAdpVgRXR and pAdpIND SP1 iNOS or the latter alone and induced with varying concentrations of Pon A.

In another experiment, HT-1080 wild-type cells were seeded at $1x10^5$ cells/well in a 6-well plate and infected after 3 h with varying moi of either pAdpIND SP1 iNOS alone (moi 0,20,50) or both pAdpIND SP1 iNOS (moi 0,20,50) and pAdpVgRXR (moi 0,2,5). The cells were induced the following day with 20 µM Pon A for 24 h after which the cells were immunostained with iNOS antibodies and assayed using flow cytometry **(Fig. 5.16)**.

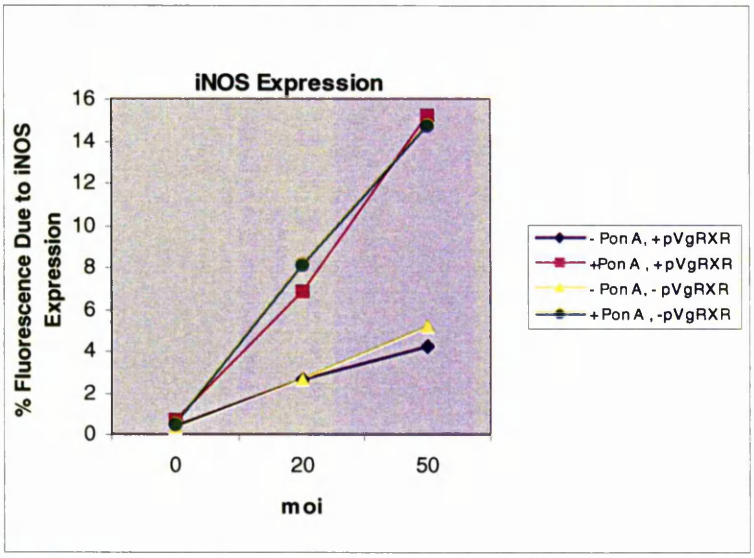

Fig 5.16 iNOS gene expression as determined by flow cytometry. Wild-type HT-1080 cells were infected with varying moi of pAdpVgRXR and pAdpIND SP1 iNOS or the latter alone and induced with 0 or 20 µM Pon A.

Both results indicated that pAdpVgRXR was not needed to induce gene expression, which increased in response to Pon A and depended on the moi used.

5.6.6 Testing the Functionality of the Ecdysone pShuttle Vectors

In order to clarify whether the disruption in gene regulation occurred at the stage of plasmid ligation (pShuttle) or viral generation (pAd), HEK 293 cells were seeded at $2x10^5$ cells/well in 6- well plates and transiently transfected with pShuttle pVgRXR and pShuttle pIND SP1 *Lac* Z vectors (1 μg/well of each vector) using Lipofectamine (10 μl/well). The following day, the cells were induced with Pon A for 24 h after which the cells were formalin-fixed and X-gal stained. Blue cells were counted in each well **(Fig 5.17 A)**. Then, the content of each well was dissolved in 1 ml DMSO and the absorbance was read at 650 nm **(Fig 5.17 B)**.

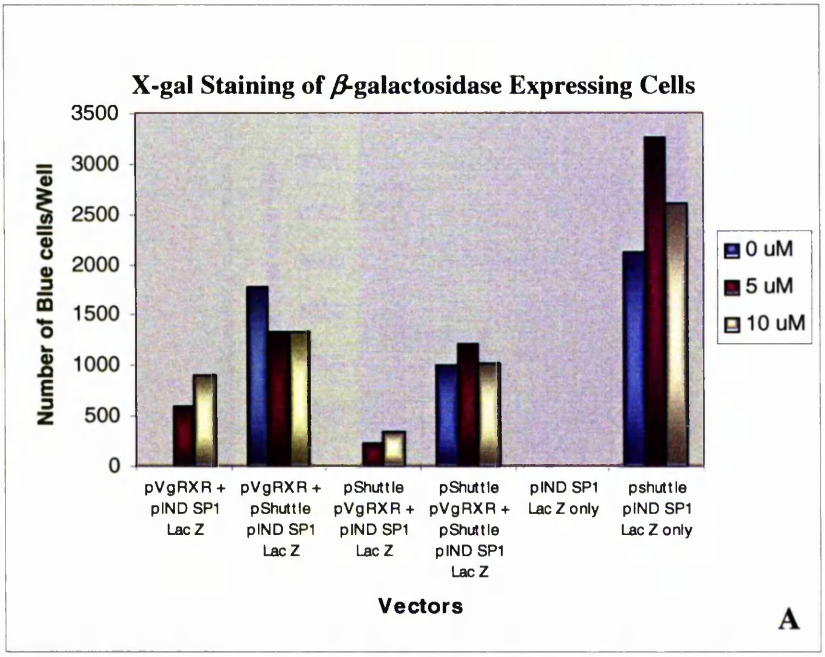

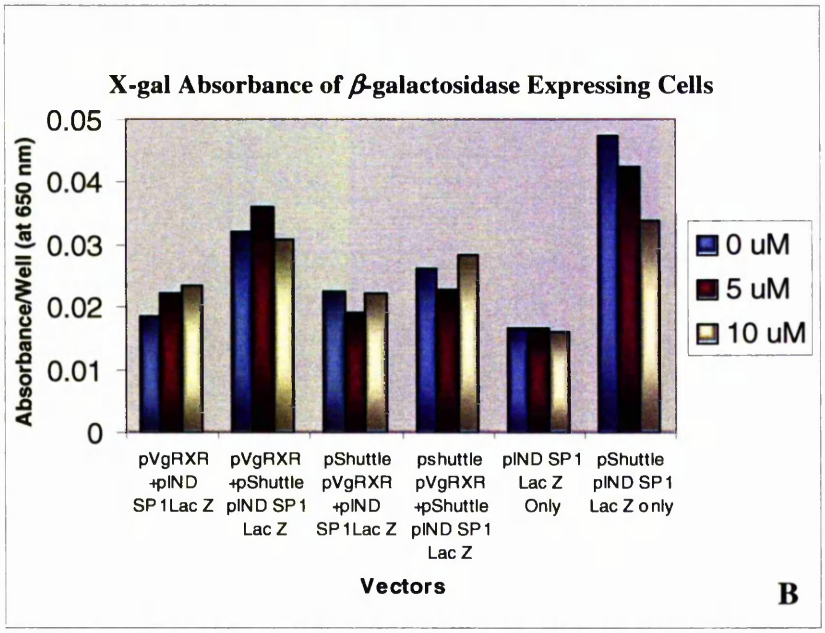

Fig 5.17 HEK 293 cells were transfected with the pShuttle ecdysone cassettes. The cells were induced with varying concentrations of Pon A and then X-gal stained. Blue cells were counted **(A)** and then the contents of each well were dissolved in 1 ml DMSO. The absorbance was read at 650 nm **(B)**.

In both cases, gene regulation was disrupted whenever pShuttle pIND SP1 *Lac* Z was used. Variations in the above results are due to human error in counting the blue cells/well. Moreover, several attempts were made to digest the ecdysone promoter out of the pShuttle

pIND SP1 *Lac* Z and pShuttle pIND SP1 iNOS vectors but all of these attempts were unsuccessful. This led to examining the inducible promoter to understand why it was behaving as a constitutive one.

5.6.7 Running the Ecdysone Promoter on a Computer Database

The sequence generated upon ligating pShuttle (at *Not* I site) and pIND SP1 (at *Sal* I site) was run on a computer database (http://bimas.dcrt.nih.gov/cgi-bin/molbio/proscan) [202] in order to confirm that this ligation did not accidentally result in a new promoter that constitutively drives gene expression. Although this was highly unlikely, yet the ligation was checked for further assurance. The results indicated that the newly generated sequence (first 29 bp that proceed the ecdysone promoter pIND SP1) did not code for any promoters **(Fig 5.18)**.

Not I / *Sal* I PIND SP1 (1 bp)

Processed sequence:

```
1       GTAATATGGTACCGCTCGACGGATCGGGGAGATCTCGGCCGCATATTAAG
51      TGCATTGTTCTCGATACCGCTAAGTGCATTGTTCTCGTTAGCTCGATGGA
101     CAAGTGCATTGTTCTCTTGCTGAAAGCTCGATGGACAAGTGCATTGTTCT
151     TGCTGAAAGCTCGATGGACAAGTGCATTGTTCTCTTGCTGAAAGCTCAGT
201     ACCCGGGTCGGAGTACTGCCCCGCCCCTAGCGATTAGCCCCGGCCCCGCA
251     TAGCTCCGCCCCGGGAGTACCCTCGACCGCCGGAGTATAAATAGAGGCGC
301     TTCGTCTACGGAGCGACAATTCAATTCAAACAAGCAAAGTGAACACGTCG
351     CTAAGCGAAAGCTAAGCAAATAAACAAGCGCAGCTGAACAAGCTAAACAA
401     TCTGCAGTAAAGTG
```

Proscan: Version 1.7

Processed Sequence: 414 Base Pairs

```
Promoter region predicted on forward strand in 4 to 254
Promoter Score: 62.37 (Promoter Cut-off = 53.000000)

Significant Signals:
 Name                    TFD #   Strand  Location  Weight
UCE.2                   S00437    +       37      1.278000
UCE.2                   S00437    -       40      1.216000
APRT-mouse_US           S00216    +       218     6.003000
EARLY-SEQ1              S01081    +       219     6.322000
(Sp1)                   S01187    +       219     8.117000
AP-2                    S01936    +       219     1.108000
Sp1                     S00801    +       220     2.755000
Sp1                     S00802    +       221     3.292000
GCF                     S01964    -       224     2.284000
Sp1                     S00781    -       225     2.772000
Sp1                     S00978    -       226     3.361000
JCV_repeated_sequenc    S01193    -       226     1.658000
Sp1                     S00979    -       227     6.023000
Sp1                     S00645    -       227     7.170000
Sp1                     S00064    -       227     5.934000
Sp1                     S01542    -       227     3.608000
UCE.2                   S00437    -       245     1.216000
```

Fig 5.18 Running of the pIND SP1 promoter that was ligated into pShuttle on a database.

The database of the newly generated sequence showed that no new promoter has been formed at the ligation site (first 29 bp that proceed the ecdysone promoter pIND SP1).

5.7 Deciphering the Cause for Gene Disruption

Since the cause for gene disruption seems to have started with the cloning of pShuttle-pIND SP1 *Lac* Z, this vector as well as pShuttle-pIND SP1 iNOS vector and the empty pShuttle-pIND SP1 vector were sequenced using the forward primer of the pShuttle vector (5' GAAGTGAAATCTGAATAATTTTGT 3') (**Fig 5.20, 5.21, 5.22**). It is important

to mention that pShuttle-pIND SP1 vector was previously sequenced using the forward primer and the ligation was confirmed **(Section 5.2.2)**. The other 2 vectors were sequenced using the reverse pShuttle primer only (5' GTGGGGGTCTTATGTAGTTTTG 3') since DNA digests confirmed the ligation of the insert (*Lac* Z Poly A) into the pShuttle pIND SP1 vector **(Sections 5.2.3 and 5.2.4)** but did not confirm the orientation and only upon using the reverse primer (that reads the Poly A) the orientation could be determined.

Upon careful sequence reading, it was realised that pShuttle-pIND SP1 *Lac* Z was not what it was thought to be. It was actually the pShuttle-CMV *Lac* Z. From the sequences, it was found that both the *Lac* Z and the iNOS vectors had a CMV promoter and no ecdysone promoter. It turned out that upon ligating the *Lac* Z Poly A (that was digested from the pShuttle CMV *Lac* Z vector) into the pShuttle pIND SP1, the colonies selected from the kanamycin-containing plates were religated pShuttle CMV *Lac* Z plasmids. This was possible since these plasmids also had a kanamycin resistance marker and upon digesting with restriction enzymes, they produced bands very similar in size to those expected with the pShuttle-pIND SP1 *Lac* Z vector. This was an extremely tricky case of ligation and the outcome was never predicted earlier. Since the iNOS cDNA was used to replace the *Lac* Z fragment, it was normal that the iNOS vector retained a CMV promoter. A second detailed analysis of the previously performed DNA digests confirmed the above explanation **(Fig 5.19)**.

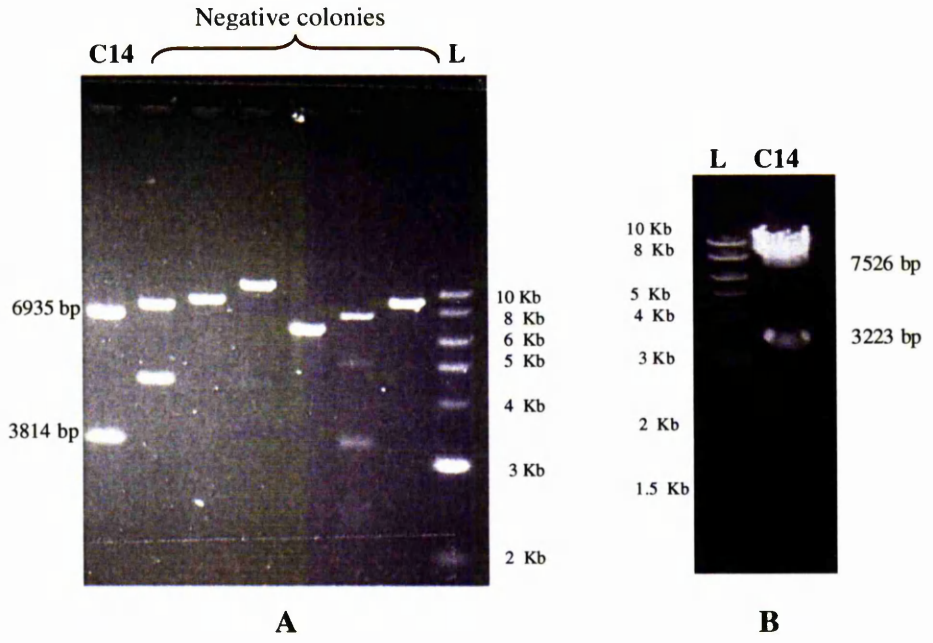

Fig 5.19 Same as **Fig 5.6**. Test digests performed after colonies were picked to check for the pShuttle pIND SP1 *Lac* Z ligation. **A** *Kpn* I and *Hind* III digests; the expected sizes were 3814 bp and 6935 bp. The marked colony was picked as it showed similar but not exactly the expected sizes. To confirm the ligation, that colony was digested using *Not* I and *Hind* III **(B)**. This digest confirmed that the ligation was correct (expected sizes: 3223 bp and 7526 bp) but did not confirm the orientation hence the need to sequence using the reverse pShuttle primer. The expected size of the relegated pShuttle CMV *Lac* Z were 3235 bp and 7356 bp upon digesting with *Kpn* I and *Hind* III. They were 3223 bp and 7368 bp if digested with *Not* I and *Hind* III. This similarity in expected sizes was not realised until after knowing that the cloned plasmid is the religated pShuttle CMV *Lac* Z.

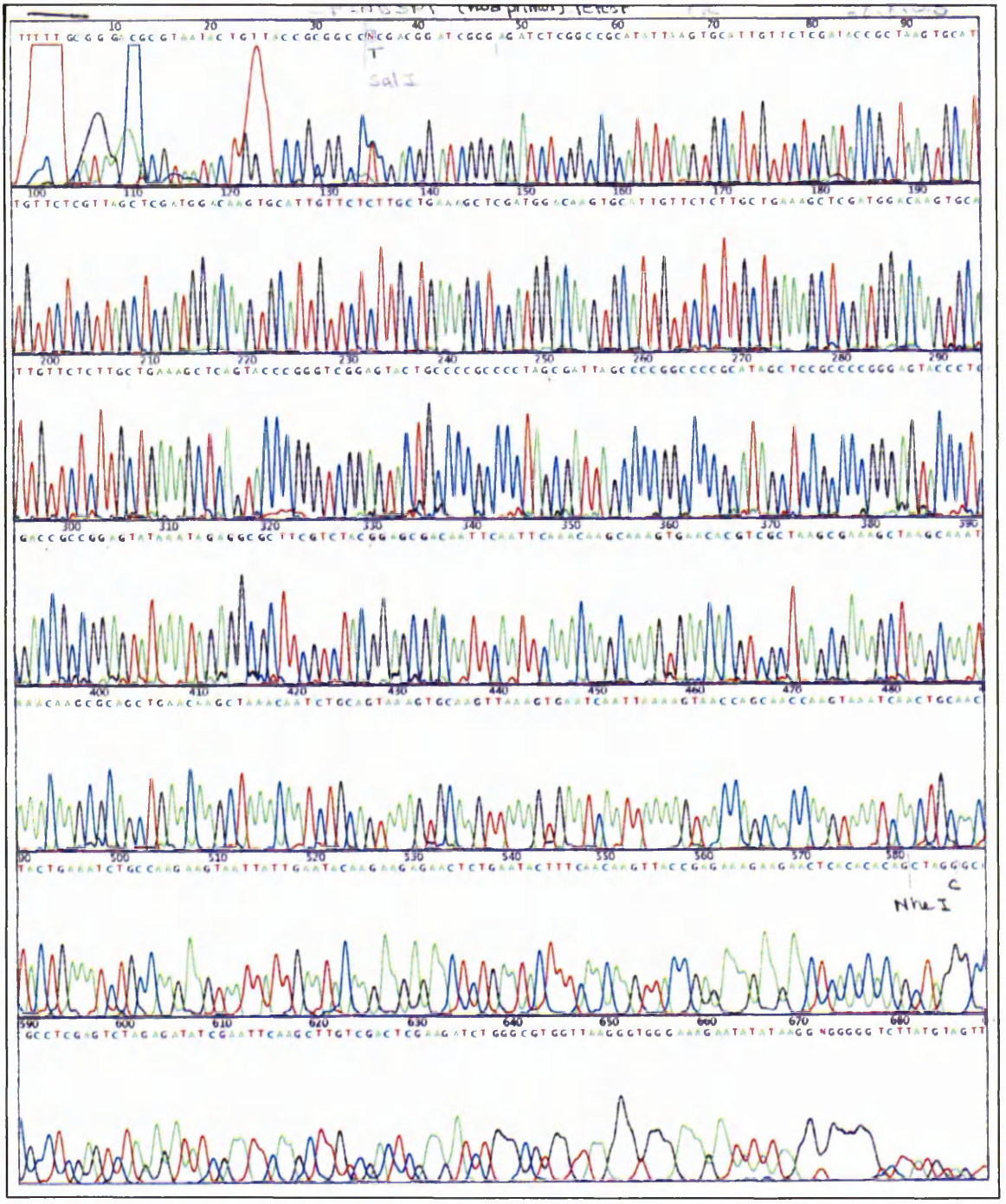

Fig 5.20 Sequence of pShuttle-pIND SP1 using the forward pShuttle primer.

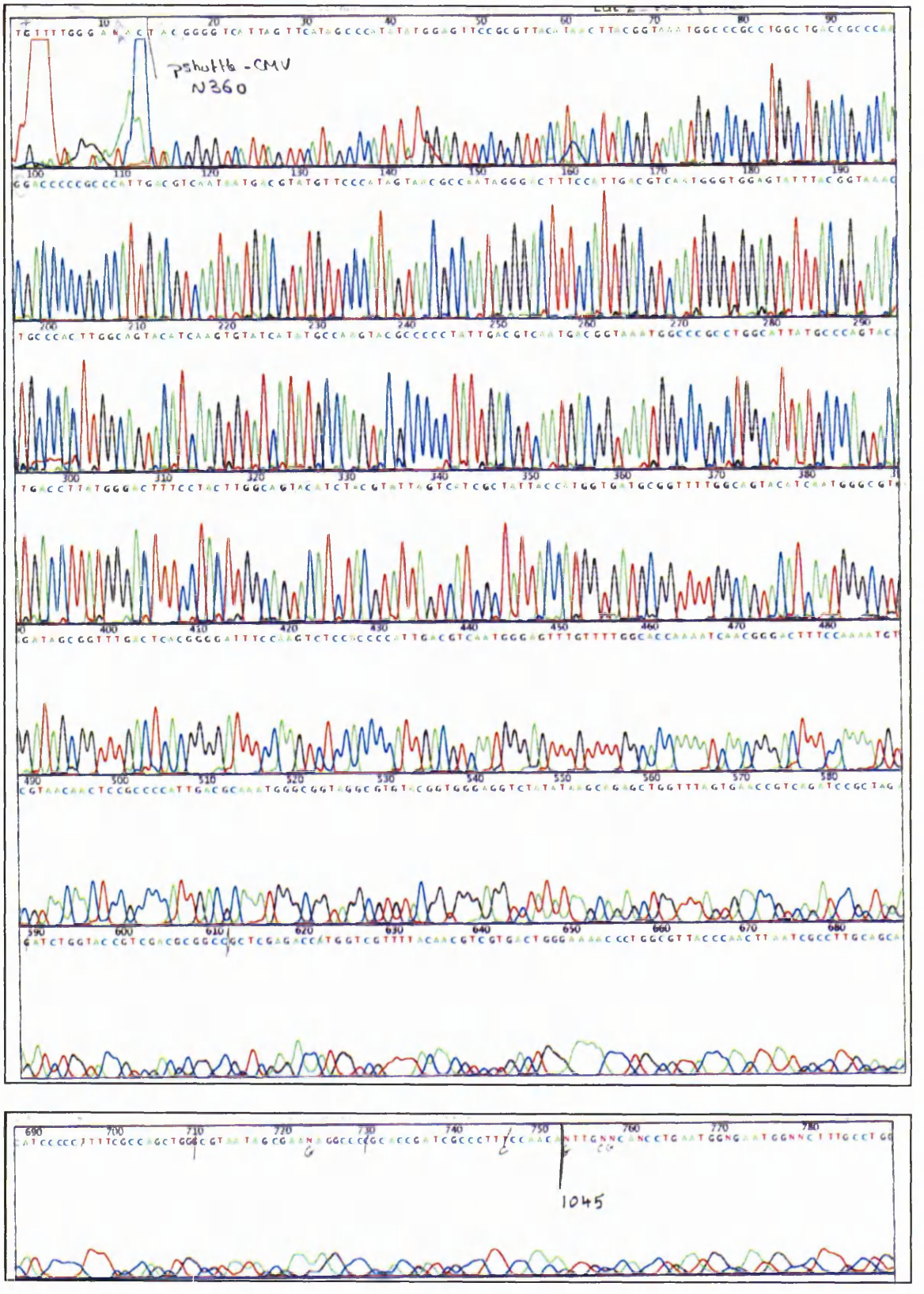

Fig 5.21 Sequence of pShuttle-CMV *Lac* Z using the forward pShuttle primer.

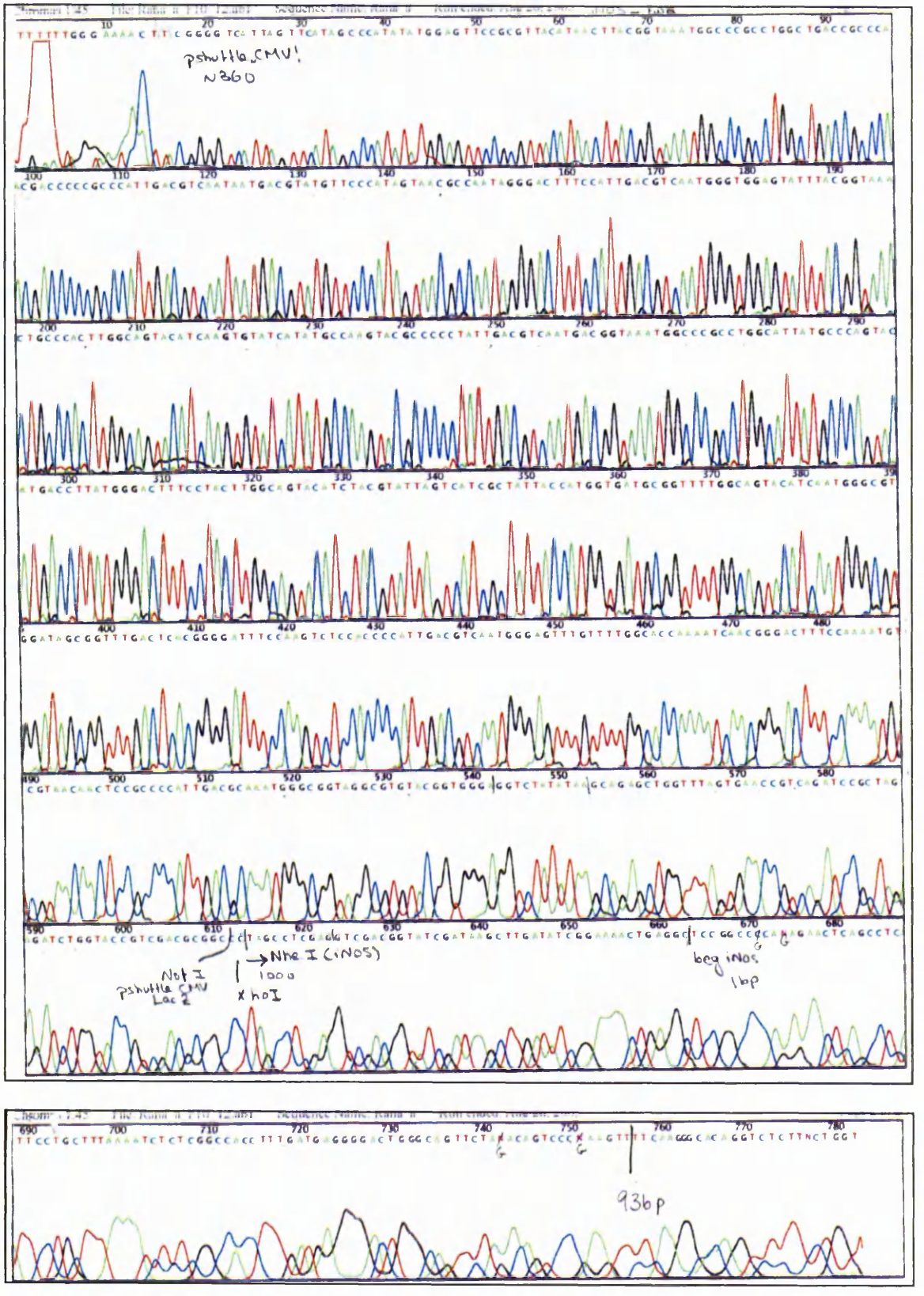

Fig 5.22 Sequence of pShuttle-CMV iNOS using the forward pShuttle primer.

5.8 Measuring Gene Expression Obtained by Viral Infection

Having realised that the established adenoviruses contain a CMV promoter, the level of *Lac* Z and iNOS gene expression obtained by these viruses was measured.

5.8.1 Determination of the Viral Transfection Efficiency of the HT-1080 Cell line

Wild-type HT-1080 cells were seeded at $5x10^4$ cell/well in a 6-well plate. After 4 h, the cells were infected with pAd CMV *Lac* Z (moi 0,2,10,30). After another 48 h, the cells were formalin-fixed and X-gal stained. Blue cells were counted **(Fig 5.23 and Table 5.3)**.

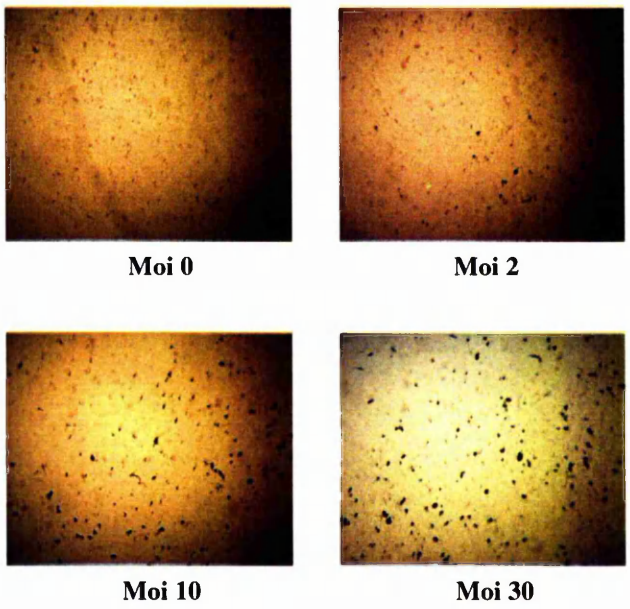

Fig 5.23 An image showing Xgal staining of HT-1080 wild type cells infected with varying moi of pAdCMV *Lac* Z (10x magnification).

PAdCMV *Lac* Z moi	0	2	10	30
Number of blue cells/field of view	0	35	151	202
Estimated Percentage (%)	0.0	6.2	26.8	35.8

Table 5.3 Number of X-gal stained cells/field of view of HT-1080 wild-type cells infected with pAd CMV *Lac* Z. The % blue cells was calculated by dividing the number of blue cells per field view (for each moi) by the total number of cells in a single field view (each field view contains approximately 564 cells).

The X-gal staining of HT-1080 wild-type cells infected with pAdCMV *Lac* Z showed that gene expression increases with viral moi. This was also expected to occur with the cells infected with pAdCMV iNOS.

5.8.2 Measuring iNOS Expression Using pAdCMV iNOS

iNOS expression generated from the constitutive iNOS adenoviruses was measured using flow cytometry. The HT-1080 wild-type cells were seeded at $5x10^4$ cells/well in 6-well plates and infected with adenoviruses at varying moi for 48 h. The *Lac* Z adenoviruses were used as a control for the effect of viral infection. The ecdysone inducible iNOS clone (16.10/T) was also included in this experiment and the cells were seeded at $5x10^4$ cells/well and induced with 20 μM Pon A the following day for 24 h. Then, the samples were formalin-fixed, permeabilised, and immunostained. A clone that was previously engineered to over express iNOS constitutively (MDA-MB-231 transfected with pEF iNOS- Dr. Edwin Chinje) was used as a positive control in this experiment. **(Fig 5.24 and Tables 5.4 and 5.5)**.

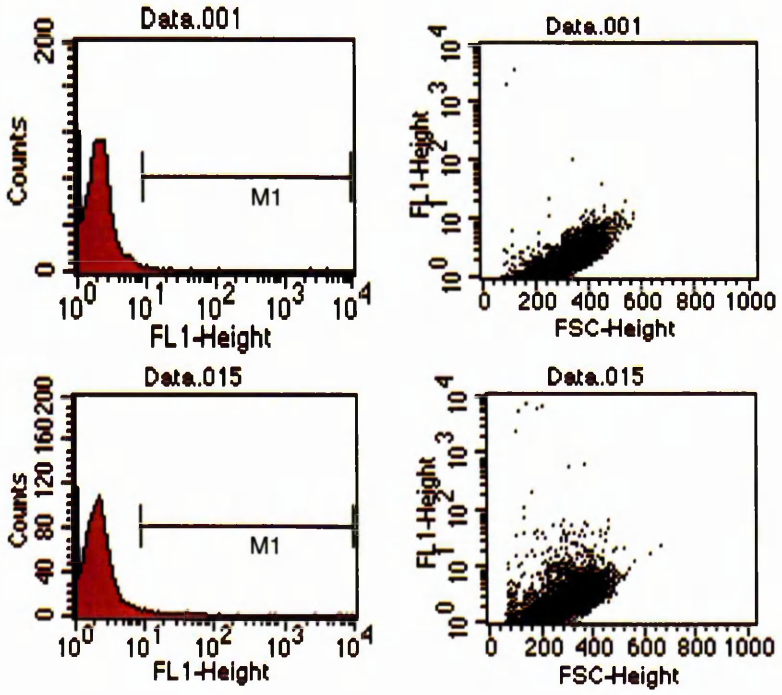

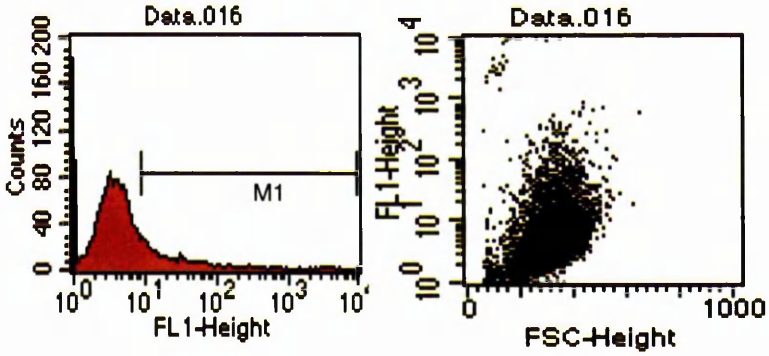

pAdCMV iNOS
Moi 10
15.3 %

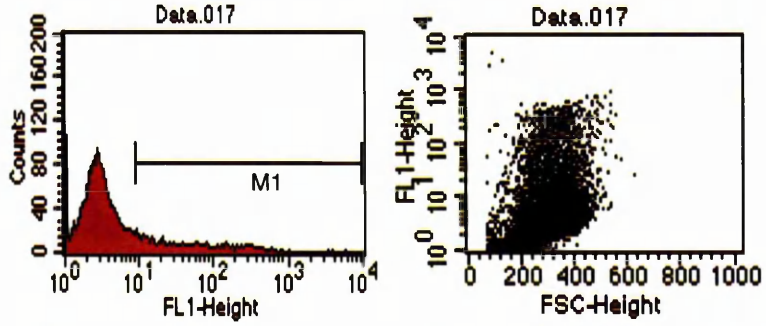

pAdCMV iNOS
Moi 30
17.51 %

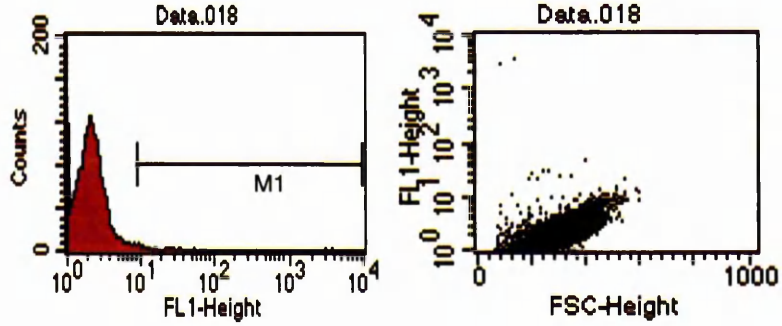

pAdCMV *Lac* Z
Moi 2
0.33 %

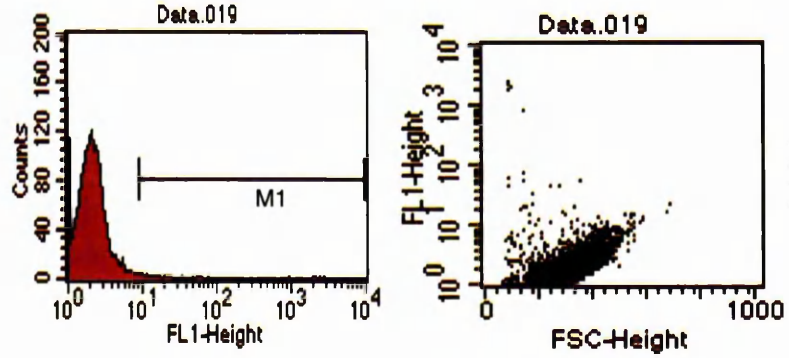

pAdCMV *Lac* Z
Moi 10
0.50 %

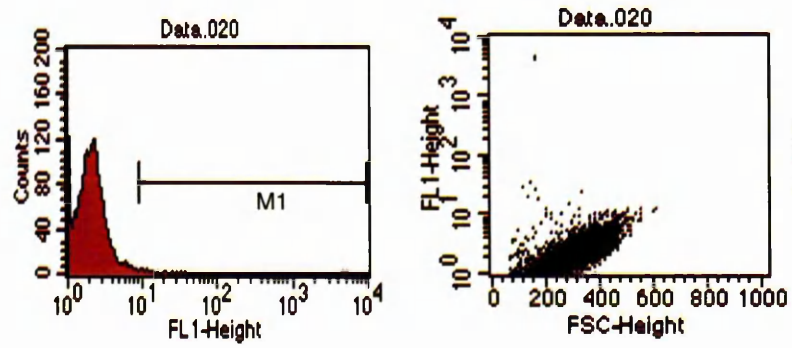

pAdCMV *Lac* Z
Moi 30
0.40 %

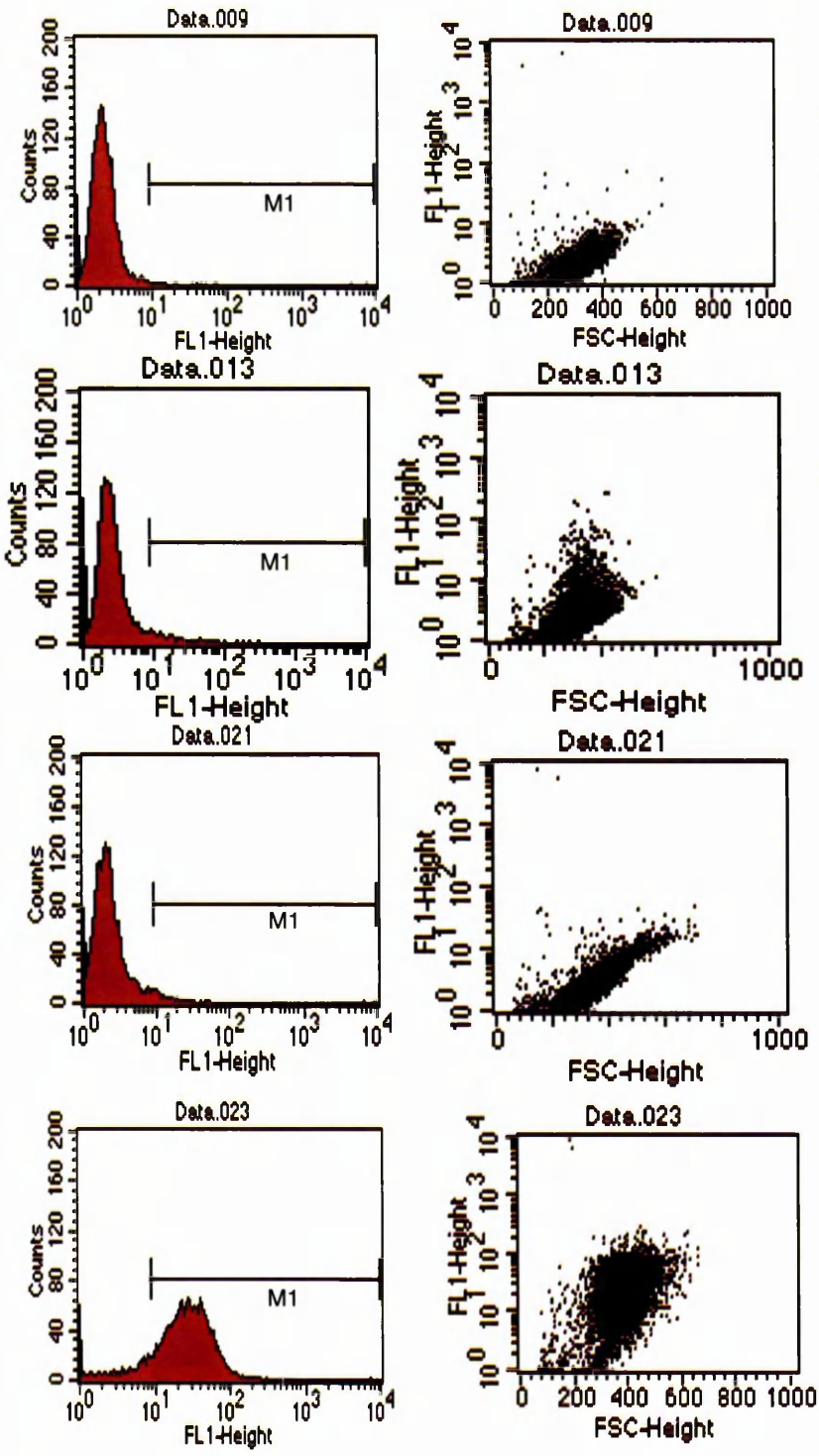

Fig 5.24 These graphs reflect the % fluorescence due to iNOS expression in HT-1080 and MDA-MB-231 cells. The % shift in peak is presented next to each sample. The graphs to the left indicate a shift in peak due to iNOS expression. M1 was set to gate for the background fluorescence in the control sample and was used to compare fluorescence of the other samples. The graphs to the right indicate (FL-1) versus side scatter (FSC). Cells exhibiting fluorescence due to high iNOS expression shift to the upper area of the quadrant.

% Fluorescence Due to iNOS Expresion:

Sample	Moi 0	PAdCMV iNOS Moi 2	PAdCMV iNOS Moi 10	PAdCMV iNOS Moi 30	PAdCMV *Lac Z* Moi 2	PAdCMV *Lac Z* Moi 10	PAdCMV *Lac Z* Moi 30
% Fluorescence	0.37	1.49	15.30	17.51	0.33	0.50	0.40
Fold		4.0	41.4	47.3	0.9	1.4	1.1

Table 5.4 % fluorescence and fold induction due to iNOS expression in the HT-1080 wild-type cells infected with pAdCMV iNOS.

Sample	HT- clone 0 μM Pon A	HT-clone 20 μM Pon A	MDA – MB-231 WT	MDA-MB-231 clone
n=1	0.24	2.93	2.39	87.02
n=2	0.21	3.31	1.71	88.37
Average	0.23	3.12	2.05	87.7
Fold		13.6		42.8

Table 5.5 A summary of the % and fold fluorescence observed in the clones that over express iNOS.

After immunostaining for iNOS expression, a 47.3 fold increase in fluorescence due to iNOS expression was observed with the cells infected with pAdCMV iNOS at moi 30 as compared to the uninfected cells. This expression is much higher than that observed with the ecdysone inducible clone (13.6 fold at 20 μM). When constitutively over expressed in the MDA-MB-231 cell line, iNOS showed a 42.8 fold increase as compared to the wild-type cells.

5.8.3 Studying the Effect of iNOS Over Expression on Apoptosis Using the iNOS Adenoviruses

The same samples that were tested for iNOS expression **(Section 5.8.2)** were also tested for apoptosis using the PI stain, which was added after immunostaining with the iNOS antibodies **(Section 2.13.2)**. This stain binds to DNA and during apoptosis; DNA is fragmented resulting in a shift in peak to the left handside [203]. The % shift in peak due to PI staining was compared in the iNOS expressing cells to that of the wild-type cells **(Figs**

5.25 and 5.26). PI is excited at 536 nm and the emission is collected at 617 nm in the FL-3 channel.

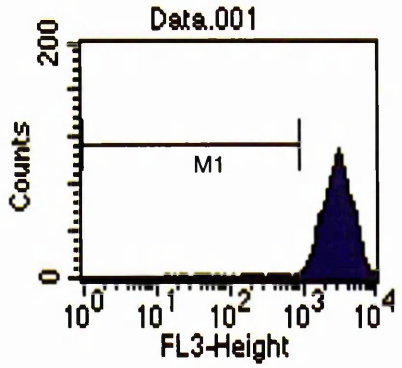

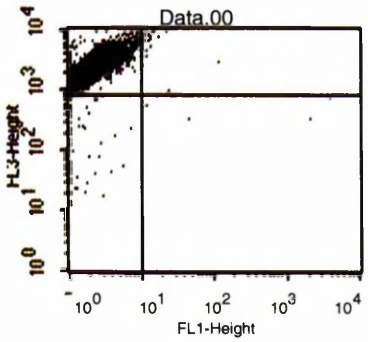

Moi 0
A 0.88 %
B 0.04 %

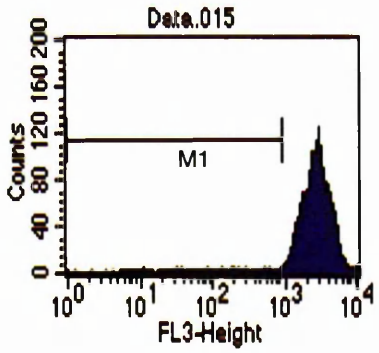

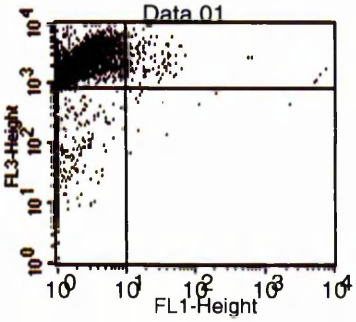

pAdCMV iNOS
Moi 2
A 3.79 %
B 0.13 %

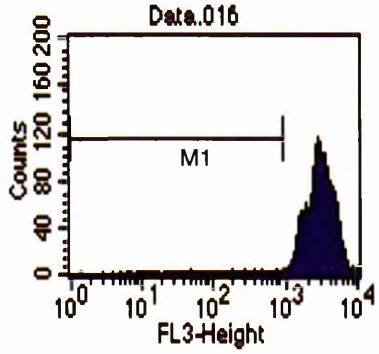

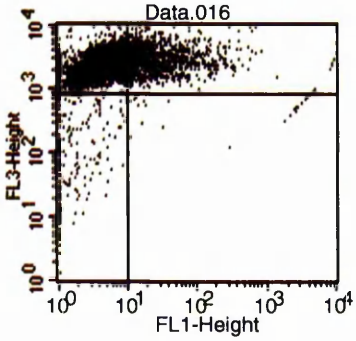

pAdCMV iNOS
Moi 10
A 2.69 %
B 0.24 %

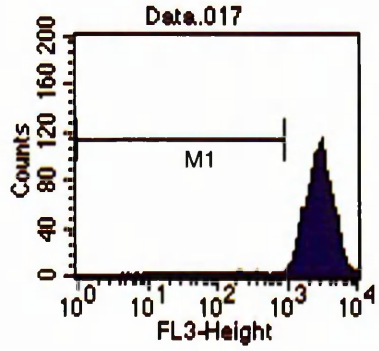

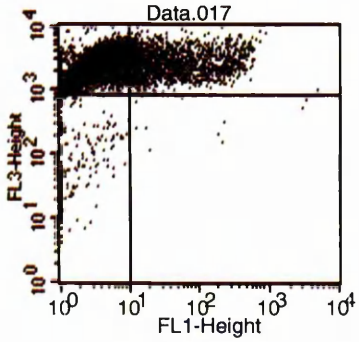

pAdCMV iNOS
Moi 30
A 2.54 %
B 0.11 %

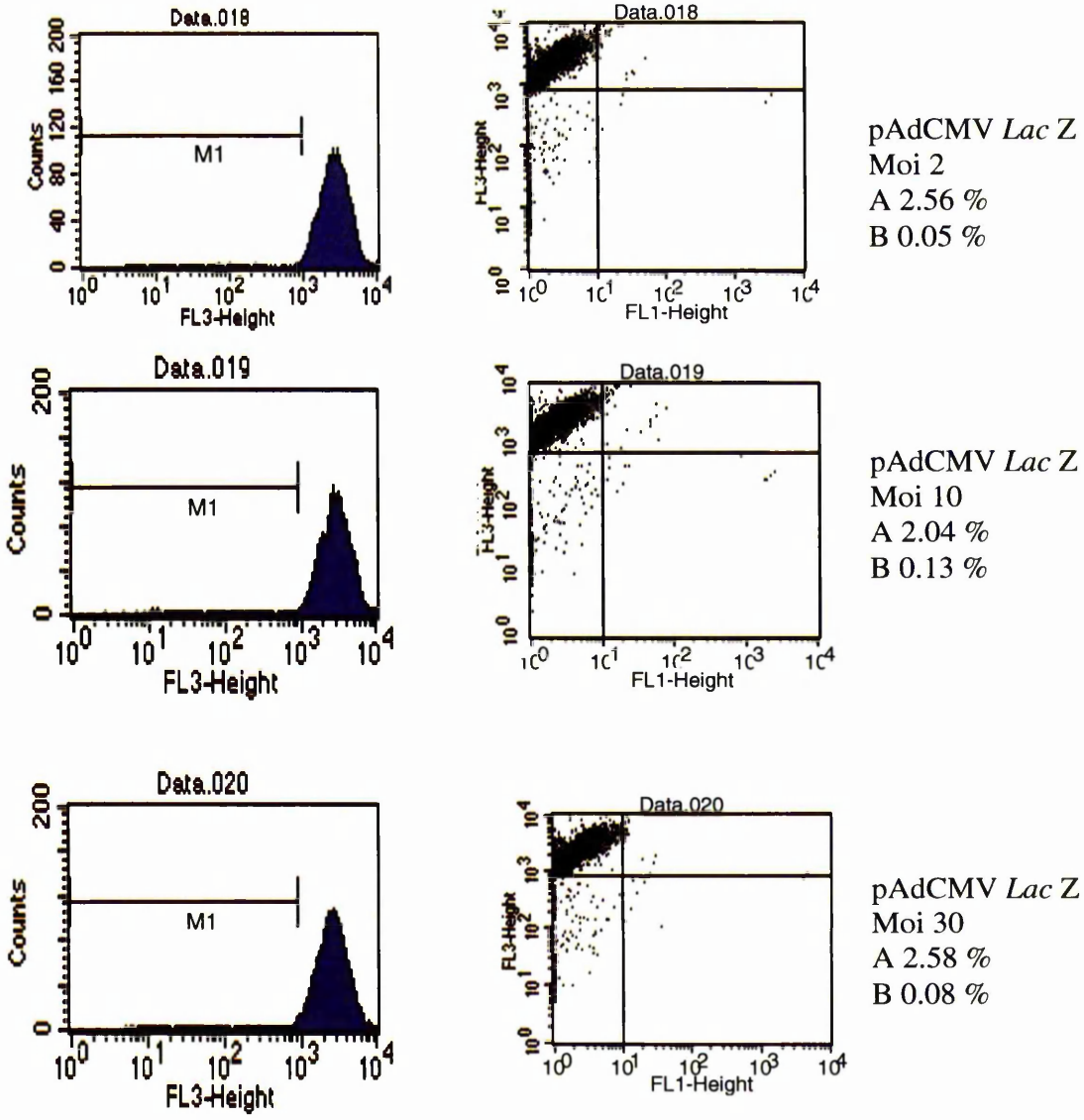

Fig 5.25 Apoptosis was measured by % fluorescence due to PI staining. HT-1080 wild-type cells were infected with pAdCMV iNOS (or pAdCMV *Lac* Z as a control). The graphs to the left represent a shift in peak indicating fluorescence due to PI staining. The M1 gate was set for background staining in the control sample and was used to compare fluorescence with the other samples. The graphs to the right represent a dot plot of the cells expressing iNOS and undergoing apoptosis. iNOS expressing cells shift to the right (FL-1), while those undergoing apoptosis shift downwards (FL-3). So, the cells that express iNOS and undergo apoptosis are represented in the lower right quadrant. Value A is the % fluorescence due to PI staining, value B represents the % of cells expressing iNOS and undergoing apoptosis.

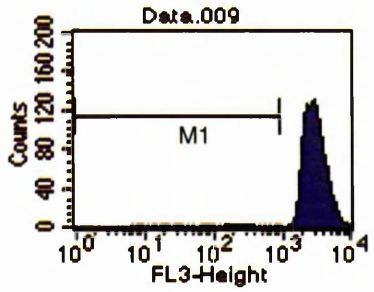

HT-1080 clone 0 μM Pon A
0.68 %

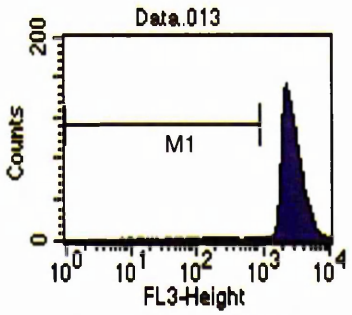

HT-1080 clone 20 μM Pon A
0.84 %

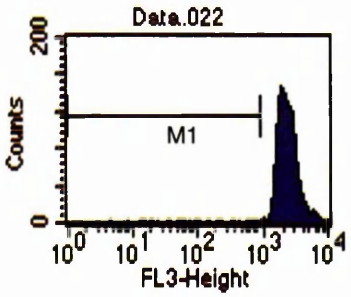

MDA-MB-231 Wild-type
0.66 %

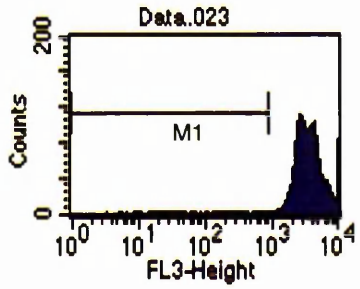

MDA-MB-231 clone
1.47 %

Fig 5.26 These graphs represent the % shift in peak due to PI staining in the iNOS expressing clones (representative graphs of n=2).

When examined for apoptosis using PI staining, there was almost no change in fluorescence due to PI staining with increasing iNOS expression. However, this was also observed with the MDA-MB-231 clone and the adenoviruses (moi 30) that express high levels of iNOS. It seems that at these levels of iNOS and under these experimental conditions, apoptosis cannot be detected.

5.9 Conclusion

In this chapter, we aimed to generate recombinant adenoviruses that express iNOS or *Lac* Z in the ecdysone cassette. However, upon evaluating the adenoviruses to determine the optimal conditions needed for inducible gene expression, high basal levels and high gene expression in the absence of the ecdysone receptor were noticed. After careful examination of all of the adenoviruses, it was discovered that although the pAdpVgRXR virus was functional and the cloning of the ecdysone promoter into the pshuttle pIND SP1 vector was successful, the pShuttle pIND SP1 *Lac* Z vector had a CMV promoter instead of an ecdysone inducible one. This explained the results that were observed earlier indicating that constitutive gene expression rather than inducible expression was taking place. A possible reason for the increase in gene expression in the presence of increasing Pon A concentration might be attributed to the toxicity of the inducer thus driving the expression of stress genes and consequently increasing the *Lac* Z or iNOS expression.

The disadvantage remains to be the inability of producing adenoviruses encoding for genes in the ecdysone reporter as this was attempted again several times but only religated plasmids were obtained. However, the advantage is the construction of adenoviruses that express *Lac* Z and iNOS under a constitutive promoter. These viruses were later used to study the various roles of iNOS in cancer gene therapy including apoptosis, bioreductive drug metabolism, and the NO-HIF-1 feedback loop. By varying the moi, this system was utilised to tightly regulate gene expression without the need to use another vector or Pon A.

Gene expression using the established adenoviruses was measured. Then, the effect of iNOS over expression on apoptosis was studied using the ecdysone inducible iNOS clone, a constitutive iNOS clone, as well as the adenoviruses that constitutively express iNOS. Apoptosis was examined *in vitro* using PI staining. High iNOS expression was observed with the MDA-MB-231 constitutive clone (87.7 %) and moderate levels were observed in the HT-

1080 cells infected with moi 30 of pAdCMV iNOS (17.51 %). Lower iNOS expression was observed in the other samples. Even though a range of iNOS expression was obtained, apoptosis was not observed in any sample including the constitutive iNOS clone. The fact that the ecdysone inducible and the constitutive iNOS clones produce NO (as observed from their activity monitored in the L-citrulline assay) indicated that these cells did not require cofactors for NO production. The reason for the inability to detect apoptosis in these samples could be due to the low level of NO generated in the ecdysone inducible clone or could be due to mutations occurring in the MDA-MB-231 clone (that constitutively generates high iNOS levels) which have lead to a blocking of the apoptotic pathway.

CHAPTER 6

Results 4 THE EFFECT OF iNOS OVER EXPRESSION ON CELL SENSITIVITY TO THE BIOREDUCTIVE DRUG TIRAPAZAMINE

6.1 Introduction

Tirapazamine is a bioreductive prodrug that upon reduction produces a toxic species, which can cause DNA damage. This drug is more toxic under hypoxic conditions as it reverts back to the non-toxic species in the presence of oxygen [72]. Studies have shown that P_{450} reductase is the major enzyme responsible for the reduction of TPZ [98]. Since NOS and P_{450} reductase share high sequence homology [7] and since some studies have found that iNOS has a higher affinity towards TPZ than the other NOSs or P_{450} reductase [69], the effect of iNOS over expression on cell sensitivity to TPZ was measured in this chapter. Previous studies in our laboratory have shown an increase in cell sensitivity towards TPZ by using clones that constitutively over express iNOS. As iNOS may be naturally over expressed in hypoxic tumours [20], it could be tailored for a therapeutic benefit by administering TPZ. A study of the effect of iNOS over expression on cell sensitivity to TPZ using the ecdysone inducible iNOS clone and the pAdCMV iNOS adenoviruses is detailed in this chapter.

6.2 Measuring Cell Sensitivity to TPZ in Stable Clones that Constitutively Over Express iNOS

Stable MDA-MB-231 clones that constitutively express iNOS were previously utilised in our laboratory to show that iNOS over expression increases the sensitivity of hypoxic cells to the bioreductive drug TPZ (Dr. Edwin Chinje). This sensitivity is specific to hypoxic conditions because TPZ reverts back to the non-toxic species in the presence of oxygen [72]. The cells were seeded at $3x10^3$ cells/well in a 96-well plate under aerobic (21 % O_2) or hypoxic (<0.1 % O_2) conditions in the presence of 250 μM L-NMA. The inhibitor was added to block the production of NO generated in the oxygenase domain of iNOS. After 3 h, the cells were incubated with varying concentrations of TPZ for another 3 h under aerobic or hypoxic conditions after which the media was replaced with fresh TPZ-free media. After 4-5 days, the cells were assayed using the MTT assay and the IC_{50} values were determined **(Table 6.1)**. The IC_{50} is the value of the drug concentration that corresponds to 50 % cell survival.

Sensitivity of MDA-MB-231 iNOS Transfected Clones to TPZ:

CLONE	*NOS Activity (pmol/min/mg)*	*TPZ IC_{50} μM (STD) Aerobic*	*TPZ IC_{50} μM (STD) Hypoxic*	*HCR*
PARENTAL	0.87 (0.11)	352.5 (27.2)	44.7 (4.6)	7.9
VECTOR	0.78 (0.17)	389.5 (15.3)	39.0 (8.4)	10.0
NOS-9	11.62 (0.93)	321.0 (26.0)	26.6 (2.3)	12.1
NOS-12	32.30 (1.57)	454.6 (76.0)	15.4 (3.2)	29.5
NOS-8	64.51 (1.41)	335.9 (19.2)	14.8 (3.6)	22.7
NOS-10	66.20 (3.11)	544.2 (86.0)	16.5 (5.1)	33.0

Table 6.1 Stable MDA-MB-231 clones constitutively expressing iNOS at different levels have been previously generated in our group. This table shows that sensitivity to TPZ increases with iNOS expression under hypoxic conditions. Cells have been exposed to hypoxic or aerobic conditions for 3 h. HCR (hypoxic cytotoxicity ratio) is the ratio of drug concentrations under normoxic to hypoxic conditions for the same level of cell kill [72]. (STD: standard deviation)

These results indicate that as iNOS expression increases, the hypoxic cytotoxicity ratio (HCR) increases. The IC_{50} values in air remain similar for the varying NOS activities whereas those of hypoxia decrease. This indicated that the cytotoxicity is occuring under

hypoxic conditions and is due to the ability of iNOS to reduce TPZ to its toxic species that remains stable only under reduced oxygen conditions.

6.3 Measuring the Cell Sensitivity to TPZ Using the MTT Assay and the Ecdysone Inducible iNOS Clone

Cells from the ecdysone inducible iNOS clone (16.10/T) were seeded at $1x10^4$ cells/well in 24-well plates and induced in air with 20 μM Pon A for 48 h in order to increase iNOS expression. Then, the plates were placed in the hypoxic chamber (<0.1 % O_2) or kept under aerobic conditions (21 % O_2) and the medium was replaced with Pon A free medium that contained TPZ. Wild-type HT-1080 cells were used as a control and glass plates were used instead of plastic plates to avoid any residual oxygen that might be retained in plastic [204]. The cells were incubated with TPZ under aerobic or hypoxic conditions for 3 h after which the media was replaced with TPZ-free RPMI media. The cells were then kept under aerobic conditions until the untreated controls became confluent (5 days after seeding) and the MTT assay was performed **(Fig 6.1 and Table 6.2)**.

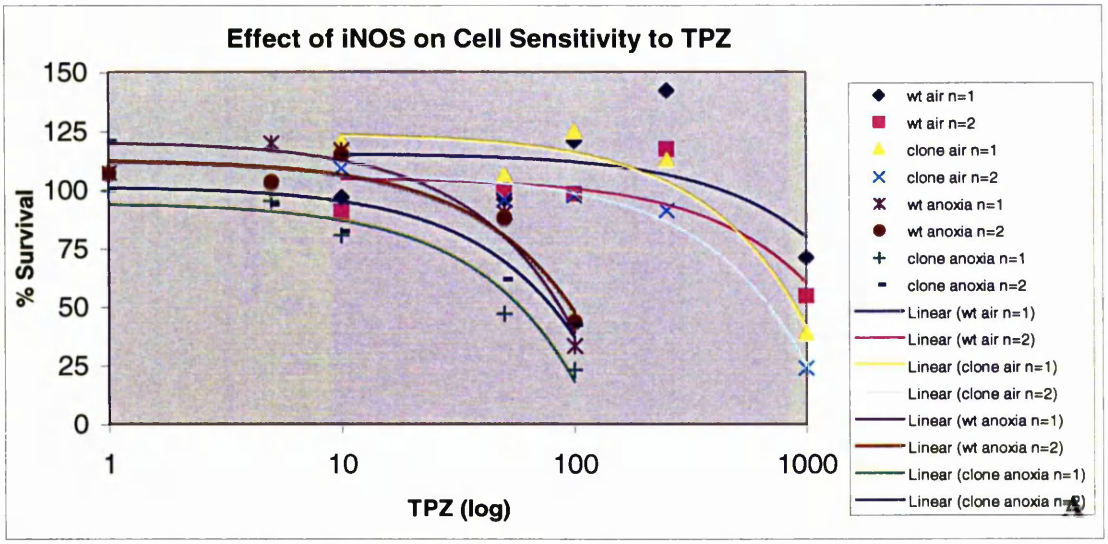

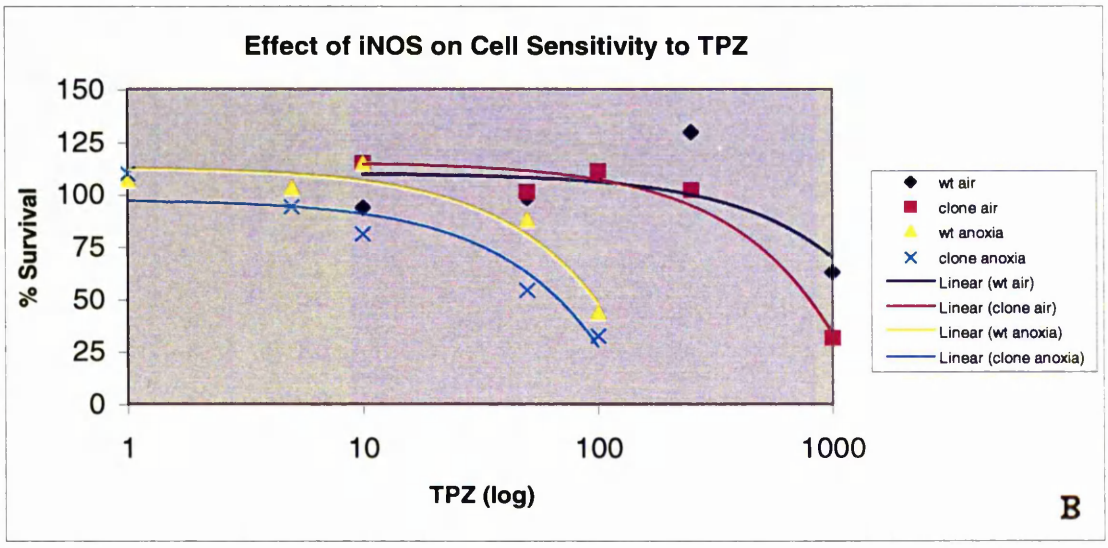

Fig 6.1 Graph showing the cytotoxicity to TPZ in air and hypoxia. Both wild-type HT-1080 and ecdysone inducible iNOS clone were induced with 20 μM Pon A (wt: HT-1080 wild-type, clone: ecdysone inducible HT-1080 iNOS clone -16.10/T) **A** is a plot of each of the 2 independent experiments (each in duplicate wells) and **B** shows the average of both experiments.

Sample	*TPZ IC_{50} μM Aerobic*	*TPZ IC_{50} μM Hypoxic*	*HCR*
wt 0 μM Pon A	1475 (2000, 950)	87.2 (90, 84.4)	16.9 (22.2, 11.3)
wt 20 μM Pon A	1355.3 (1500, 1210.5)	97.3 (85, 109.5)	13.9 (17.6, 11.1)
clone 0 μM Pon A	675.3 (802.5, 550)	134.6 (115.4, 153.8)	5.0 (6.9, 3.6)
clone 20 μM Pon A	700 (800, 600)	62.5 (45, 80)	11.2 (17.8, 7.5)

Table 6.2 Sensitivity of HT-1080 wild-type and ecdysone inducible iNOS cells to TPZ as measured by the MTT assay (average values of 2 separate experiments each in duplicate wells-shown in brackets).

The results indicated a 2.2 fold increase in hypoxic cytotoxicity to TPZ when iNOS was over expressed in the inducible clone, but the HCR values remained lower than those of the wild-type cells to the same drug. The activity of this clone was previously determined to be 21.5 pmol/min/mg at 20 μM Pon A. This slight increase in cytotoxicity could be attributed to the relatively low iNOS activity. In the MTT experiment performed using the MDA-MB-231 clones **(Section 6.2),** a 2.1 fold increase in sensitivity to TPZ was observed with an iNOS activity similar to that observed in the HT-1080 ecdysone inducible clone. The IC_{50} values of the HT-1080 cell line appear to be higher than those of the MDA-MB-231 and this could be due to the different characteristics of the different cell lines [205]. It is noteworthy to mention that several attempts were perfomed prior to this experiment in order to optimise the experimental conditions including seeding the cells at a lower density of $2.5x10^3$ cells/well, inducing with Pon A for 24 h, and incubation with TPZ for 18 h under aerobic or hypoxic conditions. However, none of these experiments showed any differential cytotoxicity, which could be due to the low iNOS activity of the ecdysone inducible clone.

6.4 Measuring TPZ-Mediated Cytotoxicity Using the Clonogenic Assay

6.4.1 Determining the Plating Efficiency of the HT-1080 Cell line

The clonogenic assay was performed as an alternative method to study the cytotoxicity to TPZ. Initially, the ideal plating efficiency was determined for the HT-1080 wild- type and ecdysone inducible clone such that enough colonies form after a certain period of culturing. The cells were seeded in 60 mm dishes at varying concentrations and fixed after 10 days with 70 % ethanol. The colonies were stained using methylene blue and counted **(Table 6.3)**.

Number of Cells Seeded/ plate	Average Number of Colonies Formed (Wild-type)	Average Number of Colonies Formed (Inducible Clone)
250	19.5 (17, 22)	18.0 (20, 16)
500	50.5 (49, 52)	53.5 (50, 57)
750	56.5 (57, 56)	60.0 (63, 57)
1000	71.5 (83, 60)	82.5 (88, 77)

Table 6.3 Average number of colonies formed 10 days after seeding. A colony contains approximately 50 cells (average values of duplicate wells, the number of colonies in each well is shown in brackets).

Based on the above experiment, a seeding number of 500 cells/plate was chosen for both wild-type and clone. This should produce a 10.1 % and 10.7 % plating efficiency in the wild-type and clone respectively 10 days after seeding and in the cells untreated with drug.

6.4.2 Over Expressing iNOS Using the Inducible Clone to Measure Cell Sensitivity to TPZ

HT-1080 wild-type and ecdysone inducible iNOS cells (16.10/T) were seeded at 500 cells /60 mm plate under aerobic (21 % O_2) or hypoxic (<0.1 % O_2) conditions. After 4 h, the cells were induced with 20 μM Pon A for 24 h under the same oxygen conditions. Then, the media was replaced with Pon A-free TPZ containing media. The cells were incubated with TPZ for 3 h following which all plates were placed under aerobic conditions and the TPZ containing media was replaced with fresh RPMI media (TPZ-free). After 7 days, the cells were fixed with 70 % ethanol, stained using methylene blue, and the colonies were counted **(Fig 6.2)**.

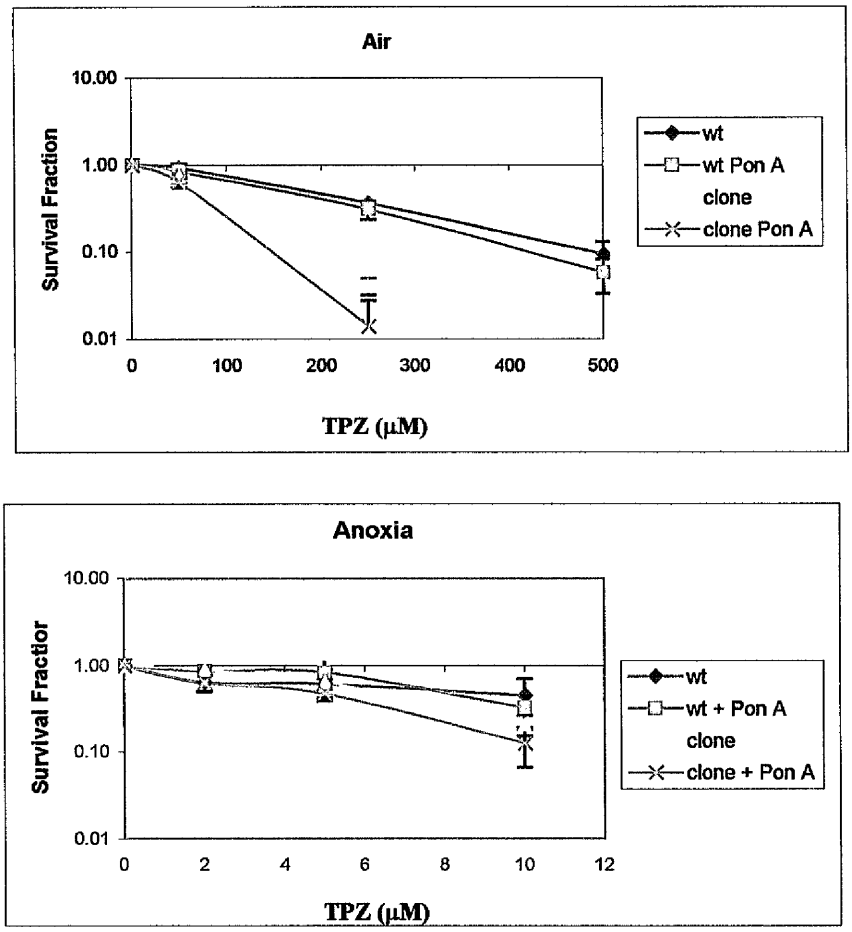

Fig 6.2 Graphs showing the survival fraction of cells that over express iNOS using the ecdysone system in comparison with uninduced cells or wild-type HT-1080. wt: wild type HT-1080, clone: ecdysone inducible iNOS HT-1080 clone-16.10/T (average values of 3 independent experiments).

Under aerobic conditions, the clone appears to be slightly more sensitive to TPZ especially when induced with Pon A. Under hypoxic conditions, a similar trend was observed with the differences being minimal.

An increase in cytotoxicity in the inducible clone under aerobic conditions was expected because upon Pon A administration, these cells can express iNOS and generate NO. However, the same cells induced with Pon A under hypoxic conditions cannot generate NO due to the absence of oxygen in this environment. This is different to the MTT experiment **(Section 6.3)** because these cells were seeded under aerobic or hypoxic conditions whereas in

the MTT experiment all the cells were seeded under aerobic conditions. The fact that the uninduced clone showed higher sensitivity than the wild-type cells could either be due to leakiness of the ecdysone system whereby even in the absence of Pon A some gene expression was observed or due to a clonal variation. Therefore, the decrease in IC_{50} observed with the Pon A induced clone under aerobic conditions may be due to NO generation, while that observed under hypxic conditions is due to TPZ cytotoxicity mediated by iNOS over expression. The HCR values for this experiment were calculated below (**Table 6.4**):

Sample	TPZ IC_{50} µM Aerobic	TPZ IC_{50} µM Hypoxic	HCR
wt 0 µM Pon A	175.0	8.0	21.90
wt 20 µM Pon A	162.5	8.0	20.30
clone 0 µM Pon A	75.0	6.3	11.90
clone 20 µM Pon A	63.0	4.6	13.70

Table 6.4 Hypoxic cytotoxicity to TPZ in iNOS over expressing HT-1080 cells.

Again, an increase in cytotoxicity was observed in the Pon A induced clone as compared to the uninduced; however, due to the low iNOS activity of this clone, the difference was modest.

6.4.3 Studying the Effect of Viral Mediated iNOS Over Expression on TPZ Cell Sensitivity

In order to study the same effect using the established adenoviruses that constitutively express iNOS, wild-type HT-1080 were seeded at 500 cells /60 mm dish under aerobic conditions. After 4 h, the cells were infected with varying moi of the pAd CMV iNOS virus or the pAd CMV *Lac* Z virus that was used as a control for viral infection. The cells were kept under aerobic conditions for 24 h and were then incubated under aerobic (21 % O_2) or hypoxic (<0.1 % O_2) conditions for another 24 h to maximise gene expression. The media was then replaced with TPZ-containing media and the cells were incubated under the same

oxygen conditions for 3 h. Then, the media was replaced with fresh RPMI (TPZ-free) and the cells were incubated under aerobic conditions for 7 additional days after which they were fixed with 70 % ethanol, stained using methylene blue, and the colonies were counted **(Fig 6.3)**.

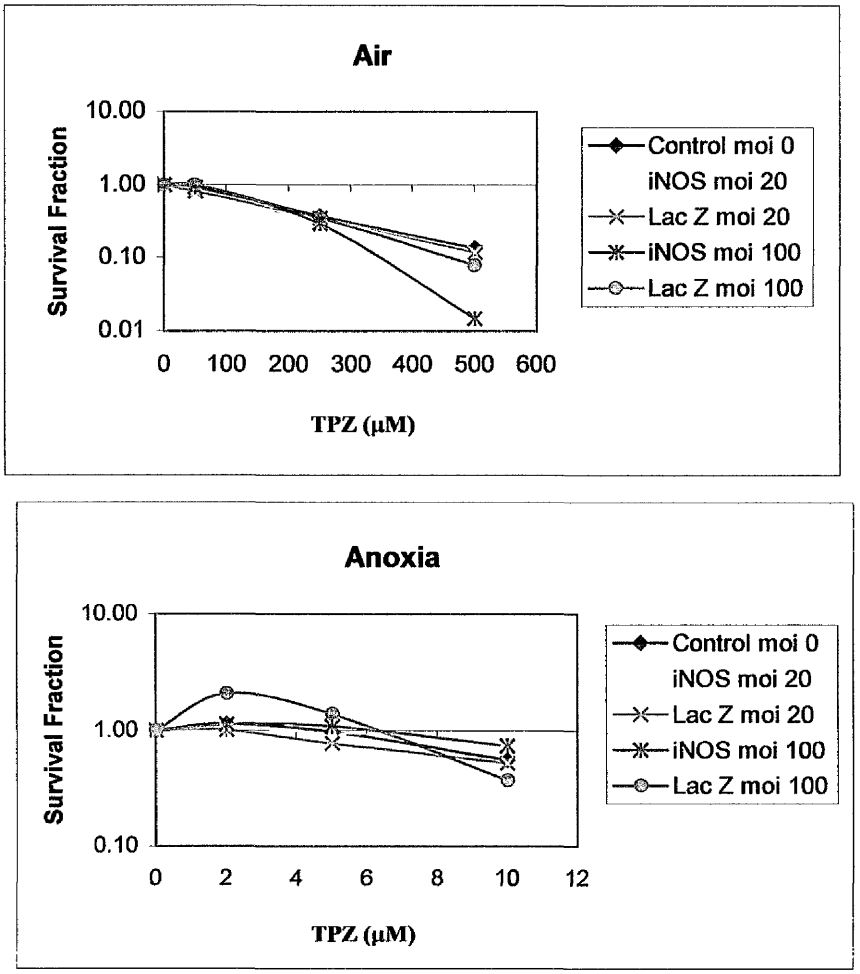

Fig 6.3 Graphs showing the survival fraction under aerobic and hypoxic conditions of cells over expressing iNOS by infecting them with pAdCMV iNOS. pAdCMV *Lac* Z was used as a control vehicle (average values of duplicate wells).

The results indicated a slight increase in sensitivity to TPZ (especially at 500 μM) upon infecting with pAd CMV iNOS in an moi dose dependent manner under aerobic conditions. However, this was not the case under hypoxic conditions. This minor difference in sensitivity might be explained by the low probability of a viral-cell encounter, as the

number of cells seeded was only 500 cells/plate in a relatively large volume of media, into which the viral inoculum was then placed. This experimental procedure could be modified such that larger numbers of cells are infected with adenoviruses in 6-well plates prior to seeding in the 60 mm plates.

6.5 Conclusion

Previous studies in our laboratory have shown that clones which constitutively over express iNOS demonstrate an increase in cell sensitivity to TPZ under hypoxic conditions. In this chapter, we have further studied this phenomenon using the ecdysone inducible iNOS clone and the pAdCMV iNOS adenoviruses. When an MTT assay was performed, a 2.2 fold increase in cytotoxicity towards TPZ was observed in the 20 μM Pon A-induced clone as compared to the uninduced clone. This low fold in the hypoxic cytotoxicity ratio could be due to the low iNOS expression observed in this clone. In addition, the clonogenic assay was performed as a second method to study the cytotoxicity of TPZ. Initially, the plating efficiency for the HT-1080 and ecdysone inducible iNOS HT-1080 clone was determined and therefore a seeding density of 500 cells/60 mm plate was chosen as it showed 10.1 % and 10.7 % plating efficiency respectively 10 days after seeding. Then, the sensitivity of iNOS over expressing cells towards TPZ was measured. Some sensitivity towards TPZ was observed using the iNOS inducible clone in the presence of 20 μM Pon A as compared to the uninduced clone; however, the fold increase in sensitivity remained modest. The increase in cytotoxicity observed under aerobic conditions could be attributed to NO production. On the other hand, an increase in cell sensitivity to TPZ should be observed using the pAdCMV iNOS adenoviruses if the cells are infected with the viruses before seeding and exposing to TPZ. These results suggest that iNOS can increase the sensitivity of cells towards TPZ and since iNOS levels are increased in clinical tumours, iNOS could be used in a therapeutic approach.

CHAPTER 7

Results 5 ROLE OF iNOS AND NO ON HIF-MEDIATED GENE EXPRESSION

7.1 Introduction

Hypoxia-inducible factor 1 (HIF-1) is a transcription factor that functions as a master regulator of oxygen homeostasis [73]. It is expressed in most cancers in response to hypoxia and it activates the transcription of genes whose protein products either increase O_2 delivery or provide metabolic adaptation under conditions of reduced O_2 availability [74]. Hypoxia regulates the expression of many genes by the interaction of HIF-1 with its DNA recognition site known as the hypoxia responsive elements (HRE) present within the the promoter region of these genes [71]. Although studies have shown that iNOS expression is up regulated under hypoxic conditions due to the HRE site available in its promoter [20], the feed back effect of NO on HIF remains largely controversial. Several studies have focused on using NO donors to study this effect and detected HIF-1 accumulation under aerobic conditions in response to the NO donor GSNO [87-89]. On the other hand, Sogawa *et al.* (1998), found that HIF mediated gene expression is reduced significantly in anoxia when GSNO was administered [93]. Deciphering the feed back effect of NO on HIF-mediated gene expression is of key importance. If NO is able to reduce HIF accumulation, this could have high therapeutic value whereby hypoxic tumours should no longer retain the ability of expressing genes that encode for growth under reduced oxygen conditions. Moreover, by over expressing iNOS in the hypoxic tumours, this enzyme could have other therapeutic benefits by combining it with TPZ administration and radiation.

In this chapter, the NO donor GSNO was used to study the effect of exogenous NO on HIF-mediated gene expression by measuring the Luciferase activity of a previously established stable clone that expresses an HRE-driven Luciferase gene. Plasmids and

adenoviruses that drive iNOS expression constitutively were then used in order to study the same effect using an endogenous, non-chemical NO sources.

7.2 Stable Expression of the Luciferase Reporter Gene in Response to Hypoxia

In order to study the effect of NO on HIF regulation, the expression of a Luciferase reporter gene in response to hypoxia was monitored. Two stable clones that were previously generated in our laboratory using the HCT-116 cell line (Dr. Rachel Cowen) were utilised. The first clone (firefly clone) had an HRE-driven luciferase cassette and therefore expresses the reporter gene firefly luciferase (luc+) under hypoxic conditions. In addition to the HRE-driven luciferase expression, the second clone encodes for the constitutive expression of the renilla luciferase gene (and so called the dual luciferase clone). Renilla was used to monitor non-specific effects on transcription that are not HIF-mediated. Initially, the experiments were performed using the HRE-luciferase clone and when changes in luciferase expression were observed, the experiments were repeated using the dual clone to test for non-specific effects.

These stable clones were generated by integrating a firefly expression cassette whose promoter comprises a trimer of the hypoxia responsive element (HRE) of mouse lactate dehydrogenase A (LDH-A) upstream of the SV40 minimal promoter followed by integration of a renilla luciferase cassette (in the dual luciferase clone) with expression driven by the human elongation factor 1 (EF1) promoter **(Fig 7.1)**.

Hypoxia driven firefly luc cassette A

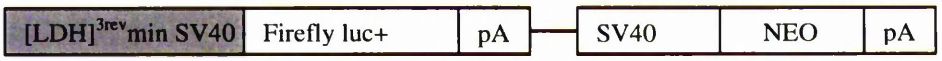

HIF-1 SITE **ChoRE**

CGG**ACGTGC**GGGAACC **CACG**TGTA

Constitutive EF1 driven renilla luc cassette B

Fig 7.1 Generation of the firefly and dual luciferase clones.

The cells were transfected with plasmid A and antibiotic selection was obtained using 0.5 mg/ml G418.Sulphate. For dual luciferase expression, the selected clone was transfected again by plasmid B and the clones were selected using 5 µg/ml puromycin.

Clone 22 (firefly luciferase) and clone 16 (dual luciferase) were used as they showed an average firefly luciferase anoxic induction of 10 folds after 18 h of hypoxic exposure followed by 3 h of reoxygenation.

7.3 Measuring the Effect of Exogenous NO on HIF Regulation Using NO Donors

The effect of exogenous availability of NO on HIF regulation was studied using the NO donor *S*-Nitrosoglutathione (GSNO). In addition to the HCT-116 cell lines, the HEK 293 cell line was also included in order to compare the results to those obtained by Metzen *et al.* (2003) who have observed that GSNO causes accumulation of HIF-1α under normoxic conditions using this cell line [89]. Initially, the HEK 293 cells were seeded at $2x10^5$ cells/well in a 6-well plate and transiently transfected by the HRE-driven luciferase cassette (2 µg/well and 10 µl/well Lipofectamine-**Section 2.8.1**) in order to express this reporter gene in this cell line. Then, each of the firefly clone, the dual luciferase clone, and HEK 293-HRE-luciferase transfected cells were seeded at $5x10^3$ cells/well in a 96-well plate under aerobic conditions (21 % O_2). After 3 h incubation under normoxic conditions, a range of GSNO

concentrations (0-1 mM) was added to the cells. The plates were immediately placed in 1 % (hypoxia) or <0.1 % (anoxia) oxygen conditions after GSNO addition. Control plates were left under aerobic conditions After 18 h, the plates were removed and reoxygenated for 3 h. The cells were then lysed and the luciferase activity was measured **(Section 2.7)**. **(Figs 7.2, 7.3, and 7.4)**

The Firefly Luciferase Clone:

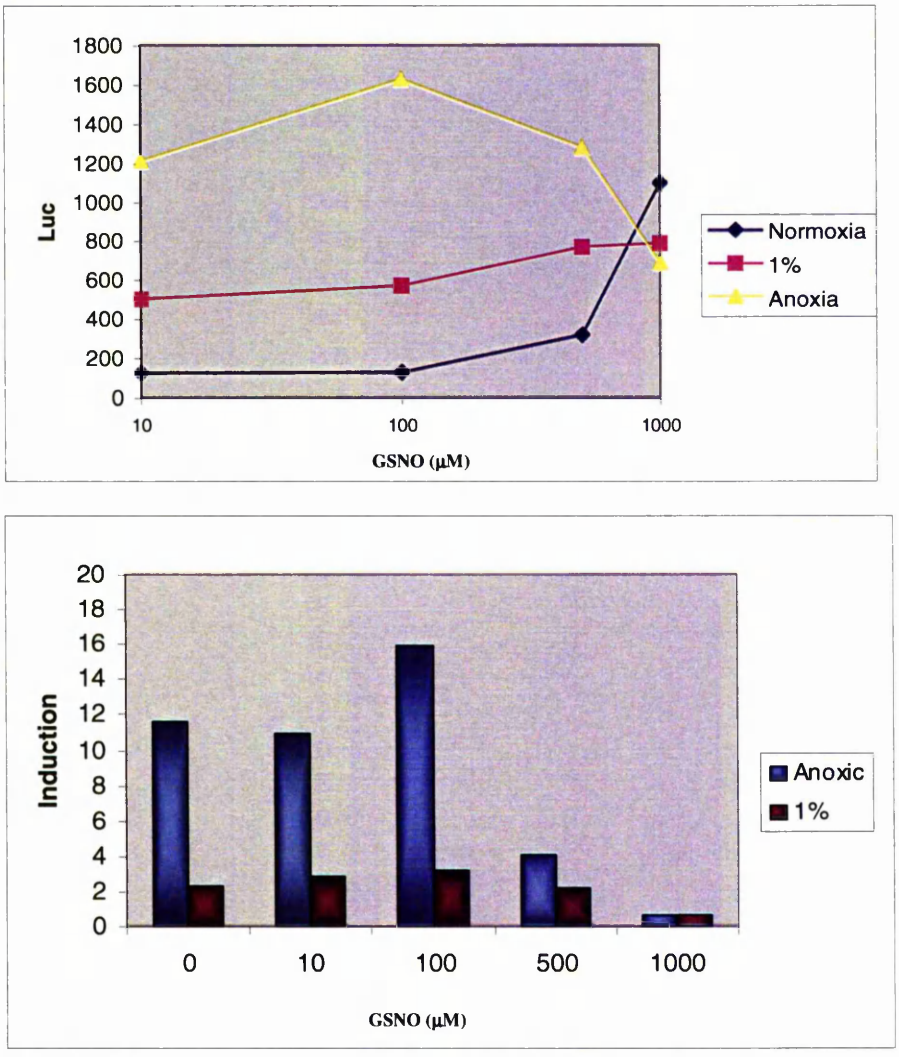

Fig 7.2 The effect of the NO donor GSNO on HIF regulated gene expression was measured using the luciferase assay. The anoxic induction was also calculated (average of 2 independent experiments each performed in triplicate wells).

The results in **Fig 7.2** indicate that GSNO causes HIF-1 accumulation under aerobic conditions especially at 500 and 1000 μM with luciferase expression reaching 2.5 and 8.5 fold above basal respectively. However, although initially a similar increase in luciferase expression was observed under 1 % and <0.1 % oxygen conditions, this expression remained constant under hypoxic conditions and appeared to decrease under anoxic conditions at concentrations of 100-1000 μM GSNO reaching levels lower than the basal. The anoxic induction in this experiment was 11.7 folds when untreated with GSNO. This induction decreased to 0.6 fold at 1000 μM GSNO. On the other hand, the hypoxic induction in this experiment was 2.3 folds and decreased to 0.7 folds when treated with the highest GSNO concentration. In order to be able to explain whether this luciferase expression was HIF-mediated or was non specific possibly due to toxicity of the drug (especially at high concentrations), this experiment was performed using the dual luciferase clone (**Fig 7.3**).

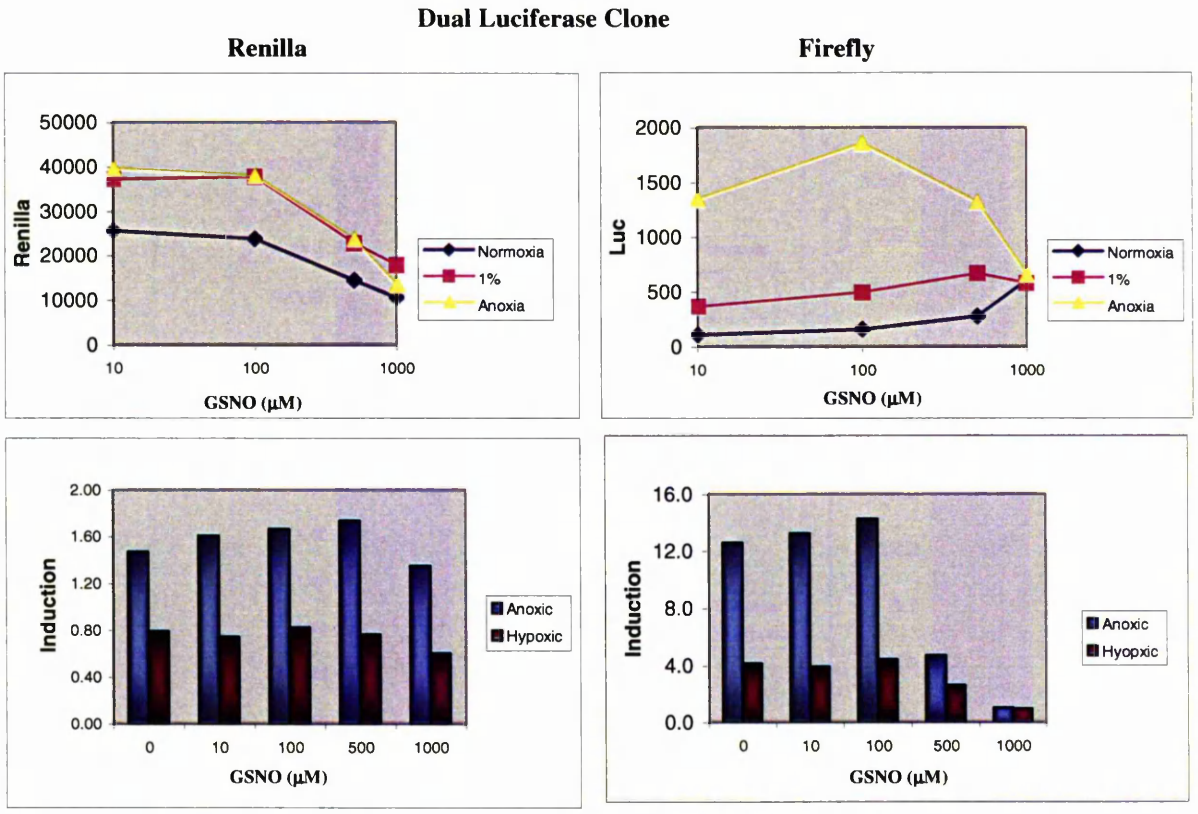

Fig 7.3 Luciferase and renilla expression under aerobic, hypoxic, and anoxic conditions after treatment with GSNO. The anoxic and hypoxic inductions are also plotted (average values of 2 independent experiments performed in triplicate wells).

Similar results were observed in the expression of the luciferase gene when the dual clone was used. This was expected because both clones contain the same HRE-driven luciferase cassette. Since the dual clone contains the renilla reporter gene, the expression of this gene was monitored (**Fig 7.3**). The Renilla values show that high concentrations of GSNO (>100 μM) are toxic which could explain the reason for HIF stabilisation to be due to stress factors in the cell mediated by this toxicity. This explains the reason for lack of aerobic HIF stabilisation at GSNO concentrations lower than 100 μM. It was also documented that GSNO produces GSSG as a by-product that at high levels could itself cause oxygen stress [92].

Luciferase gene expression was also measured in the HEK 293 cells that were transfected with the HRE-driven luciferase cassette (2 μg/well) prior to treating with GSNO (**Fig. 7.4**). This cell line was chosen in order to compare the results to those observed by Metzen *et al.* [89] who measured HIF accumulation under normoxic conditions using this cell line.

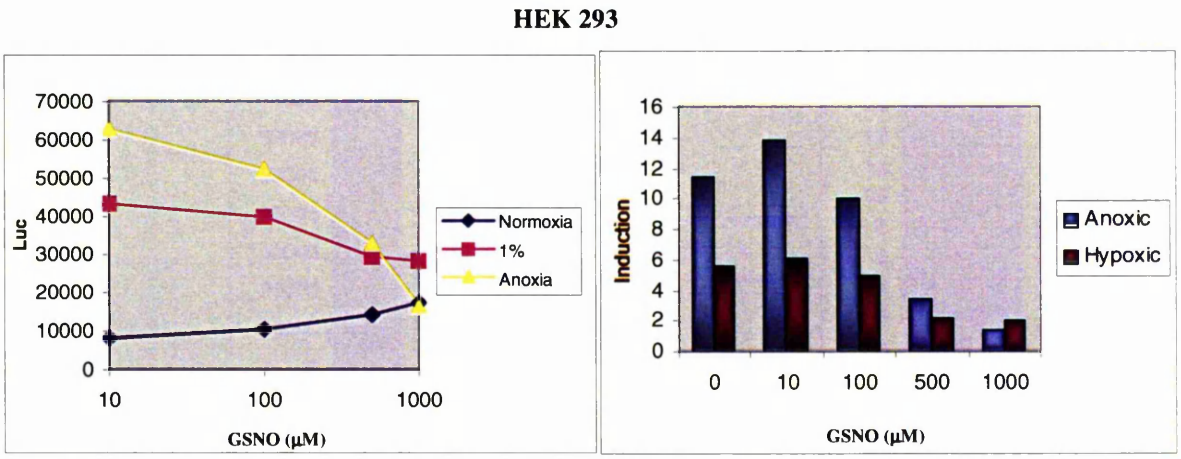

Fig 7.4 Luciferase and renilla expression measurements of the HEK 293 cells that have been transfected with 2 μg/well HRE-driven Luciferase, treated with varying concentrations of GSNO and incubated in different oxygen conditions (average of 2 independent experiments performed in triplicate wells).

Again, similar results were achieved using the HEK 293 cell line. Under aerobic conditions, the luciferase gene expression increased by 1.6 folds at 1 mM GSNO and decreased by 3.2 folds under anoxic conditions. Under hypoxic conditions, GSNO showed little effect on gene expression. So, it was suggested that the effect of GSNO on HIF-mediated gene expression depended on the concentration of the drug used as well as the oxygen gradient whereby high doses of GSNO (100-1000 μM) caused HIF stabilisation under aerobic conditions but promoted HIF degradation under anoxic conditions. The anoxic fold inductions were inversely proportional to the concentration of GSNO. This may be due to the increase of gene expression under aerobic conditions and its decrease under anoxic conditions at high GSNO concentrations. A similar trend was observed in the hypoxic inductions.

7.4 Transient Transfection of the Luciferase Clones with iNOS Plasmids

Since NO donors produce by-products that themselves could have effects on HIF regulation, an endogenous and non-chemical NO source was used to study the phenomenon of NO-HIF regulation. In this experiment, plasmids that encoded for constitutive iNOS expression were used. The firefly clone, dual luciferase clone, and HEK 293 wild-type cells were seeded at $2x10^5$ cells/well in a 6-well plate in the presence or absence of the iNOS inhibitor L-NNA (100 μM). The following day, the cells were transiently transfected **(Section 2.8.1)** with varying concentrations of pEF IRES iNOS puro or pEF IRES puro (empty vector) (0-1 μg DNA/well) using Lipofectamine (10 μl/well). The HEK 293 cells were also transfected by the HRE-driven Luciferase cassette (LDH-A SV40 at 1 μg/well). After 24 h, the cells were scraped and split equally into triplicate wells of a 96-well plate. After 4 h, the plates were placed in 1 % or <0.1 % oxygen conditions. Control plates were left under aerobic conditions. After another 18 h, the plates were removed and reoxygenated

for 3 h. The cells were then lysed and the Luciferase activity was measured. The protein content/well was measured using the protein assay **(Figs 7.5,7.6, and 7.7).**

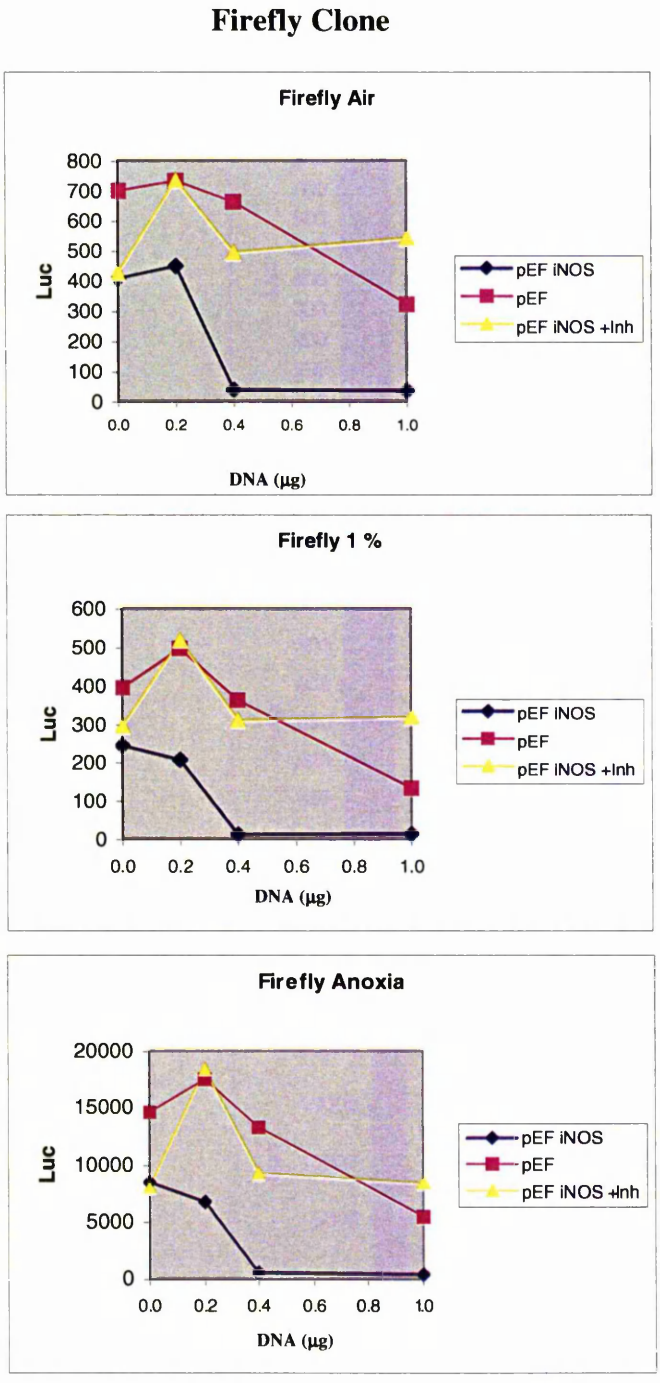

Fig 7.5 Luciferase measurements of HRE-driven luciferase expressing cells transfected with pEF IRES iNOS puro or an empty pEF IRES puro vector (representative of 3 independent experiments each performed in triplicate wells).

The Luciferase activity decreased in the cells transfected with the iNOS plasmid in a DNA-dose dependent manner. This effect was seen under all oxygen conditions but was most prominent under anoxic conditions. For example, under anoxic conditions, when 0.4 μg/well DNA was transfected, a 28.8 fold decrease was observed in the presence of the iNOS vector compared to the empty vector (p=0.0004, 2 tail t-test) and increased again by 19.9 fold (p=0.018, 2 tail t-test) in the presence of the iNOS inhibitor. Moreover, there appeared to be no HIF stabilisation in air. The decrease in luciferase gene expression that was observed in air was explained to be due to the residual HIF present in this oxygen condition; however, gene expression remained basal compared to that obtained under hypoxic and anoxic conditions. On the other hand, a decrease in gene expression was only observed at high DNA concentrations when the empty vector was used. Gene expression reverted at least partially in the presence of the NOS inhibitor L-NNA indicating that it was NO mediated. It is noteworthy to mention that NO is not generated under anoxic conditions due to lack of oxygen; however, in this experiment the cells were transfected with the iNOS plasmid under aerobic conditions to allow for NO formation prior to incubation under anoxic or hypoxic conditions. The anoxic and hypoxic inductions were calculated in this experiment **(Fig 7.6)**.

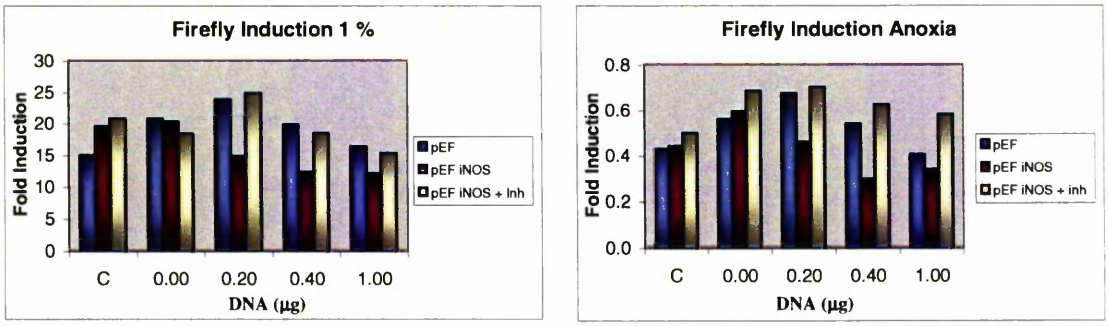

Fig 7.6 Hypoxic and anoxic inductions of the luciferase clone. The cells were transfeted with pEF IRES iNOS puro or pEF IRES puro (control vector) at varying concentrations. The cells were cultured in the presence or absence of the iNOS inhibitir L-NNA (C: untreated control, all other samples were transfected with DNA using Lipfectamine) (representative values of 3 independent experiments each performed in triplicate wells).

The induction data showed that in the presence of iNOS, HIF-driven luciferase induction was diminished ($p=0.05$ for anoxic induction when 0.4 μg/well DNA was used, 2 tail t-test) and was reversed in the presence of L-NNA ($p=0.37$ for the same DNA concentration and oxygen conditions, 2 tail, t-test). This could suggest that this effect is NO mediated. It was also observed that Lipofectamine itself caused a decrease in induction probably due to its toxic nature.

Similar results were obtained in the dual Luciferase clone with the greatest effect occurring at 0.2 μg/well of pEF IRES iNOS puro. It was also observed from the renilla expression that Lipofectamine and high DNA concentrations increased the toxicity in all the samples with the highest effect caused by pEF IRES iNOS puro and explained to be due to NO production **(Fig 7.7)**.

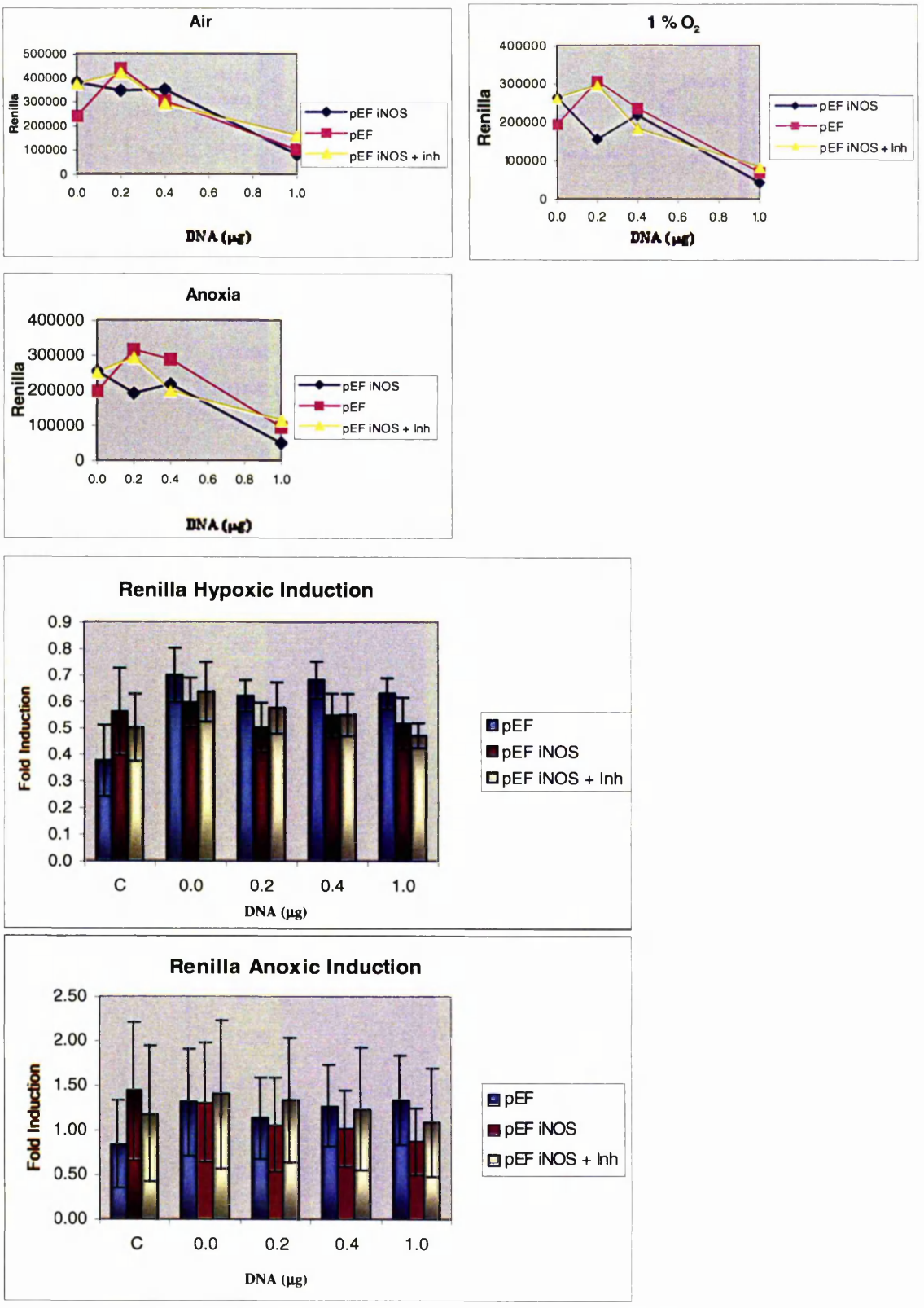

Fig 7.7 Renilla expression and induction values of the dual luciferase clone that was transiently transfected with the pEF IRES (iNOS) puro plasmids (average values of 3 independent experiments each performed in triplicate wells) (C: untreated control, all other samples were transfected with DNA using Lipfectamine).

It can be concluded from the above results that the decrease in HIF-mediated luciferase expression under anoxic conditions was caused by NO and was not due to the toxicity that accompanied the transfection process. This is because the luciferase expression was reduced by 28.8 fold under anoxic conditions whereas the renilla values were reduced by only 1.2 fold when 0.4 μg/well pEF iNOS was used. Under anoxic conditions and at 0.4 μg/well DNA, the anoxic induction dropped by 1.3 fold in the presence of iNOS ($p=0.027$, 2 tail t-test) and increased in the presence of the iNOS inhibitor 1.2 fold ($p=0.50$, 2 tail t-test).

No trend was observed using the HEK 293 cells, which could be due to the low transfection efficiency especially as this cell line was transfected with both the HRE-driven Luciferase cassette and the pEF IRES (iNOS) puro plasmids.

7.5 Studying the Effect of NO on HIF Regulation by Infecting the Luciferase Clone with pAdCMV iNOS Viruses

The effect of iNOS over expression on HIF-mediated gene expression was studied using the HCT-116 Firefly and dual luciferase clones. In this case, the previously established adenoviruses were used to allow the delivery of iNOS in a gene therapy vehicle. The cells were seeded at $5x10^3$ cells/well in a 96-well plate and infected after 4 h with varying viral moi (pAdCMV iNOS and pAdCMV *Lac* Z-as a control). After 48 h, the plates were exposed to either 18 h of anoxia or air and followed by 3 h reoxygenation. The cells were then lysed and the Luciferase expression was measured **(Figs 7.8, 7.9, 7.10)**.

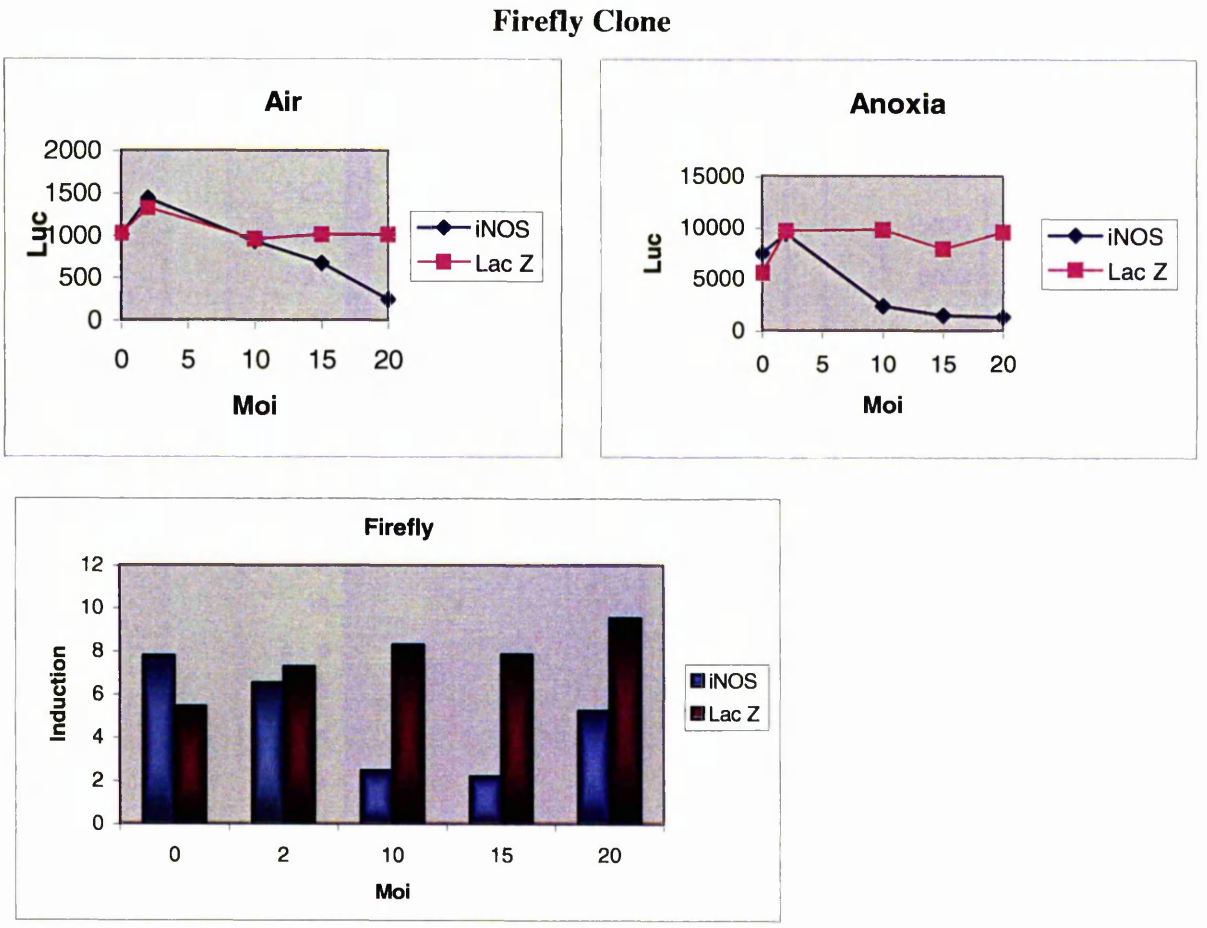

Fig 7.8 These graphs show the Luciferase activity and anoxic induction of the firefly clone after infection with pAdCMV iNOS or pAdCMV *Lac* Z (average values of duplicate wells).

The results indicated that iNOS expression caused HIF down regulation under anoxic conditions. Moreover, the fold induction was seen to decrease in a viral dose dependent manner reaching 2.2 folds in the presence of iNOS as compared to 7.9 fold in the presence of the control virus at moi 15. There was no HIF stabilisation under aerobic conditions.

The same experiment was repeated using the dual luciferase clone in order to monitor the effect of toxicity on the cells (**Figs 7.9 and 7.10**). The dual clone cells were cultured for 24 h prior to seeding in the presence or absence of the iNOS inhibitor L-NNA (100 μM) in order to monitor the ability to reverse this effect.

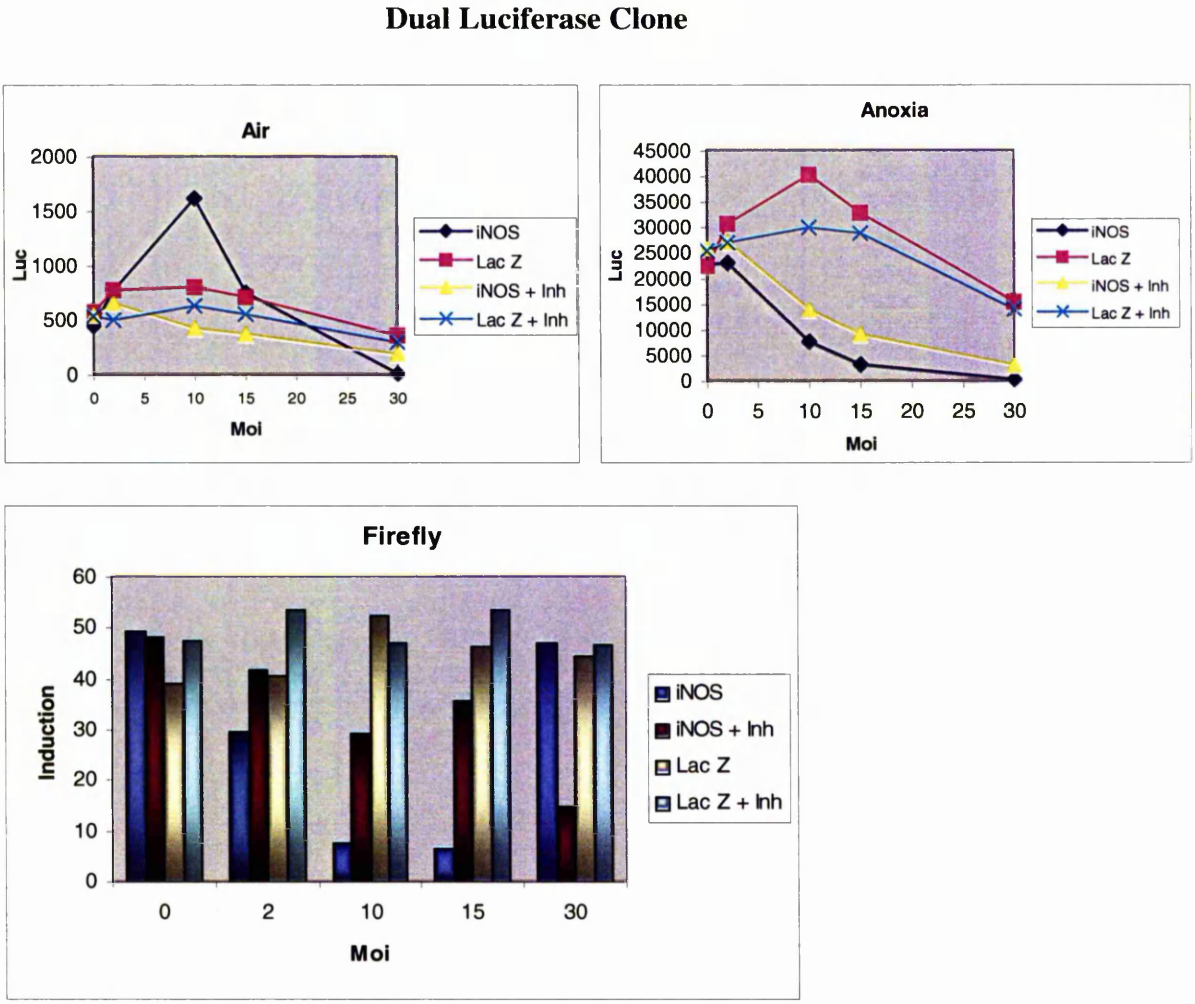

Fig 7.9 Luciferase gene expression and hypoxic induction in response to adenoviral-mediated iNOS delivery (average values for 2 independent experiments each performed in duplicate wells).

The luciferase results showed that HIF-mediated gene expression decreased in the presence of iNOS in anoxia reaching 7.3 folds at moi 15. This effect was partially reversed in the presence of L-NNA. The same effect was observed by measuring the hypoxic induction with the exception of the highest moi, which could be due to the low iNOS expression observed under normoxic conditions at this moi. In order to measure non-specific effects that could cause HIF expression, the renilla values were examined **(Fig 7.10)**

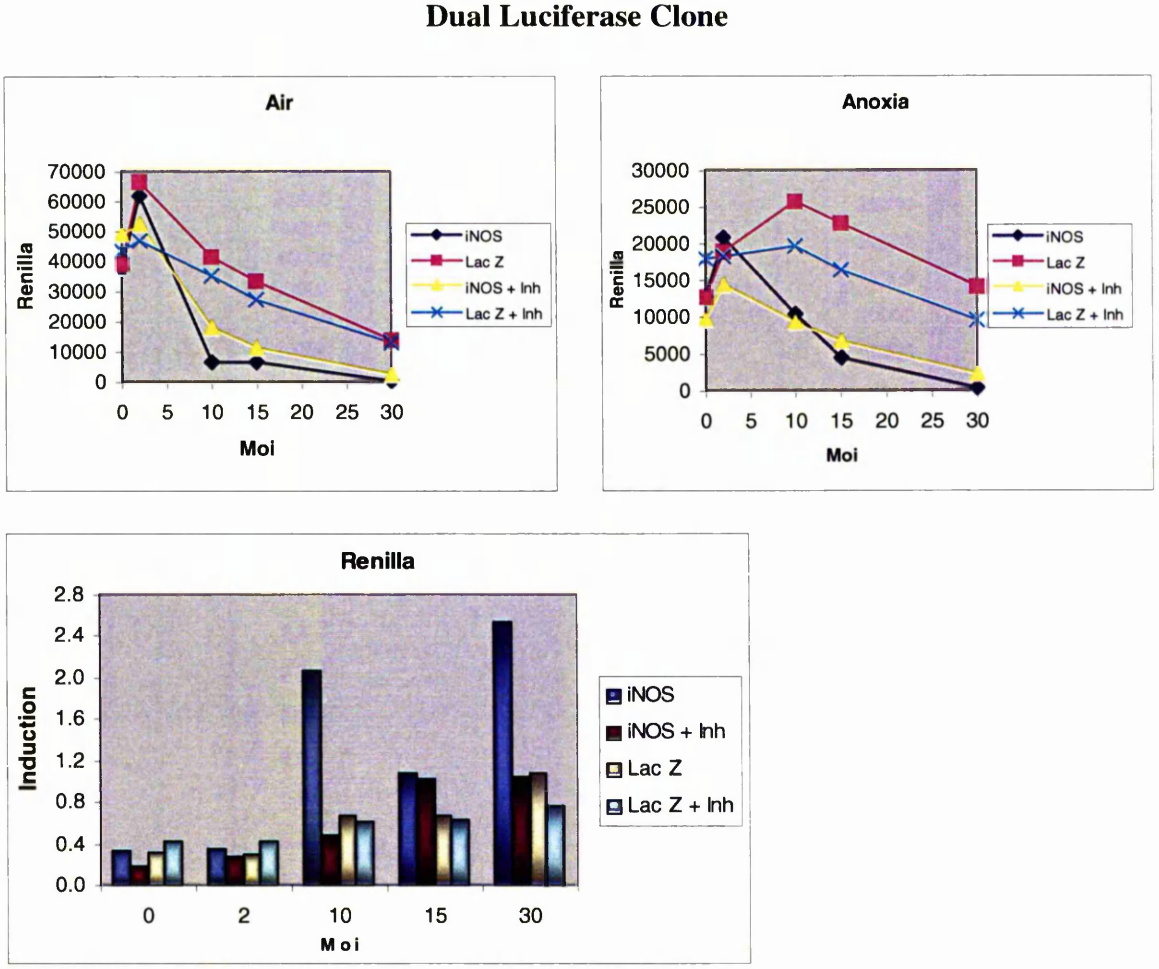

Fig 7.10 Renilla measurements of the luciferase clones infected with the pAdCMV iNOS or pAdCMV *Lac* Z (average values for 2 independent experiments each performed in duplicate wells).

The renilla hypoxic induction was higher at moi 10 and 15 compared with the other samples, particularly in the presence of iNOS expression. This was not the case in the other control samples, which could indicate that HIF-mediated gene expression was caused by NO generation. Moi 30 seems particularly toxic both under aerobic and anoxic conditions.

These experiments cannot be performed in the HEK 293 cells because these cells contain the E1 sites that will allow viral replication following infection. In addition, in this case the cells would have to be transfected with the HRE-driven Luciferase cassette followed by viral administration.

7.6 Conclusion

The importance of HIF-mediated gene expression and the controversy about the role of NO on HIF regulation prompted us to study this effect using an NO donor, an iNOS plasmid, and iNOS expressing adenoviruses. The results suggested a negative feedback loop whereby NO appeared to down regulate HIF expression especially under anoxic conditions. When high concentrations of the NO donor GSNO were used, HIF stabilisation was observed only under aerobic conditions which is in agreement with Metzen *et al.*(2003) [89]. However, we postulate that this effect is due to the toxic nature of the NO donor or its by-product GSSG. Moreover, the effect of GSNO on HIF regulation under anoxic conditions was studied in this chapter and it was observed that HIF stabilisation was reversed and that HIF-mediated luciferase expression was diminished.

In order to avoid chemical and exogenous sources of NO, the feed back effect of NO on HIF using plasmids and adenoviruses that constitutively express iNOS was studied. Again, a negative effect of NO on HIF-mediated gene expression especially under hypoxic and anoxic conditions was observed. Moreover, this effect was at least partially reversed using the iNOS inhibitor L-NNA.

The mechanism for this NO-mediated HIF down regulation remains unknown but one explanation could be due to the ability of NO to bind to heme with a higher affinity than O_2, thus binding to a heme sensor localised in the cell membrane. This binding of NO to the sensor would cause a conformational change that shuts down signal transduction even under hypoxic conditions [92]. Finally, the effects of iNOS over expression in cancer therapy appear to be promising whereby in addition to reducing tumour growth, high levels of iNOS sensitise hypoxic cells to bioreductive drugs, radiosensitise hypoxic cells, and might have a negative effect on HIF-mediated gene expression.

CHAPTER 8 DISCUSSION

8.1 Introduction

Inducible nitric oxide synthase has shown a dual effect on tumourigenesis [12]. In some cases, iNOS expression was observed in the diagnosed cancers [25-28] and was correlated with angiogenesis [41,43] and metastasis [30,31]. In other cases, however, higher levels of iNOS expression showed pro-apoptotic [54,55] and anti-metastatic [33] effects. Moreover, some studies demonstrated the ability of iNOS to sensitise cells to TPZ [97] and other bioreductive drugs including doxorubicin and menadione [69]. Other studies showed that iNOS is up regulated under hypoxic conditions [20] but failed to determine its feedback effects on HIF-mediated gene expression. All of these findings indicated that iNOS could be used in cancer therapy only if its expression levels were tightly regulated. This study focuses on the effects of iNOS rather than cNOS as the former is capable of producing higher NO levels for longer periods of time and is produced by macrophages in response to inflammatory signals. Since previous experiments performed in our laboratory showed that cells constitutively expressing high levels of iNOS are difficult to culture due to the continuous production of NO, an inducible approach to regulate iNOS expression was sought.

In this study, several strategies have been presented to optimise the therapeutic potential of iNOS for the use in cancer gene therapy. Inintially, tools were developed to control the expression of iNOS by establishing stable clones expressing the iNOS gene in the ecdysone system and adenoviruses that encode for constitutive expression of iNOS. Then, the generated systems were evaluated and their benefits and limitations were discussed. Finally, the established tools as well as NO donors and other available plasmids and clones (that constitutively express iNOS) were used to study the role of iNOS and NO on tumourigenesis, hypoxic sensitivity to TPZ, and HIF mediated gene expression.

8.2 Establishing and Evaluating the Therapeutic Tools

Initially, the ecdysone system was evaluated *in vitro* and *in vivo* using the *Lac* Z reporter gene. This system was chosen as it has showed strict tight regulation patterns [56,149]. Low basal levels and a relatively high fold induction (5-8 fold) were observed in our experiments yet the fold induction was not as high as documented in some studies [112,120]. Gene expression was observed to be dependent on the dose of the inducer and had to be measured at least 24 h after Pon A addition in order to clearly observe this dose dependent characteristic. *Lac* Z expression increased with time in the presence of the inducer and began to decrease 24 h after removal of Pon A. However, gene expression did not promptly return to basal levels as documented by Saez *et al.* (2000) yet in their experiment 1 μM Pon A was used while here 10 and 20 μM Pon A was administered and the contrast could be due to the availability of Pon A residues at the higher concentrations even when the media was washed out [112]. Moreover, Saez *et al.* (2000) used the Luciferase reporter gene to measure induction while we have used *Lac* Z. It could be that the degradation of the β-galactosidase protein is slower than that of the Luciferase enzyme. In addition, administration of high Pon A doses (>30 μM) was correlated with cell death and caused a shift in the FL-1 peak when the wild-type cells were assayed using flow cytometry. At 50 μM, Pon A resulted in 12 % cell death when measured using the MTT assay. Hence, high doses of Pon A were inappropriate to use. On the other hand, pilot *in vivo* studies using i.p administration of 1 or 2 mg/mouse Pon A were conducted and high *Lac* Z gene expression 17 h post administration even at the lower Pon A dose was observed.

In order to improve this inducible system, the ecdysone receptor (pVgRXR) has been modified such that it expresses both components VgECR and RXR using a bicistronic cassette (Stratagene, USA) [206]. This is expected to allow a more uniform expression in the cells now that both components are expressed using the same promoter (CMV in this case),

thus further optimising the production of transgenic animals. Moreover, the CMV promoter in the (modified or unmodified) pVgRXR cassette could be replaced by a tissue specific promoter in order to allow for the genes to be inducibly expressed only in the tissues of interest [150]. Other modifications include creating a chimeric *Drosophila/Bombyx* ecdysone receptor (DB-EcR) instead of the Mammalian (Vg in VgEcR) that preserves the ability to bind to the modified ecdysone promoter even without the need of exogenous (RXR). Addition of exogenous (RXR) increases gene expression as well as basal level in this system. This system is functional using steroidal (Pon A) and non-steroidal ecdysone analogues (GS-E) Hence, this modification shall decrease the number of genes needed to be transfected in the cells as well as limit any possible side effects of over expressing (RXR) [207].

After evaluating the ecdysone system using the *Lac* Z reporter gene, an HT-1080 clone that stably expressed iNOS in the ecdysone cassette was generated. The NOS activity in this clone was 21.5 pmol/min/mg when induced with 20 μM Pon A and measured using the L-citrulline assay. After immunostaining with iNOS antibodies, the iNOS cytosolic protein was clearly visualised using the fluorescent microscope. Moreover, gene expression was observed to be Pon A dose dependent with only a minority of cells expressing iNOS at 20 μM. This observation was further confirmed upon obtaining 20 % fluorescence using flow cytometryic analysis. Higher Pon A doses could not be used in order to obtain higher levels of iNOS expression due to the toxicity observed with this ecdysone inducer, which was reflected by growth delay in the induced as compared to the uninduced wild-type and ecdysone inducible *Lac* Z and iNOS cells. Thus, new attempts were performed to generate more inducible iNOS clones using other cell lines and a range of antibiotic concentrations was used in order to increase the selection pressure. It is important to note that only few studies have generated stable clones expressing toxic genes like iNOS using the ecdysone system. After detailed screening of the generated ecdysone inducible iNOS clones, it became

clear that all the obtained clones showed lower gene expression than the previously generated ecdysone inducible HT-1080 iNOS clone (16.10/2). The inability to produce clones that highly express iNOS could be due to the fact that 2 plasmids have to be expressed in every cell as per the requirements of this system, and although different selection markers are needed for each plasmid, the cells seem to be able to survive under the selection pressure even when the antibiotic doses were increased. This is possibly because the cells initially contain the ecdysone plasmids and the iNOS cDNA but later manage to remove the iNOS gene from the ecdysone receptor, probably due to the toxic product of iNOS thus causing a survival pressure and also from the relatively large iNOS insert size (4.2 Kb) compared to the ecdysone receptor (5.1 Kb). The ability of wild-type cells to over grow the iNOS clone cells in the same culture could also explain both the lower gene expression obtained with the iNOS clone than the *Lac* Z clone and the observed decrease in gene expression when the iNOS clone was cultured for long periods of time, which was slightly improved by the addition of iNOS inhibitors. In order to overcome this decrease in gene expression, the clone was not cultured for more than 4 weeks. Other methods that can be used in order to optimise the technique of generating stable clones and produce cells that fully express iNOS at 20 μM Pon A, include ligating an IRES-GFP cDNA next to the iNOS gene in the pIND SP1 iNOS vector. This method allows the expression of the GFP protein from the same ecdysone promoter that expresses iNOS without the need of fixing and immunostaining the cells. Hence, after inducing the cells with 20 μM Pon A, flow cytometry techniques could be used to sort out and collect the cells that fluoresce due to iNOS and GFP expression from the ones that do not without the need to fix the cells in the process. The iNOS expressing cells can then be cultured. These cells should therefore give 100 % expression at 20 μM Pon A.

In addition, in order to facilitate the screening for positive clones, an IRES-Luc (or GFP) gene could be ligated next to the iNOS gene in the ecdysone reporter vector. Hence, iNOS gene expression could be monitored indirectly through Luc or GFP expression without the need for immunostaining and antibody binding. Since varying the Lipofectin/Lipofectamine transfection protocol did not benefit the final outcome, another transfection technique such as calcium phosphate could be used. Finally, instead of generating stable clones, viral delivery vehicles could be produced in order to integrate the gene of interest in the cells.

The inducible iNOS clone was implanted *in vivo* and induced with Pon A. Only the tumour that was induced with 1 mg/mouse Pon A showed NOS activity when measured using the L-citrulline assay. The fact that the other 2 tumours that were even induced with higher doses of Pon A did not show any activity could indicate the loss of gene expression in these tumours. Moreover, the take rate was extremely low which could hint to some leakiness of the ecdysone system *in vivo* whereby the implanted cells possibly died due to the unexpected production of NO in the absence of the inducer. When cultured *ex vivo*, cells derived from the 1 mg/mouse Pon A tumour (16.10/T) showed similar gene expression patterns when induced to those observed with the pre-*in vivo* clone (16.10/2) indicating that this particular clone was able to maintain stability during the full *in vivo* and *ex vivo* process.

It is noteworthy to mention that the techniques used to measure the activity of iNOS have some limitations. In order to use the L-citrulline assay large cell numbers were needed (at least a T-75 flask) to detect any activity, which in some experiments may be inconvenient (particularly when high viral moi was used). In addition, the detection limit of the griess assay seemed very minimal in our experiments as even when high activity was observed with the L-citrulline assay, barely any nitrite was detected. It is important to note that many studies have used this assay but also used FCS-containing media and experiments performed

in our group have shown that FCS contains high nitrite levels and hence when the cells were induced with Pon A, the FCS-free media was used. Other techniques to quantify iNOS expression include western blotting. The flow cytometry technique is semi-quantitative but was used in experiments where the L-citrulline assay could not be utilised.

In order to deliver iNOS in a gene therapy vehicle, the ecdysone cassettes were cloned in type 5 adenoviruses. This approach was chosen as adenoviruses constitute a good gene therapeutic tool. The advantages of adenoviruses are their high titres, ability to infect dividing and non-dividing cells, as well as their large host tropism. Moreover, they do not integrate their DNA in the host genome and although they cause some immune reaction, this might be therapeutically beneficial if directed towards viral-infected tumour cells. Generating adenoviruses encoding for the ecdysone cassettes has been reported in the literature [133,172-174] and no disruption of inducible gene regulation by the viral backbone was documented. Some studies have also reported the use of adenoviruses encoding for iNOS controlled by a CMV promoter [208]. Here, the ecdysone receptor cassette (pVgRXR) was successfully cloned in the pShuttle vector and adenoviruses were generated although the size of the insert was 7.4 Kb and the vector can only accommodate 7-8 Kb. However, after detailed examination, the plasmids that were expected to be encoding for the ecdysone reporter turned out to contain a CMV promoter instead of an inducible one. Although the outcome was unexpected, the obtained viruses were still used to over express iNOS. Gene expression was controlled using the multiplicity of infection (moi) instead of Pon A induction. This approach was also useful as it excluded the toxicity of Pon A and minimised the number of adenoviruses that are needed to infect each cell. High titres of adenoviruses encoding for the iNOS gene were particularly difficult to generate probably due to the constitutive generation of NO at high levels thus killing the HEK 293 cells that were used for

viral replication. This was optimised by the addition of the iNOS inhibitor L-NNA (100 μM). Cesium chloride purification could also be used to increase the titre.

8.3 Studying the Therapeutic Effects of iNOS Using the Established Tools

Having generated tools that can tightly regulate iNOS expression, the role of iNOS on hypoxia and blood perfusion was studied. Cells from the inducible clone were implanted in nude mice and dosed with Pon A when the tumours reached 200-250 mm^3. The mice were also injected with markers to study the hypoxic fraction and blood perfusion. Pimonidazole stainining of hypoxic regions did not show any correlation with iNOS expression; however, a slight increase in Hoechst 33342 staining was observed with the mice induced with 1 mg Pon A for 24 h. This hinted to an increase in blood perfusion under these experimental conditions. Higher doses of Pon A could not be administered in order to monitor these effects further due to the high cost of the inducer.

In order to evaluate the effect of iNOS in a gene-directed-enzyme-prodrug therapy (GDEPT), the previously generated tools were used to measure the ability of iNOS to increase the sensitivity of hypoxic cells to the bioreductive drug TPZ. These experiments were conducted as previous studies showed that iNOS and P_{450} Reductase share high sequence homology [7] and that the latter reduces TPZ [98]. Cell cytotoxicity to TPZ was primarily measured in the iNOS inducible clone using the MTT assay. Several attempts were performed to optimise the experimental conditions and the final results showed a slight increase in sensitivity to TPZ in the induced cells as compared to the uninduced clone cells. In order to study the effect of iNOS over expression on cell sensitivity to TPZ further, a clonogenic assay was performed. Initially, the plating efficiency for the HT-1080 and ecdysone inducible iNOS HT-1080 clone was determined, and then the sensitivity of iNOS over expressing cells towards TPZ was measured. When the inducible clone was assessed, an increase in cytotoxicity was observed in the Pon A induced clone cells as compared to the

uninduced; however, due to the low iNOS activity of this clone, the difference was modest. In addition, the observed increase in cytotoxicity under aerobic conditions could be attributed to NO production under this oxygen condition. This is because the cells seeded under aerobic conditions produce NO in the presence of oxygen whereas those seeded under anoxic conditions cannot produce NO due to the lack of oxygen, which is an essential cofactor. This cytotoxicity cannot be due to TPZ as the toxic species of this drug reverts back to the non-toxic prodrug in the presence of oxygen. This experiment can be further optimised by culturing the cells in the epresence of an iNOS inhibitor to block the production of NO in the oxygenase monomer of iNOS. When the adenoviruses were used, very little difference in sensitivity was observed. This could be further optimised by decreased drug concentrations under aerobic or increased viral moi but more importantly by infecting a larger number of cells with the adenoviruses prior to seeding to allow a higher probability of viral-cell encounter, as with the current design, the small cell number and large container volume reduces this probability. These results indicated that iNOS can increase the sensitivity of hypoxic cells towards TPZ and since iNOS levels are increased in clinical tumours, iNOS could be used in a therapeutic approach. Moreover, studies have shown that TPZ can inhibit iNOS activity and because NO is implicated in maintaining tumour vascular homeostasis, TPZ could therefore potentiate its own toxicity by increasing the degree of hypoxia [69].

In the last chapter, the role of NO on HIF-mediated gene expression was studied. A previously established clone that expresses Luciferase in response to hypoxic conditions was used. This effect was studied because HIF constitutes a key molecule in the regulation of gene expression promoting cell survival under reduced oxygen conditions. HIF down regulation could result in a breakthrough in cancer therapy. The NO donor GSNO was used as an exogenous source of NO and particularly because studies by Metzan *et al.* (2003) have postulated a mechanism by which GSNO-derived NO causes HIF stabilisation under aerobic

conditions at a 1 mM concentration using the HEK 293 cell line [89]. The results in this study indicated that NO down regulates HIF-mediated Luciferase expression under anoxic conditions. Some increase in Luciferase expression under aerobic conditions was observed but only at high GSNO concentrations (0.5 and 1 mM). This was later explained by using an internal constitutive renilla control to be due to the toxic nature of the compound. These experiments were also repeated using the HEK 293 cell line that was transfected with HRE-driven Luciferase cassette prior to GSNO addition and the same conclusions were made. To avoid the toxic nature of NO donors, the effect of endogenous NO on HIF-mediated gene expression was studied using the Luciferase clones and the HEK 293 cells-HRE Luciferase. These HRE-Luciferase expressing cells were either transiently transfected with plasmids that constitutively express iNOS or infected with the previously established adenoviruses. Similar results were obtained and the effect was partly reversed by the addition of the iNOS inhibitor L-NNA.

The use of NO donors appears to be far from ideal. GSNO produces GSSG as a by-product and this compound is toxic and has shown oxidative stress at high doses [92]. Another donor SNP also produces cyanide by-products that have their own effects on HIF-1 binding activity [92]. Moreover, these donors are chemical compounds that have shown extremely contradictory results based on the time of incubation of the cells with these donors, the concentration of these donors, the rate of NO release, and the oxygen concentrations used. In order to optimise the study of the effect of NO on HIF-mediated gene expression, cells were transiently transfected with iNOS plasmids to provide an endogenous non-chemical source of NO. To overcome any Lipofectamine toxicity and low transfection efficiency, the cells reporting the luciferase gene were infected with the pAdCMV iNOS adenoviruses in a gene therapeutic approach. It was concluded from the obtained results that the down regulation of the HIF-mediated gene expression is due to NO and that this effect

was partially inhibited using the iNOS inhibitor L-NNA. The NO scavanger carboxy PTIO or the N-acetyl-L-cysteine (NAC) which is an antioxidant could also be used to reverse these effects. The mechanism for this NO mediated HIF down regulation remains unknown but one explanation could be due to the ability of NO to bind to heme with a higher affinity than O_2, thus binding to a heme protein localised in the cell membrane. The binding of NO to the sensor would cause a conformational change that shuts down signal transduction even under hypoxic conditions [93].

8.4 Conclusion

In this study, new tools that tightly regulate the expression of iNOS to achieve therapeutic benefit for the treatment of cancer were generated. These tools were then used to study some therapeutic effects of iNOS on tumour growth, to explore the potentials of iNOS to reduce TPZ under hypoxic conditions in a GDEPT approach, and finally to down regulate HIF-mediated gene expression by NO over production.

CHAPTER 9 FUTURE DIRECTIONS

9.1 Further Optimisation of the Gene Expression Tools

Although this study presented tools that can tightly regulate gene expression, these vehicles should be further optimised for the use in the clinic. The administration of Pon A has been limited due to its toxicity and high price and therefore cheaper and less toxic replacements should be found. Moreover, the ability of Pon A to be quickly washed out of the body could be useful in the cases where only a single dose is needed but becomes a disadvantage when longer intervals are a must and for this case Pon A pellets could be used. The ecdysone receptor consists of two cassettes encoded by different promoters, so the use of the bicistronic cassette could be more useful especially if the CMV promoter is replaced with a tissue specific one. Since the ecdysone system requires the infection (or transfection) of each cell with 2 vectors, it would be ideal to generate a single adenovirus that expresses both cassettes. This has been performed by Mizuguchi and Hayakawa (2002) but using the tetracycline system and adenoviruses that have the E1 and E3 site deleted to allow for the cloning of large inserts [209]. This is expected to increase gene expression further. So, although adenoviruses that constitutively express iNOS were generated, it would also be beneficial to generate adenoviruses that encode iNOS in the ecdysone cassette. This will allow increasing the gene expression further using a high moi and a high Pon A dose. This approach could also be compared to stable clones or adenoviruses that express iNOS in the tetracycline system, as we have already cloned the iNOS cDNA in the tetracycline cassette.

9.2 Tissue Targeting of iNOS Expression

Nitric Oxide is known to play pleiotropic roles in the body. For example, the role of NO as a pro-angiogenic factor cannot be underestimated in cases were blood vessels need to form such as in heart diseases and foetal development. Therefore, it is crucial to target the over expression of iNOS to the tissues of interest. Although iNOS is naturally over expressed

in hypoxic regions, this is not the case in our system as the iNOS cDNA was cloned in the ecdysone cassette or in adenoviruses that have an ecdysone or a CMV promoter respectively. In order to target the therapeutic effects of iNOS to hypoxic regions for example, the CMV promoter in the pVgRXR cassette or in the adenoviral cassette could be replaced with HRE promoters. Moreover, the adenoviruses themselves can be modified so that they contain a tumour specific promoter instead of the viral E1 promoter that will then allow them to grow in hypoxic cells only [210]. This will decrease the toxicity to other tissues dramatically when using a GDEPT approach because the viral vehicle, the iNOS gene, as well as the prodrug TPZ will only be active under hypoxic conditions.

9.3 Other Studies to Demonstrate the Use of iNOS in Cancer Therapy

9.3.1 Angiogenesis

To study the role of iNOS on angiogenesis *in vitro*, the inducible clone could be co-cultured with the endothelial HUVEC cell line to monitor endothelial cell migration. The previous *in vivo* experiments could also be repeated using the adenoviruses. Window chamber techniques [211] could be utilised for this purpose. Moreover, the tumours can be injected with Hoescht 33342 and Carbocyanin in order to study vasodilation. BrdU could also be administered to the tumours to study cell cycle characteristics and ELISA assays could be preformed to stain for VEGF *in vitro* and on the tumour sections.

9.3.2 Sensitisation to TPZ

The mechanism whereby iNOS sensitises the cells to TPZ can be further analysed using the High Performance Liquid Chromatography (HPLC) technique. This will monitor the formation of TPZ radicals that cause chromosome abrogation. In addition, the inducible clone as well as the adenoviruses can be used in combination with drug treatment *in vivo* to obtain reduced tumour growth.

9.3.3 Radiation

iNOS has also shown an ability to radiosensitise hypoxic cells [107]. This effect could be studied using the established tools *in vitro* and *in vivo*. Some preliminary studies were conducted, but the experimental conditions need to be optimised in order to obtain higher substance enhancement ratios.

9.3.4 HIF-mediated Gene Expression

The role of NO on HIF-mediated gene expression can be further explored by using cytokines to over express iNOS and also by co-culturing the constitutive stable iNOS clone with the Luciferase clone and monitor any bystander NO effects. Preliminary results using the latter approach in our lab (Dr. Kaye Williams and Dr. Edwin Chinje) indicate that NO produced by the stable clones down regulate HIF-mediated Luciferase expression. Western blotting could also be performed to stain for HIF-1α, HIF-1β, and HIF-2α on lysates obtained from NO-treated Luciferase clones in order to try to decipher the exact mechanism by which NO down regulates HIF-mediated gene expression.

Finally, the adenoviruses could be used to generalise the role of iNOS in cancer therapy using a variety of cell lines *in vitro* and *in vivo*.

BIBLIOGRAPHY

1. Ignarro LJ, Byrns RE, Buga GM, Wood KS: **Endothelium-derived relaxing factor from pulmonary artery and vein possesses pharmacologic and chemical properties identical to those of nitric oxide radical.** *Circ Res* 1987, **61**:866-879.

2. **The Nitric Oxide Research Group.** *http://www.sghms.ac.uk/depts/immunology/~dash/.*

3. Vanin AF: **Biological role of nitric oxide: history, modern state, and perspectives for research.** *Biochemistry (Mosc)* 1998, **63**:731-733.

4. Koshland DE, Jr.: **The molecule of the year.** *Science* 1992, **258**:1861.

5. Jadeski LC, Chakraborty C, Lala PK: **Role of nitric oxide in tumour progression with special reference to a murine breast cancer model.** *Can J Physiol Pharmacol* 2002, **80**:125-135.

6. Xie QW, Cho HJ, Calaycay J, Mumford RA, Swiderek KM, Lee TD, Ding A, Troso T, Nathan C: **Cloning and characterization of inducible nitric oxide synthase from mouse macrophages.** *Science* 1992, **256**:225-228.

7. Groves JT, Wang CC: **Nitric oxide synthase: models and mechanisms.** *Curr Opin Chem Biol* 2000, **4**:687-695.

8. Anggard E: **Nitric oxide: mediator, murderer, and medicine.** *Lancet* 1994, **343**:1199-1206.

9. Corbett JA, Mikhael A, Shimizu J, Frederick K, Misko TP, McDaniel ML, Kanagawa O, Unanue ER: **Nitric oxide production in islets from nonobese diabetic mice: aminoguanidine-sensitive and -resistant stages in the immunological diabetic process.** *Proc Natl Acad Sci U S A* 1993, **90**:8992-8995.

10. Kroncke KD, Fehsel K, Suschek C, Kolb-Bachofen V: **Inducible nitric oxide synthase-derived nitric oxide in gene regulation, cell death and cell survival.** *Int Immunopharmacol* 2001, **1**:1407-1420.

11. Wink DA, Vodovotz Y, Cook JA, Krishna MC, Kim S, Coffin D, DeGraff W, Deluca AM, Liebmann J, Mitchell JB: **The role of nitric oxide chemistry in cancer treatment.** *Biochemistry (Mosc)* 1998, **63**:802-809.

12. Kone BC: **Molecular biology of natriuretic peptides and nitric oxide synthases.** *Cardiovasc Res* 2001, **51**:429-441.

13. Taylor BS, Geller DA: **Molecular regulation of the human inducible nitric oxide synthase (iNOS) gene.** *Shock* 2000, **13**:413-424.

14. Wang Y, Newton DC, Robb GB, Kau CL, Miller TL, Cheung AH, Hall AV, VanDamme S, Wilcox JN, Marsden PA: **RNA diversity has profound effects on the translation of neuronal nitric oxide synthase.** *Proc Natl Acad Sci U S A* 1999, **96**:12150-12155.

15. Nadaud S, Soubrier F: **Molecular biology and molecular genetics of nitric oxide synthase genes.** *Clin Exp Hypertens* 1996, **18**:113-143.

16. Eissa NT, Strauss AJ, Haggerty CM, Choo EK, Chu SC, Moss J: **Alternative splicing of human inducible nitric-oxide synthase mRNA. tissue-specific regulation and induction by cytokines.** *J Biol Chem* 1996, **271**:27184-27187.

17. Soubrier F: **Nitric oxide synthase genes: candidate genes among many others.** *Hypertension* 1999, **33**:924-926.

18. Hoit BD: **Two faces of nitric oxide: lessons learned from the NOS2 knockout.** *Circ Res* 2001, **89**:289-291.

19. Prince RC, Gunson DE: **Rising interest in nitric oxide synthase.** *Trends Biochem Sci* 1993, **18**:35-36.

20. Melillo G, Musso T, Sica A, Taylor LS, Cox GW, Varesio L: **A hypoxia-responsive element mediates a novel pathway of activation of the inducible nitric oxide synthase promoter.** *J Exp Med* 1995, **182**:1683-1693.

21. Nathan C, Xie QW: **Regulation of biosynthesis of nitric oxide.** *J Biol Chem* 1994, **269**:13725-13728.

22. **http://www.inchem.org/documents/jecfa/jecmono/v33je09.htm.**

23. Cetkovic-Cvrlje M, Sandler S, Eizirik DL: **Nicotinamide and dexamethasone inhibit interleukin-1-induced nitric oxide production by RINm5F cells without decreasing messenger ribonucleic acid expression for nitric oxide synthase.** *Endocrinology* 1993, **133**:1739-1743.

24. Schini VB, Catovsky S, Schray-Utz B, Busse R, Vanhoutte PM: **Insulin-like growth factor I inhibits induction of nitric oxide synthase in vascular smooth muscle cells.** *Circ Res* 1994, **74**:24-32.

25. Wolf H, Haeckel C, Roessner A: **Inducible nitric oxide synthase expression in human urinary bladder cancer.** *Virchows Arch* 2000, **437**:662-666.

26. Lagares-Garcia JA, Moore RA, Collier B, Heggere M, Diaz F, Qian F: **Nitric oxide synthase as a marker in colorectal carcinoma.** *Am Surg* 2001, **67**:709-713.

27. Xie K, Fidler IJ: **Therapy of cancer metastasis by activation of the inducible nitric oxide synthase.** *Cancer Metastasis Rev* 1998, **17**:55-75.

28. Ekmekcioglu S, Ellerhorst J, Smid CM, Prieto VG, Munsell M, Buzaid AC, Grimm EA: **Inducible nitric oxide synthase and nitrotyrosine in human metastatic melanoma tumors correlate with poor survival.** *Clin Cancer Res* 2000, **6**:4768-4775.

29. Fidler IJ: **Critical determinants of melanoma metastasis.** *J Investig Dermatol Symp Proc* 1996, **1**:203-208.

30. Harmey JH, Bucana CD, Lu W, Byrne AM, McDonnell S, Lynch C, Bouchier-Hayes D, Dong Z: **Lipopolysaccharide-induced metastatic growth is associated with increased angiogenesis, vascular permeability and tumor cell invasion.** *Int J Cancer* 2002, **101**:415-422.

31. Zhang XM, Xu Q: **Metastatic melanoma cells escape from immunosurveillance through the novel mechanism of releasing nitric oxide to induce dysfunction of immunocytes.** *Melanoma Res* 2001, **11**:559-567.

32. Xie K, Huang S, Dong Z, Juang SH, Gutman M, Xie QW, Nathan C, Fidler IJ: **Transfection with the inducible nitric oxide synthase gene suppresses tumorigenicity and abrogates metastasis by K-1735 murine melanoma cells.** *J Exp Med* 1995, **181**:1333-1343.

33. Xie K, Dong Z, Fidler IJ: **Activation of nitric oxide synthase gene for inhibition of cancer metastasis.** *J Leukoc Biol* 1996, **59**:797-803.

34. Wang B, Xiong Q, Shi Q, Le X, Xie K: **Genetic disruption of host interferon-gamma drastically enhances the metastasis of pancreatic adenocarcinoma through impaired expression of inducible nitric oxide synthase.** *Oncogene* 2001, **20**:6930-6937.

35. Shi Q, Xiong Q, Wang B, Le X, Khan NA, Xie K: **Influence of nitric oxide synthase II gene disruption on tumor growth and metastasis.** *Cancer Res* 2000, **60**:2579-2583.

36. Shi Q, Huang S, Jiang W, Kutach LS, Ananthaswamy HN, Xie K: **Direct correlation between nitric oxide synthase II inducibility and metastatic ability of UV-2237 murine fibrosarcoma cells carrying mutant p53.** *Cancer Res* 1999, **59**:2072-2075.

37. Lala PK, Chakraborty C: **Role of nitric oxide in carcinogenesis and tumour progression.** *Lancet Oncol* 2001, **2**:149-156.

38. Risau W: **Mechanisms of angiogenesis.** *Nature* 1997, **386**:671-674.

39. Jozkowicz A, Cooke JP, Guevara I, Huk I, Funovics P, Pachinger O, Weidinger F, Dulak J: **Genetic augmentation of nitric oxide synthase increases the vascular generation of VEGF.** *Cardiovasc Res* 2001, **51**:773-783.

40. Jenkins DC, Charles IG, Thomsen LL, Moss DW, Holmes LS, Baylis SA, Rhodes P, Westmore K, Emson PC, Moncada S: **Roles of nitric oxide in tumor growth.** *Proc Natl Acad Sci U S A* 1995, **92**:4392-4396.

41. Yamasaki K, Edington HD, McClosky C, Tzeng E, Lizonova A, Kovesdi I, Steed DL, Billiar TR: **Reversal of impaired wound repair in iNOS-deficient mice by topical adenoviral-mediated iNOS gene transfer.** *J Clin Invest* 1998, **101**:967-971.

42. Franchi A, Gallo O, Paglierani M, Sardi I, Magnelli L, Masini E, Santucci M: **Inducible nitric oxide synthase expression in laryngeal neoplasia: correlation with angiogenesis.** *Head Neck* 2002, **24**:16-23.

43. Gallo O, Masini E, Morbidelli L, Franchi A, Fini-Storchi I, Vergari WA, Ziche M: **Role of nitric oxide in angiogenesis and tumor progression in head and neck cancer.** *J Natl Cancer Inst* 1998, **90**:587-596.

44. Uhlmann S, Rezzoug K, Friedrichs U, Hoffmann S, Wiedemann P: **Advanced glycation end products quench nitric oxide in vitro.** *Graefes Arch Clin Exp Ophthalmol* 2002, **240**:860-866.

45. Harris SR, Schoeffner DJ, Yoshiji H, Thorgeirsson UP: **Tumor growth enhancing effects of vascular endothelial growth factor are associated with increased nitric oxide synthase activity and inhibition of apoptosis in human breast carcinoma xenografts**. *Cancer Lett* 2002, **179**:95-101.

46. Tsurumi Y, Murohara T, Krasinski K, Chen D, Witzenbichler B, Kearney M, Couffinhal T, Isner JM: **Reciprocal relation between VEGF and NO in the regulation of endothelial integrity**. *Nat Med* 1997, **3**:879-886.

47. Chinje EC, Stratford IJ: **Role of nitric oxide in growth of solid tumours: a balancing act**. *Essays Biochem* 1997, **32**:61-72.

48. Wink DA, Kasprzak KS, Maragos CM, Elespuru RK, Misra M, Dunams TM, Cebula TA, Koch WH, Andrews AW, Allen JS, et al.: **DNA deaminating ability and genotoxicity of nitric oxide and its progenitors**. *Science* 1991, **254**:1001-1003.

49. Lepoivre M, Chenais B, Yapo A, Lemaire G, Thelander L, Tenu JP: **Alterations of ribonucleotide reductase activity following induction of the nitrite-generating pathway in adenocarcinoma cells**. *J Biol Chem* 1990, **265**:14143-14149.

50. Albina JE, Cui S, Mateo RB, Reichner JS: **Nitric oxide-mediated apoptosis in murine peritoneal macrophages**. *J Immunol* 1993, **150**:5080-5085.

51. Richter C, Gogvadze V, Laffranchi R, Schlapbach R, Schweizer M, Suter M, Walter P, Yaffee M: **Oxidants in mitochondria: from physiology to diseases**. *Biochim Biophys Acta* 1995, **1271**:67-74.

52. Eastman A: **Assays for DNA fragmentation, endonucleases, and intracellular pH and Ca2+ associated with apoptosis**. *Methods Cell Biol* 1995, **46**:41-55.

53. Nathan C: **Natural resistance and nitric oxide**. *Cell* 1995, **82**:873-876.

54. Kong G, Kim EK, Kim WS, Lee YW, Lee JK, Paik SW, Rhee JC, Choi KW, Lee KT: **Inducible nitric oxide synthase (iNOS) immunoreactivity and its relationship to cell proliferation, apoptosis, angiogenesis, clinicopathologic characteristics, and patient survival in pancreatic cancer**. *Int J Pancreatol* 2001, **29**:133-140.

55. Rieder J, Jahnke R, Schloesser M, Seibel M, Czechowski M, Marth C, Hoffmann G: **Nitric oxide-dependent apoptosis in ovarian carcinoma cell lines**. *Gynecol Oncol* 2001, **82**:172-176.

56. Xu W, Liu L, Charles IG: **Microencapsulated iNOS-expressing cells cause tumor suppression in mice**. *Faseb J* 2002, **16**:213-215.

57. Forrester K, Ambs S, Lupold SE, Kapust RB, Spillare EA, Weinberg WC, Felley-Bosco E, Wang XW, Geller DA, Tzeng E, Billiar TR, Harris CC: **Nitric oxide-induced p53 accumulation and regulation of inducible nitric oxide synthase expression by wild-type p53**. *Proc Natl Acad Sci U S A* 1996, **93**:2442-2447.

58. Ho YS, Wang YJ, Lin JK: **Induction of p53 and p21/WAF1/CIP1 expression by nitric oxide and their association with apoptosis in human cancer cells**. *Mol Carcinog* 1996, **16**:20-31.

59. Messmer UK, Ankarcrona M, Nicotera P, Brune B: **p53 expression in nitric oxide-induced apoptosis.** *FEBS Lett* 1994, **355**:23-26.

60. Ambs S, Hussain SP, Harris CC: **Interactive effects of nitric oxide and the p53 tumor suppressor gene in carcinogenesis and tumor progression.** *Faseb J* 1997, **11**:443-448.

61. Xu W, Liu LZ, Loizidou M, Ahmed M, Charles IG: **The role of nitric oxide in cancer.** *Cell Res* 2002, **12**:311-320.

62. von Knethen A, Brune B: **Cyclooxygenase-2: an essential regulator of NO-mediated apoptosis.** *Faseb J* 1997, **11**:887-895.

63. von Knethen A, Callsen D, Brune B: **NF-kappaB and AP-1 activation by nitric oxide attenuated apoptotic cell death in RAW 264.7 macrophages.** *Mol Biol Cell* 1999, **10**:361-372.

64. Tsujii M, DuBois RN: **Alterations in cellular adhesion and apoptosis in epithelial cells overexpressing prostaglandin endoperoxide synthase 2.** *Cell* 1995, **83**:493-501.

65. Rajnakova A, Moochhala S, Goh PM, Ngoi S: **Expression of nitric oxide synthase, cyclooxygenase, and p53 in different stages of human gastric cancer.** *Cancer Lett* 2001, **172**:177-185.

66. Garban HJ, Bonavida B: **Nitric oxide sensitizes ovarian tumor cells to Fas-induced apoptosis.** *Gynecol Oncol* 1999, **73**:257-264.

67. Chlichlia K, Peter ME, Rocha M, Scaffidi C, Bucur M, Krammer PH, Schirrmacher V, Umansky V: **Caspase activation is required for nitric oxide-mediated, CD95(APO-1/Fas)-dependent and independent apoptosis in human neoplastic lymphoid cells.** *Blood* 1998, **91**:4311-4320.

68. Brennan PA, Palacios-Callender M, Zaki GA, Spedding AV, Langdon JD: **Type II nitric oxide synthase (NOS2) expression correlates with lymph node status in oral squamous cell carcinoma.** *J Oral Pathol Med* 2001, **30**:129-134.

69. Garner AP, Paine MJ, Rodriguez-Crespo I, Chinje EC, Ortiz De Montellano P, Stratford IJ, Tew DG, Wolf CR: **Nitric oxide synthases catalyze the activation of redox cycling and bioreductive anticancer agents.** *Cancer Res* 1999, **59**:1929-1934.

70. Worthington J, Robson T, O'Keeffe M, Hirst DG: **Tumour cell radiosensitization using constitutive (CMV) and radiation inducible (WAF1) promoters to drive the iNOS gene: a novel suicide gene therapy.** *Gene Ther* 2002, **9**:263-269.

71. Dachs GU, Patterson AV, Firth JD, Ratcliffe PJ, Townsend KM, Stratford IJ, Harris AL: **Targeting gene expression to hypoxic tumor cells.** *Nat Med* 1997, **3**:515-520.

72. Brown JM: **Exploiting the hypoxic cancer cell: mechanisms and therapeutic strategies.** *Mol Med Today* 2000, **6**:157-162.

73. Semenza G: **Signal transduction to hypoxia-inducible factor 1.** *Biochem Pharmacol* 2002, **64**:993-998.

74. Semenza GL: **Expression of hypoxia-inducible factor 1: mechanisms and consequences.** *Biochem Pharmacol* 2000, **59**:47-53.

75. Semenza GL: **HIF-1 and tumor progression: pathophysiology and therapeutics.** *Trends Mol Med* 2002, **8**:S62-67.

76. Tendler DS, Bao C, Wang T, Huang EL, Ratovitski EA, Pardoll DA, Lowenstein CJ: **Intersection of interferon and hypoxia signal transduction pathways in nitric oxide-induced tumor apoptosis.** *Cancer Res* 2001, **61**:3682-3688.

77. McCormick CC, Li WP, Calero M: **Oxygen tension limits nitric oxide synthesis by activated macrophages.** *Biochem J* 2000, **350 Pt 3**:709-716.

78. Palmer LA, Semenza GL, Stoler MH, Johns RA: **Hypoxia induces type II NOS gene expression in pulmonary artery endothelial cells via HIF-1.** *Am J Physiol* 1998, **274**:L212-219.

79. Jaffar M, Williams KJ, Stratford IJ: **Bioreductive and gene therapy approaches to hypoxic diseases.** *Adv Drug Deliv Rev* 2001, **53**:217-228.

80. Hopfl G, Wenger RH, Ziegler U, Stallmach T, Gardelle O, Achermann R, Wergin M, Kaser-Hotz B, Saunders HM, Williams KJ, Stratford IJ, Gassmann M, Desbaillets I: **Rescue of hypoxia-inducible factor-1alpha-deficient tumor growth by wild-type cells is independent of vascular endothelial growth factor.** *Cancer Res* 2002, **62**:2962-2970.

81. Griffiths JR, McSheehy PM, Robinson SP, Troy H, Chung YL, Leek RD, Williams KJ, Stratford IJ, Harris AL, Stubbs M: **Metabolic changes detected by in vivo magnetic resonance studies of HEPA-1 wild-type tumors and tumors deficient in hypoxia-inducible factor-1beta (HIF-1beta): evidence of an anabolic role for the HIF-1 pathway.** *Cancer Res* 2002, **62**:688-695.

82. Sun X, Kanwar JR, Leung E, Lehnert K, Wang D, Krissansen GW: **Gene transfer of antisense hypoxia inducible factor-1 alpha enhances the therapeutic efficacy of cancer immunotherapy.** *Gene Ther* 2001, **8**:638-645.

83. Chen J, Zhao S, Nakada K, Kuge Y, Tamaki N, Okada F, Wang J, Shindo M, Higashino F, Takeda K, Asaka M, Katoh H, Sugiyama T, Hosokawa M, Kobayashi M: **Dominant-negative hypoxia-inducible factor-1 alpha reduces tumorigenicity of pancreatic cancer cells through the suppression of glucose metabolism.** *Am J Pathol* 2003, **162**:1283-1291.

84. Ameri K, Lewis CE, Raida M, Sowter H, Hai T, Harris AL: **Anoxic induction of ATF-4 through HIF-1-independent pathways of protein stabilization in human cancer cells.** *Blood* 2004, **103**:1876-1882.

85. Rapisarda A, Uranchimeg B, Scudiero DA, Selby M, Sausville EA, Shoemaker RH, Melillo G: **Identification of small molecule inhibitors of hypoxia-inducible factor 1 transcriptional activation pathway.** *Cancer Res* 2002, **62**:4316-4324.

86. Ivan M, Haberberger T, Gervasi DC, Michelson KS, Gunzler V, Kondo K, Yang H, Sorokina I, Conaway RC, Conaway JW, Kaelin WG, Jr.: **Biochemical purification and**

pharmacological inhibition of a mammalian prolyl hydroxylase acting on hypoxia-inducible factor. *Proc Natl Acad Sci U S A* 2002, **99**:13459-13464.

87. Sandau KB, Fandrey J, Brune B: **Accumulation of HIF-1alpha under the influence of nitric oxide.** *Blood* 2001, **97**:1009-1015.

88. Brune B, von Knethen A, Sandau KB: **Transcription factors p53 and HIF-1alpha as targets of nitric oxide.** *Cell Signal* 2001, **13**:525-533.

89. Metzen E, Zhou J, Jelkmann W, Fandrey J, Brune B: **Nitric oxide impairs normoxic degradation of HIF-1alpha by inhibition of prolyl hydroxylases.** *Mol Biol Cell* 2003, **14**:3470-3481.

90. Kimura H, Ogura T, Kurashima Y, Weisz A, Esumi H: **Effects of nitric oxide donors on vascular endothelial growth factor gene induction.** *Biochem Biophys Res Commun* 2002, **296**:976-982.

91. Kimura H, Weisz A, Kurashima Y, Hashimoto K, Ogura T, D'Acquisto F, Addeo R, Makuuchi M, Esumi H: **Hypoxia response element of the human vascular endothelial growth factor gene mediates transcriptional regulation by nitric oxide: control of hypoxia-inducible factor-1 activity by nitric oxide.** *Blood* 2000, **95**:189-197.

92. Yin JH, Yang DI, Ku G, Hsu CY: **iNOS expression inhibits hypoxia-inducible factor-1 activity.** *Biochem Biophys Res Commun* 2000, **279**:30-34.

93. Sogawa K, Numayama-Tsuruta K, Ema M, Abe M, Abe H, Fujii-Kuriyama Y: **Inhibition of hypoxia-inducible factor 1 activity by nitric oxide donors in hypoxia.** *Proc Natl Acad Sci U S A* 1998, **95**:7368-7373.

94. Huang LE, Willmore WG, Gu J, Goldberg MA, Bunn HF: **Inhibition of hypoxia-inducible factor 1 activation by carbon monoxide and nitric oxide. Implications for oxygen sensing and signaling.** *J Biol Chem* 1999, **274**:9038-9044.

95. Mateo J, Garcia-Lecea M, Cadenas S, Hernandez C, Moncada S: **Regulation of hypoxia-inducible factor-1alpha by nitric oxide through mitochondria-dependent and -independent pathways.** *Biochem J* 2003, **376**:537-544.

96. Hagen T, Taylor CT, Lam F, Moncada S: **Redistribution of intracellular oxygen in hypoxia by nitric oxide: effect on HIF1alpha.** *Science* 2003, **302**:1975-1978.

97. Chinje EC, Cowen RL, Feng J, Sharma SP, Wind NS, Harris AL, Stratford IJ: **Non-nuclear localized human NOSII enhances the bioactivation and toxicity of tirapazamine (SR4233) in vitro.** *Mol Pharmacol* 2003, **63**:1248-1255.

98. Patterson AV, Saunders MP, Chinje EC, Patterson LH, Stratford IJ: **Enzymology of tirapazamine metabolism: a review.** *Anticancer Drug Des* 1998, **13**:541-573.

99. Anderson RF, Harris TA, Hay MP, Denny WA: **Enhanced conversion of DNA radical damage to double strand breaks by 1,2,4-benzotriazine 1,4-dioxides linked to a DNA binder compared to tirapazamine.** *Chem Res Toxicol* 2003, **16**:1477-1483.

100. Wang J, Biedermann KA, Brown JM: **Repair of DNA and chromosome breaks in cells exposed to SR 4233 under hypoxia or to ionizing radiation.** *Cancer Res* 1992, **52**:4473-4477.

101. Costa AK, Baker MA, Brown JM, Trudell JR: **In vitro hepatotoxicity of SR 4233 (3-amino-1,2,4-benzotriazine-1,4-dioxide), a hypoxic cytotoxin and potential antitumor agent.** *Cancer Res* 1989, **49**:925-929.

102. Walton MI, Workman P: **Enzymology of the reductive bioactivation of SR 4233. A novel benzotriazine di-N-oxide hypoxic cell cytotoxin.** *Biochem Pharmacol* 1990, **39**:1735-1742.

103. Worthington J, Robson T, O'Rourke M, Hirst D: **Regulation of iNOS Expression and Vascular Resistance Using Radiation-Inducible Promoters.** *Abstract Submitted to the 11th Conference on Chemical Modifiers of Cancer Treatment, Banff, Aberta, Canada* 2000:185-186.

104. Mitchell JB, Wink DA, DeGraff W, Gamson J, Keefer LK, Krishna MC: **Hypoxic mammalian cell radiosensitization by nitric oxide.** *Cancer Res* 1993, **53**:5845-5848.

105. Griffin RJ, Makepeace CM, Hur WJ, Song CW: **Radiosensitization of hypoxic tumor cells in vitro by nitric oxide.** *Int J Radiat Oncol Biol Phys* 1996, **36**:377-383.

106. Kurimoto M, Endo S, Hirashima Y, Hamada H, Ogiichi T, Takaku A: **Growth inhibition and radiosensitization of cultured glioma cells by nitric oxide generating agents.** *J Neurooncol* 1999, **42**:35-44.

107. Janssens MY, Van den Berge DL, Verovski VN, Monsaert C, Storme GA: **Activation of inducible nitric oxide synthase results in nitric oxide-mediated radiosensitization of hypoxic EMT-6 tumor cells.** *Cancer Res* 1998, **58**:5646-5648.

108. Worthington J, Robson T, Hirst D: **Regulation of iNOS Expression Using Gene Therapy Sensitizes RIF-1 Tumor Cells To Radiation in vitro and in vivo.** *Abstract Submitted to the 11th Conference on Chemical Modifiers of Cancer Treatment, Banff, Aberta, Canada* 2000:V-5.

109. Hirakawa M, Oike M, Masuda K, Ito Y: **Tumor cell apoptosis by irradiation-induced nitric oxide production in vascular endothelium.** *Cancer Res* 2002, **62**:1450-1457.

110. Saez E, No D, West A, Evans RM: **Inducible gene expression in mammalian cells and transgenic mice.** *Curr Opin Biotechnol* 1997, **8**:608-616.

111. **http://www.invitrogen.com.** *Invitrogen Catalog.*

112. Saez E, Nelson MC, Eshelman B, Banayo E, Koder A, Cho GJ, Evans RM: **Identification of ligands and coligands for the ecdysone-regulated gene switch.** *Proc Natl Acad Sci U S A* 2000, **97**:14512-14517.

113. No D, Yao TP, Evans RM: **Ecdysone-inducible gene expression in mammalian cells and transgenic mice.** *Proc Natl Acad Sci U S A* 1996, **93**:3346-3351.

114. Forman BM, Goode E, Chen J, Oro AE, Bradley DJ, Perlmann T, Noonan DJ, Burka LT, McMorris T, Lamph WW, et al.: **Identification of a nuclear receptor that is activated by farnesol metabolites.** *Cell* 1995, **81**:687-693.

115. Constantino S, Santos R, Gisselbrecht S, Gouilleux F: **The ecdysone inducible gene expression system: unexpected effects of muristerone A and ponasterone A on cytokine signaling in mammalian cells.** *Eur Cytokine Netw* 2001, **12**:365-367.

116. Eliopoulos AG, Gallagher NJ, Blake SM, Dawson CW, Young LS: **Activation of the p38 mitogen-activated protein kinase pathway by Epstein-Barr virus-encoded latent membrane protein 1 coregulates interleukin-6 and interleukin-8 production.** *J Biol Chem* 1999, **274**:16085-16096.

117. Cao X, Deng X, May WS: **Cleavage of Bax to p18 Bax accelerates stress-induced apoptosis, and a cathepsin-like protease may rapidly degrade p18 Bax.** *Blood* 2003, **102**:2605-2614.

118. Reusch JE, Klemm DJ: **Inhibition of cAMP-response element-binding protein activity decreases protein kinase B/Akt expression in 3T3-L1 adipocytes and induces apoptosis.** *J Biol Chem* 2002, **277**:1426-1432.

119. Wakita K, McCormick F, Tetsu O: **Method for screening ecdysone-inducible stable cell lines.** *Biotechniques* 2001, **31**:414-418.

120. Yu B, Lane ME, Pestell RG, Albanese C, Wadler S: **Downregulation of cyclin D1 alters cdk 4- and cdk 2-specific phosphorylation of retinoblastoma protein.** *Mol Cell Biol Res Commun* 2000, **3**:352-359.

121. Albanese C, Reutens AT, Bouzahzah B, Fu M, D'Amico M, Link T, Nicholson R, Depinho RA, Pestell RG: **Sustained mammary gland-directed, ponasterone A-inducible expression in transgenic mice.** *Faseb J* 2000, **14**:877-884.

122. Welcsh PL, Lee MK, Gonzalez-Hernandez RM, Black DJ, Mahadevappa M, Swisher EM, Warrington JA, King MC: **BRCA1 transcriptionally regulates genes involved in breast tumorigenesis.** *Proc Natl Acad Sci U S A* 2002, **99**:7560-7565.

123. Wang X, Jin DY, Ng RW, Feng H, Wong YC, Cheung AL, Tsao SW: **Significance of MAD2 expression to mitotic checkpoint control in ovarian cancer cells.** *Cancer Res* 2002, **62**:1662-1668.

124. Chan C, Doctolero M, Nuttall R, Vainer M, Wang X, Hawkins P, Hohnston R, Seilhamer J, Wang B: **FlyGEM™ Performance Evaluation.** *Incyte Genomics, Fremont, CA.*

125. Li H, Zhu H, Xu CJ, Yuan J: **Cleavage of BID by caspase 8 mediates the mitochondrial damage in the Fas pathway of apoptosis.** *Cell* 1998, **94**:491-501.

126. Pastorino JG, Chen ST, Tafani M, Snyder JW, Farber JL: **The overexpression of Bax produces cell death upon induction of the mitochondrial permeability transition.** *J Biol Chem* 1998, **273**:7770-7775.

127. Kakar SS: **Inhibition of growth and proliferation of EcRG293 cell line expressing high-affinity gonadotropin-releasing hormone (GnRH) receptor under the control of an inducible promoter by GnRH agonist (D-Lys6)GnRH and antagonist (Antide).** *Cancer Res* 1998, **58**:4558-4560.

128. Cooper MK, Porter JA, Young KE, Beachy PA: **Teratogen-mediated inhibition of target tissue response to Shh signaling.** *Science* 1998, **280**:1603-1607.

129. Topham MK, Bunting M, Zimmerman GA, McIntyre TM, Blackshear PJ, Prescott SM: **Protein kinase C regulates the nuclear localization of diacylglycerol kinase-zeta.** *Nature* 1998, **394**:697-700.

130. Lin P, Yao Y, Hofmeister R, Tsien RY, Farquhar MG: **Overexpression of CALNUC (nucleobindin) increases agonist and thapsigargin releasable Ca2+ storage in the Golgi.** *J Cell Biol* 1999, **145**:279-289.

131. Pai JT, Guryev O, Brown MS, Goldstein JL: **Differential stimulation of cholesterol and unsaturated fatty acid biosynthesis in cells expressing individual nuclear sterol regulatory element-binding proteins.** *J Biol Chem* 1998, **273**:26138-26148.

132. Zhang J, Kang DE, Xia W, Okochi M, Mori H, Selkoe DJ, Koo EH: **Subcellular distribution and turnover of presenilins in transfected cells.** *J Biol Chem* 1998, **273**:12436-12442.

133. Johns DC, Marx R, Mains RE, O'Rourke B, Marban E: **Inducible genetic suppression of neuronal excitability.** *J Neurosci* 1999, **19**:1691-1697.

134. Gossen M, Freundlieb S, Bender G, Muller G, Hillen W, Bujard H: **Transcriptional activation by tetracyclines in mammalian cells.** *Science* 1995, **268**:1766-1769.

135. Burcin MM, BW OM, Tsai SY: **A regulatory system for target gene expression.** *Front Biosci* 1998, **3**:c1-7.

136. Mills AA: **Changing colors in mice: an inducible system that delivers.** *Genes Dev* 2001, **15**:1461-1467.

137. Baron U, Gossen M, Bujard H: **Tetracycline-controlled transcription in eukaryotes: novel transactivators with graded transactivation potential.** *Nucleic Acids Res* 1997, **25**:2723-2729.

138. Gossen M, Bonin AL, Bujard H: **Control of gene activity in higher eukaryotic cells by prokaryotic regulatory elements.** *Trends Biochem Sci* 1993, **18**:471-475.

139. Shockett P, Difilippantonio M, Hellman N, Schatz DG: **A modified tetracycline-regulated system provides autoregulatory, inducible gene expression in cultured cells and transgenic mice.** *Proc Natl Acad Sci U S A* 1995, **92**:6522-6526.

140. Tsai SY, Schillinger K, Ye X: **Adenovirus-mediated transfer of regulable gene expression.** *Curr Opin Mol Ther* 2000, **2**:515-523.

141. Gossen M, Bujard H: **Tight control of gene expression in mammalian cells by tetracycline-responsive promoters.** *Proc Natl Acad Sci U S A* 1992, **89**:5547-5551.

142. Stebbins MJ, Urlinger S, Byrne G, Bello B, Hillen W, Yin JC: **Tetracycline-inducible systems for Drosophila.** *Proc Natl Acad Sci U S A* 2001, **98**:10775-10780.

143. Mizuguchi H, Hayakawa T: **Characteristics of adenovirus-mediated tetracycline-controllable expression system.** *Biochim Biophys Acta* 2001, **1568**:21-29.

144. **Tet-On and Tet-Off Gene Expression Systems-Clontech Catalog.** *http://www.clontech.com*:2.

145. Liang M, Ekblad E, Lydrup ML, Nilsson BO: **Combined lack of estrogen receptors alpha and beta affects vascular iNOS protein expression.** *Cell Tissue Res* 2003, **313**:63-70.

146. Shi L, Shi SQ, Given RL, von Hertzen H, Garfield RE: **Synergistic effects of antiprogestins and iNOS or aromatase inhibitors on establishment and maintenance of pregnancy.** *Steroids* 2003, **68**:1077-1084.

147. *http://www.adenovirus.com/products/kits/adenovator/Manual%20Q-mate%20AdenoVator_version1.0_%2029may2003.pdf.*

148. Eaton RW: **p-Cymene catabolic pathway in Pseudomonas putida F1: cloning and characterization of DNA encoding conversion of p-cymene to p-cumate.** *J Bacteriol* 1997, **179**:3171-3180.

149. Senner V, Sotoodeh A, Paulus W: **Regulated gene expression in glioma cells: a comparison of three inducible systems.** *Neurochem Res* 2001, **26**:521-524.

150. Xiao YY, Beilstein MA, Wang MC, Purintrapiban J, Forsberg NE: **Development of a ponasterone A-inducible gene expression system for application in cultured skeletal muscle cells.** *Int J Biochem Cell Biol* 2003, **35**:79-85.

151. Xu ZL, Mizuguchi H, Mayumi T, Hayakawa T: **Regulated gene expression from adenovirus vectors: a systematic comparison of various inducible systems.** *Gene* 2003, **309**:145-151.

152. Stone D, David A, Bolognani F, Lowenstein PR, Castro MG: **Viral vectors for gene delivery and gene therapy within the endocrine system.** *J Endocrinol* 2000, **164**:103-118.

153. Slabiak T, revised, by, Frederickson R: **Gene Therapy.** *http://www.bio.com/newsfeatures/newsfeatures_research.jhtml?cid=54206&contentItem=54206&Page=1&action=view.*

154. Izquierdo M, Martin V, de Felipe P, Izquierdo JM, Perez-Higueras A, Cortes ML, Paz JF, Isla A, Blazquez MG: **Human malignant brain tumor response to herpes simplex thymidine kinase (HSVtk)/ganciclovir gene therapy.** *Gene Ther* 1996, **3**:491-495.

155. Ram Z, Culver KW, Oshiro EM, Viola JJ, DeVroom HL, Otto E, Long Z, Chiang Y, McGarrity GJ, Muul LM, Katz D, Blaese RM, Oldfield EH: **Therapy of malignant brain tumors by intratumoral implantation of retroviral vector-producing cells.** *Nat Med* 1997, **3**:1354-1361.

156. Dewey RA, Morrissey G, Cowsill CM, Stone D, Bolognani F, Dodd NJ, Southgate TD, Klatzmann D, Lassmann H, Castro MG, Lowenstein PR: **Chronic brain inflammation and persistent herpes simplex virus 1 thymidine kinase expression in survivors of syngeneic glioma treated by adenovirus-mediated gene therapy: implications for clinical trials.** *Nat Med* 1999, **5**:1256-1263.

157. Cowsill C, Southgate TD, Morrissey G, Dewey RA, Morelli AE, Maleniak TC, Forrest Z, Klatzmann D, Wilkinson GW, Lowenstein PR, Castro MG: **Central nervous system toxicity of two adenoviral vectors encoding variants of the herpes simplex virus type 1 thymidine kinase: reduced cytotoxicity of a truncated HSV1-TK.** *Gene Ther* 2000, **7**:679-685.

158. Senzer N, Mani S, Rosemurgy A, Nemunaitis J, Cunningham C, Guha C, Bayol N, Gillen M, Chu K, Rasmussen C, Rasmussen H, Kufe D, Weichselbaum R, Hanna N: **TNFerade biologic, an adenovector with a radiation-inducible promoter, carrying the human tumor necrosis factor alpha gene: a phase I study in patients with solid tumors.** *J Clin Oncol* 2004, **22**:592-601.

159. Albelda SM, Sterman DH: **TNFerade to the rescue? Guidelines for evaluating phase I cancer gene transfer trials.** *J Clin Oncol* 2004, **22**:577-579.

160. Kibbe MR, Tzeng E, Gleixner SL, Watkins SC, Kovesdi I, Lizonova A, Makaroun MS, Billiar TR, Rhee RY: **Adenovirus-mediated gene transfer of human inducible nitric oxide synthase in porcine vein grafts inhibits intimal hyperplasia.** *J Vasc Surg* 2001, **34**:156-165.

161. Wolff JA, Lederberg J: **An early history of gene transfer and therapy.** *Hum Gene Ther* 1994, **5**:469-480.

162. Naldini L, Blomer U, Gallay P, Ory D, Mulligan R, Gage FH, Verma IM, Trono D: **In vivo gene delivery and stable transduction of nondividing cells by a lentiviral vector.** *Science* 1996, **272**:263-267.

163. Kibbe MR, Nie S, Yoneyama T, Hatakeyama K, Lizonova A, Kovesdi I, Billiar TR, Tzeng E: **Optimization of ex vivo inducible nitric oxide synthase gene transfer to vein grafts.** *Surgery* 1999, **126**:323-329.

164. Shears LL, 2nd, Kibbe MR, Murdock AD, Billiar TR, Lizonova A, Kovesdi I, Watkins SC, Tzeng E: **Efficient inhibition of intimal hyperplasia by adenovirus-mediated inducible nitric oxide synthase gene transfer to rats and pigs in vivo.** *J Am Coll Surg* 1998, **187**:295-306.

165. Li Q, Guo Y, Xuan YT, Lowenstein CJ, Stevenson SC, Prabhu SD, Wu WJ, Zhu Y, Bolli R: **Gene therapy with inducible nitric oxide synthase protects against myocardial infarction via a cyclooxygenase-2-dependent mechanism.** *Circ Res* 2003, **92**:741-748.

166. Zanetti M, d'Uscio LV, Kovesdi I, Katusic ZS, O'Brien T: **In vivo gene transfer of inducible nitric oxide synthase to carotid arteries from hypercholesterolemic rabbits.** *Stroke* 2003, **34**:1293-1298.

167. Tzeng E, Billiar TR, Williams DL, Li J, Lizonova A, Kovesdi I, Kim YM: **Adenovirus-mediated inducible nitric oxide synthase gene transfer inhibits hepatocyte apoptosis.** *Surgery* 1998, **124**:278-283.

168. Tzeng E, Kim YM, Pitt BR, Lizonova A, Kovesdi I, Billiar TR: **Adenoviral transfer of the inducible nitric oxide synthase gene blocks endothelial cell apoptosis.** *Surgery* 1997, **122**:255-263.

169. Wang Z, Cook T, Alber S, Liu K, Kovesdi I, Watkins SK, Vodovotz Y, Billiar TR, Blumberg D: **Adenoviral gene transfer of the human inducible nitric oxide synthase gene enhances the radiation response of human colorectal cancer associated with alterations in tumor vascularity.** *Cancer Res* 2004, **64**:1386-1395.

170. Weller R, Schwentker A, Billiar TR, Vodovotz Y: **Autologous nitric oxide protects mouse and human keratinocytes from ultraviolet B radiation-induced apoptosis.** *Am J Physiol Cell Physiol* 2003, **284**:C1140-1148.

171. Gunnett CA, Lund DD, Howard MA, 3rd, Chu Y, Faraci FM, Heistad DD: **Gene transfer of inducible nitric oxide synthase impairs relaxation in human and rabbit cerebral arteries.** *Stroke* 2002, **33**:2292-2296.

172. Lee-Kwon W, Johns DC, Cha B, Cavet M, Park J, Tsichlis P, Donowitz M: **Constitutively active phosphatidylinositol 3-kinase and AKT are sufficient to stimulate the epithelial Na+/H+ exchanger 3.** *J Biol Chem* 2001, **276**:31296-31304.

173. Perez-Garcia MT, Lopez-Lppez JR, Riesco AM, Hoppe UC, Marban E, Gonzalez C, Johns DC: **Viral gene transfer of dominant-negative Kv4 construct suppresses an O2-sensitive K+ current in chemoreceptor cells.** *J Neurosci* 2000, **20**:5689-5695.

174. Holt JR, Johns DC, Wang S, Chen ZY, Dunn RJ, Marban E, Corey DP: **Functional expression of exogenous proteins in mammalian sensory hair cells infected with adenoviral vectors.** *J Neurophysiol* 1999, **81**:1881-1888.

175. Literature NEBT: **http://www.neb.com/neb/tech/tech_resource/restriction/ecoli/dam_dcm.html**.

176. Felgner PL, Gadek TR, Holm M, Roman R, Chan HW, Wenz M, Northrop JP, Ringold GM, Danielsen M: **Lipofection: a highly efficient, lipid-mediated DNA-transfection procedure.** *Proc Natl Acad Sci U S A* 1987, **84**:7413-7417.

177. Hawley-Nelson P, Ciccarone, V., Gebeyehu, G., Jessee, J., and Felgner, P.L.: *Focus* 1993.

178. Jounaidi Y, Waxman DJ: **Combination of the bioreductive drug tirapazamine with the chemotherapeutic prodrug cyclophosphamide for P450/P450-reductase-based cancer gene therapy.** *Cancer Res* 2000, **60**:3761-3769.

179. Wood KV, de Wet JR, Dewji N, DeLuca M: **Synthesis of active firefly luciferase by in vitro translation of RNA obtained from adult lanterns.** *Biochem Biophys Res Commun* 1984, **124**:592-596.

180. de Wet JR, Wood KV, Helinski DR, DeLuca M: **Cloning of firefly luciferase cDNA and the expression of active luciferase in Escherichia coli.** *Proc Natl Acad Sci U S A* 1985, **82**:7870-7873.

181. *Promega Catalogue* 4/03:2-3.

182. Matthews JC, Hori K, Cormier MJ: **Purification and properties of Renilla reniformis luciferase.** *Biochemistry* 1977, **16**:85-91.

183. **http://www.piercenet.com.**

184. Bredt DS, Snyder SH: **Isolation of nitric oxide synthetase, a calmodulin-requiring enzyme.** *Proc Natl Acad Sci U S A* 1990, **87**:682-685.

185. Geller DA, Lowenstein CJ, Shapiro RA, Nussler AK, Di Silvio M, Wang SC, Nakayama DK, Simmons RL, Snyder SH, Billiar TR: **Molecular cloning and expression of inducible nitric oxide synthase from human hepatocytes.** *Proc Natl Acad Sci U S A* 1993, **90**:3491-3495.

186. Williams CH, Jr., Kamin H: **Microsomal triphosphopyridine nucleotide-cytochrome c reductase of liver.** *J Biol Chem* 1962, **237**:587-595.

187. Luck PC, Schmitt JW, Hengerer A, Helbig JH: **Subinhibitory concentrations of antimicrobial agents reduce the uptake of Legionella pneumophila into Acanthamoeba castellanii and U937 cells by altering the expression of virulence-associated antigens.** *Antimicrob Agents Chemother* 1998, **42**:2870-2876.

188. Mosmann T: **Rapid colorimetric assay for cellular growth and survival: application to proliferation and cytotoxicity assays.** *J Immunol Methods* 1983, **65**:55-63.

189. Hardiek K, Katholi RE, Ramkumar V, Deitrick C: **Proximal tubule cell response to radiographic contrast media.** *Am J Physiol Renal Physiol* 2001, **280**:F61-70.

190. Kim JY, West CM, Valentine H, Ward TH, Patterson AV, Stratford IJ, Roberts SA, Hendry JH: **Cytotoxicity of the bioreductive agent RH1 and its lack of interaction with radiation.** *Radiother Oncol* 2004, **70**:311-317.

191. Berkner KL, Pudota BN: **Vitamin K-dependent carboxylation of the carboxylase.** *Proc Natl Acad Sci U S A* 1998, **95**:466-471.

192. He TC, Zhou S, da Costa LT, Yu J, Kinzler KW, Vogelstein B: **A simplified system for generating recombinant adenoviruses.** *Proc Natl Acad Sci U S A* 1998, **95**:2509-2514.

193. **http://www.bdbiosciences.com/clontech/products/cat/HTML/1260.shtml.**

194. Workman P, Balmain A, Hickman JA, McNally NJ, Rohas AM, Mitchison NA, Pierrepoint CG, Raymond R, Rowlatt C, Stephens TC, et al.: **UKCCCR guidelines for the welfare of animals in experimental neoplasia.** *Lab Anim* 1988, **22**:195-201.

195. Azuma C, Raleigh JA, Thrall DE: **Longevity of pimonidazole adducts in spontaneous canine tumors as an estimate of hypoxic cell lifetime.** *Radiat Res* 1997, **148**:35-42.

196. **Hydroxyprbe-1 Kit for detection of tissue hypoxia**. *http://www.radonc.unc.ecd/pimo/* Revised January 2002.

197. Raleigh JA, Miller CG, Franko AJ, Chapman JD: **Immunochemical detection of hypoxia in normal and tumor tissue**. *U.S. Patent 5,086,068* 1992.

198. Patterson AV, Williams KJ, Cowen RL, Jaffar M, Telfer BA, Saunders M, Airley R, Honess D, van der Kogel AJ, Wolf CR, Stratford IJ: **Oxygen-sensitive enzyme-prodrug gene therapy for the eradication of radiation-resistant solid tumours**. *Gene Ther* 2002, **9**:946-954.

199. Postovit LM, Adams MA, Lash GE, Heaton JP, Graham CH: **Oxygen-mediated regulation of tumor cell invasiveness. Involvement of a nitric oxide signaling pathway**. *J Biol Chem* 2002, **277**:35730-35737.

200. Latt SA, Stetten GH: **Spectral studies on 33258 Hoechst and related bisbenzimidazole dyes useful for fluorescent detection of deoxyribonucleic acid synthesis.** *Histochem. Cytochem* 1976, **24**:24-33.

201. Steinwaerder DS, Lieber A: **Insulation from viral transcriptional regulatory elements improves inducible transgene expression from adenovirus vectors in vitro and in vivo**. *Gene Ther* 2000, **7**:556-567.

202. Prestridge DS: **Predicting Pol II promoter sequences using transcription factor binding sites**. *J Mol Biol* 1995, **249**:923-932.

203. Windeatt S, Southgate TD, Dewey RA, Bolognani F, Perone MJ, Larregina AT, Maleniak TC, Morris ID, Goya RG, Klatzmann D, Lowenstein PR, Castro MG: **Adenovirus-mediated herpes simplex virus type-1 thymidine kinase gene therapy suppresses oestrogen-induced pituitary prolactinomas**. *J Clin Endocrinol Metab* 2000, **85**:1296-1305.

204. Walling J, Stratford IJ, Adams GE, Stephens MA: **Dual-function radiation sensitizers and bioreductive drugs: factors affecting cellular uptake and sensitizing efficiency in analogues of RSU 1069**. *Int J Radiat Biol Relat Stud Phys Chem Med* 1988, **53**:641-649.

205. Cowen RL, Williams KJ, Chinje EC, Jaffar M, Sheppard FC, Telfer BA, Wind NS, Stratford IJ: **Hypoxia targeted gene therapy to increase the efficacy of tirapazamine as an adjuvant to radiotherapy: reversing tumor radioresistance and effecting cure**. *Cancer Res* 2004, **64**:1396-1402.

206. Wyborski DL, Bauer JC, Vaillancourt P: **Bicistronic expression of ecdysone-inducible receptors in mammalian cells**. *Biotechniques* 2001, **31**:618-620, 622, 624.

207. Hoppe UC, Marban E, Johns DC: **Adenovirus-mediated inducible gene expression in vivo by a hybrid ecdysone receptor**. *Mol Ther* 2000, **1**:159-164.

208. Shears LL, Kawaharada N, Tzeng E, Billiar TR, Watkins SC, Kovesdi I, Lizonova A, Pham SM: **Inducible nitric oxide synthase suppresses the development of allograft arteriosclerosis**. *J Clin Invest* 1997, **100**:2035-2042.

209. Mizuguchi H, Hayakawa T: **The tet-off system is more effective than the tet-on system for regulating transgene expression in a single adenovirus vector.** *J Gene Med* 2002, **4**:240-247.

210. Cuevas Y, Hernandez-Alcoceba R, Aragones J, Naranjo-Suarez S, Castellanos MC, Esteban MA, Martin-Puig S, Landazuri MO, del Peso L: **Specific oncolytic effect of a new hypoxia-inducible factor-dependent replicative adenovirus on von Hippel-Lindau-defective renal cell carcinomas.** *Cancer Res* 2003, **63**:6877-6884.

211. Kragh M, Hjarnaa PJ, Bramm E, Kristjansen PE, Rygaard J, Binderup L: **In vivo chamber angiogenesis assay: an optimized Matrigel plug assay for fast assessment of anti-angiogenic activity.** *Int J Oncol* 2003, **22**:305-311.

APPENDIX

Maps of purchased plasmids:

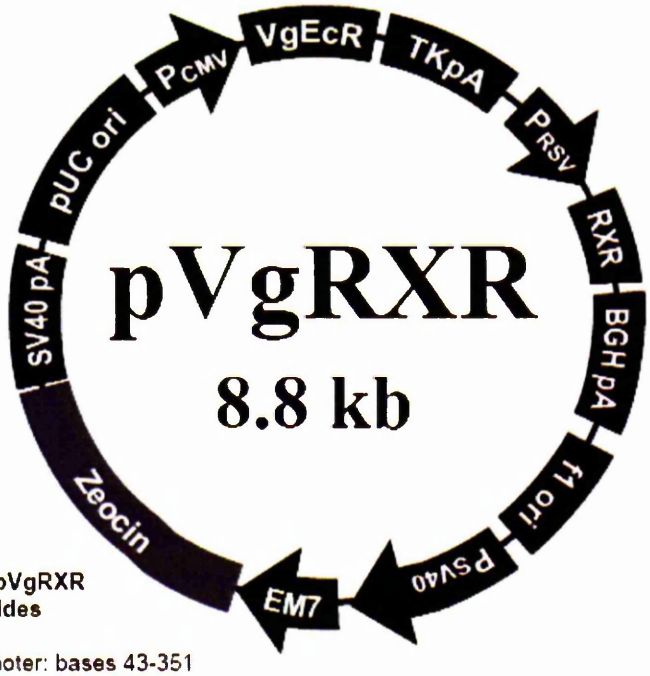

Comments for pVgRXR
8803 nucleotides

SV40 early promoter: bases 43-351
EM7 promoter: bases 778-855
Zeocin™ resistance gene (*Sh ble*) ORF: bases 856-1230
SV40 late polyadenylation sequence: base 1294-1424
pUC origin: bases 1533-2206
CMV promoter: bases 2265-2883
VgEcR fusion protein: bases 3035-5275
  modified VP16: bases 3038-3271
  EcR: bases 3302-5275
HSV-1 thymidine kinase polyadenylation sequence: bases 5470-5982
RSV 5' long terminal repeat: bases 6353-6614
RXR ORF: bases 6637-8025
BGH polyadenylation sequence: bases 8108-8332
f1 origin: bases 8502-8609

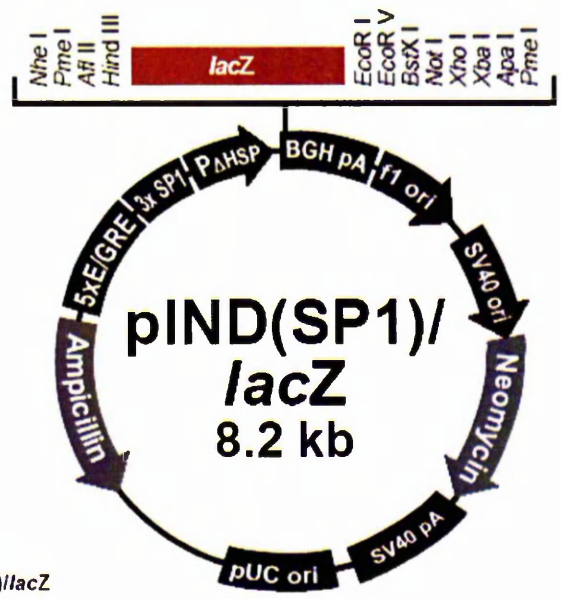

Comments for pIND(SP1)/*lac*Z
8227 nucleotides

Ecdysone/glucocorticoid Response
Elements (5x E/GREs): bases 1-174
SP1 Enhancer (3x SP1): bases 185-240
Minimal Heat Shock Promoter: bases 241-533
*Lac*Z ORF: bases 559-3729
BGH Reverse priming site: bases 3807-3824
BGH Polyadenylation sequence: bases 3806-4020
f1 origin: bases 4083-4497
SV40 promoter/origin: bases 4561-4885
Neomycin ORF: bases 4921-5715
SV40 Polyadenylation sequence: bases 5731-5970
pUC origin: bases 6402-7075
Ampicillin ORF: bases 7220-8080 (Complementary strand)

Invitrogen™
life technologies

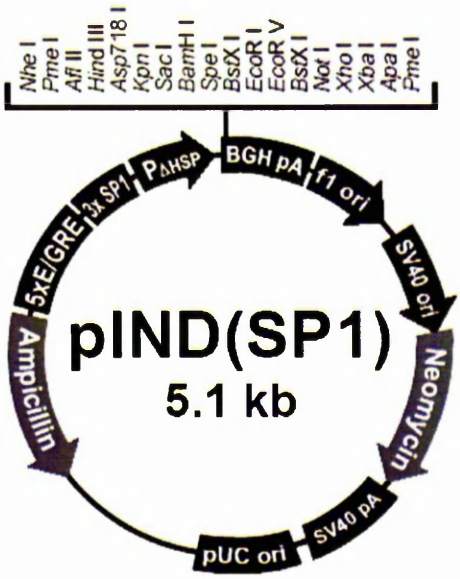

Comments for pIND(SP1)
5081 nucleotides

Ecdysone/glucocorticoid
Response Elements (5x E/GREs): bases 1-174
SP1 Enhancer (3x SP1): bases 185-240
Minimal Heat Shock Promoter: bases 241-533
Multiple Cloning Site: bases 534-659
BGH Reverse priming site: bases 661-678
BGH Polyadenylation sequence: bases 660-874
f1 origin: bases 937-1351
SV40 promoter/origin: bases 1415-1739
Neomycin ORF: bases 1775-2569
SV40 Polyadenylation sequence: bases 2585-2824
pUC origin: bases 3256-3929
Ampicillin ORF: bases 4074-4934 (complementary strand)

Invitrogen
life technologies

Biochemical and Biophysical Research Communications

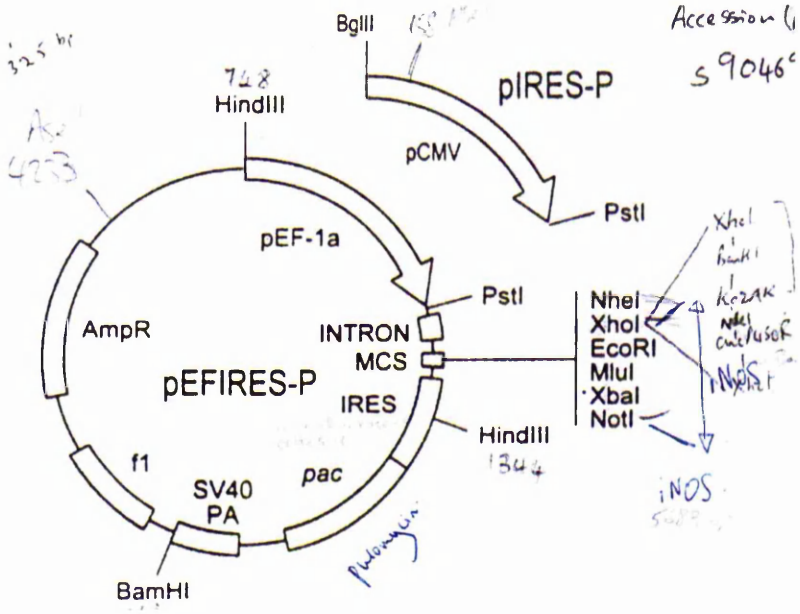

left inverted terminal repeat 1–103
encapsidation signal (ES) 183–331
multiple cloning site 345–404
Ad5 right arm homology 414–2652
Ad5 left arm homology 2701–3580
right inverted terminal repeat 3581–3683
pBR322 origin 3887–4554
kanamycin resistance ORF 5363–6154

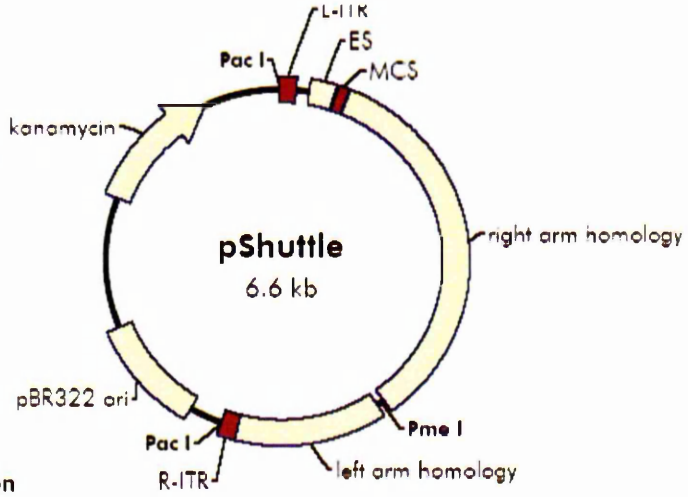

pShuttle Multiple Cloning Site Region
(sequence shown 299–459)

Forward primer binding site
GAAGTGAAATCTGAATAATTTTGTGTTACTCATAGCGCGTAATACT...

Kpn I Not I Xho I Xba I EcoR V Hind III Cla I Sal II
...GGTACCGCGGCCGCCTCGAGTCTAGAGATATCGAATTCAAGCTTGTCGACTCGAAGATCT...

Reverse primer binding site
...GGGCGTGGTTAAGGGTGGGAAAGAATATATAAGGTGGGGGTCTTATGTAGTTTTG

left inverted terminal repeat 1–103
encapsidation signal (ES) 183–331
CMV promoter 345–932
β-galactosidase (*lacZ*) ORF 967–4014
SV40 polyA 4217–4444
Ad5 right arm homology 4453–6692
Ad5 left arm homology 6740–7619
right inverted terminal repeat 7620–7722
pBR322 origin 7926–8593
kanamycin resistance ORF 9402–10193

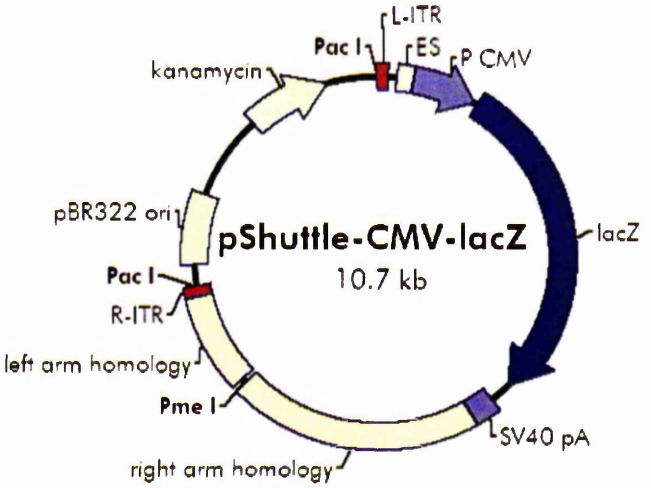

pBR322 origin 1854–2521
ampicillin resistance (*bla*) ORF 2669–3529
Ad5 right arm homology 3695–5700
Ad5 left arm homology 32462–33450

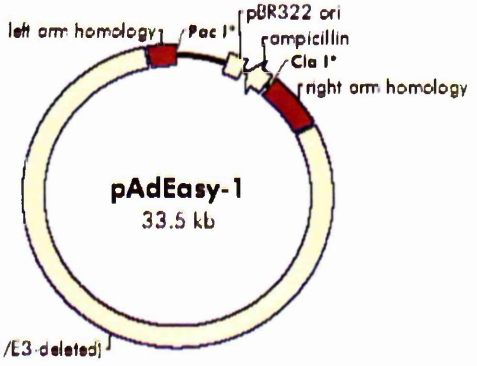

DNA Ladders:

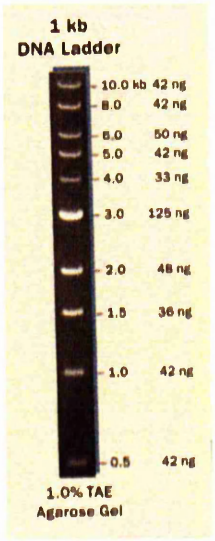

λ Hind III-digested
DNA Ladder